Universidade da Coruña

Departamento de Química Física e Enxeñería Química I

Contributions to the study of acid/base and complexation properties of natural organic matter and model substances in aqueous saline media.

Memoria presentada por Carlos Rey Castro para optar al Grado de Doctor en Química

A Coruña, 2004

MANUEL E. SASTRE DE VICENTE, Director del Departamento de Química Física e Enxeñería Química I de la Universidad de A Coruña,

CERTIFICA

que el Licenciado en Ciencias Químicas Carlos Rey Castro, realizó en este Departamento, bajo la dirección de los Drs. Manuel E. Sastre de Vicente y Roberto Herrero Rodríguez, el trabajo que, bajo el título ***Contributions to the study of acid/base and complexation properties of natural organic matter and model substances in aqueous saline media***, presenta para optar al grado de Doctor en Química.

Y para que así conste, expido y firmo la presente en A Coruña, a 11 de Marzo de 2004.

Fdo.: M. E. Sastre de Vicente

MANUEL E. SASTRE DE VICENTE, Catedrático de Química Física, y **ROBERTO HERRERO RODRÍGUEZ**, Profesor Titular del Departamento de Química Física e Enxeñería Química I de la Universidad de A Coruña,

CERTIFICAN

que el presente trabajo de investigación titulado ***Contributions to the study of acid/base and complexation properties of natural organic matter and model substances in aqueous saline media***, ha sido realizado por el Licenciado en Ciencias Químicas **Carlos Rey Castro** en el Departamento de Química Física e Enxeñería Química I, Laboratorio de Electroquímica, y que, como Directores del mismo, autorizan su presentación como Tesis Doctoral a fin de que pueda ser juzgada por el tribunal correspondiente.

Y para que así conste, expiden y firman la presente en A Coruña, a 11 de Marzo de 2004.

Fdo.: M. E. Sastre de Vicente Fdo.: R. Herrero Rodríguez

Agradecimientos

Este trabajo es el resultado de una infinidad de pequeños vectores con direcciones que cualquiera diría orientadas al azar. No obstante, y como siempre sucede en la vida, al final la suma no ha sido nula. Mi más sincero y cálido agradecimiento a todos aquellos que han caminado a mi lado:

A mis directores, Manuel Sastre y Roberto Herrero, que han demostrado una gran confianza y paciencia (en ocasiones excesivas ambas) con este trabajo y con quien lo suscribe.

Quisiera también reconocer mi deuda con los directores de mis estancias en Windermere, Messina y Barcelona-Lleida, los doctores Ed Tipping, Silvio Sammartano, Concetta de Stefano y el *tripartito* Francesc Mas, Jaime Puy y Josep Galceran. Porque han asumido responsabilidades en este trabajo más allá de sus obligaciones, y también por el estupendo trato que me han dedicado en lo personal.

Gracias al Ministerio de Educación, Cultura y Deporte por el apoyo económico a lo largo de estos cuatro años, a través de una Beca de Formación de Personal Universitario.

A los profesores y compañeros del laboratorio de Química Física II, en especial a Pablo y Bruno, por tantas aventuras, desventuras y *maratones*, y a Jose Luis Barriada, que (entre Plymouth y Coruña) siempre estuvo ahí para echar una mano. También gracias a todo el Departamento de Química Analítica (sois tantos que no me cabéis aquí uno por uno) por su ayuda técnica y su amistad. Un saludo también para Marcos Chas y Roberto Mosteiro.

A los profesores Ignacio Bárbara y Javier Cremades por la recolección y clasificación de las muestras de algas pardas.

A la gente que conocí en Windermere, en especial a Beate Michalzik y sus cuadro-paisajes, a Esther Smith, a Lucy Ball (y tu televisor!), a Bernie Simon y toda su encantadora familia; y a Steve Brian, Steve Lofts y Alan Lawlor por su asistencia profesional. A mis caseros Rachel y Hans por su paciencia con mis horarios españoles.

Agli amici di Sicilia, Ottavia, Antonio ed il loro bambino (auguri!), Ciccio, Alberto, il mio caro *cognato* Clemente, Demetrio, Pasquale, Concetta ("con la spada al cuore...") ed il *Professore* (ancora una volta), gracias a todos por una gran *maleta* roja llena de recuerdos.

A la gente de Cataluña: Encarna, Josep Lluis, Joan, y a Josep, Jaume, Francesc y sus respectivas familias. Y también a Mercé. Gracias, Francesc, en particular, por los consejos sobre la vida...

A mis amigos, por ser como sois: María, Merce (¡qué bonita es la primavera cuando llega!), Ricardo (¡saravá, irmán!), Fany y Alberto, Luz y también los *alcoanos* (¡viva la conexión astur-galaica!).

A mis padres, á miña irmá Isaura, por ser a máis valente e tamén a máis rosmona. E porque o talento non fai o que pode, senón o que debe (non o esquezas nunca). Y al resto de la familia. ¿Quién me falta?, ah, si: ¡GRACIAS, MONICA! Por tantas cosas, pero además porque a pesar de conocerme tan bien todavía sigues convencida de que merezco la pena, y porque me has ayudado con estas páginas más de lo que debería reconocer aquí.

Y ahora, comenzamos:

Resumen

En la presente memoria se detallan los principales resultados obtenidos en el estudio del efecto del medio salino sobre los equilibrios ácido-base y de complejación de diferentes ligandos orgánicos. Dicho estudio es de gran importancia en las ciencias medioambientales para la comprensión del comportamiento de los cationes metálicos en aguas naturales, ya que la interacción catión-materia orgánica desempeña un papel primordial en los diversos ciclos biogeoquímicos y afecta en gran medida a la biodisponibilidad de dicho catión. Por otro lado, esta interacción también puede tener un interés tecnológico especial, por su aplicación a métodos de descontaminación.

En el estudio de la química en disolución de los ligandos orgánicos se han tratado diferentes aspectos como el efecto de la concentración y composición del medio iónico sobre los coeficientes de actividad, el efecto polielectrolítico, la heterogeneidad, o la competición entre diferentes cationes. Los sistemas seleccionados siguen un orden ascendente en grado de complejidad, atendiendo a aspectos como el grado de heterogeneidad o la polidispersidad. En cada caso se han aplicado diferentes modelos fisicoquímicos, de mayor o menor carácter empírico. El primer capítulo de la presente memoria se ha destinado a introducir brevemente dichos modelos, con un análisis de los respectivos postulados de partida. El capítulo dos recoge información relevante sobre los detalles experimentales. Los capítulos siguientes describen los principales resultados obtenidos con los diferentes analitos estudiados a lo largo de esta tesis. La mayor parte de estos resultados han sido publicados o están en trámites de publicación, tal y como se indica en la introducción de cada capítulo. En el primer caso, el capítulo coincide con la última versión censada del artículo, con la salvedad de cambios en interlineado, fuentes, márgenes, etc. necesarios para unificar el formato de la Tesis.

Los sistemas estudiados se detallan a continuación:

1. Ligando sencillo en medios salinos concentrados: ácido o-ftálico. Este tipo de sistemas de composición química perfectamente conocida no presentan los efectos típicos de ligandos macromoleculares (carácter polielectrolítico, heterogeneidad, cambios conformacionales, etc). De esta forma, el efecto del medio iónico sobre los equilibrios ácido-base puede describirse de un modo preciso mediante la aplicación de los modelos

semiempíricos habitualmente empleados en el cálculo de coeficientes de actividad de iones sencillos, como las ecs. de Pitzer.

2. Polielectrolitos sintéticos. Se han estudiado los siguientes ácidos policarboxílicos: ác. poliacrílico (PAA), y poliacrílico-co-maleico (PAMA). Estas sustancias poseen una composición funcional conocida, pero presentan una fuerte interacción de tipo electrostático entre los grupos disociados (efecto polielectrolítico). Estos sistemas se han estudiado mediante modelos teóricos, como la ecuación de Poisson-Boltzmann no-lineal y modelos empíricos como las ecuaciones de Högfeldt y Katchalsky.

3. Equilibrios ácido-base de polisacáridos naturales: ác. algínico. Estos polielectrolitos de relativamente bajo grado de heterogeneidad funcional presentan un gran interés por su elevada afinidad hacia cationes polivalentes, lo cual convierte a las matrices naturales en que se encuentran (como las algas pardas) en excelentes materiales adsorbentes para la eliminación de metales pesados en aguas residuales.

4. Equilibrios de complejación en polielectrolitos naturales: ácidos húmicos. Estas sustancias presentan tanto efecto polielectrolítico como un elevado grado de heterogeneidad química, y determinan en gran medida la biodisponibilidad y el transporte de los metales pesados en los suelos y aguas naturales de gran contenido en materia orgánica. Se han estudiado los efectos de competición del Fe(III) con el Cu(II) por la complejación con una muestra natural purificada de ácido húmico y los resultados han sido interpretados mediante el Modelo WHAM-VI de Tipping.

5. Sistemas macroscópicos: biomasas de algas pardas. Las algas marinas son bioadsorbentes idóneos para ser utilizados en sistemas de descontaminación por su bajo coste, elevada capacidad de complejación y reducido impacto ambiental. Como primera etapa en la evaluación de su utilización tecnológica, se ha realizado un estudio del efecto del pH y la fuerza iónica sobre los equilibrios ácido-base de diferentes muestras de algas marinas de las costas gallegas. Los resultados obtenidos se han analizado a través de diferentes modelos electrostáticos, como el modelo de Donnan o el de Gouy-Chapman.

Este trabajo ha sido realizado en su mayor parte en la Universidad de A Coruña bajo la dirección de los doctores Manuel E. Sastre de Vicente y Roberto Herrero Rodríguez. Los resultados relativos a las sustancias húmicas se han obtenido a lo largo de la estancia realizada entre los meses de Septiembre y Diciembre de 2000 y Abril a Julio de 2001 en el Centre of Ecology and Hydrology de Windermere (Reino Unido), bajo la supervisión del Dr. Edward W. Tipping. Los resultados experimentales del PAMA se han obtenido en el peridodo comprendido entre Septiembre y Diciembre de 2002 en el Dipartimento di Chimica Inorganica, Chimica Analitica e Chimica Fisica de la Università di Messina (Italia), bajo la supervisión del Dr. Silvio Sammartano. Finalmente, el apartado dedicado al PAA recoge resultados experimentales y cálculos teóricos realizados entre Septiembre y Diciembre de 2003 en el Departament de Química Física de la Universitat de Barcelona y en el Departament de Química de la Universitat de Lleida, con la supervisión del Dr. Francesc Mas i Pujadas.

Table of Contents

Agradecimientos……..... i
Resumen…… iii
Table of contents…… vii

CHAPTER 1. THERMODYNAMIC MODELS FOR THE DESCRIPTION OF THE CATION BINDING EQUILIBRIA … 1
1.1. Introduction……...……...……..…… 3
1.2. Simple ligands…….…….. 6
1.3. Polyelectrolytes…….……. 9
1.3.1. Empirical models…….…… 12
1.3.1.1. Modified Henderson-Hasselbach equation ….…….. 12
1.3.1.2. Högfeldt model…….……. 14
1.3.1.3. Application to synthetic polyelectrolytes……..…… 15
1.3.2. Two-phase equilibrium models: Donnan models ……..……. 17
1.3.2.1. Permeable gels ……..…… 17
1.3.2.2. Water-soluble linear polyelectrolytes ……..……..…… 20
1.3.3. Theoretical models based on electrostatics……. 21
1.3.3.1. Linearised Poisson-Bolztmann equation (Debye-Hückel approximation)…… 22
1.3.3.2. Non-linear Poisson-Boltzmann equation (NLPB)……. 24
1.3.4. Descriptions of the chemical heterogeneity …… 26
1.3.4.1. Binding curve and average equilibrium function …..…… 26
1.3.4.2. The affinity spectrum formalism …….……. 27
1.3.4.3. The master curve approach …….…….. 29
1.4. Outline of this thesis ……..…… 31
1.5 References…….. 33

CHAPTER 2. EXPERIMENTAL SECTION……. 41
2.1. Analytical techniques…… 43
2.1.1. Potentiometry…….. 43
2.1.1.1. Glass electrode…….……. 43
2.1.1.2. Cu^{2+} ISE electrode…….…… 44

2.1.2. Calorimetry……. 46
2.2. Macromolecular ligands……... 47
2.2.1. Synthetic polyelectrolytes…….…….. 47
2.2.1.1. Conductometric and potentiometric titrations…….... 48
2.2.1.2. Nuclear magnetic resonance (NMR)……...…….. 49
2.2.2. Humic acid…….…... 50
2.2.2.1. Introduction…….… 50
2.2.2.2. Isolation and purification of a humic acid sample…….. 51
2.2.2.3. Preparation of HA samples with different Fe contents….. 52
2.2.3. Algal biomass…….. 53
2.2.3.1. Introduction……. 53
2.2.3.2. Sampling…….… 54
2.2.3.3. Pretreatment……..... 54
2.2.3.4. Characterization…….. 55
2.3. References……. 59

CHAPTER 3. ACID-BASE EQUILIBRIA OF PHTHALIC ACID IN SALINE MEDIA: ION ASSOCIATION FROM PITZER EQUATIONS…… 63
3.1. Introduction……... 65
3.2. Experimental section……. 66
3.3. Theory…… 67
3.3.1. Pitzer treatment in the absence of ion-association…….…. 67
3.4. Results and discussion…….…. 70
3.4.1. Calculation of new interaction parameters……..… 75
3.5. Conclusions…….. 78
3.6. References…… 79

CHAPTER 4. ACID-BASE PROPERTIES OF SYNTHETIC POLYELECTROLYTES…… 83
4.1. Interaction of acrylic-maleic copolymers with H^+, Na^+, Mg^{2+}, and Ca^{2+}: thermodynamic parameters and their dependence on medium……..… 85
4.1.1. Introduction.....….. 85
4.1.2. Reagents……. 86

4.1.3. Equipments and Procedure..... 87
4.1.3.1. Potentiometric measurements..... 87
4.1.3.2. Calorimetric measurements..... 87
4.1.3.3. Procedure..... 88
4.1.4. Calculations..... 89
4.1.5. Results..... 91
4.1.5.1. Protonation constants..... 91
4.1.5.2. Formation constants of weak complexes..... 95
4.1.5.3. Alkaline earth metal complexes..... 98
4.1.5.4. Enthalpies and Entropies of protonation for PAM3..... 101
4.1.5.5. Literature comparison..... 103
4.1.6. Final remarks..... 105
4.1.7. References..... 107
4.2. Effect of the divalent cation on the proton binding equilibria of the polyacrylic acid in mixed 1-1/1-2 electrolyte solutions: A non-linear Poisson-Boltzmann study..... 111
4.2.1. Introduction..... 111
4.2.2. Theoretical background..... 112
4.2.2.1. Effect of the proportion of divalent cation at infinite polymer dilution in absence of specific metal binding..... 113
a. Surface charge / surface potential relationship and potential profile over distance..... 113
b. Calculation of counterion accumulation / coion exclusion..... 115
4.2.2.2. Coupling of the NLPB electrostatic model with proton/metal competitive isotherms 116
4.2.3. Experimental..... 117
4.2.4. Results and Discussion..... 119
4.2.4.1. NLPB simulations of the divalent cation effect at constant ionic strength, in absence of specific metal binding..... 119
4.2.4.2. Comparison with experimental data 127
4.2.4.3. Effect of the finite polymer concentration..... 129
4.2.4.4. Simulations of the influence of specific divalent cation binding 132
4.2.5. Conclusions and future work 135
4.2.6. References..... 136

CHAPTER 5. GIBBS-DONNAN AND SPECIFIC ION INTERACTION THEORY DESCRIPTIONS OF THE EFFECT OF IONIC STRENGTH ON PROTON DISSOCIATION OF ALGINIC ACID……..……. 139

5.1. Introduction……..…… 141

5.2. Models…….. 142

5.2.1 Gibbs-Donnan model for a weak acid polyelectrolyte…… 142

5.2.2. Application of a specific ion interaction theory (SIT)…… 146

5.3. Experimental……. 147

5.4. Results and discussion…….. 148

5.4.1. pK^* vs. α behaviour…… 148

5.4.2 Estimation of the amount of water associated with the polymer phase……. 151

5.4.3. Ionic strength dependence…….. 153

5.5. Conclusions…….. 157

5.6. References…… 157

CHAPTER 6. COMPLEXATION EQUILIBRIA IN HUMIC SUBSTANCES: EFFECT OF FE(III) ON THE BINDING OF CU(II) BY A HUMIC ACID SAMPLE……...……..… 163

6.1. Introduction……. 165

6.2. Experimental section…… 166

6.3. Theory……. 167

6.3.1. Humic Ion-Binding Model VI…….. 167

6.3.2. Solubility of Iron (Hydr)oxides…… 173

6.4. Results and discussion…… 174

6.5. Conclusions……. 175

6.6. References…… 176

CHAPTER 7. PROTON BINDING TO SEAWEED BIOMASS……. 179

7.1. Acid-base properties of brown seaweed biomass considered as a Donnan gel. A model reflecting electrostatic effects and chemical heterogeneity……..……... 181

7.1.1. Introduction…….. 182

7.1.2. Model…… 184

7.1.2.1. Estimation of the counterion activity in the gel phase…… 185

7.1.2.2. Estimation of ion activity coefficients……. 186
7.1.2.3. Calculation of the charge vs. pH curves…… 187
7.1.2.4. Estimation of the amount of water associated with the "active" gel phase……... 188
7.1.2.5. Description of the master curve with a proton binding isotherm…….. 190
7.1.2.6. Correction for electrostatically bound protons…….. 191
7.1.2.7. Data fitting……. 192
7.1.3. Materials and methods…… 192
7.1.3.1. Biomass……. 192
7.1.3.2. Experiments…….. 193
7.1.4. Results and discussion…… 194
7.1.4.1. Influence of systematic errors……... 194
7.1.4.2. Influence of activity coefficients……... 196
7.1.4.3. Parameter estimates. Swelling behavior…… 197
7.1.4.4. Intrinsic proton binding……. 202
7.1.5. References…….. 206

7.2. Surface charge and permeable gel descriptions of the ionic strength influence on proton binding to seaweed biomass……. 213
7.2.1. Introduction…… 213
7.2.2. Models…… 215
7.2.2.1. Donnan permeable gel…….. 216
7.2.2.2. Non-permeable planar surface…….. 218
7.2.2.3. Intrinsic heterogeneity…….. 219
7.2.3. Methodology…….. 220
7.2.4. Results and discussion…… 220
7.2.4.1. Analysis of the master curves……... 220
7.2.4.2. Analysis of the dependency of the apparent pK on I and α. 226
7.2.4.3. Consideration of activity coefficients……... 228
7.2.4.4. Consideration of electrostatically bound protons……. 229
7.2.5. Conclusions…… 229
7.2.6. References…….. 230

APPENDIX A. Study of acrylic-maleic copolymers. Supplementary data. 235

APPENDIX B. Numerical solution of the NLPB equation in mixed 1-1/1-2 electrolyte solutions. ……. 245

CHAPTER 1

Thermodynamic models for the description of the cation binding equilibria

1.1. Introduction. Complexing agents in aquatic systems.

The chemical compounds present in aqueous solution can be classified into two categories (Buffle, 1988):

(a) Species of fully characterized nature, structure and properties: hydrated inorganic cations, inorganic anions and simple organic components such as aminoacids, hydroxyacids, amines or simple carboxylic acids (acetic, benzoic, phthalic, etc).

(b) Species that cannot be fully isolated, but can be separated into groups of homologous compounds possessing operationally similar properties. These species are *polidisperse*, showing a more or less broad range of molecular weights and molecular compositions. As a consequence, they are usually characterized by average parameters. Examples of this category are humic substances, natural polysaccharides (e.g. alginic acid), synthetic polyelectrolytes (e.g. polyacrylic acid), colloidal particles, etc.

The study of macromolecular complexation shows significant differences with the study of the equilibria of simple ligands, due to the following reasons:

(a) Usually, a macromolecule has a relatively high number of complexing sites. Therefore, the number of chemical species involved in the system may become enormously large. For a system with n sites that can be alternatively protonated or not, the total number of species (not including possible different conformations or energy states) is 2^n. If we take into account that complex organic ligands may have up to hundreds or thousands of sites, we can understand why the description of the system is usually done in terms of a *distribution of species*.

(b) Even though the binding reaction takes place between the inorganic cation and each complexing site, several "secondary" effects may influence the overall complexation process in greater o lesser extent (Buffle, 1988):

- *Polyfunctionality*. The binding sites can be chemically heterogeneous in various ways: the coordinating groups may be of different type (carboxylic, fenolic, sulphonic, amino, etc), and/or they can show different electronic (aliphatic chains, aromatic rings) or steric environments.

- *Conformational changes*. The steric conformation of the complexants can vary with the chemical conditions of the medium, such as pH, ionic strength

or amount of complexed cation. For instance, linear polyelectrolytes may experiment conformational transitions depending on the degree of dissociation, as a consequence of the electrostatic repulsions among charged groups along the molecule chain (a classical example is the helix-coil transition of the poly(L-glutamic) acid (Nagasawa, 1971)). Colloidal aggregation processes and gel-sol transitions can also be included in this section.

- *Polyelectrolytic effect*. Many of the macromolecular complexing sites are often charged at a given pH, ionic strength, and cation concentration. Therefore, the macromolecules carry a high local charge concentration, which influences the stability of the complexes. We can consider, for instance, the particular case of proton dissociation from an initially uncharged polyprotic acid. As the dissociation proceeds, the net charge becomes progressively more negative, and therefore each proton experiences a larger net attractive Coulombic force than the previous one, which means that the apparent dissociation constant decreases, i.e. the polyacid becomes weaker.

The polyelectrolytic properties of macromolecules have a sizable effect on their acid-base and complexation properties. The high sensitivity of the charged polymeric molecules to ionic strength contrasts quantitatively with the behaviour of simple ligands. For instance, the maximum variation of the stoichiometric dissociation constant with ionic strength for monocarboxylic acids, in aqueous alkali chloride solutions between 0 and 3.5 $mol \cdot L^{-1}$, is typically ± 0.5 logarithmic units (Barriada *et al.*, 2000). On the other hand, the apparent dissociation constant of rigid polyelectrolytic gels may increase one pK unit for each tenfold decrease in ionic strength (Marinsky, 1987). Polyelectrolytes can even show a variation of a few pK units as the dissociation degree changes, at a low (constant) ionic strength (see an example below, in **Figure 1.2**).

An additional problem in the study of cation binding to organic matter is the competition among different cations. In general, a variety of different inorganic ionic species co-exist in natural systems. Therefore, two or more of these species may compete with each other for the same complexing site of the macromolecule or surface. Even in the simplest case, the study of the complexation of only one metal ion, the competition with protons is always present.

In general, the previous physicochemical effects are coupled, that is, they occur simultaneously. For instance, the competitive equilibria of two particular cations depend on the charge of the macromolecule (i.e., on the

proportion of ionised sites), and this, in turn, depends on the amount of bound cations. Nevertheless, it is generally assumed that, under certain conditions, the relative contribution of each effect can be accounted for by means of a suitable model, like in the conventional treatments of the polyelectrolytic effect by means of an electrostatic model in order to obtain a set of intrinsic binding constants (master curve) that only depend on the chemical heterogeneity.

For all these reasons, the study of macromolecular complexation equilibria is a challenging task from a theoretical and experimental point of view. Despite this fact, the study of complex organic ligands has an enormous interest in environmental sciences.

In first place, macromolecular substances occur in natural systems at a relatively high abundance. The concentration of dissolved organic matter in natural waters is typically in the range 1-100 mg of carbon per litre (dissolved organic carbon, DOC). Typical average values in freshwaters are: 1 $mg \cdot L^{-1}$ in ground and rainwater, 2-10 $mg \cdot L^{-1}$ in lakes and rivers, and 10-50 $mg \cdot L^{-1}$ in bogs and marshes; whereas in seawater DOC varies from 1 to 10 $mg \cdot L^{-1}$ (Morel and Hering, 1993). Most of this dissolved organic matter is poorly characterized. For example, in seawater, 50-90% of DOC cannot be identified and it is thus operationally classified as humic substances (Buffle, 1988). On the other hand, only 2-10 % of marine DOC has been identified as simple ligands (free amino acids and monosaccharides, urea, etc).

As regards the humic substances, these abundant and poorly defined natural organic components exert a ubiquitous chemical influence on the environment (Tipping, 2002). Among others, we can mention their important role in the binding and transport of heavy metals, which determines their geochemical cycles and bioavailability.

In the study of the macromolecular complexation it has also a great importance the knowledge of the acid-base and complexation properties of simple ligands. For instance, compounds such as malonate, phthalate, salicylate, etc. may represent model compounds for the coordinative properties of humic acids (Morel and Hering, 1993). In fact, the values of the metal binding constants of humic acids were proved to lie between those of these simple organic acids (Tipping *et al.*, 1988).

There is also an ongoing interest in the study of the acid-base and complexation properties of some materials of biological origin, oriented to their

practical application in wastewater treatment techniques. The process of passive (not metabolically mediated) retention of a species by means of an inert biological substrate is called *biosorption* (Volesky, 1990). In the last years a great number of studies have focused on the study of the sorptive properties of different materials such as seaweeds, which show a number of advantages with respect to other conventional techniques, namely, their low cost, high sorbing capacity and low environmental impact.

Apart from their interest as model compounds, some synthetic polyelectrolytes, such as polyacrylic and polymethacrylic acids, are also employed in wastewater treatment as flocculants or dispersants because of their complexing capabilities towards metal ions (De Stefano *et al.*, 2002).

1.2. Simple ligands

The description of the medium effect on the acid-base equilibria of low molecular weight ligands in electrolytic solutions has been thoroughly studied throughout the last decades (see for instance Sastre de Vicente (1997) and references therein).

The dependence of the pK values on the ionic strength is a function of the activity coefficients of the species involved (ions and neutral molecules). The simplest mathematical formulation of this fact is the equation:

$$K^T = K^* \cdot Q(\gamma_i) \tag{1.1}$$

where K^T is the thermodynamic equilibrium constant, K^* the stoichiometric constant, and $Q(\gamma_i)$ the ratio of activity coefficients of the species associated to the equilibrium. The goal of most of the studies regarding the ionic strength effect on stoichiometric constants is to model the $Q(\gamma_i)$ term. If an explicit equation for the activity coefficient dependence on the ionic medium composition is available, we can obtain a relationship like

$$pK^T = pK^* + f(I, \text{parameters}) \tag{1.2}$$

In general, it is assumed that the mean activity coefficient of an electrolyte consists of two contributions, namely: long-range (coulombian) interactions and short-range (specific) interactions. The first term is independent of the nature of the salt concerned, whereas the second is associated to the specific differences. As concentration approaches infinite dilution, the second factor becomes negligible, and it is the electrostatic force among charges the

only effect that determines the deviations from the ideal state. This limiting behaviour of the electrolyte solutions is described by the well-known Debye-Hückel equation (Bockris and Reddy, 1998):

$$\log \gamma_{\pm} = \frac{-A|z_{+}z_{-}|\sqrt{I}}{1+Ba\sqrt{I}} \tag{1.3}$$

where z_+ and z_- are the ionic charges, A and B are constants that depend on the solvent dielectric constant and temperature, and a is an ion size parameter.

In the mid 1930's, Guggenheim suggested the following general equation for a salt $M_{\nu+}X_{\nu-}$ in a mixed electrolyte solution:

$$\ln \gamma_{\pm} = \frac{-A'|z_{+}z_{-}|\sqrt{I}}{1+\sqrt{I}} + \frac{2\nu_{+}}{\nu_{+}+\nu_{-}}\sum_{a}\beta_{Ma}m_{a} + \frac{2\nu_{-}}{\nu_{+}+\nu_{-}}\sum_{c}\beta_{cX}m_{c} \tag{1.4}$$

where A'=2.303·A, the sums in a and c are over all anions and cations, respectively, m is the molality, and β_i are specific interaction coefficients that can be obtained from measurements on pure electrolytes. The first term in this equation corresponds to the Debye-Hückel expression for a value near 3 Å for the hard-core diameter. The following terms account for the deviations from the purely electrostatic behaviour. This model is the basis of the so-called *specific interaction theories* (Ciavatta, 1980).

Nevertheless, the β_i coefficients of the Guggenheim model show a non-negligible dependence on concentration, at moderate to high ionic strengths. This fact led Pitzer to a further elaboration of this general system, and, in the 1970's, he proposed a set of semi-empirical equations for pure and mixed electrolytes applicable over wide concentration ranges.

The general Pitzer expression for the single ion activity coefficient of the cation M in a mixed electrolyte solution is (Pitzer, 1991):

$$\begin{aligned}\ln \gamma_{M^{+}} &= z_M^2 f^{\gamma} + 2\sum_{a} m_a \left[B_{Ma} + \left(\sum mz\right)C_{Ma}\right] + 2\sum_{c} m_c \theta_{Mc} + \\ &+ \sum_{c}\sum_{a} m_c m_a \left(z_M^2 B'_{ca} + z_M C_{ca} + \psi_{Mca}\right) + \frac{1}{2}\sum_{a}\sum_{a'} m_a m_{a'}\left(z_M^2 \theta'_{aa'} + \psi_{Maa'}\right) + \\ &+ \frac{z_M^2}{2}\sum_{c}\sum_{c'} m_c m_{c'} \theta'_{cc'}\end{aligned} \tag{1.5}$$

where

- z_M is the ion charge.

- f^{γ} is a function of the ionic strength that includes the long-range electrostatic interactions:

$$f^{\gamma} = -A_{\phi}\left[\frac{\sqrt{I}}{1+1.2\sqrt{I}} + \frac{2}{1.2}\ln\left(1+1.2\sqrt{I}\right)\right] \qquad (1.6)$$

- A_{ϕ} is a Debye-Hückel like parameter that depends on the temperature, water density and water dielectric constant and it has a value of 0.391 ± 0.001 at 25ºC.

- B_{Ma} is a parameter that accounts for the binary interactions of the type M-M, M-a and a-a, and shows the following dependence on the ionic strength

$$B_{Ma} = \beta^{(0)}_{Ma} + \beta^{(1)}_{Ma} g\left(\alpha_1 I^{1/2}\right) \qquad (1.7)$$

with

$$g(x) = \frac{2\left[1-(1+x)\exp(-x)\right]}{x^2} \qquad (1.8)$$

where $\beta_{Ma}{}^{(0)}$ and $\beta_{Ma}{}^{(1)}$ are interaction coefficients with a constant value, characteristic of the salt Ma. B' is the ionic strength derivative of B.

Eq. (1.7), with α_1= 2 $kg^{1/2}\cdot mol^{-1/2}$, was found suitable for most types of electrolytes, but not for the 2-2 type salts, which show a strong electrostatic ion pairing effect that has usually been represented by considering the ion pair as a separate solute species. Nevertheless, a good agreement with experimental data was found without the introduction of this extra species in the equilibrium calculations (Pitzer, 1991), by simply adding another term in eq. (1.7):

$$B_{Ma} = \beta^{(0)}_{Ma} + \beta^{(1)}_{Ma} g\left(\alpha_1 I^{1/2}\right) + \beta^{(2)}_{Ma} g\left(\alpha_2 I^{1/2}\right) \qquad (1.9)$$

where now α_1=1.4 and α_2=12 (both in $kg^{1/2}\cdot mol^{-1/2}$). The $\beta^{(2)}$ coefficient is negative and, in the limit of low molality, it is related to the ion pair association constant K by $\beta^{(2)}$ = -K/2.

- C_{Ma} is a constant parameter related to the short-range triple interactions among ions of the same electrolyte (M-M-a and a-a-M).

- ψ, θ and θ' are mixing parameters (i.e., they only appear in mixed electrolyte solutions). θ is related to binary interactions between ions of the same sign (like M-M, M-c and c-c), θ' is its ionic strength derivative, and ψ takes into account the triple interactions among ions (such as M-c-a, M-M-a or c-c-a).

The situation is much simpler for uncharged species. It is usually accepted that the ion activity coefficient of a neutral solute is linearly proportional to the ionic strength (Pitzer, 1991), and the proportionality coefficient can be calculated from solubility data (Barriada *et al.*, 2001; Castro-Varela *et al.*, 2002).

The application of the Pitzer model to the acid-base equilibria of a simple dicarboxylic acid is discussed in greater detail in Chapter 3.

1.3. Polyelectrolytes

Introduction

For the sake of brevity, in the following we will mostly refer to the acid-base equilibria of polyacids. The extrapolation of the discussion to polybases and/or metal ion complexation reactions is formally straightforward.

The proton dissociation of an acid group in a macromolecule can be represented by the formal reaction

$$-\mathrm{AH} = -\mathrm{A}^- + \mathrm{H}^+ \tag{1.10}$$

For this reaction, a conventional dissociation constant, K_a, can be defined as

$$K_a = \frac{[-\mathrm{A}^-][\mathrm{H}^+]}{[-\mathrm{AH}]} \tag{1.11}$$

Note that analytical concentrations (denoted by square brackets) are used in eq. (1.11) rather than activities, and hence K_a is not a true thermodynamic dissociation constant, but an apparent constant. This equation can be written as

$$pK_a = pH - \log \frac{\alpha}{1-\alpha} \tag{1.12}$$

which is formally identical to the well-known Henderson-Hasselbach equation.

In eq. (1.12), α represents the degree of dissociation of the macromolecule, defined as

$$\alpha = \frac{\left[-A^-\right]}{\left[-A^-\right] + \left[-AH\right]} \tag{1.13}$$

In general, the value of pK_a is a function of pH, in contrast to what happens with simple ligands. In monofunctional polymers, the deviations from ideality are usually ascribed to electrostatic effects (apart from conformational effects). Therefore, we can consider two contributions to the overall standard free energy change of the dissociation process:

$$\Delta G_{diss} = \Delta G_{int} + \Delta G_{elec} \tag{1.14}$$

where ΔG_{int} represents the *chemical free energy* due to the reaction of the functional group itself and ΔG_{elec} represents the *coulombic free energy* due to the electrostatic interactions between the proton and the charges of the polyanion. For the calculation of ΔG_{elec}, we can consider a thermodynamic cycle involving the following steps (Tanford, 1961): discharge of the macromolecule, dissociation of the uncharged species and, finally, charge of the de-protonated macromolecule:

$$\begin{array}{lcll} AH^{(Q-1)-} & = & A^{Q-} + H^+ & \Delta G_{diss} \\ \downarrow & & \uparrow & \Delta G_{elec} \\ AH_{(discharged)} & = & A_{(discharged)} + H^+ & \Delta G_{int} \end{array} \tag{1.15}$$

where Q represents the overall charge of the macromolecule. Note that in eq. (1.15) the macromolecule is considered as a whole, whereas in eq. (1.10) only the dissociation reaction taking place at an acid site is considered.

The free energy change for the global discharge-charge process is then calculated as

$$\Delta G_{elec} = N_A \int_{-(Q-1)e}^{-Qe} \psi_0(q)dq \tag{1.16}$$

where $\psi_0(q)$ is the electrostatic potential at the reaction site. If Q >> 1 (that is, when the polyelectrolyte is not close to neutrality), it can be assumed that $\psi_0(q)$ remains approximately constant over the range of the integral, so that:

$$\Delta G_{electrostatic} = -F\psi_0 \tag{1.17}$$

The physical interpretation of eq. (1.17) is that it represents the work required to bring the small ion from the surface of the macromolecule to an infinite distance (bulk solution).

Consider the conditional equilibrium constant for the overall dissociation reaction of the polyion, eq. (1.15):

$$K_a = \frac{\left[A^{Q-}\right]\left[H^+\right]}{\left[AH^{(Q-1)-}\right]} = \frac{\left(A^{Q-}\right)\left(H^+\right)}{\left(AH^{(Q-1)-}\right)}\frac{\gamma_{Q-1}}{\gamma_Q \cdot \gamma_H} = K_{int}\frac{\gamma_{Q-1}}{\gamma_Q \cdot \gamma_H} \tag{1.18}$$

We can define the ratio of polyion activity coefficients as an effective activity coefficient (Morel and Hering, 1993):

$$\ln \gamma_{eff} = \ln \frac{\gamma_Q}{\gamma_{Q-1}} = -\frac{F\psi_0}{RT} \tag{1.19}$$

Hence, we readily see that this term represents a "local" ion activity correction for the proton (actually, a Boltzmann factor):

$$K_{int} = \frac{\left[A^{Q-}\right]\left[H^+\right]}{\left[AH^{(Q-1)-}\right]}\gamma_{eff} \cdot \gamma_H = \frac{\left[A^{Q-}\right]\left(H^+\right)_0}{\left[AH^{(Q-1)-}\right]} \tag{1.20}$$

where

$$\left(H^+\right)_0 = \left[H^+\right]\gamma_H \exp\left(-\frac{e\psi_0}{k_B T}\right) \tag{1.21}$$

It must be pointed out, as discussed by Bartschat *et al.* (1992), an important difference with respect to the common formulation of activity coefficients for simple ligands, which is the reference state for the dissociation constant. Whereas for simple ligands the ion activity coefficients are referred to

zero ionic strength, for polyions it is usually adopted the condition where ψ_0 is zero as the reference state, which corresponds to the limit of high ionic strength or zero dissociation degree. This difference must be taken into account when the magnitude of the intrinsic binding constant is compared with thermodynamic constants of simple ligands. For example, polyacrylic acid has been reported to have an intrinsic pK value of 4.27 (Companys, 2003), whereas the thermodynamic value found in literature for acetic acid (that may be considered as the monomer analog) is 4.78 (Barriada *et al.*, 2000). The Debye-Hückel correction of the simple ligand constant for high ionic strength conditions is minus 0.19-0.52 log units (Bartschat *et al.*, 1992), which means that both values are in good agreement.

The separate consideration of electrostatic and intrinsic energy contributions, eq. (1.14), is the starting point of most treatments of the polyelectrolytic effects in macromolecules. Some of these models will be discussed in the following sections. Finally, section 1.3.4. summarizes a physicochemical approach to the description of the intrinsic chemical heterogeneity that is obtained once the Coulombic effects have been explicitly accounted for.

1.3.1. Empirical models

This section outlines the foundations and applications of two models widely used for the description of the dependence of the protonation constants of polyelectrolytes on the degree of dissociation: the modified Henderson-Hasselbach and Högfeldt equations. These models, although purely empirical, constitute a useful tool for summarizing in an accurate and convenient way the experimental thermodynamic information regarding the acid-base and complexation equilibria under different conditions (pH, ionic strength, temperature, etc). Some examples of their application found in the literature are also briefly reviewed.

1.3.1.1. Modified Henderson-Hasselbach equation

Already in the late 1940's, Katchalsky and coworkers found that the potentiometric behaviour of diluted solutions of polymeric acids can be formally described by two empirical constants, pK_m and n, by means of the following equation (Katchalsky and Spitnik, 1947):

$$pH = pK_m + n \log \frac{\alpha}{1-\alpha} \qquad (1.22)$$

where $pK_m = pK_a$ for $\alpha = 0.5$, and $n>1$. Both constants depend on the type of polyacid, but are almost independent of the molecular weight. They vary with ionic strength, n approaching 1 (the value for monomeric ligands) and pK_m decreasing to a limiting value for high ionic strengths.

This equation has been theoretically interpreted on the assumption that the deviation from the titration behavior of monobasic acids is due to the work expended in the removal of the hydrogen ion from the field of the ionized groups, as well as to the work performed by the polymer molecule on stretching by electrostatic forces. Two extreme models were assumed, a randomly kinked macromolecule or a highly stretched polymeric chain both carrying evenly distributed negative charges (Katchalsky and Gillis, 1949; Katchalsky *et al.*, 1954).

Figure 1.1 shows an example of the application of this equation to potentiometric data of polyacrylic acid (taken from the experimental results of Chapter 4).

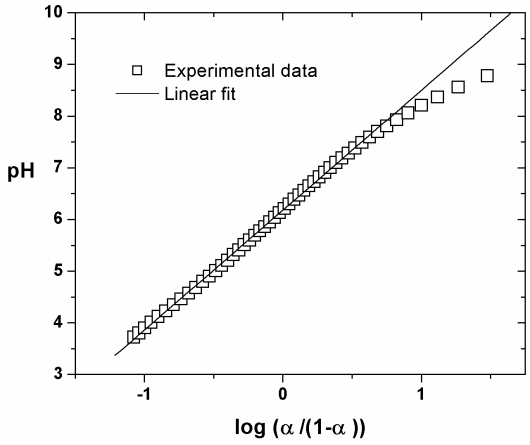

Figure 1.1 Potentiometric titration of polyacrylic acid in 0.01 M KNO_3. The line represents the fit to eq. (1.22).

By combining eqs. (1.12) and (1.22) the relationships between pK_a and α or pH can easily be obtained:

$$pK_a = pK_m - (n-1)\log\frac{\alpha}{1-\alpha} \tag{1.23}$$

$$pK_a = pK_m + \left(\frac{n-1}{n}\right)pH \tag{1.24}$$

which are formally identical to the empirical equations reported in the past by Kagawa and Kern, respectively, for polymonobasic acids (Nagasawa and Rice, 1960). Note that eq. (1.24) represents a linear relationship between pK_a and pH.

1.3.1.2. Högfeldt model

In the 1980's, a simple three-parameter model was proved useful in summarizing both thermodynamic and water uptake data for liquid and solid ion exchangers, both organic and inorganic (see Högfeldt, 1988), and references therein). The model was subsequently applicated to titration data of soluble linear polyelectrolytes, i.e. one-phase systems (Högfeldt *et al.*, 1989).

Following the Guggenheim's zero approximation, it can be assumed that any extensive thermodynamic property Y in a binary mixture of A and B (for instance, the acid and salt forms of a polyelectrolyte) can be described by

$$Y = y_A\chi_A^2 + y_B\chi_B^2 + 2y_m\chi_A\chi_B \tag{1.25}$$

where y_A and y_B correspond to the quantity Y for the pure forms, y_m refers to the mixture, and χ_i is the mole fraction of i.

Analogously, the Högfeldt model approximates the experimental function $pK_a = f(\alpha)$ to a cubic function involving three empirical constants, pK_1, pK_0 and pK_m:

$$pK_a = pK_1\alpha^2 + pK_0(1-\alpha)^2 + 2pK_m\alpha(1-\alpha) \tag{1.26}$$

where pK_1 and pK_0 are the limiting values of pK_a for $\alpha = 1$ and $\alpha = 0$, respectively. Recall that, in contrast with this model, in the Katchalsky model the pK_a is not defined for the limiting values $\alpha = 1$ and $\alpha = 0$.

The integral free energy of the dissociation reaction can be associated to the average equilibrium constant, pK_a, obtained from

$$\overline{pK}_a = \int_0^1 pK(\alpha)d\alpha = \frac{1}{3}[pK_1 + pK_0 + pK_m] \qquad (1.27)$$

A formal thermodynamic derivation of an equivalent model for ion exchange resins has been reported by Marton and Inczédy (1988), who interpreted the empirical coefficients in terms of the virial coefficients associated to pair and triplet interactions in the electrolyte mixture within the resin phase.

1.3.1.3. Application to synthetic polyelectrolytes

In the last few years, the protonation constants of different synthetic polyelectrolytes such as polyacrylic (PAA) and polymethacrylic (PMA) acids have been reported by Sammartano and cols. (Daniele *et al.*, 1999; De Stefano *et al.*, 2000; De Stefano *et al.*, 2003a) using the modified Henderson-Hasselbach and Högfeldt models. They analysed the influence of molecular weight, ionic strength and medium composition (in a variety of alkali metal chlorides and nitrates, tetraalkylammonium salts, artificial seawater (De Stefano *et al.*, 2002), etc.), the interaction with alkaline earth metal ions (De Stefano *et al.*, 2003b) and the dependence on temperature.

The variation of the apparent dissociation constant with the degree of dissociation was analysed using the models detailed above. The influence of the ionic strength on the model parameters was described by means of empirical functions of the square root of I. The differences found among the different media were interpreted in terms of complex formation. Their results led to the following considerations (De Stefano *et al.*, 2003a):

(a) A sharp difference is observed between the protonation constants obtained in alkali metal salts and in tetraalkylammonium salts. The general trend is $Et_4N^+ > Me_4N^+ >$ alkali metal cations.

(b) Among the alkali metal salts the general trend for pK_a is $K^+ \geq Na^+ > Li^+$.

(c) The influence of the anion of the supporting electrolyte is very small.

These authors have interpreted trends (a) and (b) in terms of a complexation model, in a similar way as with low molecular weight carboxylic acids (Daniele *et al.*, 1985). On the basis of the assumptions that carboxylic

groups form weak complexes with alkali metal ions and that tetraethylammonium salts do not significantly interact with carboxylic ligands (and, therefore, the protonation data in Et_4NI can be considered as a baseline), they estimated the conditional formation constants of the weak complexes with alkali metal cations. These constants are quite small, with values below 100 $mol^{-1} \cdot L$. Moreover, the differences in pK_a determined in the presence of different amounts of calcium and magnesium ions allowed the calculation of the conditional complex formation constants of the divalent metal complexes. The calculation details are described in the first part of Chapter 4.

The dependence on the molecular weight shows a slight increase of pK_a with N, the average number of monomer units in the polyelectrolyte (De Stefano *et al.*, 2003a). Measurements of PAA at different temperatures, in the range $15 \leq T/^{o}C \leq 55$, also showed a very small but constant increase of pK_a with T (De Stefano *et al.*, 2000).

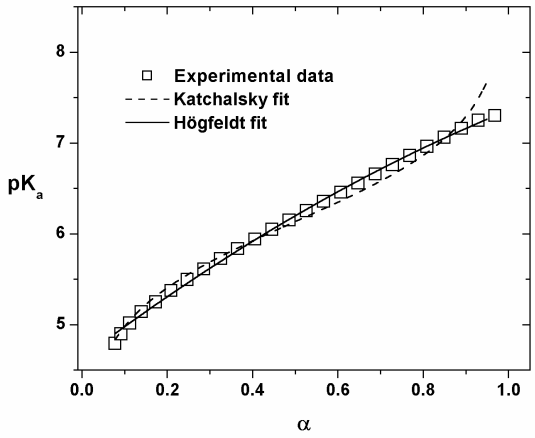

Figure 1.2. Comparison between Katchalsky and Högfeldt models applied to the potentiometric measurements of polyacrylic acid in 0.01M KNO_3.

With regard to the comparison between the modified Henderson-Hasselbach and Högfeldt models, these authors found that the latter usually shows a better fitting ability, specially at very low or high α values, where the former equation diverges. **Figure 1.2** shows some PAA titration data from Chapter 4 together with the fits to eqs. (1.23) and (1.26).

1.3.2. Two-phase equilibrium models: Donnan models

Despite the great utility of the previous models, they do not provide much insight into the physical chemistry of the cation-macromolecule binding equilibria. The empirical parameters are not straightforwardly related to the characteristic properties of the macromolecules, such as size or charge distribution. Another drawback of these simple models is that they do not include explicitly the electrostatic effect, which constitutes one of the most remarkable features of polyelectrolytic systems.

A Gibbs-Donnan concept has been proposed by Marinsky and coworkers (Marinsky, 1982; Marinsky, 1985; Marinsky *et al.*, 1985; Marinsky, 1987; Marinsky *et al.*, 1989; Marinsky and Reddy, 1991; Marinsky, 1992) for the interpretation of the counterion binding equilibria of polyelectrolytes. Initially this approach was applied to the description of ion distribution equilibria in ion exchangers (polyion gels). More recently, the concept was proved to be equally applicable for the description of water-soluble linear polyion-counterion binding systems. The formalism has also been applied to the study of less well-characterized polyelectrolytic systems, such as soil organic matter (Marinsky *et al.*, 1980; Marinsky and Reddy, 1984), humic and fulvic acids (Ephraim *et al.*, 1986; Ephraim and Marinsky, 1986; Marinsky and Ephraim, 1986) and natural polysaccharides (Lin and Marinsky, 1993). The basic concepts are also present in the electrostatic model of the NICCA-Donnan model (Benedetti *et al.*, 1996; Kinniburgh *et al.*, 1996) for humic substances. The details of the Gibbs-Donnan model and its main achievements have been reviewed by Miyajima (1995).

The Donnan model can be introduced in different ways. We will first review the thermodynamic derivation from the assumption of equilibrium between phases. An alternative derivation from the Poisson-Boltzmann equation will be discussed subsequently.

1.3.2.1. Permeable gels

The interpretation of the sensitivity of the potentiometric properties of a weakly acidic hydrophilic gel to the presence of a neutral salt MX, within the Donnan formalism, starts from the assumption of chemical equilibrium of the diffusible components between the aqueous and gel phases:

$$\overline{HX} + MX \equiv \overline{MX} + HX \qquad (1.28)$$

where the bar indicates the gel phase. From the expression of the respective chemical potentials, the following relationship can be obtained:

$$\ln\left(\frac{a_{HX}\,\bar{a}_{MX}}{\bar{a}_{HX}\,a_{MX}}\right)=\frac{\pi}{RT}\left(V_{HX}-V_{MX}\right) \tag{1.29}$$

where π is the osmotic pressure of water in the gel phase, V_i is the partial molar volume of the diffusible component i, and a_i its activity. In most gel systems, the right-side term of eq. (1.29) can be considered negligible (Marinsky, 1982), so this equation can be simplified to:

$$\frac{\bar{a}_H}{a_H}=\frac{\bar{a}_M}{a_M}=\lambda \tag{1.30}$$

The activity ratio λ is often referred to as the Donnan potential term. The substitution of eq. (1.30) into eq. (1.12) (the definition of pK_a) results in

$$pK_a=p\bar{a}_H-\log\frac{\alpha}{1-\alpha}-p\bar{a}_M+pa_M=p\bar{\bar{K}}_a+\log(\lambda) \tag{1.31}$$

where $p\bar{\bar{K}}_a$ is the intrinsic dissociation constant of the repeating acid group in the polymeric matrix of the gel. At least a slight variation of this intrinsic constant with α is usually observed, even in monofunctional (i.e., chemically homogeneous) gels. This variation is ascribed to a dependency of the activity coefficient of the dissociated functional group on the dissociation degree (the correction for deviation from ideality of the neutral group is considered negligible). The extrapolation of the pK_a - $\log(\lambda)$ vs. α curve to $\alpha = 0$ is assumed to yield the intrinsic pK of the monomer analog (Marinsky, 1985).

The Donnan term accounts for the free energy required to transfer the proton ions from the gel matrix intro the solution phase. Some assumptions must be considered for the calculation of this term: First, the titration process is modeled as an ion exchange equilibrium, i.e., for each proton ion transferred to the aqueous phase and neutralized, one counter ion enters the gel phase. As a consequence, this phase is considered electroneutral. Second, some extrathermodynamic assumptions are required in order to estimate the individual ion activity coefficients (see for instance Biesuz *et al.*, 2001). Third, the volume of the Donnan phase must be determined independently. And finally, the background salt invasion into the resin can be considered or not.

A rigorous thermodynamic formulation of the Donnan model, including the use of a specific ion interaction theory for the estimation of the activity coefficients leads to the following expression for the Donnan term in the molality scale (Biesuz *et al.*, 2001):

$$\lambda = \frac{\bar{\gamma}_M}{\gamma_{\pm(MX)}}\left(\frac{\bar{m}_{Me}}{2m_{MX}} + \sqrt{\left(\frac{\bar{m}_{Me}}{2m_{MX}}\right)^2 + \frac{\gamma^2_{\pm(MX)}}{\bar{\gamma}_M \bar{\gamma}_X}}\right) \qquad (1.32)$$

where $\bar{m}_{Me} = Q/\bar{m}_W$ is the molality (in the gel phase) of the counterion sorbed via ion exchange (Q and $\bar{m}_W$ represent the amounts of neutralized groups and water in the gel phase, respectively), and m_{MX} is the molality of the supporting salt in the bulk solution (equal to the ionic strength, for a 1:1 electrolyte). This equation can be easily derived from eq. (1.30) and considerations of mass and charge balance (see Chapter 7).

Some of the above mentioned assumptions will now be briefly analysed:

The considerations about the ion activity coefficients in the gel phase can be avoided, by introducing the following simplifications (Miyajima, 1995):

$$\frac{\gamma_H}{\bar{\gamma}_H}\frac{\bar{\gamma}_M}{\gamma_M} \approx 1 \quad \text{and} \quad \frac{\gamma^2_{\pm MX}}{\bar{\gamma}_M \bar{\gamma}_X} \approx 1 \qquad (1.33)$$

There is some experimental evicence in the ion-exchange literature to support that, at least, $\bar{\gamma}_H \approx \bar{\gamma}_{Na}$ (Marinsky, 1985). The previous simplification leads to the following equation for the Donnan term (in this case the differences between molality and molarity have been neglected, and thus a *Donnan volume*, V_D, is used instead of $\bar{m}_W$):

$$\lambda' = \left(\frac{Q}{2V_D I} + \sqrt{\left(\frac{Q}{2V_D I}\right)^2 + 1}\right) \qquad (1.34)$$

where $\lambda' = \lambda \cdot \left(\gamma_H / \bar{\gamma}_H\right)$ and the pH is now in the concentration (rather than activity) scale.

Both model formulations (with and without explicit consideration of activity coefficients) have been employed in this thesis, and some discussion about the different results has also been given.

The standard formulation of Marinsky assumes that the salt invasion is negligible, and therefore the counterion concentration in the gel is given only by the ion-exchange process, which is equivalent to consider that $\lambda' = Q/(V_D I)$. This is valid for relatively high dissociation degrees and low ionic strengths (as can be easily deduced from eq. (1.34)). Under this assumption, it was shown (Marinsky, 1985) that pK_a should be a unique function of (pH+pX), when the gel is permeable and rigid (i.e., when the Donnan volume remains constant). In this case, an increase of ca. one log unit in pK_a per tenfold decrease of the ionic strength is observed. In fact, one of the main achievements of the Marinsky model has been the analysis of the water uptake properties of different gels, from synthetic ion exchange resins of various degrees of crosslinking (Miyajima, 1995) to natural organic colloids (Marinsky and Ephraim, 1986).

The assumption of electroneutrality in the gel phase is a key point in the Donnan formulation. In fact, it can be easily demonstrated that when this condition is imposed to the Poisson-Boltzmann equation for the calculation of the electric potential in a two-phase permeable system, a "step" function for the potential profile is obtained (Wonders *et al.*, 1997), which is the characteristic profile of an ideal Donnan system. Ohshima and cols. reported a more general (although approximate) solution of the Poisson-Boltzmann equation for a permeable polyelectrolytic layer that does not entail electroneutrality in the polymer phase (Ohshima, 1998a). From this result, it can be concluded that the Donnan potential step represents a good approximation to the actual potential profile if the particle radius and the polyelectrolyte layer thickness are much larger than κ^{-1} (the Debye-Hückel parameter) and the ionic strength is not too low (Ohshima and Ohki, 1985). See section 1.3.3.2. for further details.

1.3.2.2. Water-soluble linear polyelectrolytes

The fact that the pH response of linear polyelectrolytes in (macroscopically homogenous) solution to changes in the counterion concentration level mimics that of their crosslinked analogs led Marinsky to suggest that linear polyelectrolytes present a region in which counterions tend to concentrate just like they do in a resin (Marinsky *et al.*, 1989). Separate phase

properties can therefore be assigned to this counterion-concentrated zone to facilitate the analysis following the formalism developed for ion-exchange gels.

Two important issues must be pointed out here. First, the assumption of electroneutrality in the polymer phase does not hold any longer. Therefore, the calculation of the counterion concentration must be corrected to account for the fraction of ions that escape the polyelectrolyte domain, denoted by ϕ, the osmotic coefficient (fraction of counterions that contribute to the osmotic pressure). This parameter is usually determined in salt-free polymer solutions, and its use in background salt solutions is justified by the experimentally demonstrated additivity of the colligative properties of simple salt and polyelectrolye solutions (Katchalsky, 1971).

Second, the experimental determination of the volume of solvent uptake can only be made in the case of synthetic resins, and not in water-soluble polyions, whose effective polymer phase volume is not available by any straightforward experimental procedure (Miyajima, 1995). Instead, estimates of the hypothetical volume have to be calculated from the model, which requires the intrinsic constants to be known.

1.3.3. Theoretical models based on electrostatics

As shown in the introduction to section 1.3, the theoretical treatment of the potentiometric titration of polyelectrolytes having a uniform distribution of ionizable groups leads to the following expression for the pH of the solution (Katchalsky *et al.*, 1954; Nagasawa and Holtzer, 1964):

$$pH = pK_0 + \log\left(\frac{\alpha}{1-\alpha}\right) - \frac{1}{\ln 10}\frac{e\psi_0}{k_B T} \qquad (1.35)$$

where pK_0 is the intrinsic ionization constant, e is the elementary charge, ψ_0 the electrostatic potential at the point on the molecule from which the proton is removed, k_B the Boltzmann constant and T the temperature.

The value of ψ_0 is often estimated by solving the well-known Poisson-Boltzmann equation (Bartschat *et al.*, 1992; de Wit *et al.*, 1993; Schmitz, 1993; Lyklema, 1995; Ohshima, 1998a; Borkovec *et al.*, 2001; Deserno and Holm, 2001):

$$\nabla^2\psi(r) = -\frac{eN_A}{\varepsilon}\sum_i C_i z_i \exp\left[-\frac{z_i e\psi(r)}{k_B T}\right] \qquad (1.36)$$

where N_A is the Avogadro's number, ε is the bulk dielectric constant, z_i and C_i are the valence and molar concentration of the ionic species i at an infinite distance from the polymer, respectively. In the following sections, we will only consider, for simplicity, the case of symmetric electrolytes (with $|z_+| = |z_-|$). Note that the electrostatic potential ψ(r) entering Eq. (1.36) is an averaged or mean-field potential.

1.3.3.1. Linearised Poisson-Bolztmann equation (Debye-Hückel approximation)

Eq. (1.36) can be solved analytically for an infinite plane, leading to the Gouy-Chapman model (Lyklema, 1995). However, exact analytical solutions for sperical and cylindrical geometries are not available (Ohshima, 1998a; Ohshima, 1998b).

A simplification known as the Debye-Hückel approximation is often adopted. If the electrostatic potential is sufficiently low, i.e., if

$$\left|\frac{z_i e\psi}{k_B T}\right| << 1 \qquad (1.37)$$

then all but the first term in the Taylor expansion of the exponentials in eq. (1.36) can be neglected, and the so-called *linearised Poisson-Boltzmann* equation is obtained:

$$\nabla^2\psi(r) = \kappa^2\psi(r) \qquad (1.38)$$

where κ is the Debye-Hückel parameter:

$$\kappa^2 = \frac{N_A e^2 \sum C_i z_i^2}{\varepsilon k_B T} \qquad (1.39)$$

This equation is the basis for the derivation of the Debye-Hückel limiting law for small ions (Bockris and Reddy, 1998). It has also been used in the analysis of potentiometric titration data of macromolecules such as proteins (Tanford, 1961).

The solution of eq. (1.38) depends on the particular geometry and charge distribution of the system. For instance, for a solvent-impermeable spherical macromolecule of radius R, this equation leads to

$$\psi_0 = \frac{eZ}{4\pi\varepsilon}\left(\frac{1}{R} - \frac{\kappa}{1+\kappa a}\right) \tag{1.40}$$

being Z the net charge of the macromolecule, and a the distance of closest approach of the counterion to the macro-ion.

For long rod-like molecules of radius b and length L (and ignoring end-effects), the Debye-Hückel approximation leads to (Nagasawa and Holtzer, 1964):

$$\psi_0 = \frac{eZ}{2\pi\varepsilon L}\left[\frac{K_0(\kappa a)}{\kappa a K_1(\kappa a)} + \log\left(\frac{a}{b}\right)\right] \tag{1.41}$$

where $K_i(\kappa a)$ are modified Bessel functions of the second kind. It is worth mentioning here that eq. (1.41) is used in this thesis as a starting value for the numerical solution of the non-linear Poisson-Boltzmann equation in cylindrical geometry (see Chapter 4 and Appendix B).

For partially permeable spherical macro-ions and hollow cylinders, eq. (1.38) leads to more complicated solutions (see Tanford, 1961), all of which have in common with eqs. (1.40) and (1.41) to be linear functions of the macromolecular charge:

$$\psi_0 = 2wz_i Z \tag{1.42}$$

where w is a coefficient that depends on the macromolecular geometry, the ionic strength and the temperature, but it is independent of the average net charge of the macromolecule (Z). Combining this equation with eq. (1.35) and the definition of pK_a, we obtain a linear relationship between the apparent dissociation constant and the macromolecular charge. The slope of this linear function should be related to w. In practice, however, deviations from this ideal behaviour are often observed (Nagasawa and Holtzer, 1964). For instance, the plots of pK_a vs Z may be nonlinear, indicating either a variation of the macromolecular geometry with charge (due to conformational effects) or an extrapolation of the Debye-Hückel approximation beyond the point where it is actually valid. In fact, as remarked by Nagasawa and Holtzer, this theory should not be used in those cases where ΔpK (the difference between pK_a and pK_0) is greater than 0.434 (which corresponds to $e\psi_0/k_BT = 1$).

Despite this, the use of eq. (1.42) is widespread in the environmental literature. For instance, an analogous equation is used in Models V and VI of

Tipping and cols. (Tipping *et al.*, 1990; Tipping and Hurley, 1992; Tipping, 1994; Tipping, 1998) to account for the electrostatic effects in the study of humic substances (see Chapter 6).

1.3.3.2. Non-linear Poisson-Boltzmann equation (NLPB)

If the Poisson-Boltzmann model is to be applied to polyelectrolytes with large surface charge densities, we cannot assume that the potentials are small enough to justify the linearization step used in the Debye-Hückel theory.

Ohshima and cols. reported quite accurate analytical solutions of the non-linear Poisson-Boltzmann equation for solid spheres (Ohshima *et al.*, 1982) and cylinders (Ohshima, 1998b), as well as permeable planar layers (Ohshima and Ohki, 1985). The different models have been reviewed recently (Ohshima, 1998a). We will consider here one of these approximate solutions, due to its relevance for the description of the double layer in algal cell walls (Chapter 7). The analytical solution of the potential profile across a charged permeable membrane reported by Ohshima can be used to test the accuracy of the Donnan model applied to a model system representative of a cell wall (**Figure 1.3**).

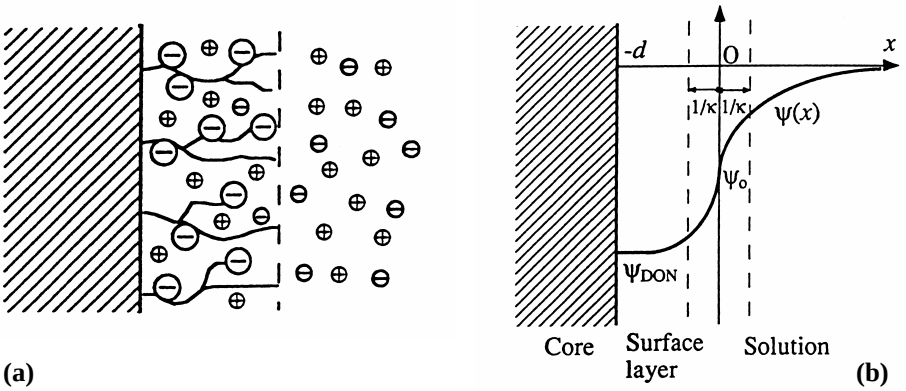

Figure 1.3. Charge distribution (a) and electric potential profile across a negatively charged polyelectrolyte layer (Ohshima, 1998a).

Consider a planar surface coated with an ion-penetrable layer of thickness d immersed in a 1-1 electrolyte solution of bulk concentration C. In the layer, membrane fixed charges are distributed at a density ρ_{fix}. In this model, the surface charge layer represents a separate phase into which the mobile ions

can diffuse (see **Figure 1.3**). The formulation of the Poisson-Boltzmann equation for the region -d < x < 0 is given by

$$\frac{d^2\psi(x)}{dx^2} = -\frac{eN_A}{\varepsilon}\left(\sum_i C_i z_i \exp\left[-\frac{z_i e\psi(x)}{k_B T}\right] + \rho_{fix}\right) \qquad (1.43)$$

whereas for x > 0, $\rho_{fix} = 0$.

If $d > \kappa^{-1}$ (the Debye length), the potential distribution inside the polyelectrolyte layer is given by the approximate expression (Ohshima, 1998a):

$$\psi(x) = \psi_{DON} + (\psi_0 - \psi_{DON}) \cdot \exp(-\kappa_m |x|) \qquad (1.44)$$

where ψ_0 is the potential at the surface, κ_m is an effective Debye-Hückel parameter that involves the contribution of the fixed charges, and ψ_{DON} is the Donnan potential:

$$\psi_{DON} = \frac{k_B T}{e} \operatorname{arcsin h}\left(\frac{\rho_{fix}}{2C}\right) = -\frac{k_B T}{e} \ln\left[\frac{\rho_{fix}}{2C} + \left(\left(\frac{\rho_{fix}}{2C}\right)^2 + 1\right)^{1/2}\right] \qquad (1.45)$$

which corresponds to the solution of (1.43) when electroneutrality is imposed, that is, when the following boundary condition is applied:

$$\sum_i C_i z_i \exp\left[-\frac{z_i e\psi(x)}{k_B T}\right] = -\rho_{fix} \quad \text{or} \quad \frac{d^2\psi(x)}{dx^2} = 0 \qquad (1.46)$$

It can be easily demonstrated that the exponential term in eq. (1.44) is negligible for large charge densities (ρ_{fix}), large layer thicknesses (d), and not too low ionic strengths.

Beyond these approximate analytical expressions, the exact solution of the NLPB equation requires the use of numerical tools (see Appendix B). In the last decades, numerical solutions of NLPB have been applied successfully in the study of synthetic polycarboxylic acids (Katchalsky, 1971; Nagasawa, 1971) and natural polyelectrolytes such as DNA (Anderson and Record, 1990; Sharp and Honig, 1990), humic substances (Bartschat *et al.*, 1992; de Wit *et al.*, 1993) and related compounds (Antelo *et al.*, 2003). The second part of Chapter 4 shows an analysis of the potentiometric behaviour of a synthetic polyelectrolyte by means of NLPB.

We can conclude that the Poisson-Boltzmann represents a relatively simple mean-field model that is able to interpret the electrostatic effects in most polyelectrolytes in terms of their geometry and charge distribution, allowing the description of the influence of macromolecular charge and medium ionic strength on the apparent ion binding constants.

1.3.4. Descriptions of the chemical heterogeneity

As a result of the presence of different reactive groups and/or different chemical and steric environments around a specific group, organic ligands often show a range of affinities for the inorganic ions. That is, the organic matter appears to be chemically heterogeneous. In the following, some of the procedures most usually adopted for the description of the chemical heterogeneity of natural complexing ligands are outlined.

1.3.4.1. Binding curve and average equilibrium function

In general, it is not possible to determine directly the concentration of each individual species involved in macromolecular complexation. In a solution containing a mixture of the ligand L and the cation M in equilibrium, the experimentally accessible information, in most of the cases, is the fraction of cation that remains free (uncomplexed) in solution and, by difference, the amount of cation bound (c_{ML}). Provided that the overall number of macromolecular sites ($c_{T,L}$) is known, we can calculate the coverage fraction of bound sites, θ, as (Buffle, 1988):

$$\theta = \frac{c_{ML}}{c_{T,L}} \tag{1.47}$$

For the particular case of proton binding reactions, we have $\theta = 1-\alpha$, where α is defined in eq. (1.13). The plot of θ vs. c_M (or log c_M) is called the *binding curve*.

An alternative way for summarizing experimental binding data is the *average equilibrium function*, K_C, which is operationally defined from the direct consideration of the following chemical process between formal species:

$$M + L \overset{K_c(c_M)}{\equiv} ML \tag{1.48}$$

so that (Buffle, 1988):

$$K_C(c_M) = \frac{c_{ML}}{c_M \cdot c_L} = \frac{1}{c_M}\frac{\theta}{1-\theta} \qquad (1.49)$$

Note that $K_C = 1/K_a$ for the particular case of proton ions, as defined in eq. (1.11).

In general, K_C is a function of the cation concentration, and it is constant only in the case of ideal complexation (Garcés, 1999). The use of K_C constitutes an analogy with the way in which thermodynamic equilibrium relations among true chemical species are expressed, applied to the formal reaction (1.48).

The microscopic interpretation of the average equilibrium function was analysed in some recent works (Garcés, 1999; Garcés *et al.*, 2002; Companys, 2003). It was shown that the macroscopic magnitude K_C represents the average of the microscopic stability constants of the sites that remain unoccupied (i.e., available) at a given free cation concentration, c_M. Thus, K_C provides a measure of the 'average affinity' of the global system as a function of the free cation concentration.

1.3.4.2. The affinity spectrum formalism

A widespread approach in environmental studies consists in assuming that the overall macromolecular coverage, θ, can be expressed as a weighted sum of local isotherms $f(c_M, k)$, each corresponding to a binding site (Buffle and Altmann, 1987; Nederlof *et al.*, 1990; Koopal *et al.*, 1994; Garcés *et al.*, 1998b):

$$\theta(c_M) = \int_0^\infty p(k) f(c_M, k)\, dk \qquad (1.50)$$

where the weighting term, p(k), is called the *affinity spectrum*. It represents the fraction of complexing sites with a value of the microscopic affinity constant between k and k+dk. Eq. (1.50) assumes that all the sites have the same local isotherm and that they do not interact. The local isotherm is most usually assumed to be a Langmuir isotherm:

$$\theta(c_M) = \int_0^\infty p(k)\frac{kc_M}{1+kc_M}\, dk = \int_{-\infty}^\infty p(\log k)\frac{1}{1+10^{-(\log k + \log c_M)}}\, d\log k \qquad (1.51)$$

For a discrete distribution of affinities, this integral is reduced to a summation.

Unfortunately, the inversion of this equation constitutes an ill-posed problem, i.e., small errors in the values of θ lead to large errors in the solution, p(k). Some authors suggested the use of simplified approximations of the local isotherm in order to obtain analytical solutions of eq. (1.51). This is the basis of the Local Isotherm Approximations (LIA) (see, for instance Nederlof *et al.*, 1990). The simplest of these methods is known as the condensation approximation (CA), which is based on replacing the local isotherm by a step function. Under this approximation, eq. (1.51) leads to

$$f_{CA}\left(\log k = -\log c_M\right) = \frac{d\theta(c_M)}{d\log c_M} \qquad (1.52)$$

However, the fact that the LIA methods require the calculation of the derivatives of the binding curve constitutes a serious drawback, due to the magnification of the experimental errors (Nederlof *et al.*, 1994).

Among the numerical methods designed to solve eq. (1.51) without requiring any approximation of the kernel, we can mention the linear regularization methods (Cerník *et al.*, 1995) or the maximum entropy formalism (Garcés *et al.*, 1998a).

Alternatively, the experimental binding curve data can be described by means of an arbitrary empirical isotherm, using a conventional fitting procedure. A great diversity of isotherms have been employed in the environmental literature so far. In a very recent work, Garcés *et al.* (2002) analysed the behaviour of some usual complexation isotherms with different underlying (symmetric) affinity spectra. The isotherms were rewritten in terms of the average, μ, and standard deviation, σ, of the affinity distribution function p(logk). It was shown that, for intermediate coverages, K_C essentially depends on the values of these two moments, being insensitive to the concrete shape of the affinity spectrum. This facilitates the direct comparison of the results obtained in studies where different isotherms are used to reproduce experimental data. On the contrary, for low macromolecular coverages, K_C strongly depends on the concrete isotherm, which warns against extrapolation of binding data obtained at intermediate concentrations to trace levels.

1.3.4.3. The master curve approach

As mentioned in the preceding sections, the binding of ions to natural organic matter is simultaneously influenced by coulombic interactions and chemical heterogeneity effects. As a result of the electrostatic effects, the experimental binding curve depends on the ionic strength. However, the assumption of eq. (1.14) allows the use of a suitable model in order to account explicitly for such electrostatic interactions. Ideally, if an appropriate electrostatic model is used, the dependence of the binding isotherms on ionic strength should vanish and the corrected isotherms will merge into a *master curve* (de Wit *et al.*, 1990), which is independent of the salt level. The above-mentioned descriptions of the intrinsic heterogeneity (e.g., the estimation of the proton affinity spectrum) can be applied to this master curve. The application of this formalism to experimental data of proton binding to seaweeds is shown in Chapter 7 and summarized in the scheme of **Figure 1.4.** Briefly, the experimental proton titration data (a) is transformed (through a charge balance) into a binding curve (b), which can be expressed as charge (Q), proton coverage (θ), dissociation degree, etc. versus pH. If the organic ligand is an acid (not amphoteric) substance initially in its fully protonated form, then the proton release from the sample (in equilibrium with an electrolyte solution) will correspond to the absolute charge (Q), otherwise a correction term is required (de Wit *et al.*, 1990). The set of charge curves obtained over a (preferably wide) range of ionic strengths (c) is used to optimize the parameters of the electrostatic model (Donnan volume, specific surface area, etc.). If the double-layer model is correct, the charge curves at different ionic strengths plotted versus pH_0, calculated from eq. (1.21), yield a single master curve (d), which can be used for the analysis of the intrinsic protonation parameters by means of an arbitary isotherm, by solving eq. (1.51) to obtain the affinity spectrum (e), etc.

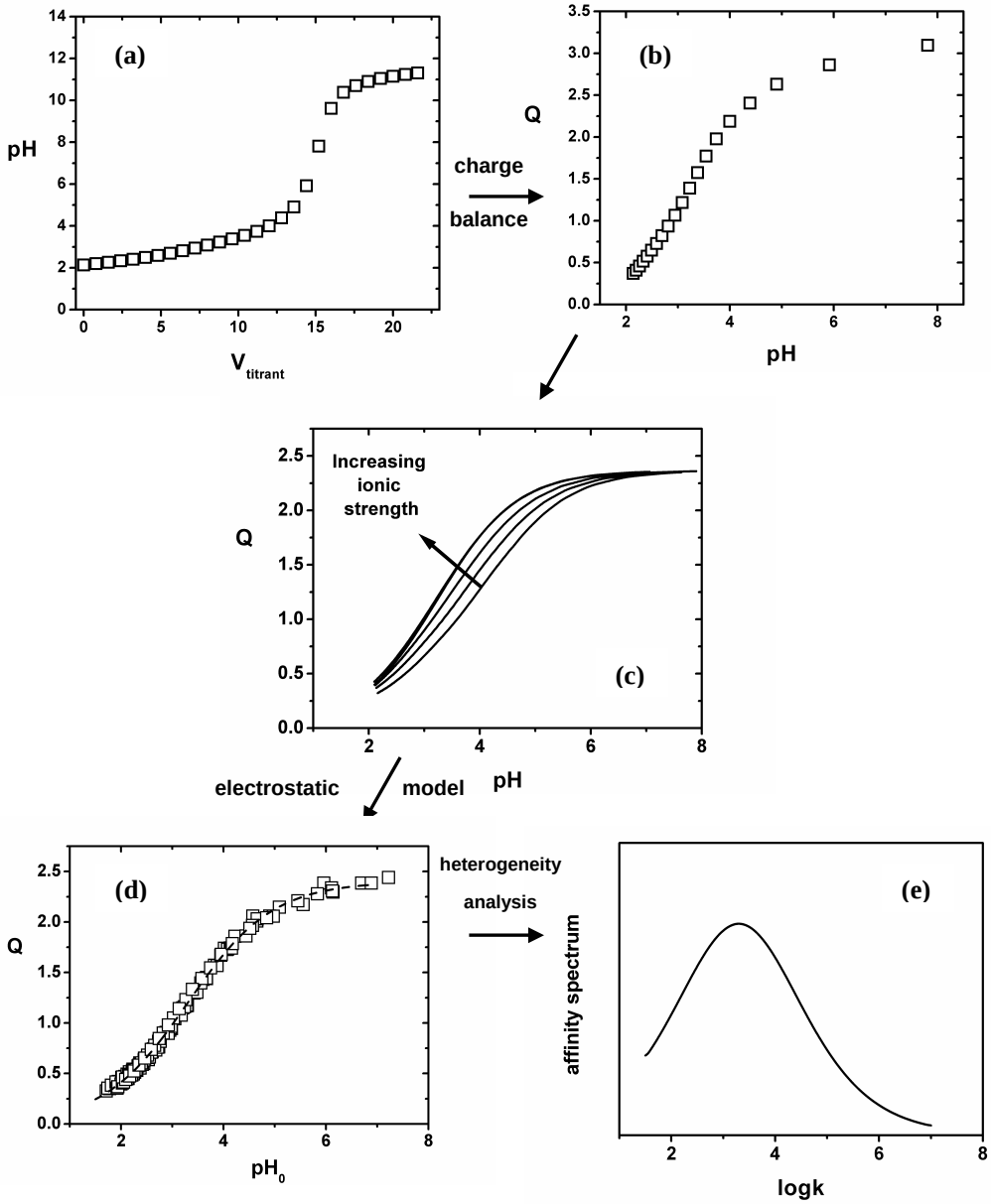

Figure 1.4. Schematic representation of the procedure for the analysis of proton titration data (adapted from de Wit *et al.* (1990), and Gondar (2003), using experimental data from Chapter 7).

1.4. Outline of this thesis

The aim of the present thesis is the study of the acid-base equilibria of natural and synthetic organic ligands, with a special emphasis on the analysis of the dependence on ionic strength and medium composition. In addition, other relevant aspects such as the influence of the intrinsic chemical heterogeneity, the complexation equilibria of metal ions (such as Ca^{2+}, Mg^{2+}, or Cu^{2+}), and competition effects among different cations are also discussed.

In most of the experimental work, the methodology used was the potentiometric titration with commercial combined glass electrodes, calibrated in proton concentration. This technique allows the direct measurement of the free proton concentrations in the aqueous phase, and therefore the estimation of the protonation constants of the different organic ligands. From the influence of the relative amount of other competing cations (such as alkaline earth cations) on the acid-base equilibria, an estimation of the metal binding properties towards these cations could be made. Other ion selective electrodes were also used, such as the Cu^{2+}-ISE for the study of copper complexation equilibria of humic substances. In some particular cases other instrumental techniques such as calorimetry were used for the characterization of the systems under study.

Some experimental details concerning the characterization of these systems and the analytical techniques are briefly discussed in Chapter 2. The subsequent chapters are dedicated to the different organic ligands studied, which are presented in order of increasing complexity, starting with phthalic acid, a simple dicarboxylic acid, and finishing with protonated marine algal biomass. All these chapters correspond to research papers already published or submitted for publication. In the former case, the chapter exactly matches the peer-reviewed definitive version of the manuscript and only minor changes (concerning fonts, spacing or section numbering) have been made in order to unify the format of this dissertation.

Chapter 3 is aimed to the description of the ionic strength dependence of the proton dissociation constants of a simple ligand, phthalic acid, in NaCl and $CaCl_2$, by means of Pitzer equations. This specific ion interaction theory accounted for the influence of the formation of Ca-phthalate weak complexes on the equilibrium constants, and removed the necessity for the introduction of an additional complex formation equilibrium.

Chapter 4 is devoted to synthetic polycarboxylic acids, and it is divided in two sections. The first one is a potentiometric and calorimetric study of the acid-base equilibria of two acrylic-maleic copolymers, using the modified Henderson-Hasselbach and Högfeldt equations. In this case, the differences in the protonation constants among different ionic media (Et_4NI, NaCl and mixtures NaCl /$CaCl_2$ or NaCl /$MgCl_2$) have been interpreted in terms of conditional formation constants for the Na^+, Mg^{2+} and Ca^{2+} complexes.

The second part of Chapter 4 consists of an analysis of the acid-base equilibria of polyacrylic acid in KNO_3/$Mg(NO_3)_2$ mixtures. In this case, the numerical solution of the nonlinear Poisson-Boltzmann for 1:1 and 1:2 electrolyte mixtures in cylindrical geometry was used to simulate the potentiometric behaviour of the polyacid. The Finite Element Method scheme for the numerical solution of NLPB was coupled with competitive isotherms in order to analyse the effect of the specific binding of the divalent cation. The theoretical predictions are compared with potentiometric titration data.

Chapter 5 deals with the study of the acid-base properties of a natural polysaccharide, alginic acid, in two different ionic media (NaCl and KNO_3). It was found that the ionic strength influences more markedly the apparent equilibrium constants than the degree of dissociation. The former effect was interpreted by means of a simplified Donnan model and an empirical equation resembling the typical specific ion interaction theory equations for simple ligands.

Chapter 6 summarizes an study of the complexation properties of a natural purified humic acid sample. The observed competition effects between Fe^{3+} and Cu^{2+} were satisfactorily described by the Humic Ion-Binding Model VI. The good simulation of the competition experiments supports the basic model assumption that metals share sites in humic matter.

Finally, Chapter 7 shows the results of a study of the proton binding equilibria of some acid-treated seaweed biomass samples, corresponding to algal species collected from the coasts of A Coruña. The first paper of this chapter consists in the application of a Donnan model with estimation of the activity coefficients for the empirical description of the experimental trends with ionic strength and dissociation degree. The second paper is aimed to the critical comparison between the Donnan and Gouy-Chapman models for the description of the acid-base data.

1.5. References

Anderson, C.F. and Record, M.T.J. 1990. Ion distributions around DNA and other cylindrical polyions: Theoretical descriptions and physical implications. *Annu. Rev. Biophys. Biophys. Chem*, **19**, 423-465.

Antelo, J., Lopez, R., Fiol, S., Antelo, J.M. and Arce, F. 2003. Study of the acid-base properties of fulvic acid-like substances extracted from senescent leaves of eucalyptus and oak. *Anal Bioanal Chem*, **375**, 523-526.

Barriada, J.L., Brandariz, I. and Sastre de Vicente, M.E. 2000. Acid-base equilibria of monocarboxylic acids in various saline media: analysis of data using Pitzer equations. *J. Chem. Eng. Data*, **45**, 1173-1178.

Barriada, J.L., Brandariz, I. and Sastre de Vicente, M.E. 2001. Salting coefficients of carboxylic acids in various saline media. *Ann. Chim.*, **91**, 615-625.

Bartschat, B.M., Cabaniss, S.E. and Morel, F.M.M. 1992. Oligoelectrolyte model for cation binding by humic substances. *Environ. Sci. Technol.*, **26**, 284-294.

Benedetti, M.F., van Riemsdijk, W.H. and Koopal, L.K. 1996. Humic substances considered as a Heterogeneous Donnan Gel Phase. *Environ. Sci. Technol.*, **30**, 1805-1813.

Biesuz, R., Zagorodni, A.A. and Muhammed, M. 2001. Estimation of Deprotonation Coefficients for Chelating Ion Exchange Resins. Comparison of Different Thermodynamic Models. *J. Phys. Chem. B*, **105**, 4721-4726.

Bockris, J.O. and Reddy, A.K.N. 1998. *Modern electrochemistry*, 2 edn. Plenum Press, New York.

Borkovec, M., Jönsson, B. and Koper, G.J.M. 2001. Ionization processes and proton binding in polyprotic systems: small molecules, proteins, interfaces, and polyelectrolytes. In: Matijevic, E. (ed.), *Surface and colloid science*, vol 16, pp. 99-399. Kluwer Academic / Plenum Press, New York.

Buffle, J. 1988. *Complexation reactions in aquatic systems: An analytical approach*. Ellis Horwood, Chichester.

Buffle, J. and Altmann, R.S. 1987. Interpretation of metal complexation by heterogeneous complexants. In: Stumm, W. (ed.), *Aquatic Surface Chemistry. Chemical Processes at the Particle-Water Interface.*, pp. 351-383. J. Wiley & Sons, New York.

Castro-Varela, R., Rey-Castro, C., Vilariño, T. and Sastre de Vicente, M.E. 2002. Potentiometric study of acetylsalicylic acid: solubility and acid-base equilibria in different saline media at 298 K. *J. Chem. Eng. Data*, **47**, 1432-1435.

Cerník, M., Borkovec, M. and Westall, J.C. 1995. Regularized least-squares methods for the calculation of discrete and continuous affinity distributions for heterogeneous sorbents. *Environ. Sci. Technol.*, **29**, 413-425.

Ciavatta, L. 1980. The specific interaction theory in evaluating ionic equilibria. *Ann. Chim.*, **70**, 551-567.

Companys, E. (2003) Speciation of heavy metals in macromolecular systems by electroanalytical techniques Departament de Química. Universitat de Lleida

Daniele, P.G., De Robertis, A., De Stefano, C., Sammartano, S. and Rigano, C. 1985. On the possibility of determining the thermodynamic parameters for the formation of weak complexes using a simple model for the dependence on ionic strength of activity coefficients: Na^+, K^+, and Ca^{2+} complexes of low molecular weight ligands in aqueous solution. *J. Chem. Soc. Dalton*, 2353-2361.

Daniele, P.G., De Stefano, C., Ginepro, M. and Sammartano, S. 1999. Salt effects on the protonation of polymethacrylate and Na^+, K^+, Ca^{2+} complex formation. *Fluid Phase Equilibr.*, **163**, 127-137.

De Stefano, C., Gianguzza, A., Piazzese, D. and Sammartano, S. 2000. Polyacrylate protonation in various aqueous ionic media at different temperatures and ionic strengths. *J. Chem. Eng. Data*, **45**, 876-881.

De Stefano, C., Gianguzza, A., Piazzese, D. and Sammartano, S. 2003a. Polyacrylates in aqueous solution. The dependence of protonation on molecular weigth, ionic medium and ionic strength. *React Funct Polym*, **55**, 9-20.

De Stefano, C., Gianguzza, A., Piazzese, D. and Sammartano, S. 2003b. Quantitative parameters for the sequestering capacity of polyacrylates towards alkaline earth metal ions. *Talanta*, **61**, 181-194.

De Stefano, C., Sammartano, S., Gianguzza, A. and Piazzese, D. 2002. Speciation of polyelectrolytes in natural fluids. Protonation and interaction of polymethacrylates with major components of seawater. *Talanta*, **58**, 405-417.

de Wit, J.C.M., van Riemsdijk, W.H. and Koopal, L.K. 1993. Proton binding to humic substances. 1. Electrostatic effects. *Environ. Sci. Technol.*, **27**, 2005-2014.

de Wit, J.C.M., van Riemsdijk, W.H., Nederlof, M.M., Kinniburgh, D.G. and Koopal, L.K. 1990. Analysis of ion binding on humic substances and the determination of intrinsic affinity distributions. *Anal. Chim. Acta*, **232**, 189-207.

Deserno, M. and Holm, C. 2001. Cell model and Poisson-Boltzmann theory: A brief introduction. *NATO Science Series, II: Mathematics, Physics & Chemistry*, **46**, 27-52.

Ephraim, J., Alegret, S., Mathuthu, A., Bicking, M., Malcolm, R.L. and Marinsky, J.A. 1986. A united physicochemical description of the protonation and metal ion complexation equilibria of natural organic acids (humic and fulvic acids). 2. Influence of polyelectrolite properties and functional group heterogeneity on the protonation equilibria of fulvic acid. *Environ. Sci. Technol.*, **20**, 354-366.

Ephraim, J. and Marinsky, J.A. 1986. A united physicochemical description of the protonation and metal ion complexation equilibria of natural organic acids (humic and fulvic acids). 3. Influence of polyelectrolite properties and functional heterogeneity on the copper ion binding equilibria in an armadale horizons Bh fulvic acid sample. *Environ. Sci. Technol.*, **20**, 367-376.

Garcés, J.L. (1999) Contribuciones al estudio de la complejación macromolecular. Análisis termodinámico. Estudios de especiación de sistemas macromolécula-metal pesado mediante técnicas voltamperométricas Dep. de Química Física. Universitat de Barcelona

Garcés, J.L., Mas, F., Cecília, J., Companys, E., Galceran, J., Salvador, J. and Puy, J. 2002. Complexation isotherms in metal speciation studies at trace concentration levels. Voltammetric techniques in environmental samples. *Phys. Chem. Chem. Phys.*, **4**, 3764-3773.

Garcés, J.L., Mas, F. and Puy, J. 1998a. Application of maximum entropy formalism in the determination of the affinity spectrum in macromolecular complexation. *Environ. Sci. Technol.*, **32**, 539-548.

Garcés, J.L., Mas, F., Puy, J., Galceran, J. and Salvador, J. 1998b. Use of activity coefficients for bound and free sites to describe metal-macromolecule complexation. *J. Chem. Soc. Faraday Trans.*, **94**, 2783-2794.

Gondar, D. (2003) Estudio de la protonación y de la complejación metálica en sustancias húmicas extraídas de una turbera Departamento de Química Física. Santiago de Compostela

Högfeldt, E. 1988. A useful method for summarizing data in ion exchange. 4. Extension and application to weak acid and chelating resins. *J. Phys. Chem.*, **92**, 6475-6476.

Högfeldt, E., Miyajima, T., Marinsky, J.A. and Muhammed, M. 1989. Application of a simple three-parameter model to titration data for some linear polyelectrolytes. *Acta Chem. Scand.*, **43**, 496-499.

Katchalsky, A. 1971. Polyelectrolytes. *Pure & Appl. Chem.* , **26**, 327-373.

Katchalsky, A. and Gillis, J. 1949. Theory of the potentiometric titration of polymeric acids. *Rec. trav. chim.*, **68**, 879-897.

Katchalsky, A., Shavit, N. and Eisenberg, H. 1954. Dissociation of weak polymeric acids and bases. *J. Polym. Sci.*, **13**, 69-84.

Katchalsky, A. and Spitnik, P. 1947. Potentiometric titrations of polymethacrylic acid. *J. Polym. Sci.*, **2**, 432-446.

Kinniburgh, D.G., Milne, C.J., Benedetti, M.F., Pinheiro, J.P., Filius, J., Koopal, L.K. and van Riemsdijk, W.H. 1996. Metal ion binding by humic acid: application of the NICA-Donnan Model. *Environ. Sci. Technol.*, **30**, 1687-1698.

Koopal, L.K., van Riemsdijk, W.H. and de Wit, J.C.M. 1994. Analytical isotherm equations for multicomponent adsorption to heterogeneous surfaces. *J. Colloid Interf. Sci.*, **166**, 51-60.

Lin, F.G. and Marinsky, J.A. 1993. A Gibbs-Donnan-based interpretation of the effect of medium counterion concentration levels on the acid dissociation properties of alginic acid and chondroitin sulfate. *React. Polym.*, **19**, 27-45.

Lyklema, J. 1995. *Fundamentals of interface and colloid science*. vol II. Academic Press, London.

Marinsky, J.A. 1982. Complexation of copper(II) by a poly(methacrylic acid) gel. *J. Phys. Chem.*, **86**, 3318-3321.

Marinsky, J.A. 1985. An interpretation of the sensitivity of weakly acidic (basic) polyelectrolyte (cross-linked and linear) equilibria to excess neutral salt. *J. Phys. Chem.*, **89**, 5294-5302.

Marinsky, J.A. 1987. A two-phase model for the interpretation of proton and metal ion interaction with charged polyelectrolyte gels and their linear analogs. In: Stumm, W. (ed.), *Aquatic Surface Chemistry. Chemical Processes at the Particle-Water Interface.*, pp. 49-81. J. Wiley & Sons, New York.

Marinsky, J.A. 1992. A Gibbs-Donnan-based interpretation of the sensitivity of the measurable acid dissociation properties of poly(acrylic acid) to concentration levels of salt and polyelectrolyte. *J. Phys. Chem.*, **96**, 6484-6487.

Marinsky, J.A., Baldwin, R. and Reddy, M.M. 1985. Interpretation with a Donnan-based concept of the influence of simple salt concentration on the apparent binding of divalent ions to the polyelectrolytes polystyrenesulfonate and dextran sulfate. *J. Phys. Chem.*, **89**, 5303-5307.

Marinsky, J.A. and Ephraim, J. 1986. A unified physicochemical description of the protonation and metal ion complexation equilibria of natural organic acids (humic and fulvic acids). 1. Analysis of the influence of polyelectrolyte properties on protonation equilibria in ionic media: fundamental concepts. *Environ. Sci. Technol.*, **20**, 349-354.

Marinsky, J.A., Miyajima, T., Högfeldt, E. and Muhammed, M. 1989. Influence of counterion concentration on equilibria and conformational properties of linear weak-acid polyelectrolytes. *React. Polym.*, **11**, 291-300.

Marinsky, J.A. and Reddy, M.M. 1984. Proton and metal ion binding to natural organic polyelectrolytes. II. Preliminary investigation with a peat and a humic acid. *Org. Geochem.*, **7**, 215-221.

Marinsky, J.A. and Reddy, M.M. 1991. Employment of Gibbs-Donnan-based concepts for interpretation of the properties of linear polyelectrolyte solutions. *J. Phys. Chem.*, **95**, 10208-10214.

Marinsky, J.A., Wolf, A. and Bunzl, K. 1980. The binding of trace amounts of lead(II), copper(II), cadmium(II), zinc(II) and calcium(II) to soil organic matter. *Talanta*, **27**, 461-468.

Marton, A. and Inczédy, J. 1988. Application of the concentrated electrolyte solution model in the evaluation of ion exchange equilibria. *React. Polym.*, **7**, 101-109.

Miyajima, T. 1995. Evaluation of the electrostatic effect on metal ion - binding equilibria in negatively charged polyion systems. In: Marinsky, J.A. and Marcus, Y. (eds.), *Ion exchange and solvent extraction*, vol 12, pp. 275-351. Marcel Dekker, New York.

Morel, F.M.M. and Hering, J.G. 1993. *Principles and Applications of Aquatic Chemistry*. J. Wiley & Sons, New York.

Nagasawa, M. 1971. Potentiometric titration and conformation of synthetic and natural polyelectrolytes. *Pure & Appl. Chem.* , **26**, 519-536.

Nagasawa, M. and Holtzer, A. 1964. The use of the Debye-Hückel approximation in the analysis of protein potentiometric titration data. *J. Am. Chem. Soc.*, **86**, 531-538.

Nagasawa, M. and Rice, S.A. 1960. A chain model for polyelectrolytes. V. A study of the effects of local charge density. *J. Am. Chem. Soc.*, **82**, 5070-5076.

Nederlof, M.M., van Riemsdijk, W.H. and Koopal, L.K. 1990. Determination of adsorption affinity distributions: A general framework for methods related to local isotherm approximations. *J. Colloid Interf. Sci.*, **135**, 410-426.

Nederlof, M.M., van Riemsdijk, W.H. and Koopal, L.K. 1994. Heterogeneity analysis for binding data using an adapted smoothing spline technique. *Environ. Sci. Technol.*, **28**, 1037-1047.

Ohshima, H. 1998a. Electrical double layer. In: Ohshima, H. and Furusawa, K. (eds.), *Electrical phenomena at interfaces. Fundamentals, measurements, and applications*, pp. 1-18. Marcel Dekker, New York.

Ohshima, H. 1998b. Surface charge density / surface potential relationship for a cylindrical particle in an electrolyte solution. *J. Colloid Interf. Sci.*, **200**, 291-297.

Ohshima, H., Healy, T.W. and White, L.R. 1982. Accurate analytic expressions for the surface charge density / surface potential relationship and double-layer potential distribution for a spherical colloidal particle. *J. Colloid Interf. Sci.*, **90**, 17-26.

Ohshima, H. and Ohki, S. 1985. Donnan potential and surface potential of a charged membrane. *Biophys. J.*, **47**, 673-678.

Pitzer, K.S. 1991. Ion interaction approach: Theory and data correlation. In: Pitzer, K.S. (ed.), *Activity coefficients in electrolyte solutions*, pp. 75-153. CRC Press, Boca Raton, Florida.

Sastre de Vicente, M.E. 1997. Ionic strength effects on acid-base equilibria. A review. *Curr. Top. Solution Chem.*, **2**, 157-181.

Schmitz, K.S. 1993. *Macroions in solution and colloidal suspension*. VCH, New York.

Sharp, K.A. and Honig, B. 1990. Electrostatic interactions in macromolecules: Theory and applications. *Annu. Rev. Biophys. Biophys. Chem*, **19**, 301-332.

Tanford, C. 1961. *Physical Chemistry of macromolecules*. John Wiley & Sons, New York.

Tipping, E. 1994. WHAM. A chemical equilibrium model and computer code for waters, sediments and soils incorporating a discrete site/electrostatic model of ion-binding by humic substances. *Computers & Geosciences*, **20**, 973-1023.

Tipping, E. 1998. Humic ion-binding model VI: An improved description of the interactions of protons and metal ions with humic substances. *Aquat. Geochem.*, **4**, 3-48.

Tipping, E. 2002. *Cation binding by humic substances*. Cambridge University Press, Cambridge.

Tipping, E., Backes, C.A. and Hurley, M.A. 1988. The complexation of protons, aluminium and calcium by aquatic humic substances: a model incorporating binding-site heterogeneity and macroionic effects. *Wat. Res.*, **22**, 597-611.

Tipping, E. and Hurley, M.A. 1992. A unifying model of cation binding by humic substances. *Geochim. Cosmochim. Acta*, **56**, 3627-3641.

Tipping, E., Reddy, M.M. and Hurley, M.A. 1990. Modeling electrostatic and heterogeneity effects on proton dissociation from humic substances. *Environ. Sci. Technol.*, **24**, 1700-1705.

Volesky, B. 1990. *Biosorption of heavy metals*. CRC Press, Boca Raton, Florida.

Wonders, J.H.A.M., Van Leeuwen, H.P. and Lyklema, J. 1997. Metal- and proton-binding properties of a core-shell latex: interpretation in terms of colloid surface models. *Colloid Surf. A: Physicochem. Eng. Asp.*, **120**, 221-233.

CHAPTER 2

Experimental section

2.1. Analytical techniques

2.1.1. Potentiometry

The potentiometric techniques allow the direct experimental measurement of the activities of the ions under study. This information must be combined with the mass balances for the ligand and the proton/metal ion, and the electroneutrality condition, in order to determine the concentrations of all the species present in solution. In this way, the equilibrium stability constants can be readily calculated.

2.1.1.1. Glass electrode

Throughout this thesis, the glass electrode was used for the calculation of the acid/base constants of the different ligands. The electrodes were calibrated to obtain the relationship between the potential and the proton concentration in the system. This calibration procedure was carried out in terms of the proton concentration, rather than in activities, in order to avoid the errors inherent to the use of the pH scale (Arce *et al.*, 1986; Covington *et al.*, 1988).

The calibrations followed the procedure described by May *et al.* (1982). Assuming that the glass electrodes exhibit a Nernstian response, the relationship between the measured potential and the proton concentration is:

$$E = E^0 + s\log\left[H^+\right] \qquad (2.1)$$

where E is the measured potential, E^0 is the formal potential, and s (the Nernst slope) is 2.303RT/zF (59.16 and 29.58 mV for monovalent and divalent ions, respectively, at 298K).

The formal potential includes different contributions, such as the standard potentials of the internal and external Ag/AgCl electrodes, the liquid junction potential and the asymmetry potential of the glass membrane. It also includes the term $s\cdot\log\gamma_H$, which is a constant in the experimental conditions of the study (constant ionic medium). Thus, the formal potential is a function of the medium composition (see **Figure 2.1**), and therefore the calibrations have to be carried out at the same ionic strength as the ligand titrations. It is also advisable to perform a certain number of replicates at each ionic strength in order to check the stability and good performance of the electrodes (Brandariz, 1994; Barriada, 2000).

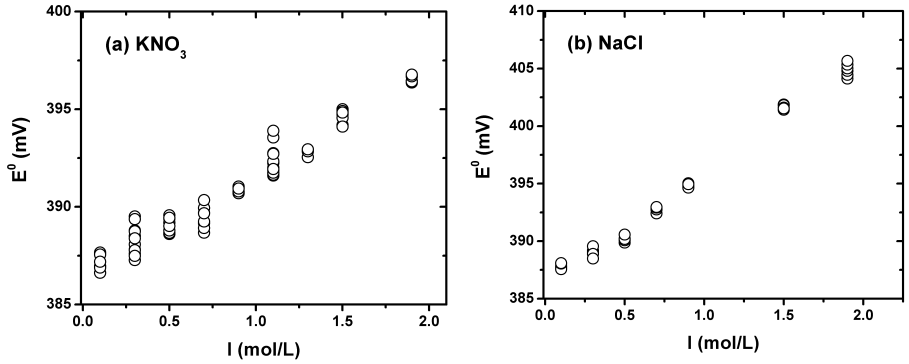

Figure 2.1. Values of the formal potential of a commercial combined glass electrode calibrated in aqueous solutions of KNO_3 and NaCl at 298K.

The typical setup for an acid/base potentiometric titration is represented schematically in **Figure 2.2**, and it basically consists of an automatic burette and a pH-meter interfaced to a PC running under DOS. The details of the equipments and procedures are described in the following Chapters.

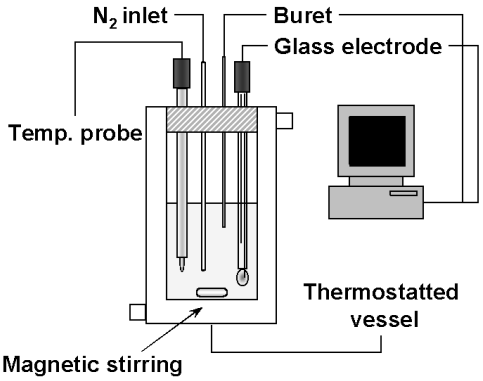

Figure 2.2. Experimental setup for a typical acid/base computer-controlled potentiometric titration.

2.1.1.2. Cu^{2+} ISE electrode

A study of the Cu^{2+} binding properties of a natural purified humic acid sample is described in Chapter 6. The copper concentrations in solution were measured potentiometrically using a sulfide-based solid-state ion selective electrode (ISE). The copper ISE was calibrated using concentration standards of

adjusted ionic strength, prepared by serial dilution of a 0.1000 mol/L standard stock solution of $Cu(NO_3)_2$, following the procedure of Bryan (2001). The electrode showed an accurate Nernstian response in the range 10^{-3}-10^{-6} M $Cu(NO_3)_2$ (see **Figure 2.3**).

In this work, an extension of the calibration using linear extrapolation (Fitch *et al.*, 1985) will be assumed. It was demonstrated that Cu ISE electrodes calibrated in well buffered solutions of organic ligands (such as ethylenediamine) show a linear response for copper activities as low as pCu 19 (Avdeef *et al.*, 1983). Other authors found a good agreement between the calculated copper activity values obtained from calibrations in buffered solutions and from extrapolations of unbuffered standards (Benedetti *et al.*, 1995; Bryan, 2001), and concluded that a linear calibration curve may be extended with confidence to lower copper concentrations in buffered solutions such as the humic solutions under study.

Furthermore, the calibration plots obtained immediately before and after the humic titrations were very reproducible (see **Figure 2.3**), which means that the performance of the Cu ISE was not irreversibly disturbed by the presence of the humic acid.

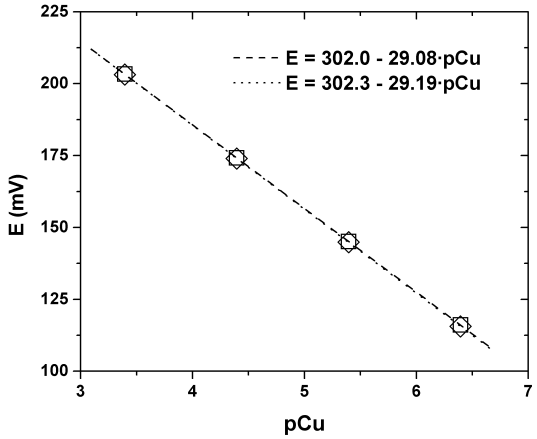

Figure 2.3. Cu^{2+} ISE calibration in KNO_3 0.1 mol/L at 20ºC, showing the performance of the electrode before (squares) and after (diamonds) the titration of a humic acid sample.

2.1.2. Calorimetry

Isoperibol titration calorimetry was used in this thesis for the experimental measurement of the protonation enthalpies of an acrylic-maleic copolymer (see Chapter 4). This technique is based on the continuous monitoring of the temperature in an adiabatic reaction vessel, which is immersed in a constant temperature bath, as a function of titrant added.

The analytical instrument used is illustrated in **Figure 2.4**. It consists of a temperature-controlled water bath that provides a constant temperature environment for the reaction vessel (a Dewar vessel) and a titrant-delivering automatic burette, which are mounted in an immersible holder. This insert assembly also holds a stirrer, a calibration heater and a thermistor. The assembly is inserted into the water bath during the experiments.

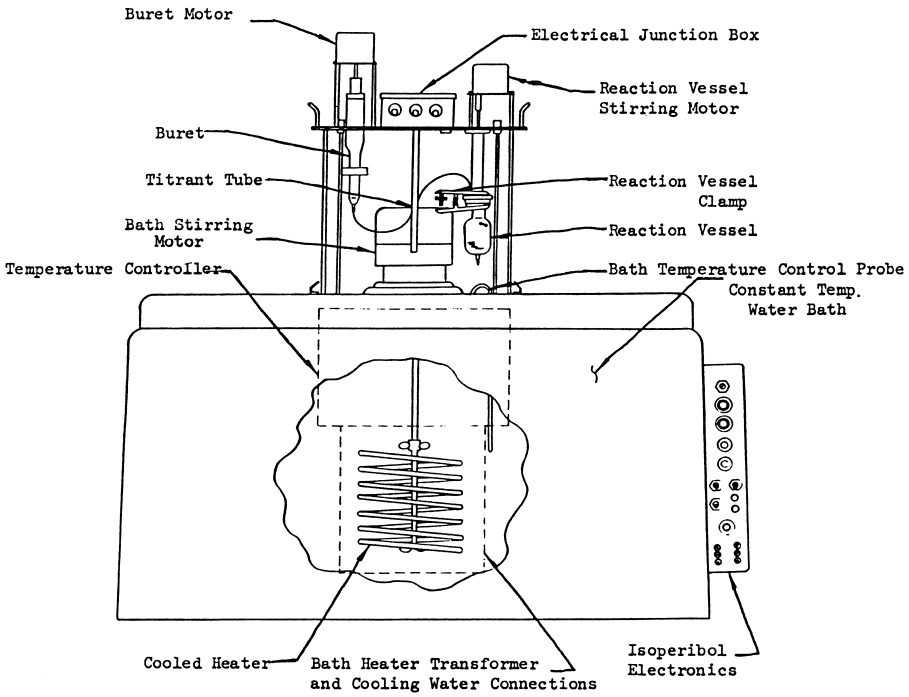

Figure 2.4. Scheme of the Tronac Model 450 isoperibolic titration calorimeter.

The thermistor continuously monitors the temperature inside the reaction vessel. The heat capacity of the reaction vessel and its content is accurately measured electrically by introducing a constant current through the resistance heater over a measured period of time. These calibration runs are performed immediately before and after each titration run.

The total energy change measured in the reaction vessel is the sum of different contributions. The heat of the reaction of interest for a given addition of titrant, $Q_{c,P}$, is determined by subtracting from the overall heat term, Q_p, the heat effects given by some correction terms (Grime, 1985; Marsh and O'Hare, 1994):

$$Q_{c,p} = \Delta H_i \Delta n_{i,p} = Q_p - Q_{NC,p} - Q_{TD,p} - Q_{D,p} - \sum \Delta H_r \Delta n_{r,p} \qquad (2.2)$$

where $\Delta n_{i,p}$ is the change in the moles of the product i formed since the beginning of the reaction to the considered point p, ΔH_i is the change in enthalpy for the reaction under study, $Q_{NC,p}$ is a non-chemical energy contribution associated with stirring of the solution, heat losses between the reaction vessel and its surroundings, etc., $Q_{TD,p}$ is due to temperature differences between titrant and titrate solutions, $Q_{D,p}$ is the heat of dilution of the titrant, and the last term represents the contributions from other reactions (such as the neutralization of H^+ and OH^-).

The $Q_{NC,p}$ and $Q_{TC,p}$ correction terms are estimated during a waiting period after and before each titration run. The heats of dilution were estimated at each ionic strength from titrations of the supporting electrolyte against the titrant solution.

2.2. Macromolecular ligands

2.2.1. Synthetic polyelectrolytes

A study of two different poly(acrylic-co-maleic) acids (PAM) is presented in Chapter 4. These polymers have average molecular weights of 3 kDa (PAM3) and 70 kDa (PAM70), and were purchased from Aldrich. Commercial PAM70 is in its sodium salt form, so an aqueous solution was passed through a Dowex 50 WX8 cation exchange resin (from Fluka) to obtain the pure acid form. PAM3 (50% w/v aqueous solution) was used without further purification.

The relevant information about the characterization of these systems was the total amount of functional groups, and the acrylic/maleic monomer ratio.

2.2.1.1. Conductometric and potentiometric titrations

The concentration of the polyacid samples (in terms of moles of acid groups per liter) was determined from potentiometric and conductometric titrations. In the latter case, aqueous solutions of PAM3 and PAM70 were prepared without supporting electrolyte and titrated against standard base solutions in glass vessels thermostatted at 25.0 ± 0.1 ºC with magnetic stirring and under nitrogen atmosphere. The conductivity was continuously monitored using a Knick Portamess conductimeter with a WTW TetraCon measuring cell. The results are shown in **Figure 2.5** and **Figure 2.6**.

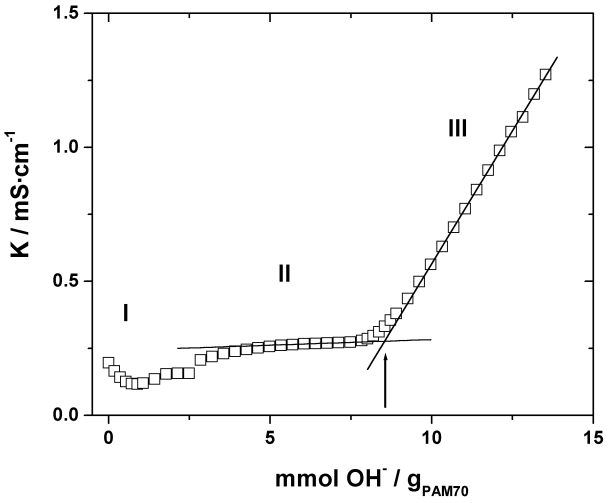

Figure 2.5. Conductometric titration of PAM70

Three different regions may be distinguished: an initial descending curve (I), typical of weak acids, due to the neutralization of free H^+; a very slow increase of the conductivity (II) owing to the increase in the concentration of negatively charged groups of the polymer and free counterions and, finally, an approximately linear part beyond the equivalence point (III), where the polymer is completely dissociated and the increase in conductivity is given by the strong base. The equivalence point can be determined as the intersection of segments II

and III. This equivalence point is in very good agreement with the value calculated from the potentiometric titrations (see **Figure 2.6**).

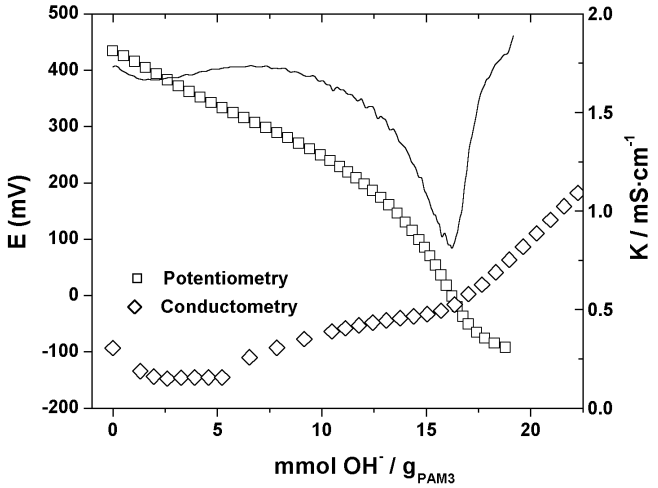

Figure 2.6. Conductometric and potentiometric titrations of PAM3. The line represents the first derivative of the potential.

It is very remarkable the fact that these polymers do not show the characteristic two-step neutralization curve typical of polymaleic acid and other copolymers of maleic acid (Chitanu *et al.*, 1999). This two-step behaviour has been explained as due to strong electrostatic correlations among neighboring functional groups (Minakata *et al.*, 1980; Kawaguchi *et al.*, 1990). For the case of the maleic-acrylic copolymers, this correlation seems to be much less significant.

2.2.1.2. Nuclear magnetic resonance (NMR)

The NMR technique can be used to estimate the relative concentration of the polymer functional groups (Chitanu *et al.*, 1999). The ^{1}H NMR spectrum of a sample of PAM3 is shown in **Figure 2.7**, as an example. The broad peaks centered at 0.8 and 1.2-2 ppm are assigned to the methylene (A) and methine protons, respectively. The integration of the latter peak yields the sum of the methine protons from the acrylic (B) and maleic (C) moieties. The acrylic/maleic monomer ratio was estimated from the relation:

$$\frac{\text{acrylic}}{\text{maleic}} = \frac{A}{C} = \frac{A}{(C+B) - A/2} = \frac{1}{1.2} \qquad (2.3)$$

Analogously, an acrylic/maleic ratio of 1.95/1 was estimated for PAM70.

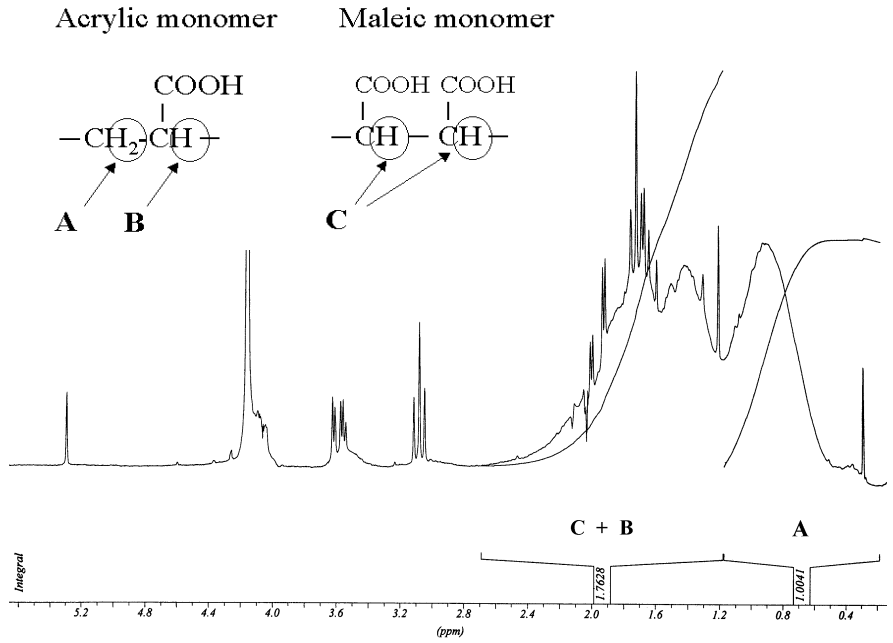

Figure 2.7. ^{1}H RMN spectrum of PAM70 in D_2O.

2.2.2. Humic acid

2.2.2.1. Introduction

Humic substances are complex, acidic organic molecules formed by the decomposition of plant, animal and microbial material. They are abundant and persistent in the biosphere and immediate subsurface, being present in particulate and dissolved forms in soils, waters and sediments (Tipping, 2002). The term *humic substances* covers a group of heterogeneous, polydisperse substances that are usually defined in an operational way, as a function of the isolation procedure (Stevenson, 1994). Traditionally, humic substances have been considered to comprise three main fractions, distinguished by their solubility and adsorption properties. Humic acids are soluble in base but

insoluble in acid, while fulvic acids (usually of lower molecular weight) are soluble in both base and acid (but are still sufficiently hydrophobic to be retained on acrylic-ester resins such as XAD-8). A third fraction, humin, is readily soluble in neither acid nor base.

Terrigenous humic compounds are usually close to 50% carbon by weight. Hydrogen contents of soil and freshwater samples centre around 5% (around 80% of which is generally bonded to carbon and the rest to oxygen). Oxygen contents are in the range 30-40%. Nitrogen and sulphur contents are quite low, though these elements are thought to play an important role in the creation of strong binding sites (Tipping, 2002). Although the detailed structure and conformation of the humic substances is, in general, complicated and ill-defined, these substances appear to contain reasonably simple and consistent functional groups for ion coordination: carboxyl, alcohol, and phenol (Buffle, 1988; Morel and Hering, 1993; Stevenson, 1994; Tipping, 2002). The total amount of titratable acid groups in humic substances is typically in the range of 10 to 20 $mmol \cdot g_C^{-1}$, of which 60-90% are considered to be carboxyl groups and the rest phenolic groups (Morel and Hering, 1993).

2.2.2.2. Isolation and purification of a humic acid sample

The procedure followed that of Swift (1996). One kilogram of moist upland peat was collected from a site in the Pennines (N. England, U.K), sieved, mixed with 1 litre of 0.1 M HCl and stirred overnight. The resulting suspension was centrifuged for 30 min at 4400g, and the supernatant discarded. The pellet was mixed with 2 litres of 0.15 M NaOH and stirred overnight under an atmosphere of N_2 in the dark. The basic soil suspension was centrifuged, the supernatant removed and acidified to pH~1 with 6 M HCl. The acid solution was stirred overnight, then centrifuged. The supernatant was discarded, and the pellet redissolved in 2.7 litres of 0.1 M KOH under N_2 in the dark. Then KCl was added to give a final K^+ concentration of approximately 0.3 M. The solution was centrifuged, the pellet discarded, and the humic acid re-precipitated with acid at pH 1. After centrifugation and removal of the supernatant, the solid was transferred to a 5 litre plastic beaker and stirred overnight with 2 litres of 0.1 M HCl / 0.3 M HF. The suspension was neutralised with 5 % (w/v) H_3BO_3 (AnalaR), and the resulting solution centrifuged. This process was repeated twice more. The humic acid product was slurried with water, placed in dialysis bags (Visking tubing size 9, MWCO 12000-14000, cleaned with hot $NaHCO_3$ and thoroughly rinsed with water), and dialysed against 0.1 M HNO_3 in the dark

at 10ºC, the outside solution being changed daily for 13 days. The final yield of humic acid was 34 g. Its ash content was 0.6%, and it contained 10.8 μmol $Fe \cdot g^{-1}$, as determined by microwave digestion with concentrated HNO_3 and measurement of iron with bathophrenanthroline in acetate buffer, after reduction with NH_2OH (Smith *et al.*, 1952). This material is referred to as HA-1. The iron content of the humic acid was diminished by repeated washing with 3 M HCl (Hering and Morel, 1988), to give a sample (HA-2) containing 3.8 μmol Fe g^{-1}.

2.2.2.3. Preparation of HA samples with different Fe contents

Two 70 cm^3 portions of HA-1 suspension (~23 g L^{-1}) in 0.1M HNO_3 were taken and mixed, while stirring thoroughly, with different amounts of a solution of 0.01M $Fe(NO_3)_3$/0.1M HNO_3. The mixtures were placed in separate dialysis bags, and dialysed against 4-litre volumes of 0.1M $NaNO_3/10^{-4}$ M HNO_3 (pH ~ 4) in the dark at 10ºC, with five changes of the outside-bag solution. Because the dialysis procedure brought about a gradual increase in pH from 1 to 4, the precipitation of ferric oxide colloids, which might have occurred if the iron salt was added immediately at pH 4, was assumed to have been avoided. The final ion activity products ($a_{Fe^{3+}}/a_{H^{+3}}$) were all appreciably lower than the solubility products of the iron oxide. The final preparations are referred to as HA-3 (14.4 μmol Fe g^{-1}) and HA-4 (35.9 μmol Fe g^{-1}). The metal content of the purified humic acid samples was determined by ICP-MS analysis of the samples after microwave digestion (see **Table 2.1**). In most cases, the metal amounts were below the detection limits.

Table 2.1. Metal contents of the humic acid samples, determined by ICP-MS ($\mu mol/g_{HA}$).

Sample	Mn	Ni	Cu	Zn	Cd	Pb
HA-1	<0.03	<0.02	0.36	0.15	<0.005	0.04
HA-2	<0.05	<0.02	0.30	0.02	<0.004	0.04
HA-3	<0.03	<0.02	0.35	0.06	<0.005	0.04
HA-4	<0.03	0.04	0.35	0.07	0.006	0.05

2.2.3. Algal biomass

2.2.3.1. Introduction

The algal division Phaeophyta (also known as brown algae) are an important assemblage of plants that are classified in about 265 genera with more than 1500 species (Lüning, 1990). They derive their characteristic colour from the large amounts of the carotenoid fucoxanthin (which yields a brown colour) contained in their chloroplasts and the presence of various tannins. They occur mainly in the marine environment, and flourish in temperate to subpolar regions where they exhibit the greatest diversity in species and morphological expression.

Biosorption in algae has mainly been attributed to the cell wall properties where both electrostatic attraction and complexation can play a role. The algal division Cryptophyta, for instance, does not have a cell wall, and it performs rather badly as heavy metal biosorbent. An excellent review on the biochemistry of biosorption by brown algae has recently been published by Davis *et al.* (2003).

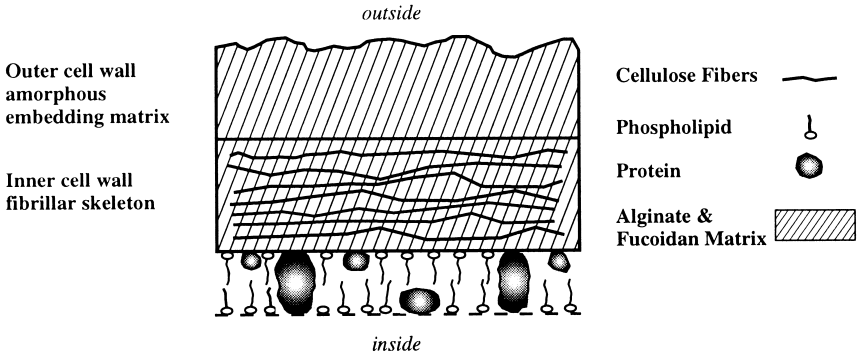

Figure 2.8. Cell wall structure in brown algae (Davis *et al.*, 2003).

The cell wall of brown algae is composed of at least two different layers. The innermost layer consists of a microfibrillar skeleton that imparts rigidity to the wall (**Figure 2.8**). The outer layer is an amorphous embedding matrix (Lobban and Harrison, 1994). Of these two components the latter is usually viewed as forming a para-crystalline matrix in which the former is embedded as a set of microfibrils. This inner and rigid fibrillar layer of brown algae is mainly comprised of the uncharged cellulose polymer. The main

components of the embedding matrix (also present in the mucilage or intercellular material) are alginic acid and fucoidan.

Alginic acid (**Figure 2.9**) is the common name given to a family of linear polysaccharides containing 1,4-linked β-D-mannuronic (M) and α-L-guluronic (G) acid residues arranged in a non-regular, blockwise order along the chain (Haug *et al.*, 1966). They can constitute between 10% and 40% of the dry weight of the algae (Percival and McDowell, 1967). Fucoidans are a group of branched polysaccharide sulfate esters with L-fucose 4-sulfate building blocks (predominantly α(1→2)-linked) as the major component, although they can also contain uronic acid residues. They are less abundant in brown algae than alginates, with dry mass percentages between 5 and 20 for some members of the family Laminariaceae.

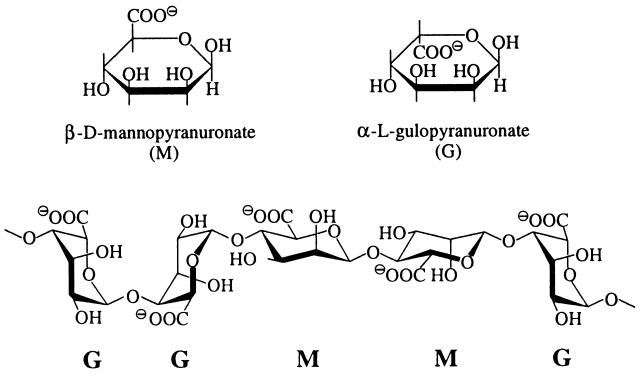

Figure 2.9. Structure of mannuronic and guluronic monomers and the alginate polymer (Davis *et al.*, 2003)

2.2.3.2. Sampling

The seaweed samples were collected in March 2001 and July 2002 from different sites along the coast near A Coruña.

2.2.3.3. Pretreatment

Immediately after collection, the seaweeds were washed with tap water and soaked in deionized water. The algae were then dried in an oven at 60º C, chopped manually and ground with an IKA M20 grinder. The ground material was sieved and the fraction between 500 μm and 1 mm was kept in polyethylene bottles at 4º C until needed.

In order to remove exchangeable cations and transform the biomass into the protonated form, the samples were acid treated before the experiments. The details of the procedure were taken from bibliography (Davis *et al.*, 2000). To do this, biomass suspensions comprised of 1 to 8 g of algae in HCl 0.1M at a 1:50 (weight/volume) ratio were shaken using a rotary shaker (Edmund Bühler model KS 15) at 175 rpm for 3 hours. Then, the biomass was filtered and the acid excess was removed by washing the samples with deionized water. The acid treatment was repeated using an algae/HCl 0.1M ratio of 1:200, and then the samples were soaked in deionized water and shaken for around 24h replacing the water as many times as needed until a constant conductivity measurement of the filtrate was attained (typically, below 10 $\mu S \cdot cm^{-1}$). Finally, the biomass was oven dried at 60ºC for at least 12 hours.

2.2.3.4. Characterization

- *Potentiometry*

The reagents and apparatus used are detailed elsewhere (see Chapter 7). The experimental procedure is essentially the same as described in section 2.1.

The electrode performance in the calibrations carried out between algae titrations has been satisfactory, with regression coefficients higher than 0.9999 in the interval 2<-Log[H+]<3 and satisfactory reproducibilities of the experimental slope and formal potential. This fact indicates that it does not seem to be a permanent interference of the biomass with the electrode (formation of insoluble deposits on the glass membrane or the junction that may modify the electrode nernstian response, for instance).

The potentiometric measurement of the activity of an ion in a heterogeneous system such as an aqueous solution in contact with a solid phase involves some problems due to the stirring rate effect, kinetic processes (intraparticle diffusion), etc. In addition, it is very important to ensure that the equilibrium conditions are reached before each measurement. For this purpose, a comparison between continuous and batch titrations was carried out.

For the batch titration, a set of biomass samples of around 0.2 g were accurately weighted and placed in 60 mL polyethylene bottles with 40mL of NaCl 0.05M and different volumes of acid and base. The bottles were shaken for 12 h in the rotary shaker (at 175 rpm) and then the suspensions were

consecutively transferred to a thermostatted cell at 25.0 ± 0.1 ºC with a combination glass electrode and a nitrogen stream.

For the continuous titration, 0.2 g of biomass were placed in the thermostatted cell, along with 40mL of background electrolyte solution, and the necessary amount of acid to get a initial pH of around 2. The suspension, magnetically stirred, was allowed to equilibrate until a constant potential reading was attained. Then successive amounts of titrant (a base solution of the same ionic strength) were added, and the potential measurements were recorded using a homemade software application, with the settings listed in **Table 2.2**.

Table 2.2. Characteristic settings for the potentiometric data acquisition.

Parameter	Value
delay after addition	180 s
number of consecutive readings (each 5 s)	5
max standard deviation of consecutive readings	0.5 mV
lapse between measurements	60 s
max variation in the lapse	0.5 mV

Figure 2.10 shows a comparison of the data obtained for S*argassum muticum* in 0.05 M NaCl. On the basis of these results we conclude that both methods lead to similar results.

The method of continuous titration was chosen, because it is quicker, it requires a smaller amount of biomass, it allows a better prevention of CO_2 absorption and thermostatting control, and it can be automated (as it does not require sample exchange between measurements).

On the other hand, continuous titrations take quite a long time (6-7 hours), as a result of the slow stabilization of the potential readings, especially near the equivalence point. Consequently, the small flow of saturated KCl through the liquid junction of the glass electrode might contaminate the sample. This source of contamination was proved to be negligible, even in such a long period of time, by measuring the KCl leak conductometrically (the average electrolyte flow rate, estimated in this way, was $2.5 \mu L \cdot h^{-1}$).

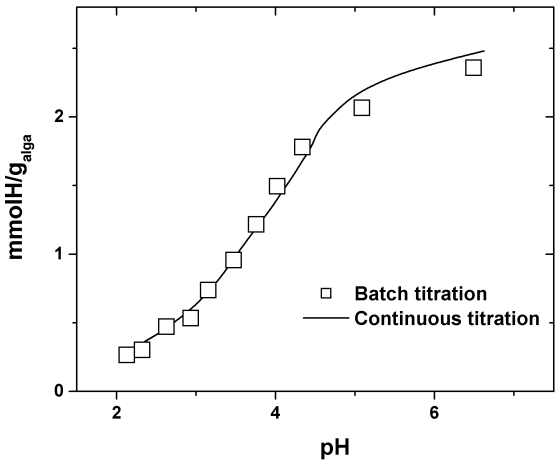

Figure 2.10. Comparison between continuous and batch titrations of *Sargassum muticum* biomass in NaCl 0.05M at 25º C.

The values of the maximum amount of acid groups, Q_{max} were estimated from the maximum of the first derivate of the glass electrode potential vs. titrant volume plots (see **Figure 2.11**). The values obtained were in the range from 2 to 3 mmol·g$^{-1}_{alga}$ (see Chapter 7).

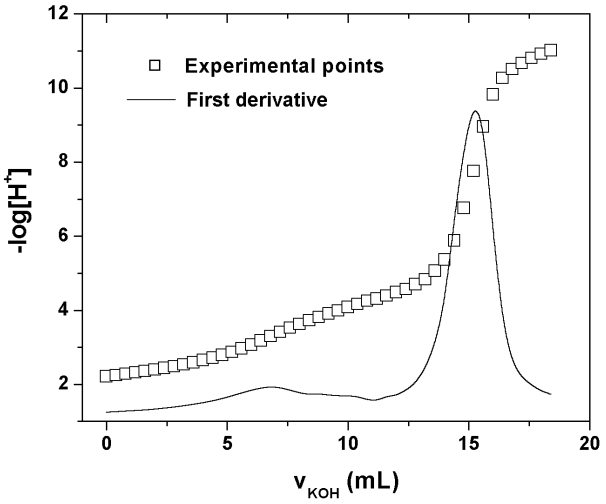

Figure 2.11. Potentiometric titration of a suspension of 0.2 g of *Saccorhiza polyschides* in 40 mL of KNO_3 0.05 M. The maximum of the derivate curve indicates the equivalence point used to estimate the maximum number of acid groups.

- *Conductometry*

Conductometric titrations of acid treated seaweed samples were performed by dispersing around 0.25 g biomass in 100mL of KNO_3 0.001M. The suspensions were titrated against standard $Ba(OH)_2$ solutions. The conductance was measured using a Crison microCM 2202 conductimeter. Potentiometric glass electrode measurements were made simultaneously.

Although in literature some authors (Fourest and Volesky, 1996) claim that the amount of strong acidic groups (identified as sulfonate groups from fucoidans) can be quantitatively estimated from the conductometric results, from our results it was not possible to distinct clearly between both kinds of groups (see **Figure 2.12**).

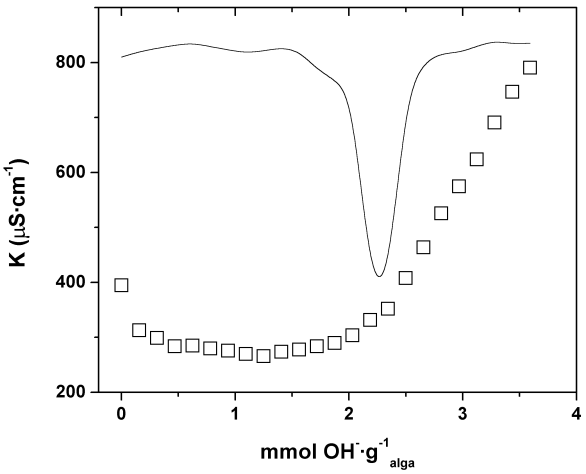

Figure 2.12. Conductometric titration of 0.25 g of *Sargassum muticum* in 0.001M KNO_3 with 0.05M $Ba(OH)_2$. The line represents the first derivative of the glass electrode potential (in arbitrary units).

2.5. References

Arce, F., Sastre de Vicente, M.E. and Santaballa, J.A. (1986). *Aspectos teórico-prácticos de la medida del pH*. Universidad de Santiago de Compostela.

Avdeef, A., Zabronsky, J. and Stuting, H. (1983). Calibration of copper ion selective electrode response to pCu 19. *Anal. Chem.*, **55**, 298-304.

Barriada, J.L. (2000). Equilibrio ácido-base de ácidos carboxílicos en medios salinos concentrados. PhD Thesis. Universidade da Coruña.

Benedetti, M.F., Milne, C.J., Kinniburgh, D.G., van Riemsdijk, W.H. and Koopal, L.K. (1995). Metal ion binding to humic substances: Application of the non-ideal competitive adsorption model. *Environ. Sci. Technol.*, **29**, 446-457.

Brandariz, I. (1994). Teorías de interacción iónica y equilibrio químico: estudio de la protonación de aminoácidos en medios salinos. PhD Thesis. Universidad de A Coruña.

Bryan, S.E. (2001). PhD Thesis. University of Lancaster.

Buffle, J. (1988). *Complexation reactions in aquatic systems: An analytical approach*. Ellis Horwood, Chichester.

Chitanu, G.C., Rinaudo, M., Desbrières, J., Milas, M. and Carpov, A. (1999). Behavior of nonalternating maleic acid copolymers in aqueous solution. *Langmuir*, **15**, 4150-4156.

Covington, A.K., Whalley, P.D., Davidson, W. and Whitfield, M. (1988). Measurement of pH in natural waters. In: West, T.S. and Nürnberg, H.W. (eds.), *The determination of trace metals in natural waters.* pp. 161-178. Blackwell Scientific Publications.

Davis, T.A., Volesky, B. and Mucci, A. (2003). A review of the biochemistry of heavy metal biosorption by brown algae. *Wat. Res.*, **37**, 4311-4330.

Davis, T.A., Volesky, B. and Vieira, R.H.S.F. (2000). Sargassum seaweed as biosorbent for heavy metals. *Wat. Res.*, **34**, 4270-4278.

Fitch, A., Stevenson, F.J. and Chen, Y. (1985). Complexation of Cu(II) with a soil humic acid: Response characteristics of the Cu(II) ion-selective electrode and ligand concentracion effects. *Org. Geochem.*, **9**, 109-116.

Fourest, E. and Volesky, B. (1996). Contribution of sulfonate groups and alginate to heavy metal biosorption by the dry biomass of sargassum fluitans. *Environ. Sci. Technol.*, **30**, 277-282.

Grime, J.K. (1985) Analytical solution calorimetry. J. Wiley, New York.

Haug, A., Larsen, B. and Smidsrod, O. (1966). A study of the constitution of alginic acid by partial acid hydrolysis. *Acta Chem. Scand.*, **20**, 183-190.

Hering, J.G. and Morel, F.M.M. (1988). Humic acid complexation of calcium and copper. *Environ. Sci. Technol.*, **22**, 1234-1237.

Kawaguchi, S., Kitano, T., Ito, K. and Minakata, A. (1990). Dissociation behaviour of poly(fumaric acid) and poly(maleic acid).2. Model calculation. *Macromolecules*, **23**, 731-738.

Lobban, C.S. and Harrison, P.J. (1994). *Seaweed ecology and physiology*. Cambridge University Press, Cambridge.

Lüning, K. (1990). *Seaweeds: their environment, biogeography, and ecophysiology*. John Wiley & Sons, New York.

Marsh, K.N. and O'Hare, P.A.G. (1994) Solution calorimetry. Blackwell Scientific, Oxford.

May, P.M., Williams, D.R., Linder, P.W. and Torrington, R.G. (1982). The use of glass electrodes for the determination of formation constants I. *Talanta*, **29**, 249-256.

Minakata, A., Matsumura, K., Sasaki, S. and Ohnuma, H. (1980). Potentiometric titration of copolymers of maleic acid. 1 A simple theory. *Macromolecules*, **13**, 1549-1553.

Morel, F.M.M. and Hering, J.G. (1993). *Principles and Applications of Aquatic Chemistry*. J. Wiley & Sons, New York.

Percival, E. and McDowell, R.H. (1967). *Chemistry and Enzymology of marine algal polysaccharides*. Academic Press, London.

Smith, G.F., McCurdy, W.H. and Diehl, H. (1952). The colorimetric determination of iron in raw and treated municipal water supplies by use of 4:7-diphenyl-1:10-phenanthroline. *Analyst*, **77**, 418-422.

Stevenson, F.J. (1994). *Humus chemistry. Genesis, composition, reactions*, 2nd edn. John Wiley & Sons, New York.

Swift, R.S. (1996). Organic matter characterization. In: Sparks, D.L. (ed.), *Methods of soil analysis. Part 3. Chemical methods*, pp. 1018-1020. Soil Scientific Society of America.

Tipping, E. (2002). *Cation binding by humic substances*. Cambridge University Press, Cambridge.

CHAPTER 3

Acid-base equilibria of phthalic acid in saline media: Ion association from Pitzer equations

Published in Talanta, 60 (2003) 93-101

3.1. Introduction

Carboxylic acids play a prominent role as acid-base functionalities in natural organic matter. As a result, the knowledge of the thermodynamics of their protonation reactions is an issue of great interest from the point of view of speciation studies in natural systems. For instance, carboxylic and phenolic groups have been reported to be the main functionalities responsible for the acid-base and metal complexation properties of humic substances (Perdue *et al.*, 1990). Among these functionalities, it has often been included the one consisting of two aromatic carboxylic groups in ortho relative position (Stevenson, 1994).

Phthalic acid has, in fact, been proposed as a simple model compound for the coordinative properties of humic acids. In particular, owing to its aromatic character, it would be more suitable for terrigenous humic substances in fresh or coastal waters, as they show a higher degree of aromaticity than humic matter from open oceans (Morel and Hering, 1993). Some attempts have also been made (Bryan *et al.*, 1997) to model the properties of humic matter using simple pre-defined metal binding sites (such as phthalic acid) by means of the so-called Random Molecular Model. Other authors (Tipping *et al.*, 1988) have compared metal binding constants of humic substances with those of simple organic acids like phthalic and salicylic acids.

Acid–base properties are known to be strongly affected by the nature and concentration of the ionic medium concerned (Daniele *et al.*, 1997; Sastre de Vicente, 1997). The knowledge of the ionic strength influence on the acid-base behaviour of simple organic compounds might contribute to a better understanding of the properties of complex substances such as natural organic matter.

One of the many problems in the study of the ionic strength dependence of equilibrium constants arises from the difficulty of making a difference between ionic interaction among components (including the background) and formation of complexes of small stability constant. The experimental estimation of the latter involves many practical and theoretical difficulties (Daniele *et al.*, 1985), namely the choice of a convenient background electrolyte, or alternatively the impossibility of assuming a constant ionic medium, the distinction between activity effects and formation of new species, the small alteration of the measured physical properties when weak complexes are

formed, etc. Implicitly, the comparison between specific interaction and ion association models lies beneath.

Traditionally, specific interaction models such as Pitzer model have been successful in describing the ionic strength dependence of carboxylic acids in weakly complexing background electrolytes such as alkali metal salts (Barriada *et al.*, 2000).

In this work, the protonation constants of phthalic acid in NaCl and $CaCl_2$ at 25ºC were determined potentiometrically, and the results were analyzed by means of Pitzer equations. Tabulated interaction parameters for the inorganic species involved (Pitzer, 1991) along with salting parameters estimated from published solubility measurements (Rivett and Rosenblum, 1914) allowed the calculation of the interaction parameters for the phthalate-Na^+/ Ca^{2+} systems, without assuming explicitly association between ions.

This alternative treatment represents a complementary point of view to the systematic studies on the estimation of stability constants of alkali and alkaline earth metal complexes of many carboxylic acids made by some authors (Daniele *et al.*, 1983; Daniele *et al.*, 1985; Daniele *et al.*, 1997).

Finally, the results were compared with data found in literature, and a discussion was made about the influence of the formation of weak complexes of phthalate on the determined acid-base equilibrium constants.

3.2. Experimental section

Carboxylic acid solutions were prepared from Carlo Erba p.a. potassium hydrogen phthalate. The HCl and NaOH standarized solutions used in the titrations were prepared from the corresponding Merck p.a. reagents.

NaCl and $CaCl_2$ (Merck p.a.) were used as background electrolytes to adjust the ionic strength (ranging from 0.1 to 2 mol/kg) of all solutions (except NaOH solutions for titrations in $CaCl_2$ where precipitation can occur at high pH values). Concentration of $CaCl_2$ was checked by alkalimetric titration with EDTA (Vogel *et al.*, 1989).

Titrations and calibrations were carried out in a glass cell furnished with a thermostating jacket at a temperature of 25.0 ± 0.1 ºC, passing a nitrogen stream through to remove dissolved O_2 and CO_2.

The titrating solutions were added from a Crison microBu 2031 automatic buret. Electromotive force measurements were made with a Crison micropH 2000 meter equipped with a Radiometer GK2401C combined glass membrane electrode (Ag/AgCl sat. as reference).

The glass electrodes were calibrated in terms of the proton concentration at a constant ionic strength following the procedure described elsewhere (Brandariz *et al.*, 1998). The calibrations were performed repeatedly for each ionic strength and electrolyte, yielding the formal potential and slope used in subsequent calculations. This procedure for the calibration of glass electrodes prior to the determination of equilibrium constants has been recommended by the IUPAC (Braibanti *et al.*, 1987).

Stoichiometric equilibrium constants were calculated from data obtained in the potentiometric titrations using the software SUPERQUAD (Gans *et al.*, 1985). Fitting of pK data to Pitzer equations was made using Origin 5.0 Professional (1997).

3.3. Theory

3.3.1. Pitzer treatment in the absence of ion-association

If we consider the proton-dissociation reactions of phthalic acid:

$$AH_2 \Leftrightarrow AH^- + H^+ \tag{3.1}$$

$$AH^- \Leftrightarrow A^{2-} + H^+ \tag{3.2}$$

The corresponding equilibrium constants will be given by:

$$K_1^T = \frac{(AH^-)(H^+)}{(AH_2)} = \frac{m_{AH^-} m_{H^+}}{m_{AH_2}} \frac{\gamma_{AH^-}\gamma_{H^+}}{\gamma_{AH_2}} = K_1^* \frac{\gamma_{AH^-}\gamma_{H^+}}{\gamma_{AH_2}} \tag{3.3}$$

$$K_2^T = \frac{(A^{2-})(H^+)}{(AH^-)} = \frac{m_{A^{2-}} m_{H^+}}{m_{AH^-}} \frac{\gamma_{A^{2-}}\gamma_{H^+}}{\gamma_{AH^-}} = K_2^* \frac{\gamma_{A^{2-}}\gamma_{H^+}}{\gamma_{AH^-}} \tag{3.4}$$

Where K^*_i, γ_j and m_j represent the i^{th} stoichiometric constant, the molal activity coefficients and the molal concentrations of species j. The substitution of the activity coefficients of the involved species by their expressions according to the Pitzer model (Pitzer, 1991) leads to the following equations:

$$\mathrm{p}K_1^* = \mathrm{p}K_1^T + 2f + \mathrm{A}_1 I + \mathrm{B}_1 g + 2\mathrm{C}h \tag{3.5}$$

$$\mathrm{p}K_2^* = \mathrm{p}K_2^T + 4f + \mathrm{A}_2 I + \mathrm{B}_2 g + 4\mathrm{C}h \tag{3.6}$$

where f, g and h are functions of the ionic strength (I):

$$f = -\frac{0.391}{\ln 10}\left[\frac{\sqrt{I}}{1+1.2\sqrt{I}} + \frac{2}{1.2}\ln\left(1+1.2\sqrt{I}\right)\right] \tag{3.7}$$

$$g = \left[1-\left(1+2\sqrt{I}\right)\exp\left(-2\sqrt{I}\right)\right] \tag{3.8}$$

$$h = I\exp\left(-2\sqrt{I}\right) \tag{3.9}$$

and A_i, B_i and C include the ionic interaction parameters β (**Table 3.1**).

Table 3.1. Coefficients of eqs. (3.5) and (3.6) as functions of Pitzer's β and λ interaction parameters (Pitzer, 1991).

	1:1 electrolyte	**1:2 electrolyte**
A_1	$\frac{2}{\ln 10}\left(\beta^{(0)}_{HX} + \beta^{(0)}_{AHC} - \lambda_{AH_2}\right)$	$\frac{2}{3\ln 10}\left(2\beta^{(0)}_{HX} + \beta^{(0)}_{AHC} - \lambda_{AH_2}\right)$
B_1	$\frac{1}{\ln 10}\left(\beta^{(1)}_{HX} + \beta^{(1)}_{AHC} - \beta^{(1)}_{XC}\right)$	$\frac{1}{3\ln 10}\left(2\beta^{1}_{HX} + \beta^{1}_{AHC} - \frac{2}{3}\beta^{1}_{XC}\right)$
A_2	$\frac{2}{\ln 10}\left(\beta^{(0)}_{HX} + \beta^{(0)}_{A^{2-}C} - \beta^{(0)}_{AHC}\right)$	$\frac{2}{3\ln 10}\left(2\beta^{(0)}_{HX} + \beta^{(0)}_{A^{2-}C} - \beta^{(0)}_{AHC}\right)$
B_2	$\frac{1}{\ln 10}\left(\beta^{(1)}_{HX} + \beta^{(1)}_{A^{2-}C} - \beta^{(1)}_{AHC} - 2\beta^{(1)}_{XC}\right)$	$\frac{1}{3\ln 10}\left(2\beta^{(1)}_{HX} + \beta^{(1)}_{A^{2-}C} - \beta^{(1)}_{AHC} - \frac{4}{3}\beta^{(1)}_{XC}\right)$
C	$\frac{1}{\ln 10}\beta^{(1)}_{XC}$	$\frac{2}{9\ln 10}\beta^{(1)}_{XC}$

The parameter $\beta^{(1)}_{XC}$ corresponds to the background electrolyte, and its value was tabulated for many compounds (**Table 3.2**).

Table 3.2. β interaction parameters for pure electrolytes at 25ºC (Pitzer, 1991).

Electrolyte	$\beta^{(0)}$	$\beta^{(1)}$
HCl	0.1775	0.2945
NaCl		0.2664
$CaCl_2$		1.614

Since the ionic strengths used were always lower than 2 mol Kg^{-1}, the mixing parameters (θ, Ψ) and the third virial coefficient (C^{ϕ}) of the general Pitzer model were discarded (Pitzer, 1973; Pitzer, 1991).

The coefficient λ_{AH_2} comes from the expression suggested by Pitzer for the activity coefficient of a neutral species (in a very low concentration) in an electrolyte solution of molality m_{el}:

$$\ln \gamma_{AH_2} = 2\lambda_{AH_2} m_{el} \tag{3.10}$$

It has been shown (Long and McDevit, 1952; Barriada *et al.*, 2001) that this coefficient can be calculated from solubility measurements in different electrolyte concentrations by means of the following equation:

$$\log \frac{S_0}{S} = \frac{2\lambda_{AH_2}}{2.303} m_{el} \tag{3.11}$$

where S_0 and S are the molal solubilities of the neutral species AH_2 in pure water and in the electrolyte solution, respectively.

The present model assumes electrolytes to be fully dissociated into ions and expresses their interactions in terms of coefficients that are generally functions of the ionic strength and various specific parameters. The notion of chemical equilibrium for the background electrolyte or for the interaction between background/acid-base couple is therefore avoided. However, as noted by Pitzer and Silvester (1976), for a weak acid the relevant equilibrium $A^- + H^+ = AH$ supersedes the binary virial interaction term between A^- and H^+. The consideration of ion association between species A^- and the background electrolyte, from Pitzer´s point of view, will be discussed in the next section.

3.4. Results and discussion

The equilibrium constants, initially obtained on the molarity scale (**Table 3.3**), were converted into molal units through the solution density (Lobo and Quaresma, 1989).

Table 3.3. Mean values of stoichiometric equilibrium constants of phthalic acid at 25ºC (molar scale), and standard deviation (SD) of a minimum of three replicates performed at each ionic strength.

NaCl					$CaCl_2$				
c_{el}(mol·L^{-1})	pK_1^*	SD	pK_2^*	SD	c_{el}(mol·L^{-1})	pK_1^*	SD	pK_2^*	SD
0.100	2.733	0.006	4.951	0.001	0.037	2.704	0.006	4.606	0.001
0.300	2.669	0.009	4.778	0.009	0.092	2.625	0.002	4.399	0.002
0.500	2.637	0.003	4.692	0.002	0.181	2.556	0.006	4.233	0.001
0.700	2.630	0.005	4.656	0.004	0.307	2.486	0.015	4.117	0.007
0.900	2.620	0.006	4.617	0.003	0.395	2.491	0.004	4.074	0.007
1.500	2.642	0.006	4.579	0.002	0.614	2.456	0.014	3.993	0.004
1.900	2.679	0.004	4.584	0.003					

Table 3.4 shows the pK^*_i values referred to the molal scale. The least-squares fitting of these values to equations (3.5) and (3.6) yielded the values of pK^T_i, A_i and B_i, which are listed in **Table 3.5** and **Table 3.6**. Experimental data and fitted curves are shown in **Figure 3.1** and **Figure 3.2**.

Table 3.4. Mean values of stoichiometric equilibrium constants of phthalic acid at 25ºC (molal scale). The standard deviations are the same as in **Table 3.3**.

NaCl			$CaCl_2$		
I(mol·Kg^{-1})	pK_1^*	pK_2^*	I(mol·Kg^{-1})	pK_1^*	pK_2^*
0.101	2.730	4.948	0.112	2.702	4.605
0.302	2.665	4.775	0.277	2.623	4.397
0.506	2.632	4.687	0.546	2.553	4.230
0.711	2.623	4.649	0.931	2.498	4.117
0.918	2.611	4.609	1.199	2.485	4.069
1.549	2.628	4.565	1.872	2.449	3.984
1.979	2.661	4.566			

Table 3.5. Parameter values obtained by fitting the pK^*_1 data to eq. (3.5). Standard errors are shown in brackets. σ^2 = Σ (Square residuals)/degrees of freedom. Some thermodynamic pK values found in literature are included for comparison.

Electrolyte	pK^T_1	A_1	B_1	$10^5\ \sigma^2$
NaCl	2.949 (0.008)	0.163 (0.011)	0.123 (0.032)	3
$CaCl_2$	2.942 (0.006)	0.088 (0.010)	0.041 (0.028)	2
(Martell and Smith, 1977)	2.950	-	-	-
(De Robertis *et al.*, 1990)	2.947	-	-	-

Table 3.6. Parameter values obtained by fitting the pK^*_2 data to eq. (3.6). Standard errors are shown in brackets. σ^2 = Σ (Square residuals)/degrees of freedom. Note that degrees of freedom are not the same in all fits.

Electrolyte	pK^T_2	A_2	B_2	B_2'	B_2''	$10^5\ \sigma^2$
NaCl	5.393 (0.006)	0.209 (0.009)	0.233 (0.026)	-	-	2
NaCl(*)	5.34 (0.11)	0.154 (0.025)	-0.2147	0.362 (0.053)	2.7 (4.5)	3
$CaCl_2$	5.108 (0.016)	0.206 (0.025)	-0.170 (0.071)	-	-	11
$CaCl_2$(*)	5.45 (0.16)	0.128 (0.033)	-0.3236	0.256 (0.066)	-13.8 (6.3)	4
$CaCl_2$(**)	5.41	0.134 (0.019)	-0.3236	0.242 (0.034)	-12.8 (0.3)	3
(Martell and Smith, 1977)	5.408	-	-	-	-	-
(De Robertis *et al.*, 1990)	5.410	-	-	-	-	-

(*) Data fitted to eq. (3.12), where B_2 has been previously estimated from B_1.

(**) The same fit as before, but using a fixed pK^T value taken from bibliography, so only parameters A_2, B_2'and B_2'' are fitted.

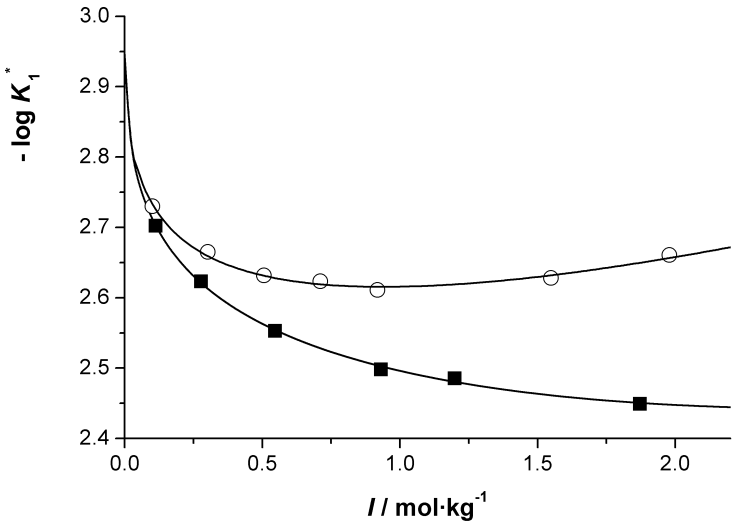

Figure 3.1. Experimental pK^* values of the first ionization equilibrium of phthalic acid in NaCl (open circles) and $CaCl_2$ (filled squares). Solid lines represent the fitting functions, eq. (3.5).

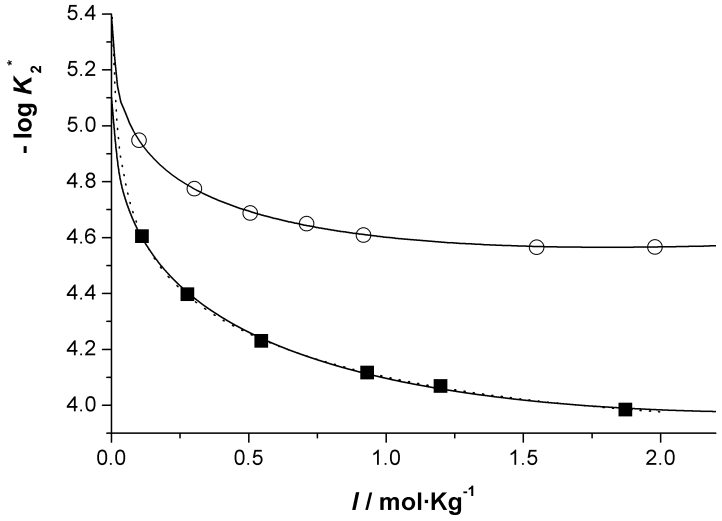

Figure 3.2. Experimental pK^* values of the second ionization equilibrium of phthalic acid in NaCl (open circles) and $CaCl_2$ (filled squares). Solid lines represent the fitting functions, eq. (3.6). Dotted line represents the Pitzer equation including the $\beta^{(2)}$ parameter, eq. (3.12).

The fitting error is reasonably low in all cases, and the extrapolated pK^{T}_{i} values are in good agreement with those found in bibliography (**Table 3.5** and **Table 3.6**). In $CaCl_2$, however, the fitting accuracy of pK^{*}_{2} was not so satisfactory, the extrapolated pK^{T} value deviates from that obtained in 1:1 electrolytes, and this deviation cannot be associated to experimental error.

It must be pointed out that an additional association equilibrium between carboxylic acid and Na^{+}/Ca^{2+} could be considered. However, for our system the inclusion of this kind of equilibrium does not lead to an improvement in the analysis of experimental data, probably due to the small order of magnitude of the associated equilibrium constants.

Regarding NaCl, the data for phthalic acid can reasonably be explained by Pitzer equations, without considering additional equilibriums for ion-pair formation. In the $CaCl_2$ case, complexation between phthalate and Ca^{2+} could be accounted for, implicitly, by including an additional $\beta^{(2)}$ term in the expression for the activity coefficient of phthalate anion, leading to the next equation for the ionic strength dependence of pK^{*}_{2}:

$$pK^{*}_{2} = pK^{T}_{2} + 4f + A_2 I + B_2 g(2) + B_2' g(1.4) + B_2'' g(12) + 4Ch \qquad (3.12)$$

where now:

$$g(x) = \frac{4}{x^2}\left[1 - \left(1 + x\sqrt{I}\right)\exp\left(-x\sqrt{I}\right)\right] \qquad (3.13)$$

and B_2, B_2' and B_2'' are given by the expressions listed in **Table 3.7**. A_2 and C have the same meaning as before. The values x = 2, 1.4 and 12 $kg^{1/2}mol^{-1/2}$ have been reported as the values that lead to better fits for a number of pure aqueous electrolyte solutions (Pitzer, 1973; Pitzer and Mayorga, 1974).

Table 3.7. Coefficients of eq. (3.12), including a $\beta^{(2)}$ interaction parameter. A_2 and C as in **Table 3.1**. For 1:1 electrolytes, similar expressions can be deduced.

	1:2 electrolyte
B_2	$\frac{1}{3\ln 10}\left(2\beta^{(1)}_{HX} - \beta^{(1)}_{AHC} - \frac{4}{3}\beta^{(1)}_{XC}\right)$
B_2'	$\frac{1}{3\ln 10}\left(\beta^{(1)}_{A^{2-}C}\right)$
B_2''	$\frac{1}{3\ln 10}\left(\beta^{(2)}_{A^{2-}C}\right)$

The use of the $\beta^{(2)}$ coefficient has been suggested by Pitzer and Mayorga (1974) for multiple charged ions like 2:2 electrolytes, in order to avoid the introduction of some extra species (the ion-pair) with its corresponding equilibrium. It is well known that the greatest practical difficulties of association models are the inability to determine association constants and the increasing complexity of equation systems as the expressions for different equilibria are introduced in the model. This $\beta^{(2)}$ term would be negative and, in the limit of low molality, it would be related to the association constant *K*, by $\beta^{(2)} = -K/2$. Values of $\beta^{(2)}$ can be found in bibliography for many sulphate salts of divalent cations like Mg, Fe, Zn or Ca. **Table 3.8** shows the values for such systems as compared to that estimated in this work for phthalic acid in $CaCl_2$. Its negative value suggests clearly the presence of ion association. Estimation of the association constant from $\beta^{(2)}$ leads to a value which is comparable to the thermodynamic constant for the ion pair obtained by other authors using different methods, so confirming Pitzer´s interpretations.

Table 3.8. $\beta^{(2)}$ values and stability constants for some 2:2 electrolytes found in literature and $^{(*)}$, $^{(**)}$ estimated in this work. Standard errors are shown in brackets.

Electrolyte	$\beta^{(2)}$	Log($-2\beta^{(2)}$)	Log$K$
$CaSO_4$	-54.24 [(a)]	2.04	2.31 [(b)]
$FeSO_4$	-42 [(a)]	1.92	2.2 [(b)]
$MgSO_4$	-37.23 [(a)]	1.87	2.36 [(b)]
$ZnSO_4$	-32.81 [(a)]	1.82	2.1 [(b)]
Ca-Phthalate	-95 (44) [(*)]	2.3 (0.2) [(*)]	2.42[(c)]
Ca-Phthalate	-88.4 (2.1) [(**)]	2.25 (0.01) [(**)]	2.49[(d)]

[(a)] Data taken from (Pitzer, 1991) (Errors in parameters not reported).

[(b)] Data taken from (Morel and Hering, 1993).

[(c)] Data taken from (Martell and Smith, 1977).

[(d)] Data taken from (Daniele *et al.*, 1985). Values of Log$K$ refer to 25ºC and zero ionic strength.

The fitting of experimental data using eq. (3.12) is shown in **Figure 3.2**, where four parameters have been fitted (B_2 could be previously estimated from pK_1 fitting results). In this case, the extrapolated pK^T value agrees quite well with the value obtained in 1:1 electrolytes and found in literature. The large standard errors associated to the fitted parameters may indicate the presence of multicollinearity among the explanatory variables of the model (Herrero *et al.*, 1993; Fiol *et al.*, 1994). In order to give more reliable values for the interaction parameters, the value of pK^T was fixed to 5.41 and only three parameters were fitted. The results are given in **Table 3.6**.

Contrary to what is observed in the case of phthalic acid in $CaCl_2$, the fitting of the experimental data from the second ionization equilibrium in NaCl to eq. (3.12) shows no substantial increase in the accuracy of fit, nor a significant change in the extrapolated pK^T (see **Table 3.6**). Also, the positive value of $\beta^{(2)}$ obtained in this way suggests no significant ion association, within Pitzer's theory framework.

3.4.1. Calculation of new interaction parameters

As has been remarked by Barriada *et al.* (2000), the very often adopted assumption of a unity activity coefficient for the neutral species (that is, the

assumption of $\lambda_{AH_2} = 0$ in eq. (3.5)) may lead to non-negligible errors using Pitzer equations, even at moderate ionic strengths. Nevertheless, recent papers (Chan *et al.*, 1995) reported β values for the phthalic system within this approximation.

In order to calculate the λ_{AH_2} coefficient for phthalic acid in NaCl and $CaCl_2$, we made use of solubility data obtained from the original work of Rivett and Rosenblum (1914). To our concern, this paper, also quoted by the extensive review by Long and McDevit (1952), was the only systematic study on phthalic acid solubility in aqueous salt solutions found in the literature.

The next steps were followed:

a) The pK^*_i (molal) values corresponding to the ionic strengths at which solubilities are given were interpolated using the fitted Pitzer equations reported in this work (eqs.(3.5) and (3.6) with parameters given in **Table 3.5** and **Table 3.6**).

b) as Rivett's data (Rivett and Rosenblum, 1914) consisted of total dissolved phthalate at each ionic strength, the concentration of undissociated dissolved species (AH_2) had to be calculated by using previously interpolated pK^*_i values;

c) finally, $\log(S_0/ S)$ versus I (molal) plots were constructed (**Figure 3.3**), and least squares fits of data were performed. From the slopes of these plots, λ_{AH_2} values for each background electrolyte were calculated (results shown in **Table 3.9**).

The values of the different β coefficients calculated from eqs. listed in **Table 3.1** and **Table 3.7** are shown in **Table 3.9**, together with the estimated standard errors.

Table 3.9. Values of β and λ interaction parameters obtained from the results in previous tables and **Figure 3.3**. Standard errors are shown in brackets.

Electrolyte	λ_{AH_2}	$\beta^{(0)}_{AHC}$	$\beta^{(1)}_{AHC}$	$\beta^{(0)}_{A2-C}$	$\beta^{(1)}_{A2-C}$
NaCl	0.189 (0.002)	0.199 (0.011)	0.256 (0.074)	0.262 (0.017)	1.030 (0.095)
NaCl[(a)]	0	0.01	0.50	0.44	-0.465
$CaCl_2$	0.146 (0.002)	0.095 (0.035)	0.77 (0.19)	0.451 (0.093)	1.16 (0.52)
$CaCl_2$ [(**)]	0.146 (0.002)	0.095 (0.035)	0.77 (0.19)	0.203 (0.074)	1.67 (0.23)

[(a)] Values assumed in (Chan *et al.*, 1995).

[(**)] see caption in **Table 3.6**.

Figure 3.3 clearly shows that the activity of the neutral species deviates significantly from unity as ionic strength rises (in other words, the slopes are statistically different from zero), in contradiction with the assumption mentioned above. This fact might account for the differences found with β parameters previously estimated for the phthalate-Na system (Chan *et al.*, 1995). Contrarily to these values, the results given here for the system AH^-,Na^+/Ca^{2+} agree quite well with the empirical relationship between $\beta^{(0)}$ and $\beta^{(1)}$ for 1:1 electrolytes reported by Pitzer (1973).

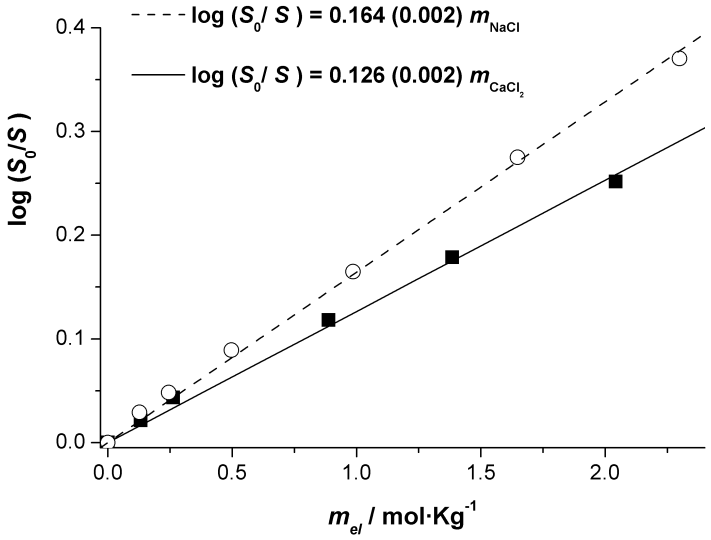

Figure 3.3. Plot of the logarithm of the relative solubility of undissociated phthalic acid versus molality of NaCl (open circles) or $CaCl_2$ (filled squares). Values were calculated from data reported in bibliography (Rivett and Rosenblum, 1914) as was described in the text. Solid and dashed lines represent the linear fitting functions, eq. (3.11).

3.5. Conclusions

The results of this work show how Pitzer equations can reasonably account for the dependence of stoichiometric equilibrium constants of an aromatic di-carboxylic acid with ionic strength even in weakly complexating media such as $CaCl_2$, although extrapolation to zero ionic strength can be affected by complex formation. In this case, the use of an additional coefficient ($\beta^{(2)}$) is proposed, by analogy with models for aqueous solutions of 2:2 electrolytes. This additional term leads to a better fit.

We must point out that the maximum degree of ion association for these weak complexes is often reached at a moderately low ionic strength (even lower than 0.1 mol·L^{-1}) (Davies, 1962). In fact, as **Figure 3.2** shows, the difference between fitting eqs. (3.6) (no $\beta^{(2)}$ included) and (3.12) (with $\beta^{(2)}$) is very small above that concentration. Consequently, in order to obtain reliable values of $\beta^{(2)}$, data in more diluted media are needed (Pitzer and Mayorga, 1974). Nevertheless, the constant ionic medium approximation (Sastre de Vicente,

1997) places a restriction on the lower ionic strength of the experiments. Thus, the $\beta^{(2)}$ value reported here should be considered merely as a reference.

The methodology applied in this work represents a reasonable alternative to ion association models, in those cases where the determination of ion pair constants shows many practical difficulties.

3.6. References

(1997) Microcal^{TM} Origin^{TM}. Microcal Software, Inc., Northampton, MA (USA).

Barriada, J.L., Brandariz, I. and Sastre de Vicente, M.E. 2000. Acid-base equilibria of monocarboxylic acids in various saline media: analysis of data using Pitzer equations. *J. Chem. Eng. Data*, **45**, 1173-1178.

Barriada, J.L., Brandariz, I. and Sastre de Vicente, M.E. 2001. Salting coefficients of carboxylic acids in various saline media. *Ann. Chim.*, **91**, 615-625.

Braibanti, A., Ostaroli, G., Paoleti, P., Petit, D. and Sammartano, S. 1987. *Pure & Appl. Chem.*, **59**, 1721.

Brandariz, I., Vilariño, T., Alonso, P., Herrero, R., Fiol, S. and Sastre de Vicente, M.E. 1998. Effect of ionic strength on the formal potential of the glass electrode in various saline media. *Talanta*, **46**, 1469-1477.

Bryan, N.D., Robinson, V.J., Livens, F.R., Hesketh, N., Jones, M.N. and Lead, J.R. 1997. Metal-humic interactions: A random structural modelling approach. *Geochim. Cosmochim. Acta*, **61**, 805-820.

Chan, C.Y., Eng, Y.W. and Eu, K.S. 1995. Pitzer single-ion activity coefficients and pH for aqueous solutions of potassium hydrogen phthalate in mixtures with KCl and with NaCl at 298.15 K. *J. Chem. Eng. Data*, **40**, 685-691.

Daniele, P.G., De Robertis, A., De Stefano, C., Sammartano, S. and Rigano, C. 1985. On the possibility of determining the thermodynamic parameters for the formation of weak complexes using a simple model for the dependence on ionic strength of activity coefficients: Na^+, K^+, and Ca^{2+} complexes of low molecular weight ligands in aqueous solution. *J. Chem. Soc. Dalton*, 2353-2361.

Daniele, P.G., De Stefano, C., Foti, C. and Sammartano, S. 1997. The effect of ionic strength and ionic medium on the thermodinamic parameters of protonation and complex formation. *Curr. Top. Solution Chem.*, **2**, 253-274.

Daniele, P.G., Rigano, C. and Sammartano, S. 1983. The formation of proton and alkali metal complexes with ligands of biological interest in aqueous solution. Thermodynamics of Li^+, Na^+ and K^+ -dicarboxylate complex formation. *Thermochim. acta*, **62**, 101-112.

Davies, C.W. 1962. *Ion Association*. Butterworths, London.

De Robertis, A., De Stefano, C., Rigano, C. and Sammartano, S. 1990. Thermodynamic Parameters for the Protonation of Carboxilic Acids in Aqueous Tetraethylammonium Iodide Solutions. *J. Solution Chem.*, **19**, 569-587.

Fiol, S., Brandariz, I., Herrero, R., Vilariño, T. and Sastre de Vicente, M.E. 1994. The Protonation Constants of Glycine in Nacl at 25ºC Based on the Pitzer and Scatchard Models Data-Analysis by Ridge-Regression. *Ber. Bunsenges Phys. Chem*, **98**, 164-171.

Gans, P., Sabatini, A. and Vacca, A. 1985. SUPERQUAD: an improved general program for computation of formation-constants from potentiometric data. *J. Chem. Soc. Dalton Trans.*, 1195-1200.

Herrero, R., Brandariz, I., Fiol, S., Vilarino, T. and Sastre de Vicente, M.E. 1993. Errors Encountered in the Determination of Pitzer Parameters from Stoichiometric Equilibrium-Constants. *An. Quím*, **89**, 602-610.

Lobo, V.M.M. and Quaresma, J.L. 1989. *Handbook of electrolyte solutions*. Elsevier, Amsterdam.

Long, F.A. and McDevit, W.F. 1952. Activity coefficients of nonelectrolyte solutes in aqueous salt solutions. *Chem. Rev.*, **51**, 119-169.

Martell, A.E. and Smith, R.M. 1977. *Critical stability constants,* vol 3. Plenum Press, New York.

Morel, F.M.M. and Hering, J.G. 1993. *Principles and Applications of Aquatic Chemistry*. J. Wiley & Sons, New York.

Perdue, E.M., Gjessing, E.T. and Glaze, W. 1990. *Organic acids in aquatic ecosystems: report of the Dahlem Workshop on Organic Acids in Aquatic Ecosystems, Berlin 1989, May 7-12*. Wiley, Chichester.

Pitzer, K.S. 1973. Thermodynamics of electrolytes. I. Theoretical basis and general equations. *J. Phys. Chem.*, **77**, 268-395.

Pitzer, K.S. 1991. Ion interaction approach: Theory and data correlation. In: Pitzer, K.S. (ed.), *Activity coefficients in electrolyte solutions*, pp. 75-153. CRC Press, Boca Raton, Florida.

Pitzer, K.S. and Mayorga, G. 1974. Thermodynamics of electrolytes. III. Activity and osmotic coefficients for 2-2 electrolytes. *J. Solution Chem.*, **3**, 539.

Pitzer, K.S. and Silvester, L.F. 1976. Thermodynamics of electrolytes. VI. Weak electrolytes including H_3PO_4. *J. Solution Chem.*, **5**, 437-446.

Rivett, A.C.D. and Rosenblum, E.I. 1914. The influence of a second solute on the solubility of ortho-phthalic acid. *Trans. Faraday Soc.*, **9**, 297-309.

Sastre de Vicente, M.E. 1997. Ionic strength effects on acid-base equilibria. A review. *Curr. Top. Solution Chem.*, **2**, 157-181.

Stevenson, F.J. 1994. *Humus chemistry. Genesis, composition, reactions*, 2nd edn. John Wiley & Sons, New York.

Tipping, E., Backes, C.A. and Hurley, M.A. 1988. The complexation of protons, aluminium and calcium by aquatic humic substances: a model incorporating binding-site heterogeneity and macroionic effects. *Wat. Res.*, **22**, 597-611.

Vogel, A.I., Jeffery, G.H., Bassett, J., Mendham, J. and Denney, R.C. 1989. *Vogel´s Textbook of Quantitative Chemical Analysis*, 5th edn. Longman, Harlow.

CHAPTER 4

Acid-base properties of synthetic polyelectrolytes

Section 4.1 has been submitted to: Reactive & Functional Polymers
Section 4.2 is in preparation for submission.

4.1. Interaction of acrylic-maleic copolymers with H^+, Na^+, Mg^{2+} and Ca^{2+}: thermodynamic parameters and their dependence on medium

Thermodynamic parameters for the interaction of two acrylic-maleic copolymers (MW = 3 kDa and 70 kDa) with H^+, Na^+, Mg^{2+} and Ca^{2+} were obtained from potentiometric and calorimetric measurements. Apparent protonation constants were expressed as a function of α (dissociation degree) using the three parameter model proposed by Högfeldt and the formation constants of Na^+, Mg^{2+} and Ca^{2+} complexes were calculated from the differences in protonation constants in the different ionic media. The salt effects on protonation were interpreted in terms of both activity coefficient variations and cation complex formation. Enthalpy changes for protonation, obtained by direct calorimetry (always quite low, the stabilization being mainly of entropic nature), were also expressed as a function of α and I using empirical equations. The formation constants obtained for alkali and alkaline earth metal complexes are quite low for Na^+ species (depending on α and on ionic strength, we always found $K < 10$ L mol^{-1}), and fairly high for Mg^{2+} and Ca^{2+} species, ML and ML_2.

Comparison is made with analogous results obtained for polyacrylic and polymethacrylic acids.

4.1.1. Introduction

Natural organic matter is quite rich in carboxylic groups, and these act as binding sites for inorganic and organic cations over a wide pH range. As regards most physical and chemical properties, humic substances (Stevenson, 1982) can be regarded as high molecular weight polyelectrolytes and for this reason polyacrylates and polymethacrylates have been studied as model molecules of more complicated natural macromolecules. In particular, high molecular weight polycarboxylates represent a very good model for acid-base properties and for interacting capabilities with almost all cations, both organic and inorganic. In turn, both protonation and cation complex formation depend on several factors, such as molecular weight, distance between carboxylic groups, even distribution of binding sites and structure (in terms of cross linking, etc.). Some general rules have already been outlined by different research groups and include the slight enhancement of basicity with increasing molecular weight and consequent increasing stability of alkali and alkaline earth metal complexes.

In some previous papers we studied the acid-base properties of polyacrylates and polymethacrylates (Daniele *et al.*, 1999; De Stefano *et al.*, 2000; De Stefano *et al.*, 2002; De Stefano *et al.*, 2003a; De Stefano *et al.*, 2003b; De Stefano *et al.*, 2003c; De Stefano *et al.*, 2004) of different molecular weights, and their binding properties towards alkali and alkaline earth metal cations (Daniele *et al.*, 1999; De Stefano *et al.*, 2002; De Stefano *et al.*, 2003b; De Stefano *et al.*, 2004) and open chain polyammonium cations (Crea *et al.*, 2001). In these studies we found several regularities as concerns binding properties *vs*. ionic strength and molecular weight. Moreover these investigations were performed in different ionic media (alkali metal chlorides, tetraethylammonium halides, artificial seawater) in order to obtain thermodynamic protonation and complexation parameters in a wide range of conditions that might be useful in the speciation of any biological fluid or natural water. This picture was completed with the determination of protonation ΔH values (De Stefano *et al.*, 2003c).

Recently, several studies have been performed in different laboratories on the acid-base properties of naturally occurring substances (Katchalsky and Spitnik, 1947; Fukushima *et al.*, 1995; Masini *et al.*, 1998; Ritchie and Perdue, 2003), such as humic and alginic acids. In these macromolecules the distribution of carboxylic groups is not very even and this mutual mean distance is often very different from that of simple polyacrylic or polymethacrylic electrolytes. The acid-base properties of natural macromolecules reflect this fact and to study these properties using appropriate models it is necessary to make comparisons with other polycarboxylic high molecular weight ligands. An interesting class of polyelectrolytes, which can help in such studies, is represented by acrylic-maleic copolymers.

4.1.2. Reagents

Standard solutions of poly(acrylic-co-maleic) acids (molecular weight 3 kDa and 70 kDa, or PAM3 and PAM70 respectively), previously trailed over a strong cationic exchange resin (Dowex 50) in H^+ form, were prepared from Aldrich product without further purification. PAM3 was a polyacid at ≈ 50% concentration in water, while PAM70 was sodium salt. The solutions of NaCl were prepared from solid product (Fluka, puriss., p.a.) by weighing pure salt previously dried in a stove at 110 °C, while Et_4NI solutions were prepared after recrystallization from methanol-acetone and vacuum-dried before use. HCl was prepared by diluting concentrated ampoules (Fluka) and standardized with

sodium carbonate. Et_4NOH and NaOH were prepared from concentrated products and standardized with potassium biphtalate. Standard solutions of $MgCl_2 \cdot 6H_2O$ and $CaCl_2 \cdot 2H_2O$ were prepared from solid product (Fluka, puriss) and the amounts of Mg^{2+} and Ca^{2+} were determined by complexometric titrations using EDTA (Fluka, puriss., p.a). All solutions were prepared using analytical grade water (R = 18 MΩ cm^{-1}) and grade A glassware and preserved from atmospheric CO_2 by means of soda lime traps.

4.1.3. Equipments and Procedure

4.1.3.1. Potentiometric measurements

Potentiometric technique was used to determine the protonation constants of both poly(acrylic-co-maleic) acids and complex formation constants with Mg^{2+}, Ca^{2+}. Free hydrogen concentrations were measured by two different electrodes; the first was an Orion combination glass-electrode (Ross type 8102), while the second was a model 8101 Orion glass-electrode coupled with a standard calomel electrode. The electrodes were connected with a Metrohm model E654 potentiometer with a resolution of ±0.1 mV and a reproducibility of ±0.15 mV. The titrant was delivered by a Metrohm 665 automatic burette with a minimum reading of ±0.001 ml and 10 ml capacity. The automatic burette and the potentiometer were connected to a personal computer, and the acquisition of e.m.f. values was performed by a computer program which reads and saves experimental data and adds pre-established volumes of titrant via the automatic burette when the equilibrium is reached; this computer program makes it possible to automate other parameters in a potentiometric titration, such as the addition of minimum volumes of titrant at the equivalence point. All potentiometric measurements were carried out in thermostatted cells at 25.0±0.1 °C; the solutions were preserved from atmospheric O_2 and CO_2 by a stream of purified N_2 in the measurement cells and magnetically stirred. For all potentiometric measurements the electrode couple was standardized, in terms of $pH = -\log [H^+]$, by titrating a 10 mmol L^{-1} HCl solution (having the same ionic strength value as the solution under study) with standard NaOH or Et_4NOH, in order to determine the standard potential E° before each experiment.

4.1.3.2. Calorimetric measurements

The protonation enthalpy changes of copolymer (PAM3) were determined using a model 450 Tronac isoperibolic titration calorimeter coupled with a Keithley 196 system Dmm digital multimeter at 25.000±0.001 °C. The

whole system was connected to a PC for the acquisition of reaction heats by a suitable computer program. The titrant was delivered by a 2.5 ml capacity model 1002 TLL Hamilton syringe; the accuracy of calorimetric apparatus was Q±0.008 J and the accuracy of the titrant volume was ±0.001 ml. Accuracy was checked by titrating a THAM (tris-(hydroxymethyl)amino-methane) buffer with HCl.

4.1.3.3. Procedure

The standardization of poly(acrylic-co-maleic) acids was performed by potentiometric and conductometric titrations with the aim of determining the total concentration of carboxylic groups.

The solutions containing different concentrations of two copolymers were titrated with NaOH or Et_4NOH solutions for both the potentiometric and conductometric measurements. Titration curves (performed without adding any supporting electrolytes) were comparable for both the copolymers and show a single transition at the equivalence. These investigations were completed by NMR analysis with the aim of calculating the ratio of acrylic to maleic acid units in the copolymer chain; small quantities of copolymers were dissolved in D_2O and the measurements performed with a model AMX R-300 Bruker instrument. Experimental data showed the ratio to be 1:1.2 (acrylic:maleic units) in the copolymer PAM3, while in the copolymer PAM70 it was 1.95:1.

Protonation constants for both copolymers were determined in two different ionic media, NaCl and Et_4NI and in the ionic strength ranges $0.05 \leq I/mol\ L^{-1} \leq 2.0$ in NaCl and $0.1 \leq I/mol\ L^{-1} \leq 0.5$ in Et_4NI. The measurements were carried out by titrating 25 ml of the solution containing the acrylic-maleic copolymers in a concentration range 15-30 mmol L^{-1} and the background salt (in order to obtain the pre-established ionic strength value) with NaOH or Et_4NOH. The same procedure was followed to determine the complex formation constants of Mg^{2+} and Ca^{2+}-copolymers at 25 °C in NaCl. Studies of alkaline earth metal-copolymer complexes were performed by titrating with NaOH solutions containing the metal (Ca^{2+} or Mg^{2+}) at concentrations of 1.6-10 mmol L^{-1}, the poly(acrylic-co-maleic) acid at concentrations of 5-30 mmol L^{-1} and NaCl in order to obtain a total ionic strength value of 0.1 mol L^{-1} or 0.5 mol L^{-1}. For the copolymer PAM3 we report formation constants with Mg^{2+} and Ca^{2+} only at I = 0.1 mol L^{-1}, while for the copolymer PAM70 the formation constants with Mg^{2+} are reported only at I = 0.1 mol L^{-1} and with Ca^{2+} at I = 0.1 and 0.5 mol L^{-1}. For each measurement some 80-100 experimental points were collected, and for

each experimental condition, independent titrations of hydrochloric acid solutions with NaOH or Et_4NOH were performed in the same experimental conditions as the systems under study to determine formal electrode potential as indicated in the potentiometric measurements section.

Calorimetric measurements were performed only on the PAM3 copolymer by titrating 50 ml of solution containing the standard solution of poly(acrylic-co-maleic) acid, which was neutralized with standard NaOH. The measurement solution contained the neutralized copolymer at 5-12 mmol L^{-1} and NaCl in order to obtain the total ionic strength value $0.05 \leq I/\text{mol L}^{-1} \leq 2.0$; this solution was subsequently titrated with HCl 0.5004 mol L^{-1}. For each experimental condition we measured the heat of dilution using solutions having the same ionic strength values as the solutions under study and in the absence of the poly(acrylic-co-maleic) acid (PAM3).

4.1.4. Calculations

The protonation constants of high molecular weight polyanions cannot be calculated as simply as those for small polyacids. To study quantitatively the interacting ability of polyelectrolytes one must preliminarly investigate their acid-base properties and, in particular, the protonation constants at different pH values, since it is not possible to determine log K^H values for each carboxylic group. Therefore one must consider a variable protonation constant as a function of the degree of dissociation (α).

The protonation constants of a generic polyacid can be expressed by the following equation

$$K^H = \frac{[HL]}{\left([L^-][H^+]\right)} \tag{4.1.1}$$

and the degree of dissociation can be written as

$$\alpha = \frac{[L^-]}{C_L} = \frac{C_{OH} + [H^+] - \frac{K_W}{[H^+]}}{C_L} \tag{4.1.2}$$

where L^- is the monomer anion of the polyelectrolyte, C_L is the analytical concentration, C_{OH} is the concentration of strong base added for the partial neutralization of the polyacid at each α value and K_w is the ionic product of

water. If we express the protonation constants of a polyacid as a function of the degree of dissociation using the most popular model derived from the modified Henderson-Hasselbalch equation (Katchalsky and Spitnik, 1947), we can write:

$$\mathrm{pH} = \log \mathrm{K}_{\mathrm{n}}^{\mathrm{H}} - \mathrm{n} \log \frac{1-\alpha}{\alpha} \tag{4.1.3}$$

or

$$\log \mathrm{K}^{\mathrm{H}} = \log \mathrm{K}_{\mathrm{n}}^{\mathrm{H}} - (\mathrm{n}-1) \log \frac{1-\alpha}{\alpha} \tag{4.1.4}$$

where n is an empirical parameter which generally does not exceed the value of 2-2.5 and K^H_n is the protonation constant at half neutralization. Other models for the calculation of protonation constants of polyacids are reported in literature, such as the simple three parameters model proposed by Högfeldt (Högfeldt, 1988; Högfeldt *et al.*, 1989):

$$\log \mathrm{K}^{\mathrm{H}} = \alpha^2 \log \mathrm{K}_1^{\mathrm{H}} + (1-\alpha)^2 \log \mathrm{K}_0^{\mathrm{H}} + 2\alpha(1-\alpha) \log \mathrm{K}_{\mathrm{m}}^{\mathrm{H}} \tag{4.1.5}$$

where K_1^H and K_0^H are the protonation constants at $\alpha = 1$ and $\alpha = 0$, respectively; K_m^H is an intermediate value that accounts for the non-linearity of K^H_m *vs.* α. The thermodynamic protonation constant can be represented by a mean constant ($\overline{\mathrm{K}}^{\mathrm{H}}$) obtained by the integral of the experimental curve $\log K^H = f(\alpha)$, in the range $0 \le \alpha \le 1$, i.e.

$$\log \overline{\mathrm{K}}^{\mathrm{H}} = \int_0^1 \log \mathrm{K}^{\mathrm{H}} \mathrm{d}\alpha = \frac{\log \mathrm{K}_1^{\mathrm{H}} + \log \mathrm{K}_0^{\mathrm{H}} + \log \mathrm{K}_{\mathrm{m}}^{\mathrm{H}}}{3} \tag{4.1.6}$$

All the calculations were performed using least squares computer programs. ESAB2M (De Stefano *et al.*, 1985) was used to determine all the parameters of the acid-base titration (analytical concentration of reagents, formal electrode potential E°, coefficient j_a for junction potential $E_j = j_a [H^+]$ and the ionic product of water K_w). LIANA (De Stefano *et al.*, 1997), was used to calculate protonation and alkaline earth metal complex formation constants and relative parameters for dependence on ionic strength, and to determine the weak complexes formed between the poly(acrylic-co-maleic) anions and the sodium ion at different degrees of dissociation (α). A modified version of the computer program ES5CM (De Robertis *et al.*, 1989) was used in calorimetric

investigations to calculate enthalpy changes for protonation, while parameters for the dependence of ΔH e TΔS on ionic strength were calculated by LIANA.

4.1.5. Results

4.1.5.1. Protonation constants

The three parameter equation proposed by Högfeldt was used to determine the protonation constants of both copolymers because it fit the experimental data better (especially at $\alpha<0.2$; $\alpha>0.8$) than the modified Henderson-Hasselbalch equation.

Table 4.1.1 shows mean protonation parameters (K_1^H, K_0^H, K_m^H and $\overline{K}^H$) at different ionic strengths (experimental protonation constants are reported as Supplementary Data in **Tables A.1-A.4**, Appendix A) for PAM3 and PAM70 in NaCl and Et_4NI respectively. The data in **Table 4.1.1** show that for the same copolymer, all protonation constants in Et_4NI are higher than the corresponding ones in NaCl , and for log K^H_1 the differences are of about one logarithmic unit (**Figure 4.1.1**).

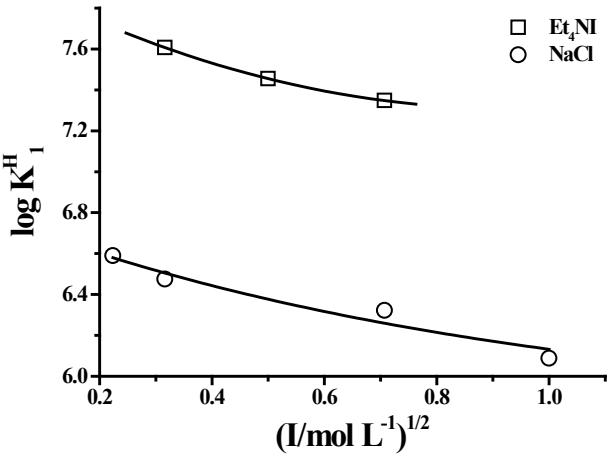

Figure 4.1.1. log K^H_1 *vs*. $(I/mol\ L^{-1})^{1/2}$ for PAM70 in different ionic media at T = 25 °C

Table 4.1.1. Mean protonation constants of poly(acrylic co-maleic) acids (PAM3, PAM70) in NaCl and Et_4NI at different ionic strengths obtained by Högfeldt model at T = 25 °C

I/mol L^{-1}	$\log K^H_1$	$\log K^H_0$	$\log K^H_m$	$\log \overline{K}^H$
	PAM3 (NaCl)			
0.05	6.538±0.017[a]	3.822±0.008	4.886±0.004	5.082
0.10	6.343±0.012	3.786±0.004	4.670±0.010	4.933
0.25	6.080±0.006	3.701±0.005	4.402±0.005	4.727
0.50	6.008±0.015	3.693±0.006	4.230±0.005	4.643
1.0	5.758±0.003	3.599±0.004	4.141±0.003	4.499
2.0	5.794±0.018	3.541±0.007	4.518±0.012	4.618
	PAM3 (Et_4NI)			
0.10	7.199±0.007[a]	3.899±0.008	4.398±0.007	5.165
0.25	7.150±0.003	3.885±0.007	4.291±0.007	5.109
0.50	6.922±0.003	3.856±0.006	4.335±0.008	5.038
	PAM70 (NaCl)			
0.05	6.590±0.005[a]	3.941±0.008	5.229±0.004	5.253
0.10	6.475±0.007	3.876±0.004	4.927±0.010	5.093
0.50	6.322±0.005	3.836±0.002	4.291±0.004	4.816
1.0	6.088±0.004	3.709±0.004	4.146±0.005	4.648
	PAM70 (Et_4NI)			
0.10	7.607±0.003[a]	3.825±0.006	4.890±0.006	5.441
0.25	7.455±0.006	3.814±0.002	4.718±0.003	5.329
0.50	7.348±0.004	3.834±0.005	4.682±0.005	5.288

[a] ± std. dev.

Figure 4.1.2 is a comparison of the protonation constants of both copolymers at $\alpha = 1$ at different ionic strength values in NaCl; as we can see, the protonation constants of PAM70 are higher than those of PAM3 at the same ionic strength values. This may due to the different structure of the two polyanions and also to their different molecular weight; indeed, an increase in molecular weight increases total polyelectrolyte charge and, therefore, the strength of interactions. We should also remember that the ratio of acrylic to

maleic units along the polymeric chain is different in the two poly(acrylic-co-maleic) anions (see the procedure section).

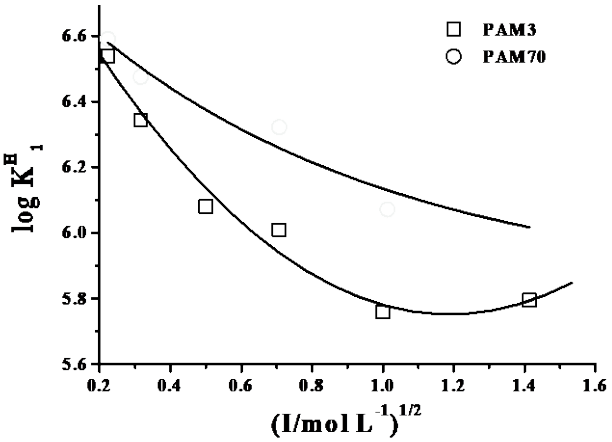

Figure 4.1.2. log K^H_1 *vs.* (I/mol L^{-1})$^{1/2}$ for both copolymers in NaCl and T = 25 °C

In order to compare the protonation constants of copolymers obtained by analysis of experimental data using equations (4.1.4) and (4.1.5), **Tables A.1** and **A.2** (Appendix A) show the protonation constants obtained using the Högfeldt model and the log K^H_n and n values obtained using the two parameter model at different ionic strength values in NaCl and Et_4NI for PAM3. The standard deviations obtained by processing experimental data using the Henderson-Hasselbalch equation are higher than those obtained using the three parameter model, in particular in Et_4NI aqueous solutions. In Et_4NI we have (mean values) σ_{fit} = 0.027 and σ_{fit} = 0.063 for the three and two parameter models, respectively; analogously in NaCl, σ_{fit} = 0.018 and σ_{fit} = 0.023. These results indicate that the three parameter model is more suitable than the two parameter one; moreover, Högfeldt model provides two useful parameters, i.e., log K^H at $\alpha = 0$ and $\alpha = 1$.

For PAM3, the dependence of K^H_1, K^H_0 and K^H_m on ionic strength is reported in **Figure 4.1.3** in the ionic strength range 0.05 ≤ I/mol L^{-1} ≤ 1.0 in NaCl aqueous solutions; it can be seen, as observed for other polycarboxylic acids already studied (Daniele *et al.*, 1999; De Stefano *et al.*, 2000; Crea *et al.*, 2001; De Stefano *et al.*, 2002; De Stefano *et al.*, 2003a; De Stefano *et al.*, 2003b; De Stefano *et al.*, 2003c; De Stefano *et al.*, 2004), that protonation constants decrease with an increase in ionic strength. This behaviour can be

explained by considering the decrease in ion activity coefficients provoked by an increase in ionic strength, and by considering the decrease in the number of polyelectrolyte charges effectively available for interaction with the proton, due to the salt-screening effect of Na^+ ions.

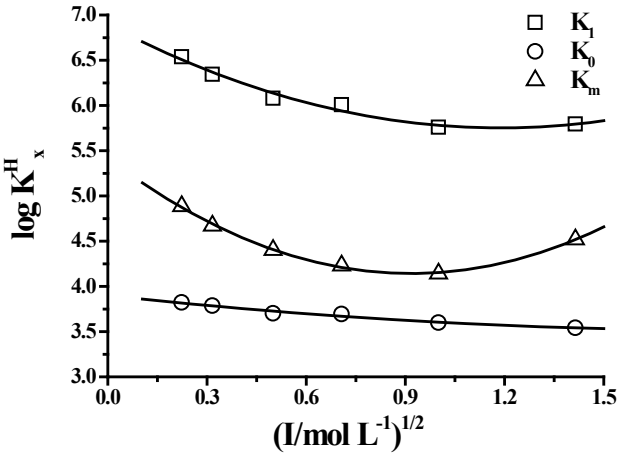

Figure 4.1.3. Protonation constants of PAM3 *vs*. $(I/mol\ L^{-1})^{1/2}$ in NaCl and T = 25 °C

The dependence of protonation constants on ionic strength was taken into account using the following equations. For $\log K^H_1$, where the difference between data in NaCl and Et_4NI is quite high, two different expressions were used

$$\log K_1^H = \log {}^T K_1^H + P_1 I^{1/2} - \log(1 + 10^{P_2} I) \qquad (4.1.7)$$

(protonation constants in NaCl), and

$$\log K_1^H = \log K_1^{H'} + P_3 I \qquad (4.1.8)$$

(protonation constants in Et_4NI). For $\log K^H_m$ and $\log \overline{K}^H$, in both ionic media, a single equation was used.

$$\log K_X^H = \log {}^T K^H + P_4 I^{1/2} + P_5 I \qquad (4.1.9)$$

In all cases the parameter at infinite dilution ($\log {}^T K^H$) was constrained to be equal in both NaCl and Et_4NI media. The protonation constants at infinite dilution and the empirical parameters of equations (4.1.7), (4.1.8) and (4.1.9) are reported in **Table 4.1.2**.

Table 4.1.2. Empirical parameters for the dependence on ionic strength of protonation constants, at T = 25 °C

	ligand	medium	log $^{T}K^{H}$	P1	P2	P3	P4	P5	σ_{fit}[a]
$logK^{H}_{l}$	PAM3		7.28±0.04						
		NaCl	-	0.658	2.12	-	-	-	0.043
		Et_4NI	-	-	-	-0.71	-	-	0.027
	PAM70		7.65±0.05						
		NaCl	-	0.987	2.48		-	-	0.093
		Et_4NI	-	-	-	-0.61	-	-	0.026
$logK^{H}_{m}$	PAM3		5.40±0.05						
		NaCl	-	-	-	-	-2.75	1.50	0.015
		Et_4NI	-	-	-	-	-4.32	3.99	0.037
	PAM70		5.89±0.06						
		NaCl	-	-	-	-	-3.52	1.77	0.023
		Et_4NI	-	-	-	-	-4.18	3.51	0.029
$\log \overline{K}^{H}$	PAM3		5.40±0.04						
		NaCl	-	-	-	-	-1.72	0.82	0.022
		Et_4NI	-	-	-	-	-0.88	0.52	0.012
	PAM70		5.54±0.07						
		NaCl	-	-	-	-	-1.44	0.55	0.025
		Et_4NI	-	-	-	-	-0.37	0.023	0.020

[a] std. dev. on the fit of equations (4.1.7), (4.1.8) and (4.1.9)

Measurements were also performed in mixtures NaCl-$MgCl_2$ and NaCl-$CaCl_2$ at different ionic strengths (and relative protonation constants are reported, in Appendix A, **Tables A.5** and **A.6**). From the lowering of protonation constants it was possible to calculate the formation constants of Mg^{2+} and Ca^{2+} complexes (see here after).

4.1.5.2. Formation constants of weak complexes

The differences in protonation constants in both ionic media can be interpreted in terms of interactions between the poly(acrylic-co-maleic) anion and the background salt cation; this interaction can be neglected when we use a tetraalkylammonium salt, such as Et_4NI, whose cation does not interact

significantly with carboxylic anions. The differences in log K^H in different salt solutions can be analysed by the following equation:

$$\log K^{H^*} = \log K^{H}_{(Baseline)} - \log\left(1 + K^{Na}\left[Na^+\right]\right) \quad (4.1.10)$$

where log $K^H_{(Baseline)}$ is the protonation constant determined in an arbitrarily chosen salt as Et_4NI, log K^{H^*} is the protonation constant (apparent protonation constant) in a solution containing a cation which interacts more significantly with polyelectolytes and K^{Na} is the formation constant of the weak complex (Na^+, PAM3 and PAM70 in our case).

This equation is strictly valid for simple monoprotic acids, but can be extended to polyacids under the following assumptions:

a) The activity of free ions does not change in different ionic media at the same ionic strength;

b) The formation constant is a function of α and of the polyelectrolyte charge;

c) True protonation constants have the same value in the presence and in the absence of interacting cations.

As concerns point c) one may calculate log K^{H^*} and log $K^H_{(Baseline)}$ at the same pH value, where it is reasonable to assume that the effective charge is the same in both media. At a certain value of α, $\alpha^* = \alpha$, the pH value for the polyanion solution in the supporting electrolyte containing the cation which forms a weak complexes species, i.e. pH*, is

$$pH^* = \log\frac{\alpha^*}{1-\alpha^*} + \alpha^{*2}\log K_1^{H^*} + (1-\alpha^*)^2\log K_0^{H^*} + 2\alpha^*(1-\alpha^*)\log K_m^{H^*} \quad (4.1.11)$$

The value of α at the same pH values, in the baseline salt, can be obtained iteratively from

$$\log\frac{\alpha}{1-\alpha} + \alpha^2\log K_1^{H} + (1-\alpha)^2\log K_0^{H} + 2\alpha(1-\alpha)\log K_m^{H^*} - pH = 0 \quad (4.1.12)$$

Therefore we may calculate the formation constants of weak complexes at different α and ionic strengths using the equation (4.1.10) in the form: log $K^H(\alpha)$ - log $K^{H^*}(\alpha^*)$ = log (1 + K^{Na} [Na^+]).

The formation constants of weak complexes are reported in **Table 4.1.3** and, as an example, **Figure 4.1.4** shows dependence on α for the sodium complexes of PAM3 at I = 0.1 mol L^{-1} and 0.5 mol L^{-1}. This Figure evidences a monotone trend for the sodium complexes as observed for other polycarboxylic acids already studied (Daniele *et al.*, 1999; De Stefano *et al.*, 2000).

Table 4.1.3 Formation constants of sodium complexes for the poly(acrylic-co-maleic) acids (PAM3, PAM70) at T = 25 °C

α	log K^{Na}		
	I = 0.1 mol L^{-1}	I = 0.25 mol L^{-1}	I = 0.5 mol L^{-1}
	PAM3		
0.50	-0.13	0.00	-0.25
0.60	0.15	0.14	-0.14
0.70	0.40	0.30	0.00
0.80	0.65	0.44	0.18
0.90	0.98	0.70	0.36
	PAM70		
0.50	-0.38	-	-0.04
0.60	0.16	-	0.05
0.70	0.48	-	0.10
0.80	0.78	-	0.23

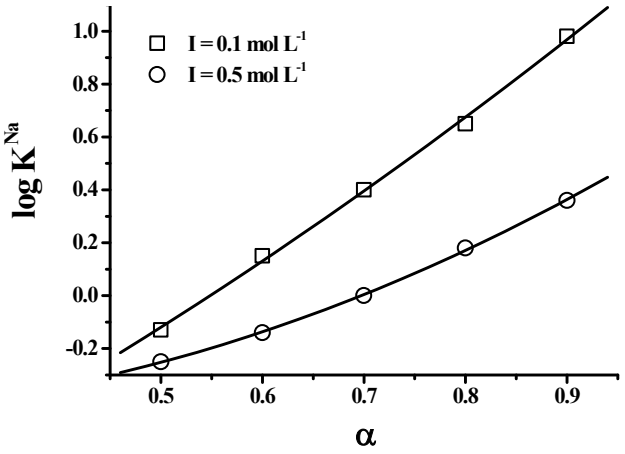

Figure 4.1.4. Sodium complexes of PAM3 *vs*. α at different ionic strengths in NaCl and T = 25 °C

The dependence of $\log K^{Na}$ on ionic strength and on α can be expressed using the relationship: $\log K^{Na} = \log {}^{T}K^{Na} + P_6 I^{1/2} + P_7 (1-\alpha) + P_8 I (1-\alpha)$

and by last squares calculation we obtained

$\log {}^{T}K^{Na} = 1.74 \pm 0.10$ (PAM3), 2.56 ± 0.18 (PAM70)

$P_6 = -1.73$ (PAM3), -3.06 (PAM70)

$P_7 = -2.75$ (PAM3), -4.53 (PAM70)

$P_8 = 2.44$ (PAM3), 7.33 (PAM70)

$\sigma_{fit} = 0.072$ (PAM3), 0.047 (PAM70)

where $\log {}^{T}K^{Na}$ is the formation constant of weak complexes at $I = 0$ mol L^{-1} and $\alpha = 1$.

4.1.5.3. Alkaline earth metal complexes

The mass balance equations for aqueous solutions containing M^{2+} ions, which form strong complexes with L^-, are written

$$C_M = \left[M^{2+}\right] + \sum \left[ML_j^{(2-j)}\right] = \left[M^{2+}\right]\left(1 + \sum \beta_j \left[L^-\right]^j\right) \qquad (4.1.13)$$

$$C_L = \left[L^-\right] + \sum \left[ML_j^{(2-j)}\right] = \left[L^-\right] + \sum j\beta_j \left[M^{2+}\right]\left[L^-\right]^j \qquad (4.1.14)$$

$$C_H = \left[H^+\right] + \left[HL\right] - \left[OH^-\right] = \left[H^+\right] + K^H \left[L^-\right]\left[H^+\right] - \frac{K_W}{\left[H^+\right]} \qquad (4.1.15)$$

If the pH is known, from equation (4.1.15) one can calculate the free concentration of L^-:

$$\left[L^-\right] = \frac{C_H - \left[H^+\right] + \left[OH^-\right]}{K^H \left[H^+\right]} \qquad (4.1.16)$$

and from equations (4.1.14) and (4.1.15) the average number of L bound to M^{2+}:

$$\bar{n} = \frac{C_L - \left[L^-\right] - K^H \left[L^-\right]\left[H^+\right]}{C_M} \qquad (4.1.17)$$

Formation constants can be calculated from the classic equation:

$$\bar{n} = \frac{\sum j\beta_j \left[L^-\right]^j}{1 + \sum \beta_j \left[L^-\right]^j} \tag{4.1.18}$$

and, if only one complex species is formed (pL = - log[L]),

$$\log \beta_j = jpL + \log\left[\frac{\bar{n}}{j - \bar{n}}\right] \tag{4.1.19}$$

In this study, the speciation model that better fits the experimental data is the one that takes into account the formation of two different species having stoichiometric coefficients 1:1 and 1:2 (M^{2+}:copolymer), whose formation constants were determined by equation (4.1.18) in which the dependence on α of formation constants was taken into account using the equation (4.1.20):

$$\log K^M = \log K_{\alpha=1} + P_q(1-\alpha) \tag{4.1.20}$$

and in particular:

$$\log K_1 = \log K_{1(\alpha=1)} + P_9(1-\alpha)$$

$$\log \beta_2 = \log \beta_{2(\alpha=1)} + P_{10}(1-\alpha)$$

Alkaline earth metal-copolymer formation constants are reported in **Table 4.1.4** together with the values of empirical parameters P_9 and P_{10}; very often we have $K_2 = \beta_2/K_1 > K_1$.

Table 4.1.4. Alkaline earth metal-copolymer complex formation constants at different dissociation degree values in NaCl at T=25°C

I/mol L^{-1}	ligand	β_1	P_9	β_2	P_{10}	σ_{fit} [b]
		Ca^{2+}				
0.1	PAM3	1.66±0.16[a]	0.43±0.21	5.66±0.04	4.21±0.15	0.08
0.1	PAM70	2.53±0.05	1.34±0.08	5.80±0.04	4.80±0.16	0.05
0.5	PAM70	2.07±0.07	1.71±0.14	5.06±0.06	6.20±0.27	0.03
		Mg^{2+}				
0.1	PAM3	2.49±0.05	2.15±0.09	5.30±0.06	6.45±0.27	0.04
0.1	PAM70	1.52±0.07	-	5.09±0.16	3.89±0.66	0.09
		log β_1		log β_2		
		$\alpha = 0$	$\alpha = 0.5$	$\alpha = 0$	$\alpha = 0.5$	
		Ca^{2+}				
0.10	PAM3	1.23	1.44	1.45	3.56	
0.10	PAM70	1.19	1.86	1.00	3.40	
0.50	PAM70	0.36	1.22	-1.44	1.96	
		Mg^{2+}				
0.10	PAM3	0.34	1.42	-1.15	2.08	
010	PAM70	1.52	1.52	1.2	3.15	

[a] ± std. dev

[b] std. dev. on the fit of the equation (4.1.18)

Similar behaviour was observed in studies on the complexing abilities of homopolymers, as polyacrylates and polymethacrylates, towards different alkaline earth metals (Daniele *et al.*, 1999; De Stefano *et al.*, 2002; De Stefano *et al.*, 2003b; De Stefano *et al.*, 2004), where the formation of a single species ML_2 (L = polyelectrolytes) or two species with $K_2 > K_1$ was observed. Depending on the ratio C_M/C_L the formation of 1:1 species can be neglected. Moreover at low α values, there is significant formation of the ML species, whilst for $\alpha \rightarrow 1$ the ML_2 species is predominant. The $K_2 > K_1$ behaviour, which is unusual for low molecular weight ligands, can easily be explained for polyelectrolytes, where effective charge changes with α: at high degrees of neutralization the metal tends to be solely bound to two coordinating groups.

This behaviour has also been observed in the formation of other dication-polyelectrolyte complexes (Morlay *et al.*, 1998; Morlay *et al.*, 1999).

Studies performed at different ionic strengths for the system Ca^{2+}-PAM70 in NaCl showed formation constant stability to decrease with an increase in ionic strength because by increasing Na^{+} concentration (ionic strength) the number of polyelectrolyte charges effectively available for interaction with Ca^{2+} decreases. In fact, the external salt screens the long-range electrostatic interactions, and it is well known that polyelectrolytes behave like neutral polymers in a large excess of salt.

4.1.5.4. Enthalpies and Entropies of protonation for PAM3

ΔH and TΔS values were calculated using an equation similar to the three parameter model proposed by Högfeldt for the calculation of protonation constants in which the terms log K^{H}_{x} (x = 0, 1, m) were substituted with ΔH_x an $T\Delta S_x$. **Table 4.1.5** reports the ΔH_x and $T\Delta S_x$ values in the ionic strength range $0.05 \leq$ I/mol $L^{-1} \leq 2.0$ in NaCl at 25 °C for PAM3. The ΔH values are always low and, as expected, they are a decreasing function of ionic strength, as are the protonation constants (**Figure 4.1.5**), while TΔS values in the same experimental conditions are all positive.

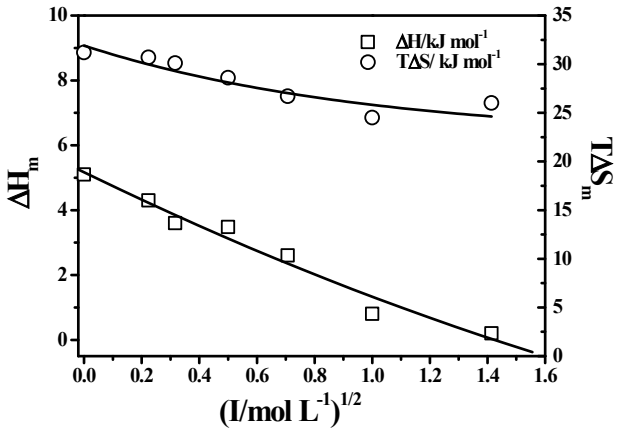

Figure 4.1.5. ΔH_m and $T\Delta S_m$ *vs.* (I/mol L^{-1})$^{1/2}$ for PAM3 in NaCl and T = 25 °C

Table 4.1.5. Thermodynamic parameters for the protonation of PAM3 at different ionic strengths in NaCl and T = 25 °C

I/mol L^{-1}	ΔG_1[a]	ΔG_0[a]	ΔG_m[a]	$\overline{\Delta G}$[a]
0.05	-37.31±0.10[b]	-21.82±0.05	-27.89±0.02	-28.44
0.10	-36.21±0.07	-21.61±0.02	-26.66±0.06	-28.16
0.25	-34.70±0.03	-21.12±0.03	-25.13±0.03	-26.98
0.50	-34.29±0.09	-21.07±0.03	-24.14±0.03	-26.50
1.00	-32.86±0.02	-20.54±0.02	-23.64±0.02	-25.68
2.00	-33.10±0.10	-20.21±0.04	-25.79±0.07	-26.37
	ΔH_1[a]	ΔH_0[a]	ΔH_m[a]	$\overline{\Delta H}$[a]
0.05	-0.70±0.15[b]	-2.40±0.13	4.30±0.13	0.40
0.10	-0.80±0.14	-2.00±0.12	3.60±0.12	0.27
0.25	-0.79±0.11	-2.73±0.10	3.48±0.10	-0.01
0.50	-1.40±0.09	-2.80±0.08	2.60±0.09	-0.53
1.00	-3.30±0.06	-3.50±0.07	0.80±0.10	-2.00
2.00	-4.20±0.06	-4.00±0.11	0.20±0.16	-2.80
	$T\Delta S_1$[a]	$T\Delta S_0$[a]	$T\Delta S_m$[a]	$\overline{T\Delta S}$[a]
0.05	35.3±0.2[b]	19.2±0.2	30.7±0.3	28.4
0.10	35.2±0.2	19.6±0.2	30.1±0.2	28.3
0.25	33.8±0.1	18.4±0.2	28.6±0.2	26.9
0.50	32.8±0.2	18.3±0.1	26.7±0.2	25.9
1.00	29.5±0.3	17.0±0.2	24.5±0.4	23.7
2.00	28.9±0.5	16.2±0.2	26.0±0.7	23.8

[a] kJ mol^{-1}

[b] ± std. dev.

The thermodynamic parameters values obtained by calorimetry point out that the stabilization of the complexes is of entropic nature. The dependence of ΔH and TΔS on ionic strength was calculated by the following simple equations

$$\Delta H = \Delta H_X^0 + aI^{1/2} \quad (4.1.21)$$

$$T\Delta S = T\Delta S_X^0 + aI^{1/2} \quad (4.1.22)$$

where *a* is an empirical parameter for dependence on ionic strength and ΔH^0_x, $T\Delta S^0_x$ are the values at infinite dilution for the three parameters proposed in the Högfeldt model. Thermodynamic and empirical parameters have been calculated using LIANA and the results obtained are: ΔH^0_1 = 0.3±0.2, ΔH^0_0 = -1.9±0.2, ΔH^0_m = 5.1±0.2 kJ mol^{-1}, and a_1 = -3.2±0.1, a_0 = -1.5±0.2, a_m = -3.6±0.2, while for TΔS we obtained: $T\Delta S^0_1$ = 36.7±0.3, $T\Delta S^0_0$ = 20.0±0.3, $T\Delta S^0_m$ = 31.2±0.4 kJ mol^{-1}, a_1 = -5.7±0.5, a_0 = -2.7±0.3, a_m = -5.0±0.8.

The last column of **Table 4.1.5** shows mean values for the enthalpy and entropy changes for protonation at different ionic strengths, calculated by equation (4.1.6) and substituting log K^H_x for ΔH_x and $T\Delta S_x$, respectively; while for the values at I/mol L^{-1} = 0 we obtain $\overline{\Delta H}^0$ = 1.16, $\overline{T\Delta S}^0$= 29.3 kJ mol^{-1}.

As observed for low molecular weight polycarboxylates, there is a strong correlation between TΔS and ΔG values. In fact we obtained:

$T\Delta S_1 = -18 - 1.48 \cdot \Delta G_1 \quad (\sigma = 1.17)$

$T\Delta S_0 = -25 - 2.06 \cdot \Delta G_0 \quad (\sigma = 0.33)$

$T\Delta S_m = -5 - 1.31 \cdot \Delta G_m \quad (\sigma = 1.43)$

$\overline{T\Delta S} = -22 - 1.82 \cdot \overline{\Delta G} \quad (\sigma = 0.82)$

This suggests that most of experimental data at different ionic strengths can be avoided using appropriate predictive linear relationships.

4.1.5.5. Literature comparison

Many authors describe a pH transition at alpha = 0.5 in the titration curve of many copolymers of maleic acid (Kitano *et al.*, 1987; Chitanu *et al.*, 1999). This effect has traditionally been explained to be the result of unequal intercharge distances along the polymer chain, so short-range electrostatic

interaction between adjacent COOH groups becomes very strong. Nervertheless, the titration curves of the poly(acrylic-co-maleic) acids studied here do not follow the same trend; in fact, the tritation curves are very similar to those of simple polyelectrolytes, as observed by potentiometric and conductometric measurements. This might be due to the relative numbers of maleic and acrylic units in the polimer chain, as already observed by Nemtoi (Nemtoi and Colonescu, 1999) in a previous paper.

Some paper in literature have reported on the sequestering abilities of acrylic-maleic copolymers; one interesting example is that of Nicholson, (2000), which examines the interactions of a poly(acrylic-co-maleic) copolymer towards some alkali and alkaline earth metals, and towards some heavy metals (Zn^{2+}, Al^{3+}, Fe^{3+}). Nicholson hypothesizes electrostatic interaction between the copolymer and the alkali and alkaline earth metals, in which the salts occupy atmospheric rather than site-bound locations. Moreover for Zn^{2+}, Al^{3+} and Fe^{3+}, IR studies show that in the presence of these ions chelation occurs and higher formation constant values are observed. The low formation constant values obtained in our studies suggest that electrostatic interaction occur, for the poly(acrylic-co-maleic) acids studied here. Other studies performed by Rivas and Seguel (1999) have shown how poly(acrylic-co-maleic) acids forms complexes with metals via their carboxylic groups involving only one functional group of maleic acid.

Table A.7 (Appendix A) shows a comparison of protonation constants at I = 0.5 mol L^{-1} in NaCl and Et_4NI for the poly(acrylic-co-maleic) acids studied here, and for polyacrylic (PAA) and polymethacrylic (PMA) acids previously studied at different molecular weights (De Stefano *et al.*, 2002; De Stefano *et al.*, 2003a). The protonation constants of PAM3 are significantly higher than those of polycarboxylic acids with the same mass (PMA: MW = 4 kDa; PAA: MW = 2.2 kDa), especially at α = 1; for example, protonation constant values at I = 0.5 mol L^{-1} in NaCl are: PAM3, log K_1^H = 6.01; PAM MW = 4 kDa, log K_1^H =5.67; PAA MW = 2.2 kDa, log K_1^H =.5.54, respectively. Moreover, for the protonation constants of other polyelectrolytes (**Table A.7**, Appendix A) we observed the following trend: PMA70 > PAA (MW = 22 kDa) > (MW = 5.4 kDa). This sequence can be explained by considering the dependence of formation constants on molecular weight, as already discussed (De Stefano *et al.*, 2003a).

Using the data reported here, it is possible to compare the alkaline earth metal-copolymer complex formation constants with those of simple

polyacrylates and polymethacrylates reported in other papers (Daniele *et al.*, 1999; De Stefano *et al.*, 2003b; De Stefano *et al.*, 2004); for example, the values of formation constants with Mg^{2+} and Ca^{2+} for PAA (MW = 2 kDa) at I = 0.5 mol L^{-1} and $\alpha = 1$, are log $K_1 = 2.43$, log $\beta_2 = 2.78$ for Mg^{2+}, and log $K_1 = 2.00$, log $\beta_2 = 4.52$ for Ca^{2+} (De Stefano *et al.*, 2004), respectively. These values are significantly lower than the alkaline earth-copolymer complex formation constants here reported, indicating copolymers to have a higher sequestering capability towards Mg^{2+} and Ca^{2+} than simple homopolymers.

In literature we found no further information on enthalpy and entropy changes in the protonation for poly(acrylic co-maleic) copolymers, but we can compare the values obtained by direct calorimetry with those obtained for the simple polyacrylates and polymethacrylates already studied by De Stefano *et al.* (2003c); for example the ΔH_m/kJ mol^{-1} values obtained for PAA (MW = 2.2 kDa) and PMA (MW = 3.4 kDa) at I = 0.1 mol L^{-1} in NaCl are 1.7 and 3.6; respectively. Thess values are in agreement with those of PAM3 at the same ionic strength and in same ionic medium; moreover, comparison can also be made for other values reported in **Table 4.1.5**.

4.1.6. Final remarks

In this work we have reported a large amount of data on the protonation and alkaline earth complexation of poly(acrylic-co-maleic) acids PAM3 and PAM70. The main results obtained by calorimetric and potentiometric investigations can be summarized as follows:

1) The protonation constants in NaCl are lower than those in Et_4NI and they generally decrease with increasing ionic strength; protonation constant values (and their trend as function of I) are comparable to those of low molecular weight polycarboxylic acids;

2) The dependence of protonation constants on ionic strength was taken into account using different equations, whose empirical parameters are given in **Table 4.1.2**, for both ionic media.

3) The difference in log K^H_x in both ionic media is due to the formation of weak complexes with sodium ion, whose formation constants were determined by a simple equation (4.1.10) by considering data in Et_4NI as baseline (not interacting medium);

4) The protonation constants of PAM70 are significantly higher (about one logarithmic unit for log K^H_1) than the protonation constants of PAM3 in

the same experimental conditions. This trend, already observed for other polycarboxylic acids (see **Table A.7**, Appendix A), can be explained considering that increased molecular weight increases the availability of polyelectrolyte charges for interaction with the cations; this is confirmed by comparing the protonation constants at I = 0.5 mol L^{-1} for PAM70, PAA (MW = 22 kDa), PMA (MW = 5.4 kDa).

5) The protonation constant values reported for both copolymers in electrolyte mixtures (NaCl-$MgCl_2$ and NaCl-$CaCl_2$) show that in multi-component mixtures (**Tables A.5** and **A.6**, Appendix A), protonation constants are much lower than corresponding constants in pure salt solution (NaCl), as a consequence of alkaline earth metal-copolymer complexation; the protonation constants in NaCl-$MgCl_2$ are higher than the corresponding constants in NaCl-$CaCl_2$;

6) Alkaline earth metal-copolymer complexes were determined by equation (4.1.20) which takes into account the dependence of formation constants on the degree of dissociation (α); the speciation model, which better fits the experimental data is the one that allows the formation of the species with stoichiometric coefficient 1:1 and 1:2 (metal:copolymer);

7) Alkaline earth metal-copolymer complex formation constants showed the same dependence on ionic strength and molecular weight as protonation constants; the stability of these complexes can be compared to that of tri-tetracarboxylic acids, denoting higher sequestering ability of poly(acrylic-co-maleic) acids towards Mg^{2+} and Ca^{2+}; for example for the systems BTC-Mg^{2+} and BTC-Ca^{2+} (BTC = 1,2,3,4 butantetracarboxylic acid) at I = 0.1 mol L^{-1} in NaCl we observe the following formation constant values, log K_{ML} = 3.01, 3.08 respectively; while for the systems TCA- Mg^{2+} and TCA-Ca^{2+} (TCA = 1,2,3 propantricarboxylic acid) at the same ionic strength values and the same ionic medium we have log K_{ML} = 2.20 and 2.24 (De Robertis *et al.*, 1993; De Stefano *et al.*, 1994). These values are lower than the stepwise formation constants values obtained for the most important species (ML_2) in the alkaline earth metal-copolymer systems (see **Table 4.1.4**). A comparison with alkaline earth metals-PAA and –PMA complex formation constants can also be made by the data reported in Daniele *et al.(*1999); De Stefano *et al.* (2003b); De Stefano *et al.*, (2004).

8) ΔH and $T\Delta S$ values for the protonation of PAM3 were determined by direct calorimetry and the results obtained show that their values are lower

and decrease with increasing ionic strength; we also determined enthalpy and entropy changes for protonation at infinite dilution and the dependence on ionic strength of ΔH and TΔS using simple equations. The TΔS values obtained show that the entropic contribution is the most important in the protonation reactions;

9) A linear relationship between TΔS and ΔG was found and this makes it possible to reduce experimental determinations.

4.1.7. References

Chitanu, G.C., Rinaudo, M., Desbrières, J., Milas, M. and Carpov, A. (1999). Nonalternating maleic acid copolymers in aqueous solution. *Langmuir*, **15**, 4150-4156.

Crea, F., De Robertis, A., De Stefano, C., Sammartano, S., Gianguzza, A. and Piazzese, D. (2001). Binding of acrylic and sulphonic polyanions by open-chain polyammonium cations. *Talanta*, **53**, 1241-1248.

Daniele, P.G., De Stefano, C., Ginepro, M. and Sammartano, S. (1999). Salt effects on the protonation of polymethacrylate and Na^+, K^+, Ca^{2+} complex formation. *Fluid Phase Equilibr.*, **163**, 127-137.

De Robertis, A., De Stefano, C., Rigano, C. and Sammartano, S. (1989). Computer analysis of equilibrium data in solution. ES5CM fortran and basic programs for computing formation enthalpies from calorimetric measurements. *Thermochim. acta*, **138**, 141-146.

De Robertis, A., Foti, C. and Gianguzza, A. (1993). Studies on polyfunctional O-ligands. Alkali and alkaline earth metal complexes of butanetetracarboxylate in aqueous solution. *Ann. Chim.*, **83**, 485-497.

De Stefano, C., Princi, P., Rigano, C. and Sammartano, S. (1985). Computer analysis of equilibrium data in solution. ESAB2M: an improved version of the ESAB program. *Ann. Chim.*, **77**, 643.

De Stefano, C., Foti, C. and Gianguzza, A. (1994). Salt effects on the protonation and on alkali and alkaline earth metal complex formation of 1,2,3-propanetricarboxylate in aqueous solution. *Talanta*, **41**, 1415-1722.

De Stefano, C., Sammartano, S., Mineo, P. and Rigano, C. (1997). Computer tools for the speciation of natural fluids. In: Gianguzza, A., Pellizzetti, E. and

Sammartano, S. (eds.), *Marine chemistry. An environmental analytical chemistry approach.*, pp. 71-83. Kluwer Academic Publishers, Amsterdam.

De Stefano, C., Gianguzza, A., Piazzese, D. and Sammartano, S. (2000). Polyacrylate protonation in various aqueous ionic media at different temperatures and ionic strengths. *J. Chem. Eng. Data*, **45**, 876-881.

De Stefano, C., Sammartano, S., Gianguzza, A. and Piazzese, D. (2002). Speciation of polyelectrolytes in natural fluids. Protonation and interaction of polymethacrylates with major components of seawater. *Talanta*, **58**, 405-417.

De Stefano, C., Gianguzza, A., Piazzese, D. and Sammartano, S. (2003a). Polyacrylates in aqueous solution. The dependence of protonation on molecular weigth, ionic medium and ionic strength. *React Funct Polym*, **55**, 9-20.

De Stefano, C., Gianguzza, A., Piazzese, D. and Sammartano, S. (2003b). Quantitative parameters for the sequestering capacity of polyacrylates towards alkaline earth metal ions. *Talanta*, **61**, 181-194.

De Stefano, C., Giuffrè, O., Pettignano, A. and Sammartano, S. (2003c). Thermodynamics of proton association of polyacrylates and polymethacrylates in NaCl(aq). *J. Solution Chem.*, **32**, 967.

De Stefano, C., Gianguzza, A., Piazzese, D. and Sammartano, S. (2004). Speciation of organic matter in natural waters-interaction of polyacrylates and polymethacrylates with major cation components in seawater. *Mar. Chem.*, **86**, 33-44.

Fukushima, M., Tanaka, S., Hasebe, K., Taga, M. and Nakamura, H. (1995). Interpretation of the acid-base equilibrium of humic acid by a continous pK distribution and electrostatic model. *Anal. Chim. Acta*, **302**, 365-373.

Högfeldt, E. (1988). A useful method for summarizing data in ion exchange. 4. Extension and application to weak acid and chelating resins. *J. Phys. Chem.*, **92**, 6475-6476.

Högfeldt, E., Miyajima, T., Marinsky, J.A. and Muhammed, M. (1989). Application of a simple three-parameter model to titration data for some linear polyelectrolytes. *Acta Chem. Scand.*, **43**, 496-499.

Katchalsky, A. and Spitnik, P. (1947). Potentiometric titrations of polymethacrylic acid. *J. Polym. Sci.*, **2**, 432-446.

Kitano, T., Kawaguchi, S., Anazawa, N. and Minakata, A. (1987). Dissociation behavior of an alternating copolymer in isobutilene and maleic acid by potenciometric tritatoin and intrinsic viscosity. *Macromolecules*, **20**, 2498-2506.

Masini, J.C., Abate, G., Lima, E.C., Hahn, L.C., Nakamura, M.S., Lichtig, J. and Nagatomy, H.R. (1998). Comparison of methodologies for determination of carboxylic and phenolic groups in humic acids. *Anal. Chim. Acta*, **364**, 223-233.

Morlay, C., Cromer, M., Mouginot, Y. and Vittori, O. (1998). Potentiometric study of Cu(II) and Ni(II) complexation with two high molecular weight poly(acrylicacids). *Talanta*, **45**, 1177-1188.

Morlay, C., Cromer, M., Mouginot, Y. and Vittori, O. (1999). Potentiometric study of Cd(II) and Pb(II) complexation with two high molecular weight poly(acrylic acids); comparison with Cu(II) and Ni(II). *Talanta*, **48**, 1159-1166.

Nemtoi, G.H. and Colonescu, L. (1999). Potentiometric tritation and electrostatic free energy of the copolyacid poly(acrylic acid-co-maleic acid) in aqueous solution. *Analele Stiintifice Ale Universitatii "Al. I. Cuza" Chimie*, **7**, 213-218.

Nicholson, J.W. (2000). Metal salts interaction with acrylic acid-maleic acid copolymer: an infrared spectroscopic study. *J. Appl. Polym. Sci.*, **78**, 1680-1684.

Ritchie, J.D. and Perdue, E.M. (2003). Proton-binding study of standard and reference fulvic acids, humic acids, and natural organic matter. *Geochim. Cosmochim. Acta*, **67**, 85-96.

Rivas, B.L. and Seguel, G.V. (1999). Poly(acrylic acid-co-maleic acid)-metal complexes with copper(II), cobalt(II), and nickel(II) synthesis, characterization and structure of its metal chelates. *Polyhedron*, **18**, 2511-2518.

Stevenson, F.J. (1982). *Humus chemistry, composition, reactions*. Wiley Interscience, New York.

4.2. Effect of the divalent cation on the proton binding equilibria of polyacrylic acid in mixed 1-1/1-2 electrolyte solutions: A non-linear Poisson-Boltzmann study

The influence of the relative amount of divalent salt on the acid/base behaviour of polyacrylic acid (PAA) in aqueous $KNO_3/Mg(NO_3)_2$ mixtures at 25ºC was simulated by means of the non-linear Poisson-Boltzmann (NLPB) equation in cylindrical geometry. The Finite Element Method scheme for the numerical solution of NLPB was coupled with ideal competitive isotherms in order to analyze the effect of the specific binding of the divalent cation. It is shown that, even in the absence of specific metal binding, a relatively small proportion of divalent ion may modify notably the surface potential on the macromolecule at low ionic strengths. The theoretical predictions are compared with experimental potentiometric titration data. The consideration of specific binding is able to account for the high screening effect of the magnesium ion observed experimentally and, also, for the dependence of the apparent protonation constants on the polymer concentration. The model is able to approximately describe the experimental data obtained at two different ionic strengths, using values of the structural parameters and intrinsic proton binding constant taken from literature, which were obtained from potentiometric experiments in pure KNO_3 aqueous solutions. Only one new additional parameter had to be incorporated, namely, the equilibrium constant for the magnesium ion - acrylate monomer complex.

4.2.1. Introduction

The complexation equilibria of synthetic polyelectrolytes have been extensively studied in the last decades (Katchalsky, 1971; Nagasawa, 1971; Högfeldt, 1988; Marinsky *et al.*, 1989; Marinsky, 1992; Porasso *et al.*, 1999; De Stefano *et al.*, 2003) due to their interest as model molecules of many biological and environmental systems such as polysaccharides, proteins or humic substances. As a result of the polyelectrolytic nature of these macromolecules, the dissociation of their ionisable groups and, consequently, the binding of inorganic ions, is greatly influenced by the net electric charge of the polyion.

The application of Poisson-Boltzmann equation to the modelling of electrostatic interactions in polyelectrolytes has become widespread in the last

decades (see, for instance, the reviews of Anderson and Record, 1990, Sharp and Honig, 1990, and Borkovec *et al.*, 2001). The fact that polyions often develop high local charge densities at environmental conditions requires carrying out the exact solution of the NLPB equation through numerical methods, since the Debye-Hückel approximation (that leads to the linearised PB equation) is not justified.

As well known, the Poisson-Boltzmann approach involves several rough simplifications (Lyklema, 1995). For instance, correlations among salt ions are neglected, and they are considered as point charges (so their finite size is disregarded); the solvent is considered to be a structureless continuum of constant permittivity; the surface charge is assumed to be homogeneous and smeared-out; etc. Despite these severe limitations, it has proved to work surprisingly well for the description of many thermodynamic properties of natural and synthetic macromolecules. As an example, in a very recent paper, Ni *et al.* (1999) compared the numerical solutions of the cylindrical Poisson-Boltzmann equation with canonical Monte Carlo simulations of the ion distributions around a DNA macromolecule in mixtures of univalent/divalent cations, finding a good agreement between both methods.

In this work, the interaction between diluted polyacrylic acid and divalent counterions in the presence of a supporting 1-1 salt is analyzed using the Poisson-Boltzmann equation for cylindrical geometry. Two types of interactions are considered: purely electrostatic interaction and site-specific binding. The influence of these effects is analyzed theoretically through numerical simulations. Experimental results of potentiometric titrations using a glass electrode are given for comparison. The goal here is not to obtain accurate fits to experimental data, but to explore how well a simple thermodynamic model of ion-polyion interactions may explain the major qualitative features of the experimental results. In this way, it is expected to gain insight into the physical-chemical nature of polyelectrolyte complexation and the parameters that control it.

4.2.2. Theoretical background

The proton binding equilibria of a polyelectrolyte can be described by the Henderson-Hasselbach equation:

$$\log K^{H} = pH - \log \frac{\alpha}{1-\alpha} \qquad (4.2.1)$$

where K^H is the apparent (i.e., conditional) protonation constant of the polyacid, and α is the dissociation degree. In this work, α will be defined as the fraction of sites *that are not protonated*, that is:

$$\alpha = \frac{c_{L,t} - c_{LH}}{c_{L,t}} \qquad (4.2.2)$$

where c_{LH} and $c_{L,t}$ are the concentrations of protonated sites and total functional groups, respectively. In the absence of specific binding, α will coincide with the fraction of *charged groups*. The use of this definition ensures that eq. (4.2.16), which is used for the experimental measurement of α (see below), will still be valid if specific metal binding occurs.

In general, K^H is a function of the dissociation degree (in contrast with simple ligands), as a consequence of different aspects such as the polyelectrolytic nature of these substances (Buffle, 1988). The observable change in Gibbs free energy related to the dissociation process is often split into two contributions, one representing the energy necessary to bring the proton from the surface site (at a potential ψ_0) to the bulk solution, and another representing an intrinsic binding term. Thus, the corresponding equilibrium constants will be related by:

$$\log K^{H} = \log K^{H}_{int} - \frac{F}{RT \ln 10}\psi_0 = \log K^{H}_{int} - \frac{1}{\ln 10}\tilde{\psi}_0 \qquad (4.2.3)$$

where $\tilde{\psi}_0 = F\psi_0/(RT)$ is a dimensionless potential, and K^H_{int} (the intrinsic constant) is assumed to be independent of α (the electrostatic effect is considered the only source of non ideal behaviour).

4.2.2.1. Effect of the proportion of divalent cation at infinite polymer dilution in absence of specific metal binding

Surface charge / surface potential relationship and potential profile over distance

Let us consider the following model for the polyelectrolyte solution (Anderson and Record, 1990): The solvent is regarded as a structureless continuum of constant permittivity, and the polyion molecule is modelled as an infinitely long and uniformly charged cylinder immersed in a mixed aqueous solution of 1:1 and 1:2 electrolytes of concentrations C_1 and C_2, respectively. It must be stressed that the use of the rod model for this linear polyelectrolyte only requires that its radius of curvature be large compared to the ionic atmosphere around the polyion skeleton. The macromolecule is considered long enough so that the coulombic end effects can be considered negligible.

Assuming that the spatial distributions of the salt ions surrounding the polyion follow the Boltzmann distribution, the variation of the mean-field electrical potential, $\psi(r)$, around the polyion can be obtained by solving the equation

$$\nabla^2\psi(r) = -\frac{eN_A}{\varepsilon}\sum_i C_i z_i \exp\left[-\frac{z_i e\psi(r)}{k_B T}\right] \qquad (4.2.4)$$

where r is the distance from the polyion axis, e is the elementary charge, N_A is the number of Avogadro, ε is the bulk dielectric constant, z_i and C_i are the valence and molar concentration of the ionic species i at an infinite distance from the polymer, respectively, k_B is the Boltzmann constant, and T is the temperature. For a mixture of 1:1 and 1:2 background electrolytes, this equation reads (see Appendix B):

$$\nabla^2\tilde{\psi} = \kappa^2\left\{\alpha_1 \sinh\tilde{\psi} + \alpha_2\left[\exp(\tilde{\psi}) - \exp(-2\tilde{\psi})\right]\right\} \qquad (4.2.5)$$

where κ is the reciprocal of Debye's length, $\tilde{\psi}$ is the dimensionless electrical potential, defined as above, and the coefficients α_i are defined in terms of the ratio $\rho = C_2/C_1$ as

$$\alpha_1 = \frac{1}{1+3\rho} \quad \text{and} \quad \alpha_2 = \frac{\rho}{1+3\rho} \qquad (4.2.6)$$

Note that when C_2=0, then α_1=1 and α_2=0 and thus the NLPB equation for a pure 1:1 salt solution is obtained. Similarly, if C_1=0, then α_1=0 and α_2=1/3, and hence the equation for a 1:2 electrolyte solution is recovered.

The boundary conditions for the present problem are:

$$\psi(\infty) = 0 \quad \text{and} \quad \left(\frac{d\psi}{dr}\right)_{r=a} = -\frac{\sigma}{\varepsilon} \tag{4.2.7}$$

where a is the radius of the cylinder and σ is the surface charge density, which is usually expressed in terms of ξ^{cyl}, the structural linear charge density, defined as

$$\xi^{cyl} = \frac{l_B}{b} \tag{4.2.8}$$

This parameter relates the distance between consecutive functional groups (mean axial charge spacing), b, with the Bjerrum length, l_B (see Appendix B).

Eq. (4.2.5) was solved in cylindrical geometry using the Finite Element Method in order to obtain the potential profile ψ(r) and, in particular, the value of the surface potential, ψ_0. The details are described in Appendix B.

Calculation of counterion accumulation / coion exclusion

The local density, $c_i(r)$, of each ion *i*, in units of molarity, can be represented as a function of the radial coordinate r. The counterion accumulation and co-ion exclusion arising from salt ion-polyion interactions can be evaluated by integrating the difference between the nonuniform radial distributions of the salt ions surrounding the macromolecule and the uniform ion distribution in a corresponding reference solution, where interactions involving the polyion are absent (Ni *et al.*, 1999):

$$\Gamma_i = 2\pi b N_A 10^{-24} \int_a^R (c_i(r) - C_i) r dr - \pi b N_A 10^{-24} C_i a^2 \tag{4.2.9}$$

In this equation Γ_i represents the excess (or defect) number of moles of the ion species i in the diffuse layer around the macromolecule per mol of polyion monomer unit. Note that the distances are expressed in nanometers and the concentrations in mol/L. The second term on the right represents the contribution of the volume excluded to the salt ions by the polyion (considered a hard cylinder). In general, this term can be considered negligible for the supporting salt ions. The upper integration limit in eq. (4.2.9), R, should be infinite, for an infinitely diluted polymer solution, or the cell radius if a cell

model of the polyelectrolytic solution is considered (Katchalsky, 1971; Deserno and Holm, 2001). In practice, integration is carried over the annular volume around the cylinder where $c_i(r)$ and C_i are significantly different.

If we assume that the local ion concentrations in the diffuse layer follow the Boltzmann distribution, eq. (4.2.9) becomes:

$$\Gamma_i = 2\pi b N_A 10^{-24} C_i \int_a^R \left\{ \exp\left[- z_i \tilde{\psi}(r) \right] - 1 \right\} r dr \qquad (4.2.10)$$

The values of Γ_i have been obtained by numerical integration using the $\tilde{\psi}(r)$ profiles calculated as explained in Appendix B.

4.2.2.2. Coupling of the NLPB electrostatic model with proton/metal competitive isotherms

The specific binding of proton and metal ions were assumed to be described by the following ideal competitive Langmuir isotherms for 1:1 metal binding:

$$\theta_H = \frac{K^H_{int}\left[H^+\right]_0}{1 + K^H_{int}\left[H^+\right]_0 + K^M_{int}\left[M^{2+}\right]_0} \qquad (4.2.11)$$

$$\theta_M = \frac{K^M_{int}\left[M^{2+}\right]_0}{1 + K^M_{int}\left[H^+\right]_0 + K^M_{int}\left[M^{2+}\right]_0} \qquad (4.2.12)$$

where θ_H and θ_M are the macromolecular coverages of proton and metal ions, respectively, K^M_{int} is the intrinsic formation constant of the metal ion-carboxylate complex, and the subscript $_0$ denotes local concentrations at the polymer surface.

The charge on the polymer molecule, Z, now depends on both θ_H and θ_M, and may be calculated as:

$$Z = N\left(1 - \theta_H - 2\theta_M\right) \qquad (4.2.13)$$

where N is the average number of acid groups per macromolecule. Note that it has been assumed (a) that each divalent ion neutralizes two charges of the polymer and (b) that proton and metal ions compete for the same sites.

In eqs. (4.2.11) and (4.2.12) the proton and metal concentrations at the surface of the macromolecule are related to the bulk solution concentrations through the following equations:

$$\left[H^+\right]_0 = \left[H^+\right]_{bulk} \exp\left(-\tilde{\psi}_0\right) \text{ and } \left[M^{2+}\right]_0 = \left[M^{2+}\right]_{bulk} \exp\left(-2\tilde{\psi}_0\right) \qquad (4.2.14)$$

where $\tilde{\psi}_0$ is given by the NLPB equation.

Moreover, the free metal ion concentration is calculated from the total concentration, $[M^{2+}]_{total}$, through the mass balance

$$\left[M^{2+}\right]_{bulk} = \left[M^{2+}\right]_{total} - c_{L,t}\theta_M \qquad (4.2.15)$$

For simplicity, the amount of cation accumulated in the diffuse layer (i.e., non specifically bound) has not been taken into account in this equation. As will be discussed in Section 4.2.4, this amount may be significant for finite polymer concentrations, at the conditions of the present study. Hence, a more accurate model should be developed in the future (for instance, by explicitly including the mass balance of all the ions in the Finite Element Method scheme for the numerical solution of NLPB).

The nonlinear set of equations (4.2.11)-(4.2.15) was solved iteratively using the Newton-Raphson method with numerical estimates of the partial derivatives of the jacobian matrix (Press *et al.*, 1986). The tolerance criterion for the proton and metal coverages was 10^{-6}.

4.2.3. Experimental

Reagents

Polyacrylic acid, PAA, (35% solution in water, average molecular weight 250 kDa) was purchased from Aldrich and used without further purification treatment. KNO_3 and $Mg(NO_3)_2$ Merck p.a. were used as supporting electrolytes. HNO_3 and KOH 0.1 M Merck Titrisol were used as standard

solutions. Ultrapure water (Milli-Q system, from Millipore) was used throughout the experiments.

Equipments and procedure

Potentiometric measurements were carried out with an Orion Research Ionanalyzer 720A and a Metrohm 665 Dosimat automatic burette attached to a personal computer through a RS232 card, and controlled by means of home-made data acquisition software. The titrations were performed in a glass jacketed cell thermostated at 25.0 ± 0.1 ºC, and the sample solutions, magnetically stirred, were preserved from atmospheric O_2 and CO_2 by a stream of pure N_2. Antidiffusing tips were used with the automatic burette, to avoid slow diffusion of the titrant between additions.

The free hydrogen concentrations were measured using an Orion 8101 glass electrode coupled with a Ag/AgCl reference electrode. The electrode couple was standarised in terms of pH = -log[H^+] by titrating aqueous solutions of HNO_3 and supporting electrolyte having the same ionic strength as the sample solutions, following Gran method (Gran, 1952; Gans and O'Sullivan, 2000).

From the experimental pH vs. titrant volume data, the degree of dissociation of PAA, α, can be easily calculated from simple charge balance considerations:

$$\alpha = 1 - \theta_H = \left(\left[H^+\right] + \frac{vC_{KOH}}{V_0 + v} - \frac{K_w}{\left[H^+\right]} \right) \frac{1}{c_{L,t}} \qquad (4.2.16)$$

where v and C_{KOH} are the volume and molar concentration of the titrant solution, V_0 is the initial sample volume, K_w is the ionic product of water, and $c_{L,t}$ is the polymer concentration on a monomer basis (where dilution due to the titrant addition must be properly accounted for). Recall from eq. (4.2.2) that α represents the fraction of sites that are not bound to protons. Therefore, eq. (4.2.16) is valid even in the presence of specific metal binding, if one neglects the accumulated concentration in the diffuse layer (non-specific binding).

4.2.4. Results and Discussion

The values of the structural and intrinsic parameters of PAA were taken from Companys (2003) (see **Table 4.2.1**). In this work, the NLPB model was applied to the analysis of PAA potentiometric titrations in KNO_3 at different ionic strengths (from 0.005 to 0.1 M), and it was found that the values listed in **Table 4.2.1** provided a good correction for the electrostatic effects. These values are in agreement with the results of Nagasawa *et al.*, 1965. Moreover, the value of pK^H_{int} agrees with the published thermodynamic constant for acetic acid, 4.78 (Barriada *et al.*, 2000), if we take into account the different reference states for the activity coefficients (zero surface potential for the polyelectrolyte and zero ionic strength for the acetic acid). A Debye-Hückel correction term of minus 0.19-0.52 log units was suggested by Bartschat *et al.*, 1992 in order to correct the simple ligand constant. The parameters listed in **Table 4.2.1** will be used throughout this work, and, therefore, they will be considered independent of the amount of magnesium nitrate. The effects of short range repulsions between the polyion and each small ion could be included, in a restricted primitive model, by means of a suitable choice of *a* (Anderson and Record, 1990), which could account for the different radii of the hydrated counterions. However, this effect will not be considered in this study.

Table 4.2.1. Structural and intrinsic parameters for PAA in aqueous KNO_3 solutions, obtained by solving Poisson-Boltzmann in cylindrical symmetry (Companys, 2003).

Parameter	Value
cylinder radius, a (nm)	0.55
separation between carboxylate groups, b (nm)	0.25
structural charge density, ξ^{cyl}	2.85
pK^H_{int}	4.27 ± 0.04

4.2.4.1. NLPB simulations of the divalent cation effect at constant ionic strength, in absence of specific metal binding

The calculated values of the dimensionless surface potential, $\tilde{\psi}_0$, as a function of the degree of dissociation and the percentage of divalent cation at different overall ionic strengths are plotted in **Figure 4.2.1**. We notice that at a

fixed dissociation degree and medium composition, the surface potential decreases as the overall ionic strength increases, as a result of the higher screening effect from the ionic environment. Furthermore, it can be observed that, even at constant ionic strength and polymer charge density, the surface potential decreases as the relative amount of 1-2 salt increases, due to the more effective screening effect of the divalent ion with respect to the monovalent one. As a consequence, the ionic strength alone does not constitute an appropriate magnitude to characterize the potentiometric behaviour of the polyelectrolyte.

It is interesting to note that the potential (and, therefore, the apparent dissociation constant) is very sensitive to a small proportion of divalent salt, which is especially remarkable at low ionic strengths. This fact is more clearly noticeable in **Figure 4.2.2**, which shows a plot of the derivative of $\tilde{\psi}_0$ (with respect to y_0) versus $-\log(y_0)$. Recall from Appendix B that $y_0 = \kappa \cdot a$, and hence y_0 is proportional to $I^{1/2}$. Therefore, these plots can be regarded as an indication of the surface potential response to small variations in the medium ionic strength, for different monovalent/divalent ratios. For the particular case of α = 0.5, it can be noted that below an approximate ionic strength of 0.05 $mol \cdot L^{-1}$ (which corresponds to a $-\log(y_0)$ value of around 0.3), the presence of a very small amount of divalent cation induces the slope of $\tilde{\psi}_0$ vs. I to change abruptly and to approach the value for a pure 1-2 salt solution. Bearing this in mind, the overall ionic strengths of 0.01 and 0.1 $mol \cdot L^{-1}$ (below and above the value of the maximum in **Figure 4.2.2** for α = 0.5) were chosen as experimental conditions for this study.

The potential profiles in the diffuse layer, calculated through NLPB, are shown in **Figure 4.2.3** (overall ionic strength: 0.01 M) and **Figure 4.2.4** (overall ionic strength: 0.1M). From these results, we can point out the following comments. The absolute value of the dimensionless potential is a monotonically decreasing function of the distance that becomes almost zero at a few Debye lengths from the polymer axis, regardless of the ionic strength and the proportion of divalent ion. The slope of the potential at r = a is proportional to the surface charge density (this is one of the boundary conditions, eq. (4.2.7)). As a result, the value of the slope at the polymer surface remains constant regardless of the bulk composition (for a fixed dissociation degree).

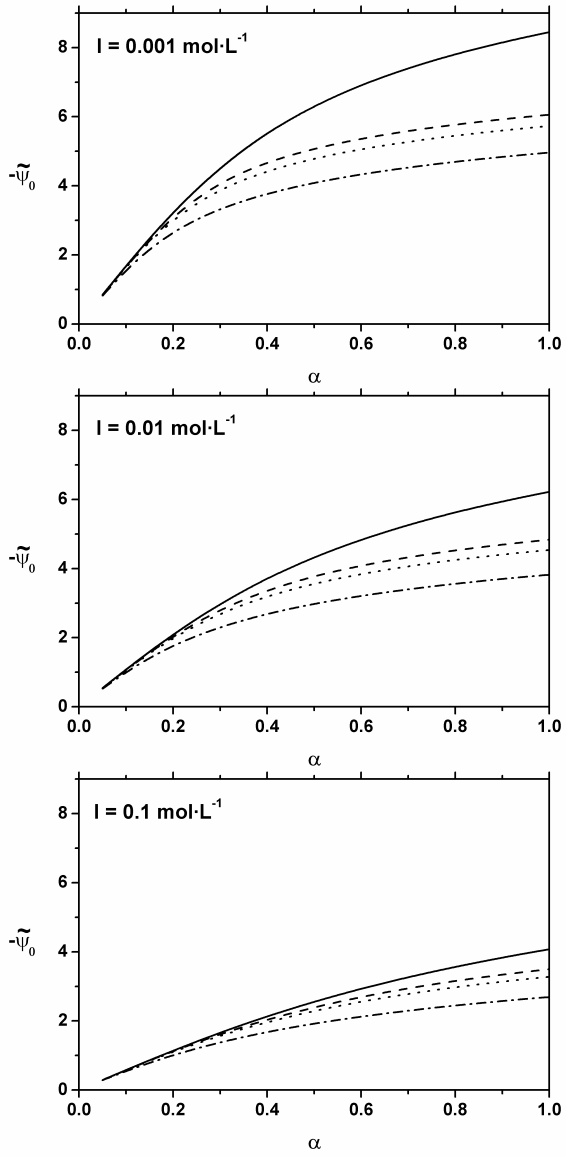

Figure 4.2.1. Dimensionless surface potential calculated through NLPB for PAA in different electrolyte mixtures at a constant overall ionic strength (indicated in the legends): pure 1-1 salt solution (solid lines), 10% of the ionic strength due to the 1-2 salt (dashed lines), 20% of the ionic strength due to the 1-2 salt (dotted lines), and pure 1-2 salt solution (dash-dotted lines).

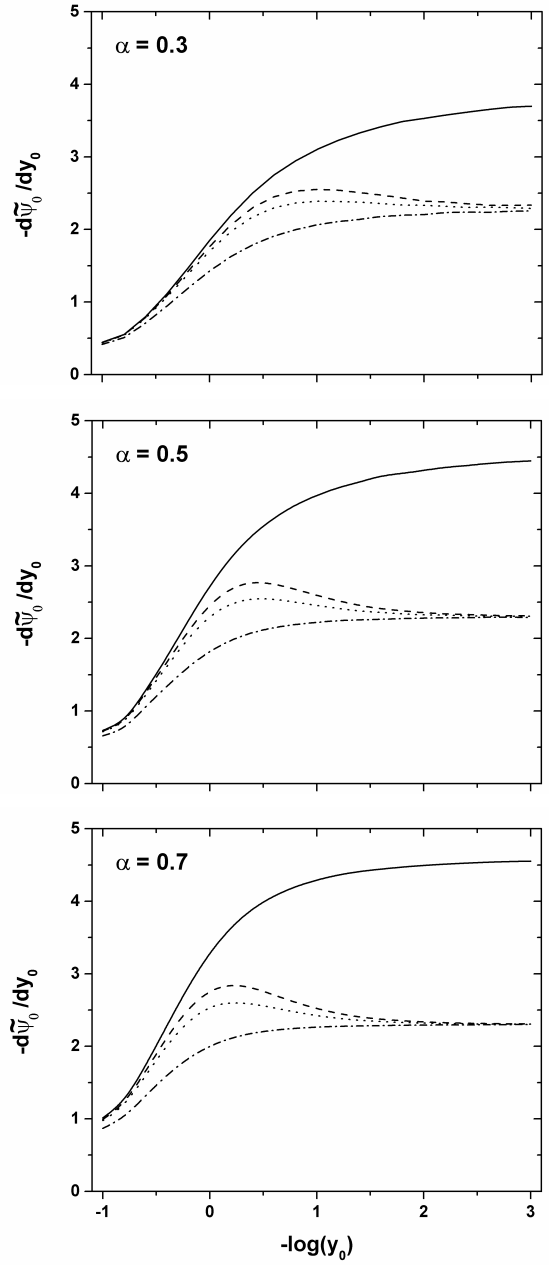

Figure 4.2.2 Derivative of the surface potential (with respect to $y_0=\kappa a$) versus $-\log(y_0)$, in different electrolyte mixtures: pure 1-1 salt solution (solid lines), 10% of the ionic strength due to the 1-2 salt (dashed lines), 20% of the ionic strength due to the 1-2 salt (dotted lines), and pure 1-2 salt solution (dash-dotted lines).

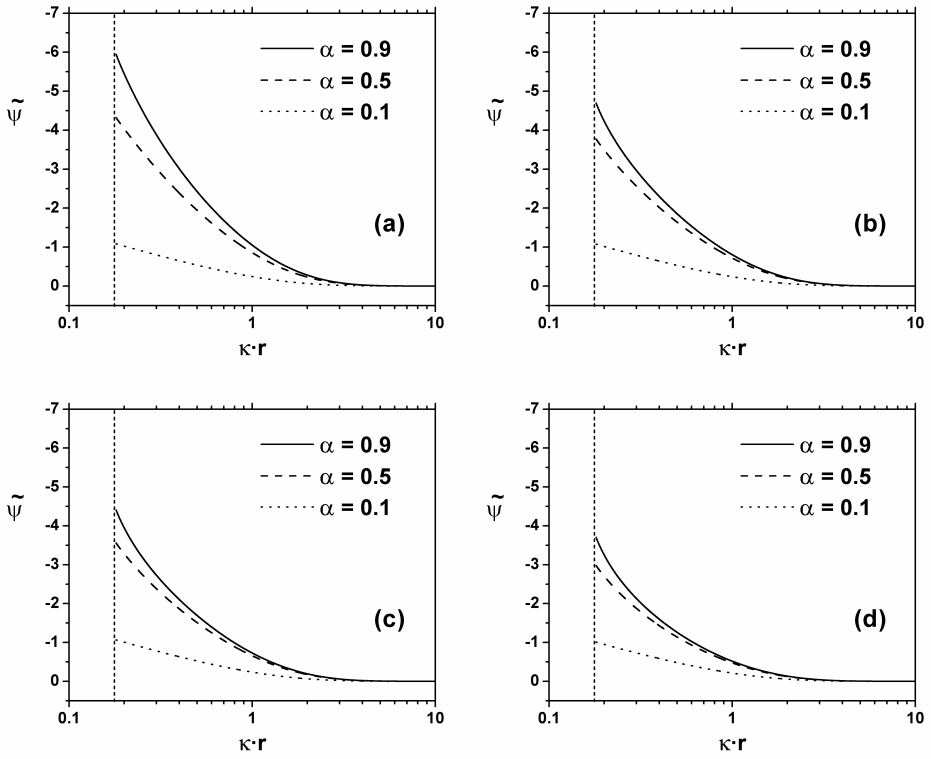

Figure 4.2.3 Dimensionless potential versus y = κr, calculated by NLPB (without considering specific metal binding) in different electrolyte mixtures: pure 1-1 salt solution (a), 10% of the ionic strength due to the 1-2 salt (b), 20% of the ionic strength due to the 1-2 salt (c), and pure 1-2 salt solution (d). Overall bulk ionic strength: 0.01 M. Note the logarithmic scale of the x-axis.

The impact of the dissociation degree on the potential profile is greater than that of the mixture composition. Despite this, it can be noticed that the effect of the divalent ion is much more evident at high α values. For instance, if we compare **Figure 4.2.3** panels (a) and (d) we see that in the pure 1-2 salt solution at α = 0.9 the surface potential is 38% lower than in the absence of divalent ion, whereas at α = 0.1 it has just decreased by 7%. The influence of the bulk composition decreases as ionic strength increases (compare with **Figure 4.2.4**). These observations are in agreement with **Figure 4.2.1**.

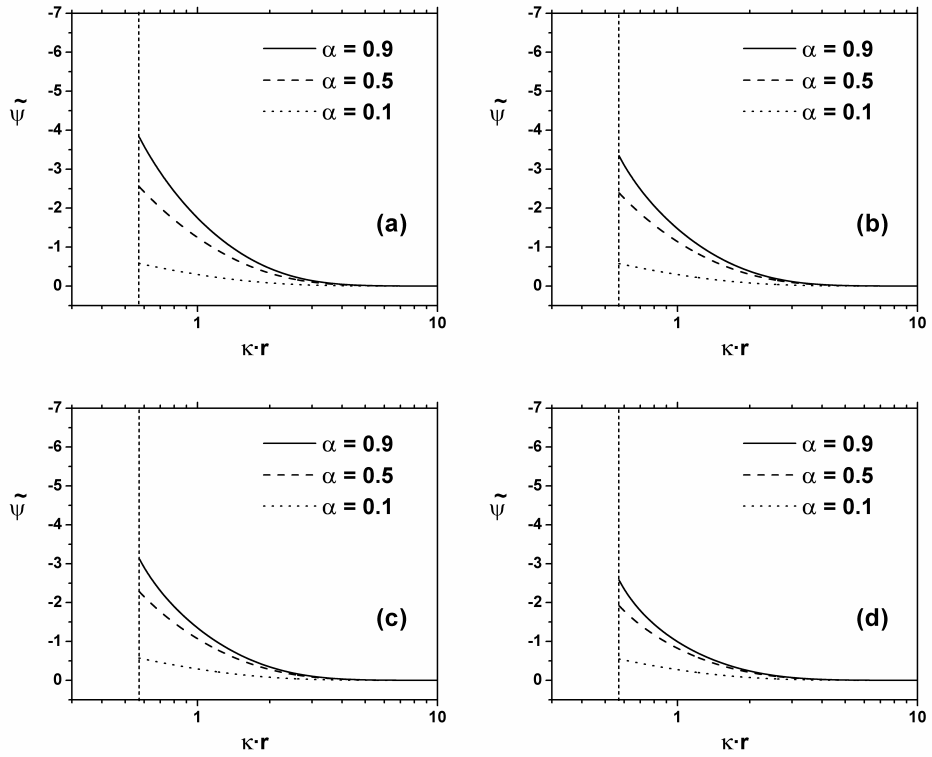

Figure 4.2.4. Dimensionless potential versus y = κr, calculated by NLPB (without considering specific metal binding) in different electrolyte mixtures: pure 1-1 salt solution (a), 10% of the ionic strength due to the 1-2 salt (b), 20% of the ionic strength due to the 1-2 salt (c), and pure 1-2 salt solution (d). Overall bulk ionic strength: 0.1 M. Note the logarithmic scale of the x-axis.

A logarithmic plot of the NLPB radial distributions of divalent and monovalent cations is shown in **Figure 4.2.5**. We notice that the local concentration of both ions increases in several orders of magnitude throughout the diffuse layer from the bulk solution to the polymer surface. The steepness of the ion concentration gradient increases with the dissociation degree, and shows much higher values for the divalent ion. Besides, it may be observed that the presence of the divalent cation in the ionic cloud is greatly favoured over the monovalent one: for instance, in panels (b) and (c) of **Figure 4.2.5** the surface/bulk concentration ratio for Mg^{2+} is around two orders of magnitude larger than for K^+.

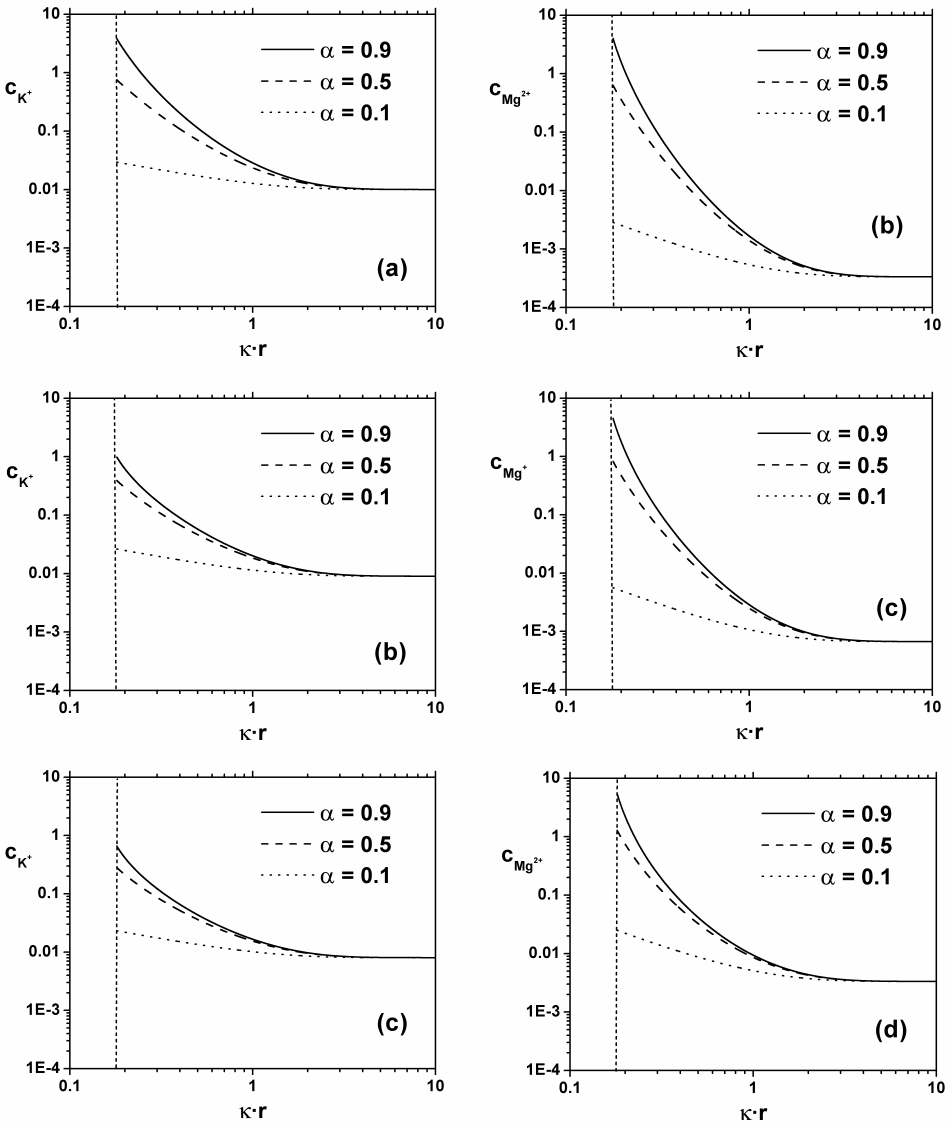

Figure 4.2.5 Counterion local concentration versus y = κr, calculated by NLPB (without considering specific metal binding) in different electrolyte mixtures: pure 1-1 salt solution (a), 10% of the ionic strength due to the 1-2 salt (b), 20% of the ionic strength due to the 1-2 salt (c), and pure 1-2 salt solution (d). Overall bulk ionic strength: 0.01 M. Note the logarithmic scale of both axes.

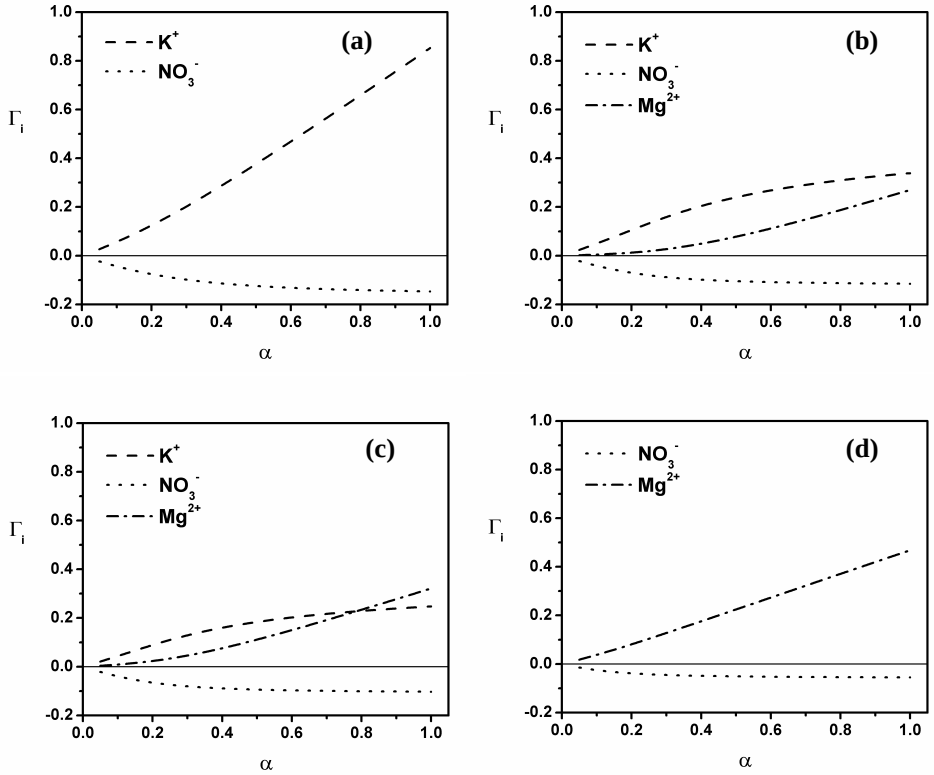

Figure 4.2.6 Excess/defect moles of counter/co-ions in the diffuse layer per mol of PAA monomer, calculated from eq. (4.2.10) for different electrolyte mixtures (in absence of specific metal binding): pure 1-1 salt solution (a), 10% of the ionic strength due to the 1-2 salt (b), 20% of the ionic strength due to the 1-2 salt (c), and pure 1-2 salt solution (d). Overall bulk ionic strength: 0.01 M.

The integration of the difference between the local and bulk ion concentrations over the whole thickness of the diffuse layer allows to calculate the ion accumulation/exclusion, eq. (4.2.10). The results are plotted in **Figure 4.2.6**. We may notice a practically linear dependence of Γ with α for pure electrolyte compositions, especially for the divalent case (d). Note also that Γ for the monovalent cation in mixtures barely increases above $\alpha = 0.6$ (b and c). It may be observed that the excess of divalent ion increases rapidly as the polymer charge density and the bulk M^{2+} concentration increase.

4.2.4.2. Comparison with experimental data

Some results obtained in the absence of divalent cation are shown in **Figure 4.2.7**. It can be observed that the reproducibility of the titrations is excellent. Moreover, the repetition of the titrations with a polymer concentration one order of magnitude lower shows virtually no difference at this ionic strength (as shown in the figure), which means that these results were obtained within the high salt regime (Borkovec *et al.*, 2001). Therefore, in these conditions the assumption of infinite polymer dilution seems justified. In fact, at the highest ionic strength no influence of the polymer concentration was observed in the range 2.5-0.25 mM at any monovalent to divalent counterion ratio (see **Figure 4.2.8**).

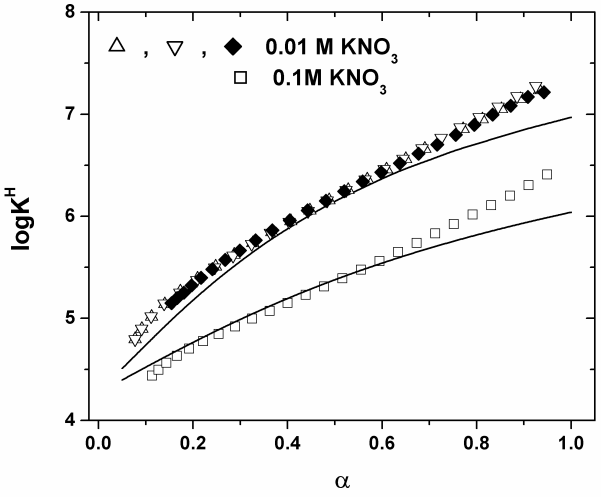

Figure 4.2.7. Experimental potentiometric titration data for PAA in 0.01 M KNO_3 and 0.1 M KNO_3. In the former case, two polymer concentrations are displayed, showing the good reproducibility of the experiments and the fulfilment of the high salt regime test for the data obtained in absence of divalent cation. The lines represent the NLPB calculations. Polymer concentrations (on a monomer basis): $2.5 \cdot 10^{-3}$ M (open symbols) and $2.5 \cdot 10^{-4}$ M (filled symbols).

From **Figure 4.2.7** we also notice that the spacing between the experimental titration curves obtained at both ionic strengths is in good agreement with the NLPB model predictions (with no adjustable parameter to improve the fitting), as expected for a good correction of the electrostatic effects. However, the theoretical curves do not reproduce very well the experimental data at the lowest and highest α values. The deviation at low values of α may probably be due, apart from the limitations of the PB model, to the flexibility of the backbone chain (Nagasawa *et al.*, 1965).

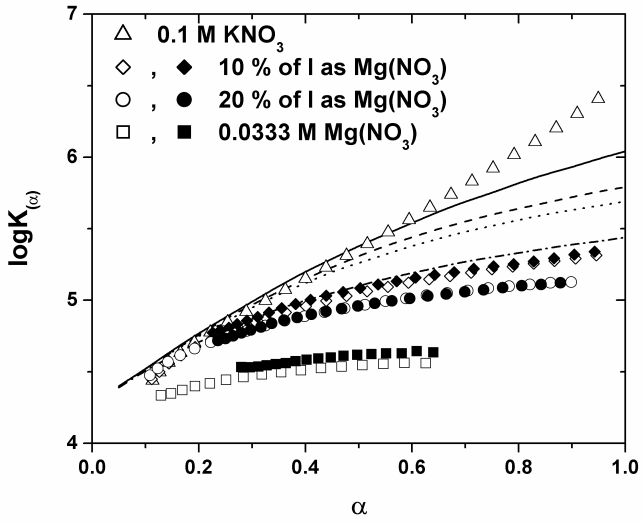

Figure 4.2.8. Apparent protonation constant of PAA at an overall ionic strength of 0.1 M in different electrolyte mixtures. PAA monomer concentration: $2.5 \cdot 10^{-3}$ M (open symbols) and $2.5 \cdot 10^{-4}$ M (filled symbols). The lines represent NLPB calculations assuming infinite polymer dilution and absence of Mg^{2+} specific binding (the key to the line styles is the same as in **Figures 4.2.1** and **4.2.2**).

Even though the NLPB equation predicts the trend, the variation of the experimental titration curves with the ratio of divalent/monomer cation (**Figure 4.2.8**) is larger than calculated by the model, as if the screening effect of the divalent ions was more effective than expected from purely electrostatic interactions. Furthermore, the fact that NLPB predicts unrealistic divalent ion concentrations at the macromolecule surface for the highest dissociation degrees (see **Figure 4.2.5** panels b, c and d), may indicate the necessity of considering the existence of local binding to the polymer carboxylic groups (see below).

4.2.4.3. Effect of the finite polymer concentration

While the titrations performed in pure 0.01M KNO_3 seem to belong to the high salt regime conditions (see **Figure 4.2.7**), in the presence of divalent cation at the same ionic strength, the apparent protonation constant shows a striking dependence on the polymer concentration (see **Figure 4.2.9** and **Figure 4.2.10**), especially for large α values. It is especially remarkable that the observed behaviour (the apparent pK decreases on decreasing the concentration of PAA) is just opposite to the trend observed by Nagasawa *et al.* (1965) with PAA in pure KNO_3 solutions (at higher polymer concentrations than the present study). This author reported an inverse linear relationship between $\log K^H$ and the square root of the polymer concentration.

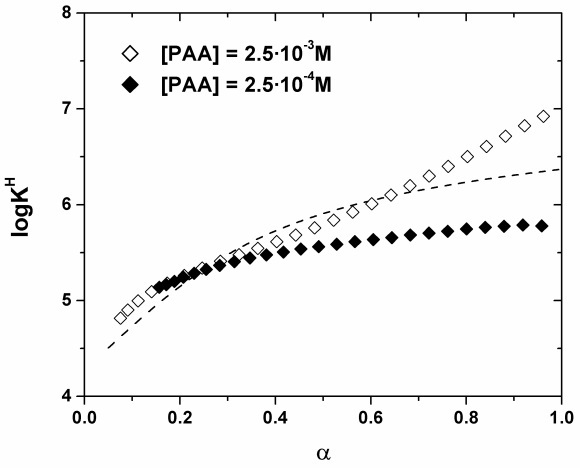

Figure 4.2.9. Apparent protonation constants of PAA at an overall ionic strength of 0.01 M, in the presence of 0.33 mM $Mg(NO_3)_2$. (10% of the ionic strength due to the 1-2 salt) The PAA concentrations are indicated in the legends. The line represents the NLPB calculations assuming infinite polymer dilution and absence of Mg^{2+} specific binding.

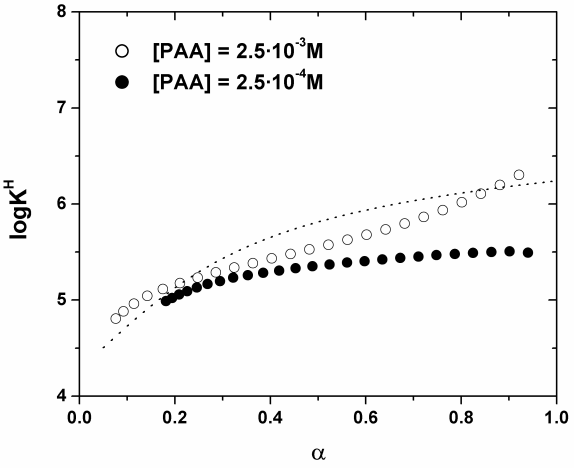

Figure 4.2.10. Apparent protonation constants of PAA at an overall ionic strength of 0.01 M, in the presence of 0.66 mM $Mg(NO_3)_2$ (20% of the ionic strength due to the 1-2 salt). The PAA concentrations are indicated in the legends. The line represents the NLPB calculations assuming infinite polymer dilution and absence of Mg^{2+} specific binding.

So far, it has been implicitly assumed that C_i (the ion concentration at the region of the solution where $\psi = 0$) is equal to the bulk concentration of species i. This assumption is strictly valid only at infinite polymer dilution. For polymer solutions of finite concentrations, Katchalsky *et al.* (1966) proposed the consideration of a *cell model*. This model assumes that charged colloidal particles repel each other so that the average inter-particle distances are maximum. Therefore, a unit volume of a solution containing c_p polyions can be divided into c_p cells of volume V_{cell}, so that $c_p V_{cell} = 1$. Each cell is considered electroneutral. The centrally located macroion creates within the cell an electrostatic potential of cylindrical symmetry (see **Figure 4.2.11**). Due to symmetry reasons, the potential reaches a minimum in the cell boundary (R). As pointed out by Katchalsky, the terms C_i in eq. (4.2.4) *are not*, in general, equal to the average salt ion concentrations (that, is, the analytical concentrations). Instead, they represent, the concentrations at the cell boundary (R), where the potential is defined as $\tilde{\psi}(R) = 0$. The boundary concentrations can be rigorously defined by the normalization conditions (Katchalsky *et al.*, 1966):

$$C_i \int_V \exp\left[-z_i \tilde{\psi}(r)\right] dV = C_{iT} V_{cell} \qquad (4.2.17)$$

where C_i and C_{iT} represent the ion concentration at the cell boundary and the average (analytical) concentration, respectively. The integration is carried out over the cell volume, V_{cell}.

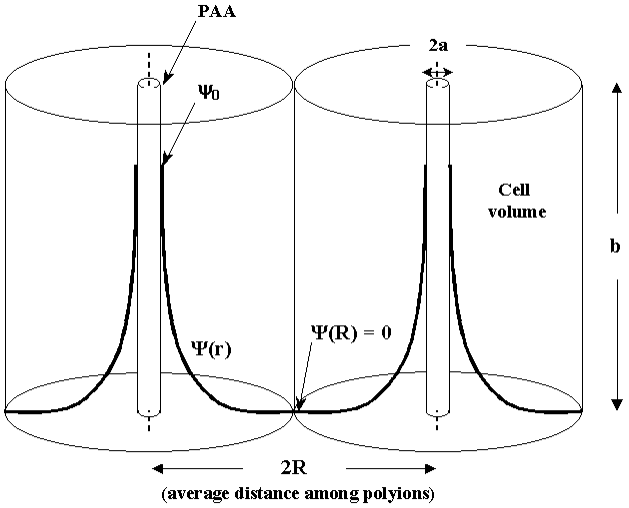

Figure 4.2.11. Cell model for a polyelectrolyte solution of finite concentration (after Katchalsky *et al.*, 1966)

Only in the limiting case of excess of supporting salt and infinite dilution of polyelectrolyte, we can assume $C_i = C_{iT}$. Throughout this chapter, the calculations have been carried out for this limiting case, which can be considered adequate for most studies of diluted polyelectrolyte solutions with excess of 1:1 supporting salts. Anderson and Record (1990) reported that the errors involved in this assumption are usually less than 5-10%, as long as $c_{L,t} < 0.3 \cdot C_{iT}$ for all i. However, in mixed 1:1/1:2 electrolyte solutions at moderately low ionic strengths, even at very diluted polymer concentrations, it may happen that the approximation $C_i = C_{iT}$ for the divalent cation is not justified. This is demonstrated, in our particular case, by the calculated values of the divalent ion accumulation in the diffuse layer (**Figure 4.2.6**). As a matter of example, for PAA in the presence of a background salt solution composed of 9 mM KNO_3 and 0.33 mM $Mg(NO_3)_2$, we see from the results of **Figure 4.2.6** (b) that around 0.2 mol of Mg^{2+} would theoretically be accumulated in the diffuse layer per mol of carboxylate groups at $\alpha = 1$, which represents the same order of magnitude as the total amount of magnesium ion for a polymer concentration of

2.5 mM. Obviously, this effect will have a significant influence on the experimental titration behaviour of the polyelectrolyte.

4.2.4.4. Simulations of the influence of specific divalent cation binding

The influences of the intrinsic metal binding constant, overall ionic strength, relative amount of divalent cation, and polymer concentration on the conditional protonation constants were investigated through numerical simulations, as detailed above. The value of 1.3, close to the thermodynamic formation constant of the complex Mg-acetate, which is 1.27 (Martell and Smith, 1977), was chosen as a starting value for $\log K^{M}_{int}$ in eqs. (4.2.11) and (4.2.12), by analogy with the correspondence between the intrinsic protonation constant of PAA and that of the acetic acid. Recall that the simple ligand constant must be corrected for the zero potential reference state, and therefore the appropriate value should be somewhat lower than 1.3.

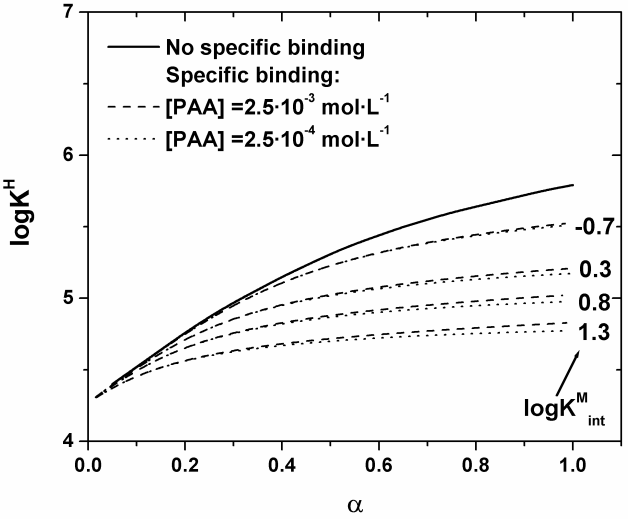

Figure 4.2.12. Theoretical estimates of the apparent protonation constants of PAA in the presence of 3.33 mM $Mg(KNO_3)_2$ (at an overall ionic strength of 0.1 M), calculated using NLPB coupled with ideal Langmuir competitive isotherms for the 1:1 binding of Mg^{2+} ions. The values of $\log K^{M}_{int}$ are indicated in each case. The solid line represents the NLPB calculations assuming negligible specific binding and infinite polymer dilution.

One can see in **Figure 4.2.12** that increasing the $\log K^{M}_{int}$ value leads to diminishing the conditional proton binding. For a fixed α, a stronger specific binding constant of the divalent cation means that a larger proportion of the macromolecule charge is neutralized with metal cations and thus the maximum available charge is smaller, which, in turn, decreases the calculated surface potential and, therefore, the apparent protonation constant. In addition, the non-specific binding of counterions due to accumulation in the diffuse layer is expected to decrease as the effective surface charge decreases.

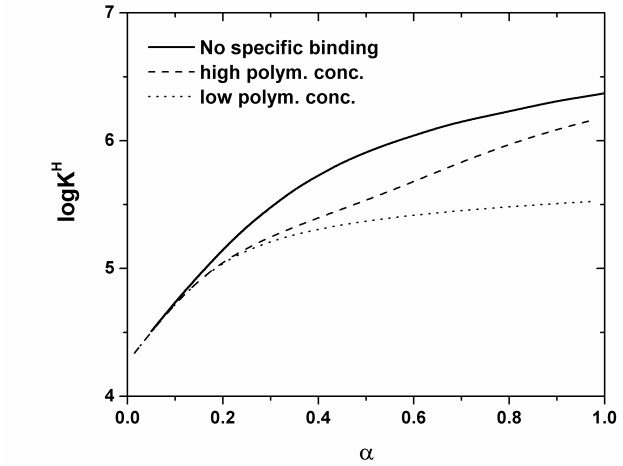

Figure 4.2.13. Theoretical estimates of the apparent protonation constants of PAA in 9 mM KNO_3 and 0.33 mM $Mg(NO_3)_2$ (total ionic strength: 0.01M), calculated through NLPB coupled with ideal Langmuir competitive isotherms for the 1:1 binding of Mg^{2+} ions, using $\log K^{M}_{int} = 0.8$. Dashed lines: [PAA] = 2.5 mM; dotted lines: [PAA] = 0.25 mM; solid line: NLPB calculations assuming negligible specific binding and infinite polymer dilution.

Although the rigorous calculation of NLPB should consider the normalization condition within the cell, eq. (4.2.17), in order to accurately account for the polymer concentration effect, we may suggest an explanation for experimental results shown in **Figure 4.2.9** and **Figure 4.2.10** in terms of the specific binding of metal ions. The mass balance for the metal ions, eq. (4.2.15), imposes a constraint on the NLPB-competitive Langmuir model. It may happen that the specific binding of metal ions causes a depletion of these ions in the bulk and, therefore, the charge neutralization of the polymer does not reach the same level as in large metal excess conditions. In other words, the difference

between high and low polymer concentration might be due to the competition for a different number of binding sites in the solution volume. This explanation is supported by the numerical simulations shown in **Figure 4.2.13** and **Figure 4.2.14**. On the other hand, at the highest ionic strength (0.1 M) almost no difference in the NLPB-competitive Langmuir calculations is observed between 0.25 and 2.5 mM polymer concentrations (compare dashed and dotted lines in **Figure 4.2.12**).

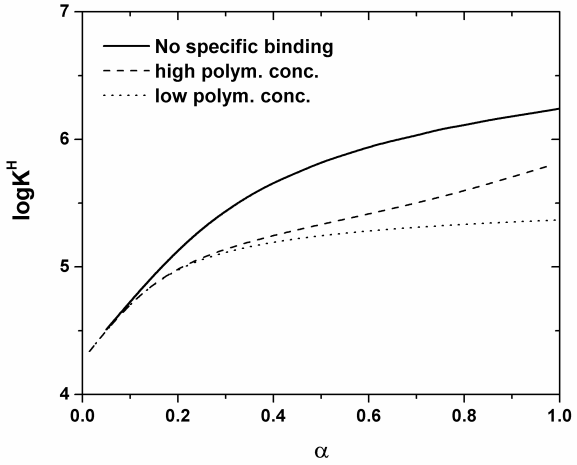

Figure 4.2.14. Theoretical estimates of the apparent protonation constants of PAA in 8 mM KNO_3 and 0.66 mM $Mg(NO_3)_2$ (total ionic strength: 0.01M), calculated through NLPB coupled with ideal Langmuir competitive isotherms for the 1:1 binding of Mg^{2+} ions, using $\log K^M_{int}$ = 0.8. Dashed lines: [PAA] = 2.5 mM; dotted lines: [PAA] = 0.25 mM; solid line: NLPB calculations assuming negligible specific binding and infinite polymer dilution.

Finally, we may also see that the NLPB model coupled with 1:1 competitive isotherms is able to describe the large screening effect due to the magnesium ions, observed at the highest ionic strength (**Figure 4.2.15**). It can be observed that the use of a value of 0.3 for the intrinsic metal binding constant yields a satisfactory (though not perfect) agreement between theoretical and experimental results.

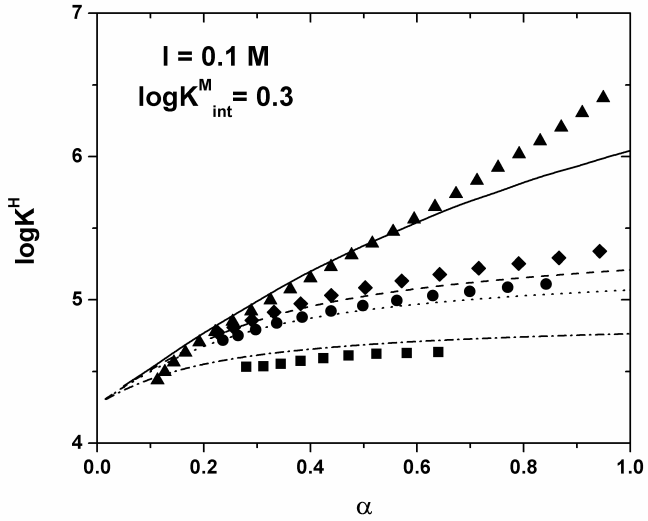

Figure 4.2.15. Apparent protonation constants of PAA at an overall ionic strength of 0.1 M in different electrolyte mixtures. PAA monomer concentration: $2.5 \cdot 10^{-4}$ M (filled symbols). The lines represent the NLPB calculations coupled with Mg^{2+} specific binding using $\log K^{M}_{int} = 0.3$ (the key to the line styles is the same as in **Figures 4.2.1** and **4.2.2.**).

4.2.5. Conclusions and future work

A theoretical study based on the NLPB equation concerning the effect of a divalent cation on the proton binding equilibria of a synthetic linear polyelectrolyte was shown. Simulations suggest a great sensitivity of the electrostatic description to the divalent/monovalent counterion ratio. Experimental results of proton binding to polyacrylic acid in $KNO_3/Mg(NO_3)_2$ mixtures reflect a screening effect of the magnesium ions that is even higher than expected from purely coulombic interactions (within the NLPB formalism). They also show a striking effect of the polymer concentration at low ionic strengths. The coupling of the NLPB scheme with ideal Langmuirian proton/metal competitive isotherms provided a simple framework for the interpretation of both effects. Future work will be aimed to the improvement of the Finite Element Method implementation for the numerical solution of NLPB within an electroneutral cell model for polymer solutions of finite concentration. In addition, a more advanced analysis of the specific metal binding will involve

the use of competitive isotherms that consider the simultaneous co-existence of 1:1 and 1:2 metal-site complexes (Koper and Borkovec, 2001).

4.2.6. References

Anderson, C.F. and Record, M.T.J. (1990). Ion distributions around DNA and other cylindrical polyions: Theoretical descriptions and physical implications. *Annu. Rev. Biophys. Biophys. Chem*, **19**, 423-465.

Barriada, J.L., Brandariz, I. and Sastre de Vicente, M.E. (2000). Acid-base equilibria of monocarboxylic acids in various saline media: analysis of data using Pitzer equations. *J. Chem. Eng. Data*, **45**, 1173-1178.

Bartschat, B.M., Cabaniss, S.E. and Morel, F.M.M. (1992). Oligoelectrolyte model for cation binding by humic substances. *Environ. Sci. Technol.*, **26**, 284-294.

Borkovec, M., Jönsson, B. and Koper, G.J.M. (2001). Ionization processes and proton binding in polyprotic systems: small molecules, proteins, interfaces, and polyelectrolytes. In: Matijevic, E. (ed.), *Surface and colloid science*, vol 16, pp. 99-399. Kluwer Academic / Plenum Press, New York.

Buffle, J. (1988). *Complexation reactions in aquatic systems: An analytical approach*. Ellis Horwood, Chichester.

Companys, E. (2003). Speciation of heavy metals in macromolecular systems by electroanalytical techniques. PhD Thesis. Universitat de Lleida.

Deserno, M. and Holm, C. (2001). Cell model and Poisson-Boltzmann theory: A brief introduction. *NATO Science Series, II: Mathematics, Physics & Chemistry*, **46**, 27-52.

Gans, P. and O'Sullivan, B. (2000). GLEE, a new computer program for glass electrode calibration. *Talanta*, **51**, 33-37.

Gran, G. (1952). Determination of the equivalence point in potentiometric titrations. Part II. *Analyst*, **77**, 661-671.

Katchalsky, A. (1971). Polyelectrolytes. *Pure & Appl. Chem.* , **26**, 327-373.

Katchalsky, A., Alexandrowicz, Z. and Kedem, O. (1966) *Polyelectrolyte solutions.* In: Conway, B.E. and Barradas, R. (eds), *Chemical physics of ionic solutions*, New York, pp 295-346.

Koper, G. and Borkovec, M. (2001). Binding of metal ions to polyelectrolytes and their oligomeric counterparts: An application of a generalized Potts model. *J. Phys. Chem. B*, **105**, 6666-6674.

Lyklema, J. (1995). *Fundamentals of interface and colloid science*. Vol 2. Academic Press, London.

Martell, A.E. and Smith, R.M. (1977). *Critical stability constants*. Vol 3. Plenum Press, New York.

Nagasawa, M., Murase, T. and Kondo, K. (1965). Potentiometric titration of stereoregular polyelectrolytes. *J. Phys. Chem.*, **69**, 4005-4012.

Ni, H., Anderson, C.F. and Record, M.T.J. (1999). Quantifying the thermodynamic consequences of cation (M^{2+}, M^{+}) accumulation and anion (X^{-}) exclusion in mixed salt solutions of polyanionic DNA using Monte Carlo and Poisson-Boltzmann calculations of ion-polyion preferential interaction coefficients. *J. Phys. Chem. B*, **103**, 3489-3504.

Press, W.H., Flannery, B.P., Teukolsky, S.A. and Vetterling, W.T. (1986). *Numerical recipes*. Cambridge University Press, Cambridge.

Sharp, K.A. and Honig, B. (1990). Electrostatic interactions in macromolecules: Theory and applications. *Annu. Rev. Biophys. Biophys. Chem*, **19**, 301-332.

CHAPTER 5

Gibbs-Donnan and specific ion interaction theory descriptions of the effect of ionic strength on proton dissociation of alginic acid

Published in J. Electroanal. Chem., 564 (2004) 223-230

5.1. Introduction

Biosorption, that is, the ability of biomass to sequester heavy metals and other pollutants, has been considered an alternative technique for the removal of toxic metals from industrial effluents (Volesky, 1990). Among the diversity of materials available, macroalgae have proved to be the most promising biosorbents for heavy metal recovery. The main mechanism of metal sorption to marine algae involves the interaction of the metal cations with the abundant sites of alginate existing in the algae (Schiewer and Volesky, 1997; Crist *et al.*, 1999). Therefore, the study of the acid-base chemistry of alginic acid under different ionic strength conditions is a matter of great interest in the field of biosorption, from an environmental point of view.

Alginic acid (AA) is a natural polysaccharide found in brown seaweeds (it may constitute 14 to 40% of the dry solids (Percival and McDowell, 1967)) that consists of linear chains of 1,4-linked β-D-mannuronic and α-L-guluronic acids (Lobban and Harrison, 1994). Several studies (Haug, 1961; Cesàro *et al.*, 1990) showed that the acid properties of AA depend on the particular monomer composition.

Specific ion interaction models, such as Guggenheim, Scatchard, or Pitzer models (Sastre de Vicente, 1997), have been successful in describing the ionic strength dependence of the proton binding properties of simple organic ligands like aminoacids (Fiol *et al.*, 1998), amines (Taboada-Pan *et al.*, 2001) and carboxylic acids (Daniele *et al.*, 1985; Foti *et al.*, 1998; Barriada *et al.*, 2000; Rey-Castro *et al.*, 2003a) in many ionic strength conditions and different background salts.

In the case of natural polyelectrolytes, however, several factors complicate the modeling of the proton binding reactions (Buffle, 1988): a) polyfunctionality (chemical heterogeneity), due to the presence of sites of different nature and/or steric environment; b) possible conformational changes; and c) polyelectrolytic nature, due to the presence of charged functional groups.

A number of papers can be found which deal with the ionic strength dependence of the protonation equilibria of polyelectrolytes. Many of them are focused on the determination of a set of thermodynamic parameters to summarize the experimental data. Simple models have been proposed, such as

Katchalsky *et al.* (1954) or Högfeldt (1988) models, which provide successful descriptions of the polyelectrolyte titration curves, although the experimental dependence on the ionic strength of the thermodynamic parameters involved has not a simple theoretical explanation. As a result, different empirical functions have been proposed, often polynomials of the square root of I (De Stefano *et al.*, 2002), by analogy with the behaviour of simple ligands. Sammartano and coworkers (Daniele *et al.*, 1999; De Stefano *et al.*, 2000; De Stefano *et al.*, 2001) have extensively studied the application of the above-mentioned models to synthetic polyelectrolytes. In a very recent work (De Stefano *et al.*, 2003), these authors have also proposed the application of the SIT model to the protonation data of polyacrylic acid.

The available information regarding the proton dissociation of alginic acid is scarce, and only few papers dealing with salt effects can be found (Jang *et al.*, 1989; Lin and Marinsky, 1993; Fukushima *et al.*, 1999). The purpose of this work is to analyze the dependence of the AA apparent dissociation constants on the ionic strength by means of two empirical functions derived from the SIT model and the Gibbs-Donnan theory for polyelectrolytes.

5.2. Models

5.2.1 Gibbs-Donnan model for a weak acid polyelectrolyte

The similarity between the acid-base behaviour of linear polyelectrolytes and that of their gel analogs has led to the hypothesis that a counterion-concentrating solvent sheath develops around the surface of the charged polyelectrolyte molecule in solution. A two-phase model based on the Gibbs-Donnan formalism has been proposed to explain the properties of these substances by Marinsky and coworkers (Marinsky, 1987; Marinsky *et al.*, 1989; Marinsky and Reddy, 1991).

From the postulates of this model, it has been shown that:

$$\frac{\bar{a}_H}{a_H} = \frac{\bar{a}_M}{a_M} \tag{5.1}$$

where a_i is the activity of *i*, M represents the counterion (here, Na^+ or K^+), and the bar indicates an association with the water of the polymer subphase.

The proton dissociation reaction of the polyelectrolyte:

$$AH = A^- + H^+ \tag{5.2}$$

can be described by an apparent dissociation constant, $K_{(\alpha)}$, as follows:

$$pK_{(\alpha)} = pa_H - \log\frac{\alpha}{1-\alpha} \tag{5.3}$$

where a_H is the proton activity in the bulk solution, and α is the dissociation degree.

The Gibbs-Donnan approach defines an intrinsic equilibrium constant for the dissociation reaction in the polyelectrolyte domain, $\overline{K}$, independent of the bulk ionic strength:

$$p\overline{K}_{(\alpha)} = p\bar{a}_H - \log\frac{\alpha}{1-\alpha} \tag{5.4}$$

where now $\bar{a}_H$ corresponds to the proton activity in the polyelectrolyte domain.

The difference between the two constants is given by (pa_M - $p\bar{a}_M$), the so-called Donnan term, which may be regarded as a partition coefficient for the counterion activity between the polymer subphase and the bulk solution:

$$pK_{(\alpha)} = p\overline{K}_{(\alpha)} + \left(pa_M - p\bar{a}_M\right) \tag{5.5}$$

If we refer to the corresponding stoichiometric constants, this equation becomes:

$$pK^*_{(\alpha)} = p\overline{K}^*_{(\alpha)} + \left(pa_M - p\bar{a}_M\right) + \log\left(\frac{\gamma_H}{\bar{\gamma}_H}\right) \tag{5.6}$$

where γ_H is the proton activity coefficient.

For the calculation of the Donnan term, the equilibrium of the background electrolyte, MX, between the bulk solution and the hypothetical polymer subphase must be considered:

$$a_M a_X = \bar{a}_M \bar{a}_X \tag{5.7}$$

where

$$a_M a_X = \left(m_s + \alpha m_p \phi_p\right)\left(m_s\right)\gamma^2{}_{\pm MX} \tag{5.8}$$

and

$$\bar{a}_M \bar{a}_X = \left(\frac{\alpha V m_p \left(1-\phi_p\right)}{\bar{W}_p} + \bar{m}_s\right)\left(\bar{m}_s\right)\bar{\gamma}_M \bar{\gamma}_X \tag{5.9}$$

in these equations m_s represent the molality of the background salt in the bulk solution (equivalent to the molal ionic strength, I, in a 1:1 electrolyte), m_p is the polymer molality, on a monomer basis, ϕ_p is the osmotic coefficient of the salt-free polyelectrolyte, V is the total volume of the solution, $\bar{m}_s$ is the molality of the salt that permeates the polymer domain, and $\bar{W}_p$ represent the amount of water associated with the polymer phase (usually referred to as *Donnan volume*). ϕ_p represents the fraction of counterions that effectively "escapes" from the polyion domain. Under the additivity rule of the colligative properties of simple salt and linear polyelectrolyte solutions, this magnitude is a unique function of α, and almost independent of the ionic strength (Alexandrowicz and Katchalsky, 1963; Katchalsky *et al.*, 1966).

In the range of ionic strengths studied, $m_s >> \alpha m_p \phi_p$, due to the high background salt to monomer concentration ratios.

The Donnan term would thus be given by:

$$\frac{\bar{a}_M}{a_M} = \frac{\bar{\gamma}_M}{\gamma_{\pm(MX)}}\left(\frac{\alpha V m_p \left(1-\phi_p\right)}{2\bar{W}_p m_s} + \sqrt{\left(\frac{\alpha V m_p \left(1-\phi_p\right)}{2\bar{W}_p m_s}\right)^2 + \frac{\gamma_\pm{}^2}{\bar{\gamma}_M \bar{\gamma}_X}}\right) \tag{5.10}$$

If the activity coefficient quotients are assumed to be equal to unity, a simplified expression is obtained for the dependence of pK^* on the ionic strength at a constant α:

$$pK^{*}_{(\alpha)} = \overline{pK}^{*}_{(\alpha)} + \log\left(\frac{D_{(\alpha)}}{I} + \sqrt{\left(\frac{D_{(\alpha)}}{I}\right)^{2} + 1}\right) \qquad (5.11)$$

where $D_{(\alpha)} = \alpha Vm_p(1-\phi_p)/2\,\overline{W}_p$.

In the limit of high ionic strength, where the difference in the counterion concentration between the two phases vanishes, the ratio of the ion activity coefficients is exactly equal to one and, therefore, $\lim_{I\to\infty} pK^{*}_{(\alpha)} = \overline{pK}^{*}_{(\alpha)}$. This will be useful for the estimation of $\overline{W}_p$ (see the Results and Discussion section).

$D_{(\alpha)}$ is proportional to the counterion concentration within the polymer phase (not including the permeated salt). This term would be constant for a given α value, provided that $\overline{W}_p$ is constant or a unique function of α. Thus, eq. (5.11) constitutes an empirical function that may describe the ionic strength dependence of $pK_{(\alpha)}$ with only two fitting parameters.

Nevertheless, a dependence of $\overline{W}_p$ on both the dissociation degree and ionic strength has been reported for alginic acid (Jang *et al.*, 1989; Lin and Marinsky, 1993). Thus, it would be assumed the next empirical relationship:

$$\frac{\overline{W}_p}{Vm_p} = W'_p = a \cdot \alpha \cdot I^{-b} \qquad (5.12)$$

where W'_p is used to designate the kilograms of polymer-associated water per mole of monomer.

Substituting eq.(5.12) into eq.(5.11) gives:

$$pK^{*}_{(\alpha)} = \overline{pK}^{*}_{(\alpha)} + \log\left(\frac{D'_{(\alpha)}}{I^{c}} + \sqrt{\left(\frac{D'_{(\alpha)}}{I^{c}}\right)^{2} + 1}\right) \qquad (5.13)$$

where $c = 1 - b$, and $D'_{(\alpha)} = (1-\phi_p)/2a$.

5.2.2. Application of a specific ion interaction theory (SIT)

The behavior of AA in saline media has been considered according to a single ligand model. For the simple proton dissociation reaction:

$$AH_n^{-z} \Leftrightarrow AH_{n-1}^{-(z+1)} + H^+ \tag{5.14}$$

the corresponding thermodynamic equilibrium constant will be given by:

$$K^T = K^* Q(\gamma) \tag{5.15}$$

where K^* is the stoichiometric equilibrium constant, K^T its value at infinite salt dilution and $Q(\gamma)$ is the quotient of activity coefficients associated to species appearing in eq. (5.14).

According to a Guggenheim-like model for the activity coefficient of the species involved in eq. (5.14), the following expression for the dependence of pK^* on the ionic strength, at different degrees of dissociation, is obtained:

$$pK^*_{(\alpha)} = pK^T_{(\alpha)} + \frac{A_{(\alpha)}\sqrt{I}}{1 + B_{(\alpha)}\sqrt{I}} + C_{(\alpha)}I \tag{5.16}$$

where pK^T is the value extrapolated to zero ionic strength (note the difference with $p\overline{K}^*$ in the Donnan model), $A_{(\alpha)} = -2 \cdot 0.51 \cdot z_{(\alpha)} \approx -z_{(\alpha)}$ (average charge per molecule of AA), and B, C are parameters related to the mean ionic diameter and the specific binary interactions between species, respectively (Sastre de Vicente, 1997).

It is assumed here that the effective charge (which determines the value of A) and the diameter of the molecule (related to B) are both independent of I, for a given value of α.

Due to the polyelectrolitic nature of AA, it is expected that an analysis of the effect of ionic strength on its acid-base behavior will lead to different values of pK^T at zero ionic strength depending on the dissociation degree. Also, A, B and C in a greater or lesser extent will probably depend on α.

5.3. Experimental

Alginic acid (free acid from *Macrocystis pyrifera*) was purchased from Sigma-Aldrich, with an approximate composition of 39% of guluronic and 61% of mannuronic acid (data supplied by the manufacturer).

NaCl and KNO_3 (Merck p.a.) were used as background electrolytes to adjust the ionic strength (ranging from 0.01 to 2 $molL^{-1}$) of all the solutions. The HCl, NaOH and KOH titrating solutions were prepared from the corresponding Merck p.a. reagents and standarized against sodium tetraborate decahydrate (Aldrich) and potassium hydrogen phthalate (Carlo Erba), respectively. The base solutions were prepared in boiled and N_2-purged MilliQ water. The concentrations were accurately calculated from the Gran plots (Gran, 1988), which showed a negligible CO_2 contamination.

Titrations and calibrations were carried out in a glass cell furnished with a thermostating jacket at a temperature of 25.0 ± 0.1 ºC, passing a nitrogen stream through the samples to remove dissolved O_2 and CO_2. The titrating solutions were added from a Crison microBu 2031 automatic buret. Electromotive force measurements were made with a Crison micropH 2000 meter equipped with a Radiometer GK2401C combined glass membrane electrode (Ag/AgCl sat. as reference).

The glass electrodes were calibrated in terms of the proton concentration at a constant ionic strength following the procedure described elsewhere (Fiol *et al.*, 1992; Brandariz *et al.*, 1998). The calibrations were performed repeatedly for each ionic strength and electrolyte, yielding the formal potential and slope used in subsequent calculations. This method has the advantage that the junction potential and the proton activity coefficient are included in the intercept of the Nernst-type equation (May *et al.*, 1982), so minimizing the possible error due to the change in the medium composition when calibrating the electrode with standard buffers.

For the titrations, 40 or 100 mL of the sample solution (AA at 0.1% or 0.04%, respectively) were placed in the thermostatted vessel and a certain amount of acid was added to yield an initial pH value of ca. 2.5. The automatic buret and pH-meter were computer-controlled by means of a homemade software application. The titration runs were conducted at least in duplicate.

The concentration (in $mol \cdot L^{-1}$) of the different solutions was converted into molal units through the solution density (Lobo and Quaresma, 1989).

The values of the apparent pK at α = 0.3, 0.5 and 0.7 were interpolated from the experimental curves by means of a cubic spline calculated with Origin v.5.0 (1997). The fitting to eqs. (5.13) and (5.16) was performed by the nonlinear least squares minimization tool of Origin v.5.0, based on the Levenberg-Marquardt algorithm.

5.4. Results and discussion

5.4.1. pK^* vs. α behaviour

Figure 5.1 shows a sample of the experimental data obtained in NaCl. The pK^* vs. α titration curves show a slight shoulder in the central region of α, rather than a smooth and constant increase typical of most polyacids. This behaviour has been reported before for AA and other polyuronic acids by Cesàro and coworkers (Cesàro *et al.*, 1990; Cesàro and Sagui, 1992). These authors discuss the possible simultaneous influence of interchain disaggregation and conformational transitions on the apparent pK behaviour of these substances. Paoletti *et al.* (1997) provided an additional interpretation of such 'bumps' in the $pK_{(\alpha)}$ curves in terms of the counterion condensation theory, for polysaccharides bearing two different carboxylic groups with close pK values.

Regardless of the actual processes occurring throughout the titration, the experimental data can be analyzed by fitting them to empirical models such as the Högfeldt equation, that includes three empirical parameters, pK_0, pK_m and pK_1:

$$pK^*_{(\alpha)} = pK_0(1-\alpha)^2 + 2pK_m(1-\alpha)\alpha + pK_1\alpha^2 \qquad (5.17)$$

where pK_0, pK_1 are the limit values for $\alpha \to 0$ and $\alpha \to 1$, respectively, and pK_m is an intermediate value that accounts for the non-linear behaviour of the function $pK^*_{(\alpha)}$.

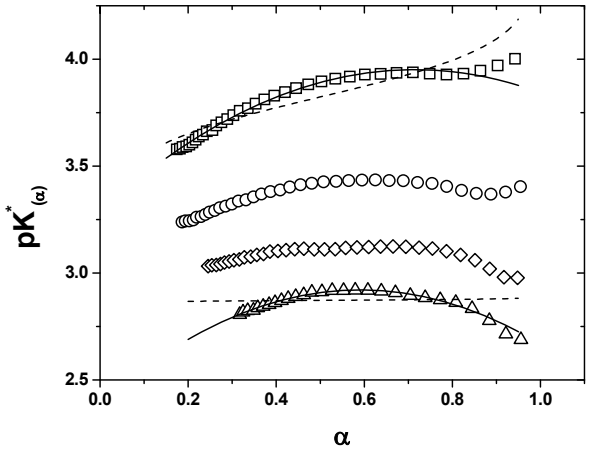

Figure 5.1. $pK^*_{(\alpha)}$ versus α curves obtained for AA in NaCl. Only four curves are shown, for clarity reasons: 0.01 $mol \cdot L^{-1}$ (squares), 0.05 $mol \cdot L^{-1}$ (circles), 0.20 $mol \cdot L^{-1}$ (diamonds) and 1.0 $mol \cdot L^{-1}$ (up triangles). The lines represent the fits to eq. (5.17) (solid line) and eq. (5.18) (dashed line), for $\alpha < 0.9$.

The Katchalsky model involves only two parameters, pK_n (equivalent to pK at $\alpha = 0.5$) and n:

$$pK^*_{(\alpha)} = pK_n + (n-1)\log\left(\frac{\alpha}{1-\alpha}\right) \tag{5.18}$$

The fitting of the experimental data to eqs. (5.17) and (5.18) is shown in **Figure 5.1** for two particular titrations obtained in NaCl. It can be observed that the three-parameter function describes much better the shape of the titration curve than the two-parameter equation.

From the results obtained, it seems that ionic strength is a more important factor in the apparent equilibrium constant than the dissociation degree (for $0.2 < \alpha < 1$). In fact, the observed values of the slope parameter n in eq.(5.18) are relatively small, lying in the range between 1.4 and 1 (the theoretical value for a monomeric acid), and decreasing as ionic strength increases. Polyacrylates, for instance, show values of n between 2.2 and 1.2 in solutions of alkali metal chlorides and nitrates of concentrations between 0.1 and 3 $mol \cdot L^{-1}$ (De Stefano *et al.*, 2003).

In theory, the value of the intrinsic equilibrium constant in the Gibbs-Donnan model could be assessed from the extrapolation of the different $pK^*_{(\alpha)}$ curves to $\alpha = 0$. This is the method usually employed in the work of Marinsky (1987). It is based on the assumption that at $\alpha = 0$ no charge in the macromomolecule is expected, and therefore the difference between the counterion activities in both phases becomes zero. From eq. (5.6) it can be deduced that:

$$pK^*_{(\alpha\to 0)} = p\overline{K}^*_{(\alpha\to 0)} \tag{5.19}$$

The stoichiometric constants must be corrected for the medium effect on the activity coefficients in order to obtain the thermodynamic constants. Once the correction is applied, the curves obtained at different ionic strengths should converge in the limit $\alpha \to 0$.

In practice, several factors complicate this procedure. The Donnan model predicts a steep change in $pK^*_{(\alpha)}$ at low α values (Marinsky, 1987). However, the limitations of the experimental technique (interference of the liquid junction potential on the glass electrode measurements at low pH) hindered the experimental acquisition of data below $\alpha = 0.2$. In addition, the uncertainties in the slope and formal potential of the glass electrode make the error in pK to increase as α decreases. Therefore, the data obtained did not allow making a reliable extrapolation.

In literature, the extrapolation to $\alpha \to 0$ is often made using a graphical method (see for instance Lin and Marinsky (1993)), rather than using a fitting function to estimate the pK value at $\alpha = 0$. The large uncertainties involved in such extrapolation are evident.

Jang *et al.* (1989) did not found a clear convergence of the AA titration curves. Instead, they estimated the intrinsic pK assuming that at a sufficiently high ionic strength all the polyelectrostatic effects are screened. In the case of the present work, this is supported by the fact that the mean slope of the $pK^*_{(\alpha)}$ curves decreases as I increases, reaching its lowest value at the highest ionic strength (see the fits to eq. (5.18) in **Figure 5.1**).

The discussion about the convergence presumes the deviations from the intrinsic constant to be due exclusively to the variable macromolecular charge. However, AA is a natural material with some degree of heterogeneity, and this

probably contributes to the shape of the curves. In a greater extent, this effect has been observed in purified peat (Marinsky *et al.*, 1980).

5.4.2 Estimation of the amount of water associated with the polymer phase

In order to derive an analytical expression of $pK^*_{(\alpha)}$ as a function of I, eq. (5.13), from the postulates of the Donnan model, it is necessary to introduce an empirical function to describe the variation of W'_p. In this work, a simultaneous influence of α and I, eq (5.12), has been considered. This assumption is in contrast, for example, with the typical expression used in the NICA-Donnan model for humic substances (Benedetti *et al.*, 1996; Companys *et al.*, 2003):

$$W'_p = a' \cdot I^{-b'} \tag{5.20}$$

where a' and b' are two empirical constants independent of pH or α.

The use of eq. (5.12) requires further discussion. It has been shown (Jang *et al.*, 1989; Lin and Marinsky, 1993) that W'_p can be estimated through use of the Gibbs-Donnan approach. The key point is the assessment of the intrinsic constant. Once $p\overline{K}^*$ is known, the Donnan volume can be obtained by solving eq. (5.11) iteratively. In this work, the assessment of $p\overline{K}^*$ by extrapolation to $\alpha \rightarrow 0$ was discarded, for the reasons detailed above. Instead, it will be assumed that all the electrostatic effects are suppressed at the highest ionic strength, and thus $pK^*_{(\alpha,\ high\ I)} = p\overline{K}^*_{(\alpha)}$. A similar approach has also been used in the study of proton binding to bacterial cell walls (Plette *et al.*, 1995) and seaweed biomass (Rey-Castro *et al.*, 2003b). The procedure adopted for the estimation of the Donnan volume can be summarized as follows:

a) The titration curves obtained at different values of I were fitted to eq. (5.17).

b) The fitted functions were used to interpolate the pK^* data at fixed values of α.

c) Eq. (5.11) was solved iteratively, assuming $pK^*_{(\alpha,\ I=2M)} = p\overline{K}^*_{(\alpha)}$. The values of ϕ_p were taken from bibliography (Katchalsky *et al.*, 1966), taking into account that the difference between the osmotic

coefficients of sodium and potassium alginate can be considered negligible (Katchalsky *et al.*, 1961).

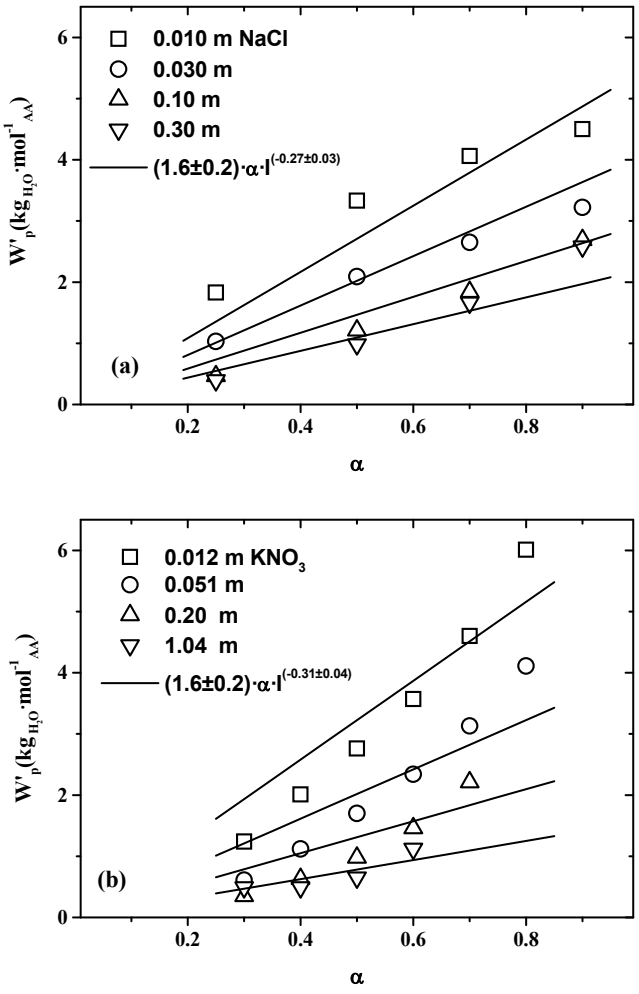

Figure 5.2. Estimates of the amount of water associated to the polymer phase calculated using a Gibbs-Donnan approach. a) Data taken from Lin and Marinsky (1993); b) Data calculated from the results of this work, assuming $pK^*_{(\alpha,\ I=2M)} = \overline{pK}^*_{(\alpha)}$. The lines represent the least-squares fits to eq. (5.12).

The results of the calculations for AA in KNO_3 are shown in **Figure 5.2**. Some data for AA in NaCl taken from bibliography (Lin and Marinsky, 1993) are included for comparison. The results show an increasing trend with α, especially at low ionic strengths. Both datasets were fitted to eq. (5.12), yielding the fitted parameters shown in the legend of **Figure 5.2**. The values obtained for b are in agreement with the results listed in **Table 5.2**. The fitted functions show a remarkable coincidence between the two electrolytes and provide a satisfactory support for the use of eq. (5.12). It is interesting to note that a similar trend in the Donnan volumes has been reported in a study of the proton binding to seaweed biomass (Rey-Castro *et al.*, 2003b).

It must be pointed out that when no independent experimental measurements of the specific volume are available, a certain degree of ambiguity in the definition of the electrostatic model may exist (Benedetti *et al.*, 1996), and therefore different models for the Donnan volume may lead to equally satisfactory fits of the experimental data (Rey-Castro *et al.*, 2003b). In fact, eq. (5.20) would lead to an expression formally identical to eq. (5.13), but with a different expression of $D'_{(\alpha)}$. Once again, the empirical nature of eq. (5.13), which is proposed only as a useful expression to describe the behaviour of pK^*, must be highlighted.

5.4.3. Ionic strength dependence

The pK^* values interpolated at α = 0.3, 0.5 and 0.7 are plotted in **Figure 5.3** together with the fits according to eqs. (5.13) and (5.16). The fitted parameters are summarized in **Table 5.1** (SIT) and **Table 5.2** (Donnan).

It can be noted that a good fit was obtained using eq. (5.16), in the sense that the function closely follows the trend of the experimental points. Nevertheless, very large errors in parameters A, B and C are obtained, and the pK^T values extrapolated to zero ionic strength show a large uncertainty, probably due to the high sensitivity of the SIT function to errors in the data at low I. The large errors associated to A and B parameters are a result of the presence of multicollinearity among the explanatory variables of the model, which has already been studied in the analysis of the dissociation equilibria of simple ligands (Herrero *et al.*, 1993; Fiol *et al.*, 1994). This problem may be expected for this type of ill-defined functions, when the number of experimental points is low, as it has been shown in the above-mentioned works. However, it

must be pointed out that the analysis of salt effects using less than ten different ionic strength values is commonplace in most (not only potentiometric) works.

Table 5.1. Parameters obtained by fitting the experimental $pK^*_{(\alpha)}$ data (in the $mol \cdot kg^{-1}$ scale) to eq.(5.16). The errors are shown in brackets.

α	$pK^T_{(\alpha)}$	A(α)	B(α)	C(α)	$10^3 \cdot \sigma_{fit}^2$ [a]
			AA in KNO_3		
0.3	4.58 (0.25)	-15.7 (6.0)	8.2 (2.2)	-[b]	1.6
0.5	4.54 (0.36)	-14.3 (8.9)	8.5 (3.7)	-[b]	3.1
0.7	5.60 (0.56)	-44 (23)	15.7 (5.1)	-[b]	1.3
			AA in NaCl		
0.3	4.35 (0.14)	-9.4 (2.7)	4.8 (1.3)	0.10 (0.03)	1.0
0.5	4.94 (0.12)	-19.2 (3.2)	8.2 (1.1)	0.09 (0.01)	0.2
0.7	4.90 (0.11)	-16.5 (2.5)	6.84 (0.9)	0.12 (0.02)	0.3

[a] σ_{fit}^2 = Σ (Square residuals)/degrees of freedom.
[b] the values of C are statistically compatible with zero.

Table 5.2. Parameters obtained by fitting the experimental $pK^*_{(\alpha)}$ data (in the $mol \cdot kg^{-1}$ scale) to eq.(5.13). The errors are shown in brackets.

α	$\mathbf{p\overline{K}}^*_{(\alpha)}$	D'	c	$10^3 \cdot \sigma_{fit}^2$ [a]
		AA in KNO_3		
0.3	2.72 (0.04)	0.37 (0.09)	0.56 (0.04)	1.6
0.5	2.95 (0.02)	0.16 (0.03)	0.70 (0.04)	1
0.7	2.95 (0.02)	0.15 (0.02)	0.75 (0.03)	0.5
		AA in NaCl		
0.3	2.74 (0.04)	0.30 (0.07)	0.61 (0.04)	1.6
0.5	2.88 (0.02)	0.17 (0.03)	0.73 (0.03)	0.8
0.7	2.86 (0.02)	0.18 (0.03)	0.76 (0.04)	1.2

[a] σ_{fit}^2 = Σ (Square residuals)/degrees of freedom.

It must also be noted that the highest errors are obtained with AA in KNO_3, where no minimum in $pK^*_{(\alpha)}$ was found within the investigated range of ionic strengths. The presence of a minimum in NaCl, suggested only by the data at the highest ionic strength, entails the use of the linear term in eq. (5.16).

The differences in pK^* between both electrolytes, although relatively small, taking into account the reproducibility of the data, follow the trend $K^+ > Na^+$, according to the different complexing ability of the alkali metal cations towards carboxylates (De Stefano *et al.*, 2002).

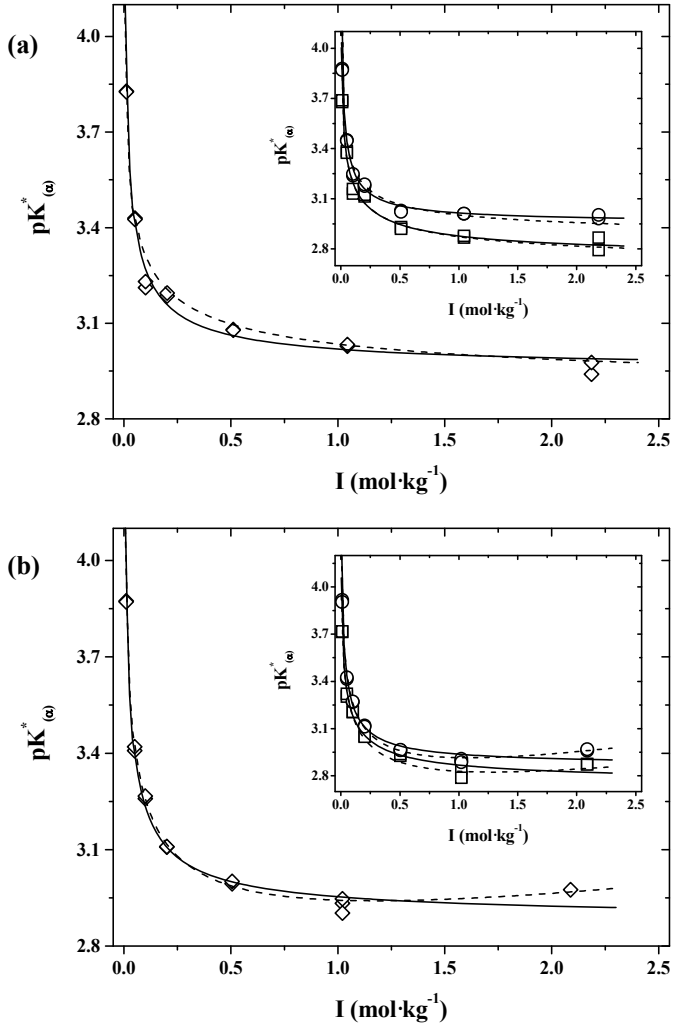

Figure 5.3. $pK^*_{(\alpha)}$ values of AA in KNO_3 (a) and NaCl (b) at three different degrees of dissociation: α = 0.5 (diamonds), α = 0.3 (squares) and α = 0.7 (circles). The two latter are shown in the inset for clarity reasons. Data fitted according to Donnan (solid lines) and SIT (dashed lines) models.

An increase in the parameters A and pK^T on increasing α is observed (**Table 5.1**), which might be explained by the growth of the negative charge of AA as the titration proceeds. Moreover, the increasing trend in B, parameter associated to size, (see **Table 5.1**) may be accounted for by the repulsion among negative charges of AA.

In a recent paper regarding the AA dissociation in different sodium salts, Fukushima *et al.* (1999) proposed the application of a Debye-Hückel electrostatic model equivalent to eq. (5.16) with C = 0. Their study was restricted to the analysis of pK_n (eq. (5.18)) at ionic strengths ≤ 1 M, and no clear evidence of a minimum in $pK^*_{(\alpha)}$ was found. The average charge reported in this work ($z(\alpha=0.5) = 50$ for AA in NaCl) is of a similar order of magnitude than the parameter A listed in **Table 5.1**. However, the errors in the parameters are not mentioned by the authors, which makes a precise comparison difficult. They calculated independently a value of 9.6 for the B parameter, from an estimate of the AA molecule radius. This result agrees quite well with the value listed in **Table 5.1**.

The Gibbs-Donnan approach has already been applied to the interpretation of the acid dissociation of alginic acid (Jang *et al.*, 1989; Lin and Marinsky, 1993), although an explicit function to describe the influence of the ionic strength on the dissociation constant has not been reported. These works agree in their conclusion that alginic acid behaves like a flexible polymer with a sizeable variability in the water content of the counterion-concentrating domain of the polyelectrolyte. The polymer subphase volume estimates reported in these papers for AA in NaCl and $NaNO_3$, respectively, are in agreement with the results of this work, showing an almost linear relationship with α, with an I-dependent slope (see **Figure 5.2**). By including this trend (in the form of eq. (5.12)) in an equation derived from the Gibbs-Donnan postulates, an empirical expression (eq. (5.13)) was obtained which describes satisfactorily the experimental behaviour of $pK^*_{(\alpha)}$ as a function of I (see **Figure 5.3**).

In addition, this model seems to avoid the presence of multicollinearity and, consequently, the errors in the optimized parameters are smaller (see **Table 5.2**). On the other hand, it does not reflect the presence of a minimum in pK^* insinuated by the results in NaCl shown in this work. In contrast to the SIT model, the Gibbs-Donnan approach can also be used for the simultaneous

description of the dependence of pK^* on I and α, provided that the variation of $\overline{pK}^*_{(\alpha)}$ is properly accounted for (Biesuz *et al.*, 2001; Rey-Castro *et al.*, 2003b).

5.5. Conclusions

SIT and Gibbs-Donnan models have been applied to the study of the ionic strength influence on the proton dissociation of AA in NaCl and KNO_3. Both of them lead to a similar description of the experimental data, although the initial assumptions, the accuracy of the fitted parameters and the thermodynamic information involved are different. The SIT approach essentially represents a methodology analogous to that previously employed in the study of simple ligands, based in the Debye-Hückel theory. This model yields a thermodynamic constant extrapolated to infinite dilution of the background salt and, in the simplest case, two parameters related to the average charge and size of the molecule. The optimized values of the parameters are affected by large errors, due to a problem of multicollinearity.

The Gibbs-Donnan approach, on the contrary, starts from a two-phase model postulated for linear polyelectrolytes and gels, and it leads to a function that includes a dissociation constant extrapolated to high ionic strength and two additional empirical parameters, related to the variation of the water content of the polymer subphase. The values of these parameters, obtained by least squares minimization, show lower associated errors than in the previous case.

5.6. References

(1997) Microcal™ Origin™. Microcal Software, Inc., Northampton, MA (USA)

Alexandrowicz, Z. and Katchalsky, A. 1963. Colligative properties of polyelectrolyte solutions in excess of salt. *J. Polym. Sci.*, **A1**, 3231-3260.

Barriada, J.L., Brandariz, I. and Sastre de Vicente, M.E. 2000. Acid-base equilibria of monocarboxylic acids in various saline media: analysis of data using Pitzer equations. *J. Chem. Eng. Data*, **45**, 1173-1178.

Benedetti, M.F., van Riemsdijk, W.H. and Koopal, L.K. 1996. Humic substances considered as a Heterogeneous Donnan Gel Phase. *Environ. Sci. Technol.*, **30**, 1805-1813.

Biesuz, R., Zagorodni, A.A. and Muhammed, M. 2001. Estimation of Deprotonation Coefficients for Chelating Ion Exchange Resins. Comparison of Different Thermodynamic Models. *J. Phys. Chem. B*, **105**, 4721-4726.

Brandariz, I., Vilariño, T., Alonso, P., Herrero, R., Fiol, S. and Sastre de Vicente, M.E. 1998. Effect of ionic strength on the formal potential of the glass electrode in various saline media. *Talanta*, **46**, 1469-1477.

Buffle, J. 1988. *Complexation reactions in aquatic systems: An analytical approach*. Ellis Horwood, Chichester.

Cesàro, A., Delben, F. and Paoletti, S. 1990. Thermodynamics of the proton dissociation of natural polyuronic acids. *Int. J. Biol. Macromol.*, **12**, 170-176.

Cesàro, A. and Sagui, M.C. 1992. Effect of chain aggregation and ionic interactions on the proton dissociation equilibria of weak polyacids. *Makromol. Chem., Macromol. Symp.*, **58**, 39-61.

Companys, E., Puy, J., Torrent, M., Galceran, J., Salvador, J., Garcés, J.L. and Mas, F. 2003. Binding curve from normalised limiting currents of labile heterogeneous metal - macromolecular systems. The case of Cd / humic acid. *Electroanalysis*, **15**, 452-459.

Crist, R.H., Martin, J.R. and Crist, D.R. 1999. Interaction of metal ions with acid sites of biosorbents peat moss and *Vaucheria* and model substances alginic and humic acids. *Environ. Sci. Technol.*, **33**, 2252-2256.

Daniele, P.G., De Robertis, A., De Stefano, C., Sammartano, S. and Rigano, C. 1985. On the possibility of determining the thermodynamic parameters for the formation of weak complexes using a simple model for the dependence on ionic strength of activity coefficients: Na^+, K^+, and Ca^{2+} complexes of low molecular weight ligands in aqueous solution. *J. Chem. Soc. Dalton*, 2353-2361.

Daniele, P.G., De Stefano, C., Ginepro, M. and Sammartano, S. 1999. Salt effects on the protonation of polymethacrylate and Na^+, K^+, Ca^{2+} complex formation. *Fluid Phase Equilibr.*, **163**, 127-137.

De Stefano, C., Foti, C., Giuffrè, O. and Sammartano, S. 2001. Dependence on ionic strength of protonation enthalpies of polycarboxylate anions in NaCl aqueous solution. *J. Chem. Eng. Data*, **46**, 1417-1424.

De Stefano, C., Gianguzza, A., Piazzese, D. and Sammartano, S. 2000. Polyacrylate protonation in various aqueous ionic media at different temperatures and ionic strengths. *J. Chem. Eng. Data*, **45**, 876-881.

De Stefano, C., Gianguzza, A., Piazzese, D. and Sammartano, S. 2003. Polyacrylates in aqueous solution. The dependence of protonation on molecular weigth, ionic medium and ionic strength. *React Funct Polym*, **55**, 9-20.

De Stefano, C., Sammartano, S., Gianguzza, A. and Piazzese, D. 2002. Speciation of polyelectrolytes in natural fluids. Protonation and interaction of polymethacrylates with major components of seawater. *Talanta*, **58**, 405-417.

Fiol, S., Arce, F., Armesto, X.L., Penedo, F. and Sastre de Vicente, M.E. 1992. Analysis of Systematic Errors in Calibrating Glass Electrodes with H^+ as a Concentration Probe. *Fresenius J. Anal. Chem.*, **343**, 469-472.

Fiol, S., Brandariz, I., Herrero, R., Vilariño, T. and Sastre de Vicente, M.E. 1994. The Protonation Constants of Glycine in Nacl at 25º C Based on the Pitzer and Scatchard Models Data-Analysis by Ridge-Regression. *Ber. Bunsenges Phys. Chem*, **98**, 164-171.

Fiol, S., Vilariño, T., Herrero, R., Sastre de Vicente, M.E. and Arce, F. 1998. Protonation constants of valine, serine, and beta-alanine in artificial seawater at 25 degrees C. *J. Chem. Eng. Data*, **43**, 393-395.

Foti, C., Sammartano, S. and Signorino, G. 1998. The dependence on ionic strength of protonation constants of carboxylic acids in aqueous tetraethylammonium iodide solution, at different temperatures. *Fluid Phase Equilibr.*, **149**, 91-101.

Fukushima, M., Tatsumi, K. and Wada, S. 1999. Evaluation of the intrinsic acid-dissociation constant of alginic acid by considering the electrostatic effect. *Anal. Sci.*, **15**, 1153-1155.

Gran, G. 1988. Equivalence volumes in potentiometric titrations. *Anal. Chim. Acta*, **206**, 111-123.

Haug, A. 1961. Dissociation of alginic acid. *Acta Chem. Scand.*, **15**, 950-952.

Herrero, R., Brandariz, I., Fiol, S., Vilarino, T. and Sastre de Vicente, M.E. 1993. Errors Encountered in the Determination of Pitzer Parameters from Stoichiometric Equilibrium-Constants. *An. Quím*, **89**, 602-610.

Högfeldt, E. 1988. A useful method for summarizing data in ion exchange. 4. Extension and application to weak acid and chelating resins. *J. Phys. Chem.*, **92**, 6475-6476.

Jang, L.K., Harpt, N., Uyen, T., Grasmick, D. and Geesey, G.G. 1989. An iterative procedure based on the Donnan equilibrium for calculating the polymer-subphase volume of alginic acid. *J. Polym. Sci.*, **27**, 1301-1315.

Katchalsky, A., Alexandrowicz, Z. and Kedem, O. 1966. Polyelectrolyte solutions. In: Conway, B.E. and Barradas, R. (eds) *Chemical physics of ionic solutions*, New York, pp 295-346

Katchalsky, A., Cooper, R.E., Upadhyay, J. and Wassermann, A. 1961. Counter-ion fixation in alginates. *J. Chem. Soc*, 5198-5204.

Katchalsky, A., Shavit, N. and Eisenberg, H. 1954. Dissociation of weak polymeric acids and bases. *J. Polym. Sci.*, **13**, 69-84.

Lin, F.G. and Marinsky, J.A. 1993. A Gibbs-Donnan-based interpretation of the effect of medium counterion concentration levels on the acid dissociation properties of alginic acid and chondroitin sulfate. *React. Polym.*, **19**, 27-45.

Lobban, C.S. and Harrison, P.J. 1994. *Seaweed ecology and physiology*. Cambridge University Press, Cambridge.

Lobo, V.M.M. and Quaresma, J.L. 1989. *Handbook of electrolyte solutions*. Elsevier, Amsterdam.

Marinsky, J.A. 1987. A two-phase model for the interpretation of proton and metal ion interaction with charged polyelectrolyte gels and their linear analogs.

In: Stumm, W. (ed.), *Aquatic Surface Chemistry. Chemical Processes at the Particle-Water Interface.*, pp. 49-81. J. Wiley & Sons, New York.

Marinsky, J.A., Miyajima, T., Högfeldt, E. and Muhammed, M. 1989. Influence of counterion concentration on equilibria and conformational properties of linear weak-acid polyelectrolytes. *React. Polym.*, **11**, 291-300.

Marinsky, J.A. and Reddy, M.M. 1991. Employment of Gibbs-Donnan-based concepts for interpretation of the properties of linear polyelectrolyte solutions. *J. Phys. Chem.*, **95**, 10208-10214.

Marinsky, J.A., Wolf, A. and Bunzl, K. 1980. The binding of trace amounts of lead(II), copper(II), cadmium(II), zinc(II) and calcium(II) to soil organic matter. *Talanta*, **27**, 461-468.

May, P.M., Williams, D.R., Linder, P.W. and Torrington, R.G. 1982. The use of glass electrodes for the determination of formation constants I. *Talanta*, **29**, 249-256.

Paoletti, S., Gilli, R., Navarini, L. and Crescenzi, V. 1997. Effect of monomer composition on proton dissociation of weak polyacids. *Glycoconjugate J.*, **14**, 513-517.

Percival, E. and McDowell, R.H. 1967. *Chemistry and Enzymology of marine algal polysaccharides*. Academic Press, London.

Plette, A.C.C., van Riemsdijk, W.H., Benedetti, M.F. and van der Wal, A. 1995. pH dependent charging behavior of isolated cell walls of a Gram-positive soil bacterium. *J. Colloid Interf. Sci.*, **173**, 354-363.

Rey-Castro, C., Castro-Varela, R., Herrero, R. and Sastre de Vicente, M.E. 2003a. Acid-base equilibria of phthalic acid in saline media: ion association from Pitzer equations. *Talanta*, **60**, 93-101.

Rey-Castro, C., Lodeiro, P., Herrero, R. and Sastre de Vicente, M.E. 2003b. Acid-base properties of brown seaweed biomass considered as a Donnan gel. A model reflecting electrostatic effects and chemical heterogeneity. *Environ. Sci. Technol.*, **37**, 5159-5167.

Sastre de Vicente, M.E. 1997. Ionic strength effects on acid-base equilibria. A review. *Curr. Top. Solution Chem.*, **2**, 157-181.

Schiewer, S. and Volesky, B. 1997. Ionic strength and electrostatic effects in biosorption of protons. *Environ. Sci. Technol.*, **31**, 1863-1871.

Taboada-Pan, C., Brandariz, I., Barriada, J.L., Vilariño, T. and Sastre de Vicente, M.E. 2001. The salting coefficient and size of alkylamines in saline media at different temperatures: estimation from Pitzer equations and the mean spherical approximation. *Fluid Phase Equilibr.*, **180**, 313-325.

Volesky, B. 1990. *Biosorption of heavy metals*. CRC Press, Boca Raton, Florida.

CHAPTER 6

Complexation equilibria in humic substances: Effect of Fe(III) on the binding of Cu(II) by a humic acid sample

This chapter is part of the paper published in Geochim. Cosmochim. Acta,
66 (2002) 3211-3224.

6.1. Introduction

Iron is an abundant and reactive element, with a variety of geochemical and environmental chemical roles. In the dissolved and particulate phases of freshwaters, sediments and soils, it undergoes significant interactions with natural organic matter (chiefly humic substances). Dissolved iron-organic complexes and iron oxide-humic colloids are important in the transport and fate of the element in rivers and estuaries (Sholkovitz and Copland, 1981; Ross and Sherrell, 1999). Adsorption of humic matter alters the surface chemistry and colloid stability of iron oxides (Tipping, 1986). Photochemical processes involving Fe and natural organic matter lead to the decomposition of DOM, the production of reactive species (superoxide anion, hydrogen peroxide, hydroxyl radical), and the generation of dissolved, bioavailable, ferrous iron (e.g. Collienne, 1983; Stumm and Morgan, 1996; Voelker *et al*., 1997). Iron and humic matter influence phosphorus speciation in lakes (Jones *et al.*, 1993).

Whereas the presence in freshwaters of dissolved complexes of (monomeric) Al with natural organic matter is well established (Driscoll, 1984; LaZerte, 1984), the situation with regard to Fe(III) is less clear. According to Perdue *et al.* (1976) and Koenings (1976), soluble iron-humic complexes are significant components of surface freshwaters. Others (Shapiro, 1966; Cameron and Liss, 1984) attribute the high apparent solubility of Fe in freshwaters to the presence of small iron oxide particles stabilized by adsorbed humic matter. Estimates of the distribution of Fe(III) between the organically-complexed and colloidal oxide forms have been made by kinetic analysis, i.e. by determining the rate of conversion of Fe(III) to a spectroscopically-detectable complex, following the addition of an excess of a suitable ligand. The starting species are then identified and quantified by fitting the kinetic data to a model in which each species has a rate constant in a defined range. Tipping *et al.* (1982) found that ca. 30 % of the Fe(III) in the supernatant of a centrifuged lake water sample was present as a fast-reacting component, possibly organically-complexed Fe. Sojo and de Haan (1991) reported that ca. 60 % of the Fe(III) in a filtered (0.2 μm) neutral lake water (DOC 9 mg L^{-1}) was present as organic complexes. In both studies, Fe(III) not complexed by organic matter was considered to be present as colloidal oxides.

The interactions of Fe with humic substances affect not only the metal, but also the organic matter itself. Its binding may alter the tendency of humic substances to aggregate and to adsorb to surfaces, and may affect the binding of other metals. For instance, competition by Fe(III) for Am and Cu has been proposed (Peters *et al.*, 2001). In view of the high concentrations of Fe(III), compared to those of trace metals, such competition effects may be highly significant in natural systems. Clearly, therefore, a full understanding of metal chemistry in natural waters needs to take into account the competitive reactions of Fe and other metals with humic matter.

The aim of the present work was to examine how Fe binding by humic matter will affect interactions with trace metals, such as Cu. As a framework, Humic Ion-Binding Model VI, a discrete-site, electrostatic model of cation-humic interactions was used, which has been parametrized with a large number of data sets from experiments with isolated humic substances (Tipping, 1998). Model VI can be viewed as an encapsulation of the available knowledge, and its application to natural systems as a comparison of laboratory-based expectations with field reality. An important assumption of the model is that all binding sites are available to all metals.

In the following text, fulvic acid, humic acid are abbreviated by FA and HA respectively, dissolved organic carbon and dissolved organic matter by DOC and DOM. The variable ν represents moles of metal bound per gram of humic matter.

6.2. Experimental section

The isolation and purification of the humic acid and the preparation of samples with different Fe content is described in detail in Chapter 2. This section deals with the details of the copper titration experiments, which follow the procedure described by Brian (2001).

Measurements of pH were made with a Radiometer model GK2401C combination electrode connected to a Radiometer PHM. The electrode was calibrated with phthalate and phosphate BDH buffers, following procedures recommended by Davison (1990). Measurements of Cu^{2+} were made with an Orion cupric half-cell model 9429 ion-selective electrode, and an Orion Ag / AgCl double-junction model 90-02 reference electrode, both attached to an

Orion Microprocessor Ionanalyzer 901. The Cu electrode was prepared according to Avdeef *et al.* (1983). Each day, before calibration and titration, the electrode was polished carefully with Orion aluminium oxide (3μm) polishing strip (moistened in MilliQ water), rinsed carefully with MilliQ water, soaked in 0.025 M H_2SO_4 for approx. 10 minutes, then rinsed with more MilliQ water. The outer solution of the reference electrode was replaced daily, and the inner solution weekly. Before each experiment, the electrode was calibrated at 20ºC over a range of 10^{-6} to 10^{-3} M in $[Cu^{2+}]$. A calibration check was performed after each experiment. Calibration slopes were always within 1 % of the Nernstian value. All titrations were performed with the apparatus covered to exclude light. According to the manufacturer (Orion), Fe(III) interferes when the concentration of Fe^{3+} is greater than one-tenth of the Cu^{2+} concentration; the maximum ratio of Fe^{3+} to Cu^{2+} was calculated to be 0.003, which implies negligible interference.

To prepare the humic acid for titration, a dialysed suspension (HA-2, HA-3 or HA-4, see Chapter 2) was diluted with 0.1 M $NaNO_3$ / 10^{-4} M HNO_3 to give [HA] = 1 $g \cdot L^{-1}$. An aliquot of 100 cm^3 was taken, and bubbled at room temperature for approx. 1 h with wet air, enriched to 0.1 % with CO_2. It was then transferred to a thermostatted jacket at 20ºC, the electrodes were inserted, $Cu(NO_3)_2$ was added to give an initial total Cu concentration of 10^{-6} M, and the system was left to equilibrate for one hour, still bubbled with air. The first EMF reading was then taken, and the titration was performed by adding further known amounts of $Cu(NO_3)_2$. At each addition, the EMF reading was accepted when the electrode drift became less than 0.1 $mV \cdot min^{-1}$.

6.3. Theory

6.3.1. Humic Ion-Binding Model VI

The model was described in detail by Tipping (1998). It uses a structured formulation of discrete, chemically-plausible, binding sites for protons, in order to allow the creation of regular arrays of bidentate and tridentate binding sites for metals.

Fulvic and humic acids are assumed to be rigid spheres of uniform size. From typical measured weight-average molecular weights (1500 for FA, 15,000 for HA), and assuming an effective density (humic matter plus included solvent)

of 1.2 $g \cdot cm^{-3}$, the radii of the molecules are calculated to be 0.8 nm (FA) or 1.72 nm (HA). Ion-binding groups are positioned randomly on the molecular surfaces.

Proton dissociation is represented by postulating 8 groups with different acid strengths. The dissociation reaction can be written generally as;

$$(HumH)^{Z} = (Hum)^{Z-1} + H^{+} \qquad (6.1)$$

where Hum represents the humic molecule, and Z is the net charge. The reactions are characterised by intrinsic (i.e., separated from non-specific electrostatic effects: see below) equilibrium constants, the negative logarithms of which are denoted by pK_1 - pK_8. The four most strongly-acid groups (groups 1-4) are referred to as type A groups, and consist mainly of carboxylic acid groups, while the remaining 4 groups (type B) represent weaker acids, such as phenolic acids. The 8 pK_i values are expressed in terms of 4 constants (pK_A, pK_B, ΔpK_A and ΔpK_B) as follows:

$$\text{for } i = 1-4 \qquad pK_i = pK_A + \frac{(2i-5)}{6}\Delta pK_A \qquad (6.2)$$

$$\text{for } i = 5-8 \qquad pK_i = pK_B + \frac{(2i-13)}{6}\Delta pK_B \qquad (6.3)$$

Thus the values of pK_A and pK_B are the average pK values of the two types of group, while ΔpK_A and ΔpK_B are measures of the spread of the individual pK_i values around the means. Positive values of ΔpK_A and ΔpK_B mean that the pK_i values increase as i increases, i.e. the groups become progressively weaker acids. Each type A group is assigned an abundance of $n_A/4$ $mol \cdot g^{-1}$ humic matter, and each type B group an abundance of $n_A/8$ $mol \cdot g^{-1}$. Thus, within a type, each group is present in equal amounts, and there are half as many type B groups as type A groups. The affinity spectrum associated with this description of the proton binding is shown in **Figure 6.1**. The imposed regularity of the groups facilitates the formulation of multidentate binding sites for metals.

Metal ions (Ca^{2+}, Fe^{3+}, Cu^{2+}, etc.), and their first hydrolysis products ($CaOH^{+}$, $FeOH^{2+}$, $CuOH^{+}$, etc.), compete with each other, and with protons, for the type A and type B groups. The same intrinsic equilibirum constant is assumed to apply to the aquo ion and its first hydrolysis product. Monodentate binding takes place according to the general reaction:

$$Hum^{Z} + M^{z} = (HumM)^{Z+z} \quad (6.4)$$

The equilibrium constants for the different sites are given by:

$$\text{for sites } 1-4: \quad \log K(i) = \log K_{MA} + \frac{(2i-5)}{6}\Delta LK_{A1} \quad (6.5)$$

$$\text{for sites } 5-8: \quad \log K(i) = \log K_{MB} + \frac{(2i-13)}{6}\Delta LK_{B1} \quad (6.6)$$

where ΔLK_{A1} and ΔLK_{B1} are constants estimated from data fitting. Thus the values of log $K_{MA,i}$ are evenly spaced around the mean of log K_{MA} but the spacing is not necessarily the same as that for protons, i.e. in general ΔLK_1 is not equal to ΔpK_A. The same applies to the type B sites.

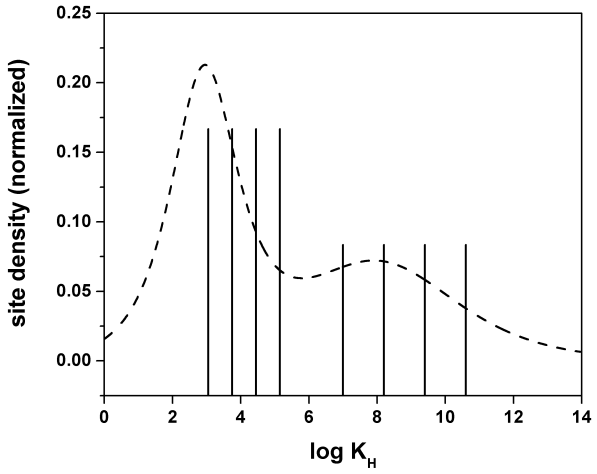

Figure 6.1. Intrinsic proton affinity distribution associated with the generic Model VI description for humic acids (vertical lines). The affinity spectrum associated with the NICA-Donnan model using the generic parameters recommended by Milne *et al.* (2001) (dashed line) is shown for comparison.

For a bidentate site comprising single sites j and k, the association constant K(j,k) is given by:

$$\log K(j,k) = \log K(j) + \log K(k) + x\Delta LK_2 \quad (6.7)$$

where ΔLK_2 is an adjustable parameter. The value of x is zero for 90.1% of the sites, one for 9%, and 2 for 0.9%. This generates heterogeneity, with a small

number of strong sites, a larger number of moderately strong ones, and a majority of weak ones. Analogous rules are used for the tridentate sites, made up of single sites l, m and n:

$$\log K(l, m, n) = \log K(l) + \log K(m) + \log K(n) + y\Delta LK_2 \qquad (6.8)$$

Here, y is 0, 1.5 or 3 for the 90.1%, 9% and 0.9% abundances, respectively. Each metal ion has a characteristic ΔLK_2.

The fractions of single sites that contribute to the bidentate or tridentate sites are determined statistically, by assuming the proton sites to be randomly positioned on the surfaces of the (spherical) molecules. Pairs of groups are considered to form bidentate sites, or triplets to form tridentate sites, if they are less than or equal to 0.45 nm apart. The fraction of sites forming bidentate sites is denoted by f_{prB}, that for tridentates is f_{prT}. For fulvic acid, f_{prB} = 0.42, f_{prT} = 0.03, while for humic acid, the corresponding values are 0.50 and 0.065. The bidentate and tridentate sites are fixed entities; with respect to metal binding, they are unable to revert to monodentate behaviour under any circumstances.

If all combinations of proton sites are allowed, 36 different bidentate sites and 120 different tridentate sites can form, for each of which there are three binding strengths, if ΔLK_2 is non-zero. Together with the eight monodenate sites therefore, there could be 476 different sites in all. The abundances of these sites depend on their composition, in terms of type A and type B sites, the latter being present at half the total abundance of the former. For example, tridentate sites comprising three type A proton sites are eight times more abundant than those comprising three type B sites. To avoid over-complication, and to speed computations, a sub-set of sites is used in the model, while maintaining the relative proportions of the contributing proton sites. To do this, bidentate or tridentate sites are allowed to consist only of different proton sites, and only 24 representative combinations are adopted. The 24 allowed combinations lead to 72 different sites, because of the heterogeneity terms (eqs. (6.7) and (6.8)). With the addition of the 8 monodentate sites, there are 80 different sites in all.

The above reactions are described with intrinsic equilibrium constants, which are referred to a state of zero charge. These constants are modified by a empirical electrostatic term, based in the Debye-Hückel theory (see Chapter 1), that takes into account the attractive or repulsive interactions between ions and

the charged macromolecule. For instance, the binding of a metal ion to a monodentate site is described by the following charge-dependent equilibrium quotient, $K_M(Z)$:

$$R^Z + M^z \equiv RM^{(Z+z)}; \qquad K_M(Z) = \frac{\left[RM^{Z+z}\right]}{\left[R^Z\right]a_M} = K_M \exp(-2wzZ) \tag{6.9}$$

where R represents the macromolecule, wich carries a net charge of Z ($mol \cdot g^{-1}$), K_M is the intrinsic association constant for the metal ion M, and w is the ionic strength-dependent electrostatic interaction factor (see Chapter 1), which is given by the empirical expression

$$w = P \cdot \log I \tag{6.10}$$

where P is an empirical constant and I is the ionic strength.

The overall accumulation of counterions in the double layer is described with a simple Donnan sub-model. The volume of this region is approximated by the following expression:

$$V_D = \frac{10^3 N_A}{M} \frac{4\pi}{3}\left[\left(r + \frac{1}{\kappa}\right)^3 - r^3\right] \tag{6.11}$$

where M and r are the molecular weight and radius, respectively, and κ is the Debye-Hückel parameter.

In Model VI, the maximum number of parameters that can be optimised to describe proton dissociation is six: K_{MA}, K_{MB}, ΔLK_{A1}, ΔLK_{B1}, ΔLK_2, K_{sel} (see **Table 6.1**). In practice however, this number can be substantially reduced. Thus, Tipping (1998) described the setting of a single universal value for ΔLK_{A1} and ΔLK_{B1}, and the estimation of ΔLK_2 by correlation with the equilibrium constant for complex formation with NH_3. For dilute systems, K_{sel} can be set to unity. Finally, K_{MA} and K_{MB} are strongly correlated. Therefore, the fitting of a new data set can be achieved by adjusting only K_{MA}, which was the approach taken in the present work. **Table 6.1** shows the values of the Model VI parameters used in the present work. It is important to note that the values of log K_{MA} for all the metals except Fe(III) have been derived by fitting experimental data; the values for Fe(III) are estimated from linear free energy relationships (Tipping, 1998). High values of log K_{MA} mean that the metal is strongly bound at the

high-abundance "weak" sites. High values of ΔLK_2 mean that the metal is favoured by the low-abundance "strong" sites, associated, according to the model, with nitrogen-containing groups. If ΔLK_2 is small, the strong sites are not favoured, and binding is predominantly due to oxygen-containing sites.

Table 6.1. Model VI parameters (Tipping, 1998)

Parameter	HA	FA	Comments
M	15000	1500	molecular weight
r (nm)	1.72	0.80	Radius
n_A (mol g^{-1})	$3.3x10^{-3}$	$4.8x10^{-3}$	number of type A groups
n_B (mol g^{-1})	$1.65x10^{-3}$	$2.4x10^{-3}$	= 0.5 x n_A
pK_A	4.1	3.2	median proton dissociation constant for type A groups
pK_B	8.8	9.4	median proton dissociation constant for type B groups
ΔpK_A	2.1	3.3	range factor for pK_A
ΔpK_B	3.6	4.9	range factor for pK_B
P	-330	-115	electrostatic parameter
f_{prB}	0.50	0.42	proximity factor for bidentate sites
f_{prT}	0.065	0.03	proximity factor for tridentate sites
ΔLK_1	2.8	2.8	range factor for metal binding
log K_{MA}			
Mg	0.7	1.1	Intrinsic equilibrium constants for monodentate binding at type A sites. Values for type B sites are obtained from the relation: log K_{MB} = 3.39·log K_{MA} – 1.15 (r^2 = 0.80)
Al	2.6	2.5	
Ca	0.7	1.3	
Fe(III)	2.5	2.4	
Cu	2.0	2.1	
Zn	1.5	1.6	
Cd	1.3	1.6	
Pb	2.0	2.2	

Table 6.1. (Cont.) Model VI parameters (Tipping, 1998)

ΔLK_2		
Mg	0.12	
Al	0.46	
Ca	0.0	Strong binding site term, obtained from the relation: $\Delta LK_2 = 0.55 \cdot \log K_{NH3}$ ($r^2 = 0.66$), where K_{NH3} is the equilibrium constant for complexation with NH_3
Fe(III)	2.20	
Cu	2.34	
Zn	1.28	
Cd	1.48	
Pb	0.93	

The humic binding model is combined with an inorganic speciation model, the species list and constants for which were given in the description of the Windermere Humic Aqueous Model (WHAM; Tipping, 1994). Ionic strength effects on the inorganic reactions are taken into account using the extended Debye-Hückel equation. Temperature effects on reactions between inorganic species are taken into account using published or estimated enthalpy data, but in the absence of experimental information, reactions involving humic substances are assumed to be independent of temperature. The combined model used in the present work is referred to as WHAM / Model VI.

6.3.2. Solubility of Iron (Hydr)oxides

Reported solubility products ($a_{Fe^{3+}}/a_{H^{+3}}$) at 25ºC for "amorphous iron oxide", "hydrous ferric oxide", ferrihydrite, etc. are in the range from $10^{2.5}$ to 10^5. The lowest value was given by Baes and Mesmer (1976), whereas the range from 10^3 to 10^5 was proposed by Nordstrom *et al.* (1990). Lower values represent aged materials, whereas the higher ones are more typical for freshly precipitated material. It can be envisaged that natural waters and soils contain phases with a range of solubility products, depending for example on the intensity of redox cycling or photochemical effects.

6.4. Results and discussion

Figure 6.1 shows the effect of Fe(III) on the binding of Cu by humic acid at pH 4, determined in the present study. The ranges of ν and [Cu^{2+}] cover substantial ranges, and especially the range of low-occupancy binding where the "strong" sites are dominant. A significant competitive effect by Fe(III) is observed. The model was applied by finding the values of log K_{MA} for Cu and Fe(III) that gave the smallest sum of squared residuals in log [Cu^{2+}]. The optimal log K_{MA} for Cu was 1.82, which is close to the default of 2.0. The optimal log K_{MA} for Fe(III) was 2.6, also very close to the default value of 2.5 (see **Table 6.1**). The ion activity products ($a_{Fe^{3+}}/a_{H^{+3}}$) are calculated to be no greater than $10^{1.7}$ for any of the solutions, so it can be assumed that there was no precipitation of $Fe(OH)_3$. The good simulation of the Fe-Cu competition experiments provides support for the basic model assumption that the metals share sites in humic matter.

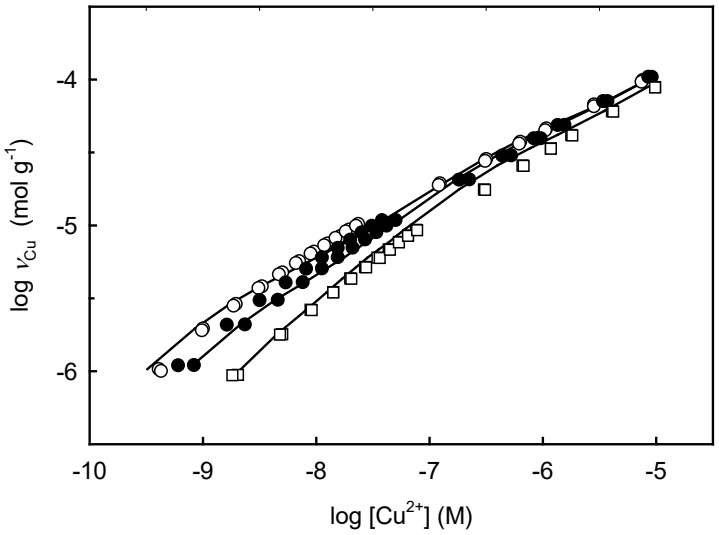

Figure 6.2. Competition by Fe(III) for Cu binding by HA, pH 4, I = 0.1 M. The ratios of Fe(III) to HA in μmol g^{-1} are: 3.5 (open circles), 14 (filled circles) and 36 (open squares). Points are experimental observations; lines are Model VI fits (see text).

Iron has a complex chemistry, and their binding by humic substances have been subjected to relatively little experimental investigation. Humic substances themselves are complex and possibly variable with respect to source.

Consequently, the ability to predict humic binding of Fe in natural waters is imprecise, so far. Nonetheless, the modelling results shown here indicate a reasonably coherent picture of the interactions of the individual metals with humic matter, and of some competitive interactions involving trace metals (such as Cu). Thus, Model VI can account for the available information if some tolerance among examples is allowed in the values of the key parameter log K_{MA}. The very limited field data for Fe(III) complexation by humic substances do not permit a full calibration, but given reasonable assumptions, the model can be made to reproduce the observed values.

If it is accepted that the model has approximate validity, then the predictive calculations raise interesting issues in freshwater metal chemistry. It is evident that competition effects among metals can be highly significant in freshwaters. For instance, the binding of Fe by humic matter is expected to have strong effects on the binding of trace metals, exemplified in the present study by Cu. Indeed, the low-abundance, high-affinity sites that have been demonstrated in isolated and purified humic matter (see e.g. Benedetti *et al.*, 1995; Kinniburgh *et al.*, 1996) may be far less important under conditions prevailing in natural freshwaters. This being so, it is difficult to attribute the strong binding of metals such as Cu in some freshwaters (e.g. Xue and Sigg, 1993) to humic matter and related complexants, as Town and Filella (2000) recently have done. The alternative explanation, proposed by Xue and Sigg (1993) is that the strong binding is by highly selective biogenic ligands, released by phytoplankton in order to control metal levels in their immediate environment. Similar conclusions have been drawn for the surface oceans (Bruland *et al.*, 1991).

6.5. Conclusions

Metal binding to humic substances can be explained approximately by the Humic Ion-Binding Model VI. The model can account for laboratory competition data involving Fe(III) and a trace element (Cu), supporting the assumption that the binding sites are common to all metals. The model suggests that, in freshwaters, Fe(III) might compete significantly with trace metals (especially a high affinity metal such as Cu). As a result of these competition effects, high-affinity sites in humic matter may be less important for trace metal binding in the field than they are in laboratory systems involving humic matter that has been treated to remove associated metals. Future work should, therefore, pay close attention to the Fe(III) content of the humic samples.

6.6. References

Avdeef, A., Zabronsky, J. and Stuting, H. (1983). Calibration of copper ion selective electrode response to pCu 19. *Anal. Chem.*, **55**, 298-304.

Baes, C.F. and Mesmer, R.E. (1976). *Hydrolysis of cations*. Wiley, New York.

Benedetti, M.F., Milne, C.J., Kinniburgh, D.G., van Riemsdijk, W.H. and Koopal, L.K. (1995). Metal ion binding to humic substances: Application of the non-ideal competitive adsorption model. *Environ. Sci. Technol.*, **29**, 446-457.

Bruland, K.W., Donat, J.R. and Hutchins, D.A. (1991). Interactive influences of bioactive trace metals on biological production in oceanic waters. *Limnol. Oceanogr.*, **36**, 1555-1577.

Bryan, S.E. (2001) Ph D thesis. University of Lancaster.

Cameron, A.J. and Liss, P.S. (1984) The stabilization of “dissolved” iron in freshwaters. *Water Res*. **18**, 179-185.

Collienne, R.H. (1983) Photoreduction of iron in the epilimnion of acidic lakes. *Limnol. Oceanogr*. **28**, 83-100.

Davison, W. (1990). A practical guide to pH measurement in freshwaters. *TRAC-Trend. Anal. Chem.*, **9**, 80-83.

Driscoll, C.T. (1984). A procedure for the fractionation of aqueous aluminium in dilute acidic waters. *Int. J. Environ. Anal. Chem*. **16**, 267-283.

Jones, R.I., Shaw, P.J., and De Haan, H. (1993) Effects of dissolved humic substances on the speciation of iron and phosphate at different pH and ionic strength. *Environ. Sci. Technol*. **27**, 1052-1059.

Kinniburgh, D.G., Milne, C.J., Benedetti, M.F., Pinheiro, J.P., Filius, J., Koopal, L.K. and van Riemsdijk, W.H. (1996). Metal ion binding by humic acid: application of the NICA-Donnan Model. *Environ. Sci. Technol.*, **30**, 1687-1698.

Koenings, J.P. (1976). In situ experiments on the dissolved and colloidal state of iron in an acid bog lake. *Limnol. Oceanogr.*, **21**, 674-683.

LaZerte, B.D. (1984). Forms of aqueous aluminium in acidified catchments of central Ontario: a methodological analysis. *Can. J. Fish. Aquat. Sci*. **41**, 766-776.

Milne, C.J., Kinniburgh, D.G. and Tipping, E. (2001). Generic NICA-Donnan model parameters for proton binding by humic substances. *Environ. Sci. Technol.*, **35**, 2049.

Nordstrom, D.K., Plummer, L.N., Langmuir, D., Busenberg, E., May, H.M., Jones, B.F. and Parkhurst, D.L. (1990). Revised chemical equilibrium data for major water-mineral reactions and their limitations. In: Melchior, D.C. and Bassett, R.L. (eds.), *Chemical modeling of aqueous systems* II., vol 1, pp. 398-413. American Chemical Society

Perdue, E.M., Beck, K.C. and Reuter, J.H. (1976). Organic complexes of iron and aluminium in natural waters. *Nature*, **260**, 418-420.

Peters, A.J., Hamilton-Taylor, J. and Tipping, E. (2001). Americium binding to humic acid. *Environ. Sci. Technol.*, **35**, 3495.

Ross, J.M. and Sherrell, R.M. (1999). The role of colloids in tracemetal transport and adsorption behaviour in New Jersey Pinelands streams. *Limnol. Oceanogr*., **44**, 1019-1034.

Shapiro, J. (1966). The relation of humic color to iron in natural waters. *Verh. Internat. Verein. Limnol.*, **16**, 477-484.

Sholkovitz, E.R. and Copland, D. (1981). The coagulation, solubility, and adsorption properties of Fe, Mn, Cu, Ni, Cd, Co and humic acids in a river water. *Geochim. Cosmochim. Acta* **45**, 181-189.

Sojo, L.E. and De Haan, H. (1991) Multicomponent kinetic analysis of iron speciation in humic lake Tjeukemeer: comparison of fulvic acid from the drainage basin and lake water samples. *Environ. Sci. Technol*., **25**, 935-939.

Stumm, W. and Morgan, J.J. (1996). *Aquatic Chemistry. Chemical Equilibria and Rates in Natural Waters.*, 3rd. edn. John Wiley & Sons, New York.

Tipping, E. (1986). Some aspects of the interactions between particulate oxides and aquatic humic substances. *Mar. Chem.*, **18**, 161-169.

Tipping, E. (1994). WHAM. A chemical equilibrium model and computer code for waters, sediments and soils incorporating a discrete site/electrostatic model of ion-binding by humic substances. *Computers & Geosciences*, **20**, 973-1023.

Tipping, E. (1998). Humic ion-binding model VI: An improved description of the interactions of protons and metal ions with humic substances. *Aquat. Geochem.*, **4**, 3-48.

Tipping, E., Woof, C. and Ohnstad, M. (1982). Forms of iron in the oxygenated waters of Esthwaite Water, U.K. *Hydrobiol.*, **92**, 383-393.

Town, R.M. and Filella, M. (2000). Dispelling the myths: Is the existence of L1 and L2 ligands necessary to explain metal ion speciation in natural waters? *Limnol. Oceanogr.*, **45**, 1341-1357.

Voelker, B.M., Morel, F.M.M. and Sulzberger, B. (1997). Iron redox cycling in surface waters: effects of humic substances and light. *Environ. Sci. Technol.*, **31**, 1004-1011.

Xue, H.B. and Sigg, L. (1993). Free cupric ion concentration and Cu(II) speciation in a eutrophic lake. *Limnol. Oceanogr.*, **38**, 1200-1213.

CHAPTER 7

Proton binding to seaweed biomass

Sections 7.1 and 7.2 were published in:
Environ. Sci. Technol., 37 (2003) 5159-5167 and
Chem. Spec. Bioavailab., 16 (2004) 61-69, respectively.

7.1. Acid-base properties of brown seaweed biomass considered as a Donnan gel. A model reflecting electrostatic effects and chemical heterogeneity

Brown seaweeds are interesting materials to be used as biosorbents for heavy metals due to their high binding ability and low cost. The study of the passive biosorption of protons on this kind of materials and its dependency on pH, ionic strength and medium composition is essential for the practical application of brown algae in waste water treatment.

This work reports the results of the study of the proton binding equilibria of dead biomass from the seaweeds *Sargassum muticum*, *Cystoseira baccata* and *Saccorhiza polyschides* by potentiometric titration with a glass electrode in the pH range between 2 and 8. Two different salts, NaCl and KNO_3, in concentrations ranging from 0.05 to 2 $mol \cdot L^{-1}$, were used as background electrolytes. The influence of the ionic strength was accounted for by means of the Donnan model in combination with the master curve approach. Different empirical expressions to describe the swelling behavior of the biosorbent were tested. On the basis of the intrinsic affinity distribution analysis a unimodal Langmuir-Freundlich isotherm was selected to describe the proton binding properties.

The results show very little influence of the type of salt. The ionic strength dependency of the proton binding is very similar for the three species, and average empirical expressions of the Donnan volume are proposed.

The maximum proton binding capacities obtained ranged between 2.4 and 2.9 $mol \cdot kg^{-1}$, with average intrinsic proton affinity constants between 3.1 and 3.3, and heterogeneity parameters of ca. 0.5 for *S. muticum* and *C. baccata*, and slightly higher (ca. 0.7) for *S. polyschides*.

The combined Langmuir-Freundlich equation and Donnan model allowed a good description of the experimental charge vs. pH curves obtained.

7.1.1. Introduction

The process of passive, not metabolically induced, binding of a chemical species to biomass is called biosorption. In recent years, a widespread concern on the cumulative properties and environmental impact of heavy metals has led to the study and development of biosorption as an alternative technique for the removal of these substances from effluents and waste waters (Volesky, 1990; Forster and Wase, 1997). Compared to conventional techniques such as precipitation or ion exchange with synthetic resins, biosorption offers the advantages of the low cost and high binding ability of the materials, and a reduced impact on the environment. These features make biosorption specially suitable to be applied to dilute effluents with a relatively low metal concentration.

Among the different biological substrates studied, algal biomass has received much attention due to its high metal binding capacity (Volesky, 1990). Many studies have been reported on heavy metal biosorption on marine algae (Holan and Volesky, 1994; Leusch *et al.*, 1995; Aderhold *et al.*, 1996; Schiewer and Volesky, 1997a; Matheickal and Yu, 1999; Davis *et al.*, 2000; Figueira *et al.*, 2000; Klimmek *et al.*, 2001). Although pH is always considered a critical factor, the number of papers dealing specifically with the acid-base properties of algal biomass is relatively small (Crist *et al.*, 1988; Crist *et al.*, 1990; Schiewer and Volesky, 1997b; Schiewer and Wong, 2000).

The cell wall plays an important role in proton and metal binding to algae (Crist *et al.*, 1988; Schiewer and Volesky, 1997b), due to its high content in polysaccharides with acid functional groups. The main substances of this type in brown algae are alginates, which usually constitute around 20-40% of the total dry weight (Jensen, 1995), and fucoidans. Alginic acid is a linear polymer of 1,4-linked β-D-mannuronic and α-L-guluronic acids. The monomer sequence and its relation with proton dissociation and metal binding equilibria has been studied by Haug and co-workers (Haug, 1961; Haug *et al.*, 1966; Haug *et al.*, 1974). The term "fucoidans" covers a group of partially sulphated heteropolysaccharides that often contain uronic acids (Lobban and Harrison, 1994). In brown algae, the carboxyl groups of alginates are more abundant than either carboxyl or amine groups of the proteins. Therefore, they are likely to be the main functionalities involved in acid-base reactions (Schiewer and Wong, 2000).

The use of biomaterials under real wastewater conditions requires a previous extensive knowledge of their proton and metal binding properties, which are known to be strongly affected by the nature and concentration of the ionic medium concerned (Sastre de Vicente, 1997).

Specific interaction models, e.g. Pitzer model (Pitzer, 1991), have been successful in describing the ionic strength dependence of the proton binding properties of simple organic ligands such as aminoacids (Fiol *et al.*, 1998), amines (Taboada-Pan *et al.*, 2001) and carboxylic acids (Daniele *et al.*, 1985; Foti *et al.*, 1998; Barriada *et al.*, 2000) in many ionic strength conditions and different background salts. Some of these simple ligands, e.g. phthalic acid (Rey-Castro *et al.*, 2003), have been reported to closely resemble the acid functionalities of natural organic matter like humic substances (Morel and Hering, 1993).

However, in the case of complex natural organic matter several factors complicate the modeling of metal and proton binding reactions (Buffle, 1988): a) polyfunctionality (chemical heterogeneity), due to the presence of sites of different nature and/or steric environment; b) possible conformational changes; and c) polyelectrolytic nature, due to the presence of charged functional groups.

Many monographs that analyze different models of cation binding to heterogeneous complexants can be found in the specialized literature (Buffle, 1988; Grenthe and Puigdomenech, 1997; Borkovec *et al.*, 2001; Tipping, 2002).

The present work reports the study of the proton binding equilibria of three different brown seaweeds, *Sargassum muticum*, *Cystoseira baccata* and *Saccorhiza polyschides* (from the coasts of Galicia, NW Spain). The effects of pH and ionic strength are analyzed in two different background electrolytes. The aim of this study is to check the ability of a physicochemically realistic model to account for the experimental results. The proposed model reflects both the polyelectrolytic and the chemically heterogeneous nature of the algal biomass.

The analysis is restricted to proton dissociation at pH < 8, which is the range of interest in biosorption studies. At higher pH values, most heavy metal cations tend to undergo hydrolysis.

The study of the properties of *Sargassum muticum* as a possible biosorbent is of particular importance. This seaweed constitutes an alien species

that was accidentally introduced in the Atlantic Ocean and the Pacific coasts of North America from Japan (Lüning, 1990). *S. muticum* competes with the local fucalean species and may also interfere with the mussel farming industry, as it often occurs in the Galician rias. Thus, it would constitute an ideal material to be used as biosorbent.

7.1.2. Model

The proton binding "active" zone of the algal biomass is supposed to be constituted of a polyelectrolyte that forms a charged, three-dimensional structure. This layer is modeled as a permeable polyelectrolytic gel. For this kind of systems, Marinsky (1987) proposed a model based on the Gibbs-Donnan formalism. This approach assumes a state of chemical equilibrium of the diffusible components between the gel and the aqueous phase. This equilibrium is defined by the reaction:

$$\overline{HX} + MX = \overline{MX} + HX \tag{7.1.1}$$

where MX is the background electrolyte, and HX its related acid. The bar is used to indicate an association with the water of the gel phase. From the expression of the respective chemical potentials, the following relationship can be obtained:

$$\ln\left(\frac{a_{HX}\,\bar{a}_{MX}}{\bar{a}_{HX}\,a_{MX}}\right) = \frac{\pi}{RT}\left(V_{HX} - V_{MX}\right) \tag{7.1.2}$$

where π is the osmotic pressure of water in the gel phase, V_i is the partial molar volume of the diffusible components, and a_i their activity. In most gel systems, the right-side term of eq. (7.1.2) can be considered negligible (Marinsky, 1987), so this equation can be simplified to:

$$\frac{\bar{a}_H}{a_H} = \frac{\bar{a}_M}{a_M} \tag{7.1.3}$$

This activity ratio will be referred to as the Donnan term (λ). The calculation of this ratio allows the estimation of the proton activity in the gel phase:

$$p\bar{a}_H = pa_H - \mathrm{Log}(\lambda) \tag{7.1.4}$$

where p refers to the negative logarithm.

For the sake of simplicity, only the case of a 1:1 electrolyte has been considered.

7.1.2.1. Estimation of the counterion activity in the gel phase

The activities of the different species in the gel phase are not accessible to direct measurement. Nonetheless, they can be predicted from the assumption of chemical equilibrium between phases and some extra-thermodynamical considerations about the calculation of the activity coefficients (Biesuz *et al.*, 2001).

Throughout the titration process, the negative charge that results from the neutralization of proton ions in the bulk solution is assumed to be compensated by the transfer of an equal amount of counterions into the gel phase. In addition, an extra amount of background salt can be present in the gel phase, as a result of permeation.

The equilibrium state is characterized by the equality of the background electrolyte activities in both phases:

$$a_M a_X = \bar{a}_M \bar{a}_X \tag{7.1.5}$$

where a_i corresponds to the ion activity of species i. The total counterion concentration in the gel will be the sum of the amount sorbed via ion exchange ($\bar{m}_{Me}$), and the amount of salt transferred ($\bar{m}_{MX}$). Their respective activities will be given by:

$$\bar{a}_M = \left(\bar{m}_{Me} + \bar{m}_{MX}\right)\bar{\gamma}_M \tag{7.1.6}$$

$$\bar{a}_X = \bar{m}_{MX}\,\bar{\gamma}_X \tag{7.1.7}$$

$$a_M a_X = m_{MX}^2\,\gamma^2_{\pm(MX)} \tag{7.1.8}$$

where $\bar{m}_i$ is expressed in moles per kg of water contained in the gel, m_{MX} is the molality of the salt in the solution, $\bar{\gamma}_i$ is the molal ion activity coefficient in the gel phase, and $\gamma_\pm$ is the mean molal activity coefficient of the salt in the solution phase.

An expression for $\overline{m}_{MX}$ can be derived from eqs. (7.1.5 – 8):

$$\overline{m}_{MX} = -\frac{\overline{m}_{Me}}{2} + \sqrt{\frac{\overline{m}_{Me}^{2}}{4} + \frac{m_{MX}^{2}\gamma^{2}_{\pm(MX)}}{\left(\overline{\gamma}_{M}\overline{\gamma}_{X}\right)}} \qquad (7.1.9)$$

This expression has to be evaluated iteratively.

The activity coefficients are calculated by means of the Pitzer equations (Pitzer, 1991), under the following assumptions:

- No explicit association between the sorbed M^+ counterions and the algal functional groups is considered. Consequently, all the counterions inside the gel phase are considered to remain as free ions.

- All proton ions are associated with the functional groups.

- The equations for the calculation of the activity coefficient of an ion inside the gel phase are the same as in aqueous solution.

The Donnan term λ can be calculated from eqs. (7.1.3), (7.1.6) and (7.1.9):

$$\lambda = \frac{\overline{\gamma}_{M}}{\gamma_{\pm(MX)}}\left(\frac{\overline{m}_{Me}}{2m_{MX}} + \sqrt{\left(\frac{\overline{m}_{Me}}{2m_{MX}}\right)^{2} + \frac{\gamma_{\pm}^{2}}{\overline{\gamma}_{M}\overline{\gamma}_{X}}}\right) \qquad (7.1.10)$$

The variation in the bulk solution concentration, m_{MX}, due to the ion exchange reaction can be considered negligible, so it is supposed to remain constant throughout the titration.

7.1.2.2. Estimation of ion activity coefficients

In the 1970's, Pitzer (1991) reported various semi-empirical equations for the activity coefficients of pure and mixed electrolytes applicable over wide concentration ranges. In the last two decades, the use of specific ion interaction theories has become widespread for the description of the ionic strength and medium composition dependency of equilibrium constants for simple substances in relatively concentrated solutions. The interested reader is referred to recent reviews published on this subject (Daniele *et al.*, 1997; Sastre de Vicente, 1997).

Despite the good results obtained with simple ligands, researchers have only recently started to apply these models to the study of acid-base equilibria in complex systems such as synthetic polymeric resins (Biesuz *et al.*, 2001). The need of an accurate model to account for the ionic strength effect on the activity coefficients in the study of polyelectrolytic systems arises from the fact that very high counterion concentration ratios between the bulk solution and the vicinity of the polymeric molecule may exist. The assumption of neglecting these deviations from ideality in the calculation of the Donnan factor is analyzed below.

In this work, estimates of the mean and individual ion activity coefficients in the molal scale have been made by means of a simplified version of the Pitzer equations (Pitzer, 1991). Thus, the ion activity coefficient of a cation M^+ in a mixture of 1:1 electrolytes would be given by:

$$\ln \gamma_M = f^{\gamma} + 2\sum_a m_a \left[B_{Ma} + I \cdot C_{Ma}\right] + \sum_c \sum_a m_c m_a \left(B'_{ca} + C_{ca}\right) \qquad (7.1.11)$$

where a and c ($c \neq M$) are the anions and cations present in solution, and m_i are their respective molal concentrations. f^{γ} is a function of the ionic strength (I) related to long-range non-specific electrostatic interactions, whereas the other terms account for specific binary (B, B') and ternary (C) interactions among ions of different charge. The additional parameters (for instance, the parameter associated to interactions between ions of the same charge) are considered negligible in the studied range of ionic strengths.

7.1.2.3. Calculation of the charge vs. pH curves

The data (pH vs. volume of titrant) from the acid-base titrations of the algal biomass at different background salt concentrations were converted to charge-pH curves. Throughout all the paper, the negative logarithm of the proton concentration (-log $[H^+]$) would be referred to as pH. The charge, Q, expressed as moles of protons dissociated per kilogram of biomass was calculated by use of the charge balance condition:

$$Q = \frac{1}{C_{algae}} \left(\left[H^+\right] + \frac{V_b C_b - V_a C_a}{V_0 + V_b + V_a} - \frac{K_w}{\left[H^+\right]} \right) \qquad (7.1.12)$$

where V_0 is the initial volume of the solution in the titration cell, C_{algae} the concentration of biomass in the cell, in kilograms of dry weight per liter, V_a, V_b, C_a and C_b are the volume and concentration of added acid and base, respectively, and K_w is the ionic product of water.

If we consider an exchange ratio of 1 mol of cations from the background electrolyte per mol of titrated protons, Q (mol per kilogram of dry algae) would correspond to the amount of counterion sorbed via ion exchange. Thus, $\bar{m}_{Me}$ can be calculated if the amount of water ($\bar{m}_w$, in kilograms per kilogram of algae) contained in the active layer of the biomass is known:

$$\bar{m}_{Me} = \frac{Q}{\bar{m}_w} \qquad (7.1.13)$$

The amount of salt transferred into the gel phase, $\bar{m}_{MX}$, was calculated iteratively from eq (7.1.9). The Pitzer ion interaction parameters used in the calculation of activity coefficients were taken from bibliography (Pitzer, 1991). The estimated activity coefficients and the values of $\bar{m}_{MX}$ allow the calculation of the Donnan term for each point of the titration, so that the proton binding curves can be transformed to Q as a function of $\bar{pa}_H$, the negative logarithm of the proton activity in the gel phase, using eq. (7.1.4). In the literature, this is often referred to as the master curve. It has been shown (de Wit *et al.*, 1990; de Wit *et al.*, 1993a) that if the electrostatic model is correct, the charge curves at different ionic strengths merge into one single master curve when plotted as a function of $\bar{pa}_H$.

7.1.2.4. Estimation of the amount of water associated with the "active" gel phase

The model used ascribes the deviations from the ideal simple-ligand behavior of the algal biomass to a combination of electrostatic effects, due to the variation of the macromolecule charge, and an inherent chemical heterogeneity. The main problem of this kind of models is the ambiguity in the separation of both effects that exists when the electrostatic model is used without further knowledge about the dimensions of the particles (in this case, the gel volume). In some cases, a unique solution to the electrostatics and hence the position of the master curve cannot be found. For instance, Benedetti *et al.* (1996b) reported that different sets of Donnan volumes may lead to different well-merging master

curves for humic substances. These authors suggested that experimental data of specific volumes should be available in order to avoid this problem.

Recently, Avena *et al.* (1999) have reported estimates of the hydrodynamic volumes and radii of different samples of humic acids from viscosimetric measurements. The reported values allowed a consistent description of the electrostatics of humic acids. On the basis of the viscosimetric data, these authors have proposed an empirical linear function of the pH with an ionic strength-dependent slope for the specific volumes of these substances.

Schiewer and cols. (Schiewer and Volesky, 1997b; Schiewer and Volesky, 1997a; Schiewer and Wong, 2000) have performed swelling experiments with biomass samples from brown algae in order to study the variations of the specific volume with pH and ionic strength. The experimentally determined values correspond to the total specific volume of the particles. Unfortunately, this data can not be used in a quantitative way for modeling, since the volume of the gel phase that takes part actively in the proton binding, i.e. the polysaccharide layer in the cell wall, constitutes an unknown fraction of the total and might even swell to a different extent than the average particle. Nevertheless, these authors have assumed that trends in the total particle volume would correspond to similar trends in the "active" volume. They have suggested the use of linear functions of pH or Q as empirical correlations for the estimation of the Donnan volumes. These authors have not found a clear trend with the ionic strength for the total particle volume of biomass of the genus *Sargassum* (Schiewer and Volesky, 1997b).

However, the main factor that determines the Donnan volume of humic substances has been reported to be the ionic strength. Traditionally, empirical relationships of the Donnan volume with the logarithm of the ionic strength have been used in NICA-Donnan models for these substances (Benedetti *et al.*, 1996a).

Recently, a modification of the Humic Ion Binding Model VI (Tipping, 1998), that includes a fixed-volume Donnan model, has been successfully applied to account for the ionic strength dependence of proton binding in complex heterogeneous systems like peat suspensions (Smith *et al.*, 2004). Other authors have also chosen a constant value of the Donnan volume for peat (Marinsky *et al.*, 1980) and marine algae (Schiewer and Volesky, 1997b).

On the basis of the different approximations mentioned before, several empirical expressions of $\overline{m}_w$ were tested in this work:

a) $\overline{m}_w$ = constant (no swelling).

b) $\overline{m}_w$ proportional to pH, pH^2, Q or Q^2 (dissociation-dependent Donnan volume).

c) $\overline{m}_w$ proportional to a potential function of I (ionic strength-dependent Donnan volume).

d) $\overline{m}_w$ as a function of both the dissociation degree and ionic strength:

$$\overline{m}_w = a + b \cdot I^c \cdot Q \qquad (7.1.14)$$

The latter function is inspired by the relatively complex swelling behavior found with humic substances (Avena *et al.*, 1999), and by the trend of the estimates of $\overline{m}_w$ calculated as detailed in the Results and discussion section.

In each case, the empirical parameters were optimized to yield the best master curve.

7.1.2.5. Description of the master curve with a proton binding isotherm

The intrinsic proton affinity distribution can be calculated by using the so-called condensation approximation (CA) (Nederlof *et al.*, 1990). In this method, the distribution function is obtained as the first derivative of the master curve:

$$F_{CA}\left(\log K_H\right) = \frac{dQ}{d\overline{pa}_H} \qquad (7.1.15)$$

with $\log K_H = \overline{pa}_H$.

F_{CA} is a non-normalized distribution function. Alternatively, the normalized function can be easily calculated if Q_{max} is known, although this amount is often very difficult to determine experimentally.

The calculation of the affinity distribution is very sensitive to random experimental error. The noise in experimental data is specially large in the case of the master curve, as it consists of a superposition of all the curves at different

ionic strengths. Different smoothing procedures have been proposed to avoid spurious peaks. Rigorous studies dealing with the effect of experimental random errors on the calculation of the affinity distribution functions have been published (see for instance (Nederlof *et al.*, 1994)).

On the basis of the wide and smooth distributions obtained for the three algae (see the Results and discussion section), we have chosen a description of the master curve in terms of a continuous distribution of affinities rather than a series of Langmuir equations for discrete ligands. The reason for this is that the CA method applied to the algae data did not allow the resolution of narrow peaks. In addition, the use of a unimodal continuous distribution has the advantage that it requires less adjustable parameters than a combination of two or more discrete Langmuir equations. This approach has also been used with humic substances (de Wit *et al.*, 1993b; Nederlof *et al.*, 1993; Benedetti *et al.*, 1996a).

The Langmuir-Freundlich isotherm, eq. (7.1.16), was chosen among the many isotherm equations that could be used for the description of the intrinsic proton binding. Garcés *et al.* (2002) have shown that different isotherms with the same average and standard deviation of the distribution function can describe ion binding data with similar accuracy at intermediate coverages.

$$Q' = Q_{max}\left(1 - \frac{\left(K_H \bar{a}_H\right)^{\Gamma}}{1 + \left(K_H \bar{a}_H\right)^{\Gamma}}\right) \qquad (7.1.16)$$

where K_H is the proton binding constant, a measure of the average free energy involved in the proton binding reaction. Log K_H corresponds to the mean value of the affinity distribution function. The empirical parameter Γ has a value between 0 and 1, and it is related to the degree of heterogeneity of the system.

7.1.2.6. Correction for electrostatically bound protons

The assumption that inside the gel phase all the proton ions are covalently associated with the acid functional groups may not be strictly correct. A certain amount of dissociated protons is expected to be present in the algae phase, so the amount of charged functional groups would be higher than calculated from eq. (7.1.12). A corrected value was calculated from eq. (7.1.17):

$$Q' = Q + \overline{m}_w \cdot \left(\overline{m}_H - m_H\right) \qquad (7.1.17)$$

where $\overline{m}_H$ and m_H are the concentration of protons calculated in the gel phase and measured in the bulk solution, respectively. Eq. (7.1.17) is a result of considering the total amount of bound cations as the sum of the specifically (covalently) and the electrostatically bound amounts (Kinniburgh *et al.*, 1996; Schiewer and Volesky, 1997b).

This correction term represents about 8% of the concentration of charged groups at the lowest pH and ionic strength, and becomes negligible (less than 1%) above pH = 3 for all the titrations.

7.1.2.7. Data fitting

The parameter values were obtained by minimizing the standard deviation of the differences between experimental and calculated moles dissociated. Function minimizations were carried out by the Nelder-Mead simplex method, and fitting of data to the isotherm equation was done by non-linear least-squares regression using the Levenberg-Marquardt algorithm. Both algorithms were used as the corresponding built-in subroutines implemented in MatLab 6.1 (2001).

7.1.3. Materials and methods

7.1.3.1. Biomass

The three brown seaweeds studied (*Sargassum muticum*, *Cystoseira baccata*, *Saccorhiza polyschides*) were collected from the coast of A Coruña (Galicia, NW-Spain). The algae were oven-dried at 60ºC, ground, sieved (size fraction of 0.5-1 mm) and stored in polyethylene bottles until use. Prior to the experiments the material was pre-treated to remove exchangeable cations and to protonate it. The treatment was carried out by soaking twice the biomass in 0.1 M HCl at a 1:50 and a 1:200 (w/v) ratio with regular shaking on a rotary shaker at 175 rpm for 3 hours. Afterwards the material was rinsed thoroughly with deionized water until constant conductivity was attained and dried in an oven at 60ºC overnight. This procedure was essentially the same as reported in bibliography (Davis *et al.*, 2000).

7.1.3.2. Experiments

Titrations and calibrations were carried out in a glass cell furnished with a thermostating jacket at a temperature of 25.0 ± 0.1 ºC. A nitrogen stream was used to remove dissolved O_2 and CO_2.

The titrating solutions were added from a Crison microBu 2031 automatic buret. Electromotive force measurements were done with a Crison micropH 2000 meter equipped with a Radiometer GK2401C combination glass electrode (Ag/AgCl sat. as reference).

The glass electrodes were calibrated in solutions of known proton concentration at a constant ionic strength following the procedure described elsewhere (Fiol *et al.*, 1992; Brandariz *et al.*, 1998). The calibrations were performed repeatedly for each ionic strength and electrolyte, yielding the formal potential and slope used in subsequent calculations. This method has the advantage that the liquid junction potential and the proton activity coefficient are included in the intercept of the Nernst-type equation (May *et al.*, 1982). Therefore, the possible error due to the change in the medium composition is minimized. As a consequence, this method allows an accurate measurement of proton concentrations, instead of activities, and does not rely on the estimation of activity coefficients for the calculation of the charge balances. On the other hand, a medium of constant ionic strength is required, which sets a limit on the minimum possible background salt concentration.

The electrodes were calibrated in the acid pH range, slopes were within 3% of the theoretical Nernst value and square regression coefficients for the Nernst type equation were always greater than 0.9999.

For each titration, ca. 0.2 g of biomass (dry weight) were placed in the cell, and 40 mL of background electrolyte solution at the desired ionic strength were added. A certain amount of HCl was also added to yield an initial pH value of ca. 2. The stirred suspension was allowed to equilibrate until the emf measure was stable, and then the titration was started. The automatic buret and pH-meter were computer-controlled by means of a homemade software application. After each addition of titrant (NaOH or KOH, prepared with boiled deionised water) the system was allowed to equilibrate until a stable reading was obtained. A whole titration typically takes 6-7 hours. The procedure was tested by comparison with a batch titration (equilibrium time of 12 h in a rotary shaker at

175 rpm), and no significant differences were found. The titrations were done at least by duplicate.

The concentration (in $mol \cdot L^{-1}$) of the different solutions, was converted into molal units through the solution density (Lobo and Quaresma, 1989).

7.1.4. Results and discussion

7.1.4.1. Influence of systematic errors

Each titration starts from an initial pH value of 2 up to a maximum pH of 10-11.5. Within this range, systematic errors may have a different weight depending upon the pH value. It has been analyzed the influence of three parameters, namely, the ionic product of water, and the intercept (E_0) and slope (s) of the Nernst type equation used to calibrate the glass electrodes. Other possible sources of systematic error (temperature, concentration of titrant, etc.) that might also contribute to bias are less important. An example of a charge curve and its first derivative (an estimate of the affinity spectrum (Nederlof *et al.*, 1990)) is shown in **Figure 7.1.1**. It corresponds to a titration of *Saccorhiza polyschides* in 0.1M KNO_3. The experimental set of raw data (V_a, V_b, potential of the glass electrode in mV) was used to calculate the charge vs. pH curve with four different combinations of pK_w, E_0 and s. The differences chosen are considered representative of the observed error. For instance, the values of E_0 and s obtained in seven successive calibrations of the same glass electrode performed in 0.05 M NaCl showed a coefficient of variation of 0.23% and 0.42%, respectively (at the lowest ionic strengths the results usually show the highest dispersion).

As can be noted from **Figure 7.1.1**, the accuracy of the calculated (Q, pH) data decreases drastically above pH 10. Consequently, the calculated affinity spectrum shows an increasing error from this point, and the study of possible acid functionalities in the zone of high pH values would be affected by large errors. Thus, our study was limited to data between pH 2 and pH 8, which is the range of interest in biosorption studies.

Values of pK_w for each electrolyte and ionic strength can be found in bibliography (Brandariz *et al.*, 1995, and references therein). The influence of

systematic errors on the calibration of the glass electrode has been discussed elsewhere (Fiol *et al.*, 1992).

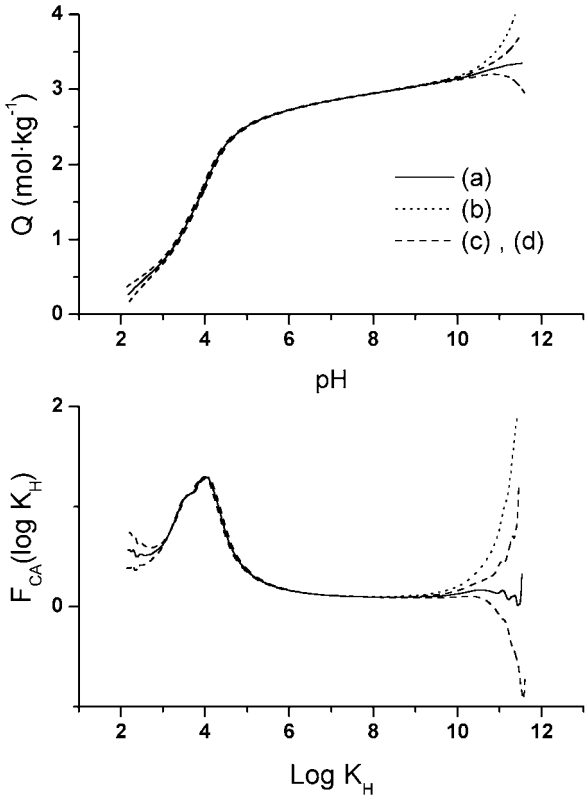

Figure 7.1.1. Influence of systematic errors in the negative logarithm of the ionic product of water (pK_w), and in the intercept (E_0) and slope (s) of the Nernst equation on the charge vs. pH curve of *Saccorhiza polyschides* in 0.1M KNO_3. (a): pK_w = 13.74 (taken from Brandariz *et al* (1995)), experimental values of E_0 and s (calculated from the calibrations at the same ionic strength); (b) the same as (a), with pK_w = 14; (c) the same as (a), but with relative errors in E_0 and s of -0.25% and +0.5%, respectively; (d) the same as (a) but with relative errors in E_0 and s of +0.25% and -0.5%, respectively. Lower panel: calculated affinity distribution function $F_{CA}(\log K_H)$ (non-normalized).

7.1.4.2. Influence of activity coefficients

The error involved in neglecting activity coefficients in the expression of the Donnan potential term has also been studied. The assumption of $\gamma_i = 1$ in eq. (7.1.10) leads to:

$$\lambda = \left(\frac{\overline{m}_{Me}}{2m_{MX}} + \sqrt{\left(\frac{\overline{m}_{Me}}{2m_{MX}} \right)^2 + 1} \right) \qquad (7.1.18)$$

Note that all the concentrations are in the mol kg^{-1} scale, and that the difference between molar and molal scale is not negligible at concentrations as high as 2 mol L^{-1}.

A hypothetical Donnan gel phase with a total functional group content, Q_{max}, of 2.5 mol kg^{-1} and a constant water content of 4 grams per gram of dry weight, in equilibrium with KNO_3 solutions of concentrations between 0.01 and 2 mol kg^{-1} was tested. The Donnan factor λ was calculated either with eq. (7.1.10) or with eq. (7.1.8). The results are shown in **Figure 7.1.2**.

As can be seen in **Figure 7.1.2**, eq. (7.1.18) overestimates the λ values, with regard to those calculated when activity coefficients are taken into account. This discrepancy tends to increase as ionic strength decreases. Such result is explained by the fact that the ratio of counterion concentrations inside and outside the gel phase and, consequently, the difference in the activity coefficients, becomes larger as the ionic strength decreases.

The influence of the activity coefficients on the estimated Donnan term would become larger as the gel water content decreases and Q_{max} increases.

It must be pointed out that the procedure used for the estimation of $\overline{\gamma}_i$ represents merely an approximation, as it is not possible to determine activity coefficients in a gel phase experimentally. Nevertheless, these results highlight the fact that neglecting activity coefficients may represent a rough simplification.

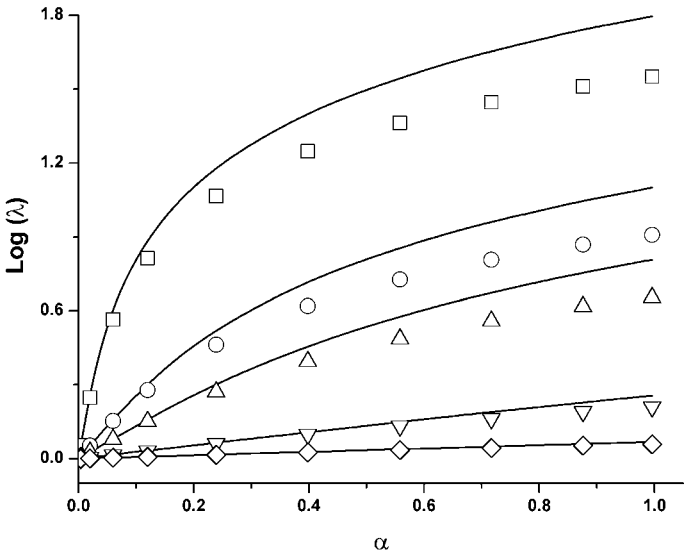

Figure 7.1.2. Logarithm of the Donnan term as a function of the dissociation degree, α. Log λ was calculated with eq. (7.1.18) (lines) and eq. (7.1.10) (symbols), at different ionic strengths: 0.01 (squares), 0.05 (circles), 0.1 (up triangles), 0.5 (down triangles) and 2 mol·kg^{-1} (diamonds).

7.1.4.3. Parameter estimates. Swelling behavior

A typical effect in most polyelectrolytic systems is the apparent negligible ionic strength effect on the proton dissociation at salt concentrations above 1 M. In our case, this general rule is confirmed by the negligible difference between the charge-pH curves at 0.7 and 2.0 M. So it seems reasonable to assume that the electrostatic effects are suppressed at 2.0 M. Therefore, the curve at this salt concentration can be considered as an approximation to the master curve. In this way estimates of $\bar{m}_w$ at each point of the other curves can be calculated, and the results may reveal a particular trend with pH, specific charge and/or salt concentration. An analogous approach has been used by Plette *et al.* (1995) in their study of the proton binding behavior of isolated bacterial cell walls.

The procedure for the estimation of $\bar{m}_w$ can be summarized in the following steps:

- For each experimental point of the titrations at 2.0 M ionic strength, the value of pa_H is assumed to be equal to $\overline{pa}_H$.

- The charge vs. $\overline{pa}_H$ curve (in 2.0 M) is fitted to a Langmuir-Freundlich equation to interpolate data.

- For the rest of the titrations, the logarithm of the Donnan term is estimated by difference: $\log \lambda = pa_{H(I)} - pa_{H(I=2M)}$.

- $\overline{m}_w$ is calculated iteratively from eqs. (7.1.10) and (7.1.13), with a tolerance of 0.001 in logarithmic units.

The results obtained for *S. muticum* in NaCl are plotted in **Figure 7.1.3**. A simultaneous influence of ionic strength and specific charge, Q, on $\overline{m}_w$ is observed.

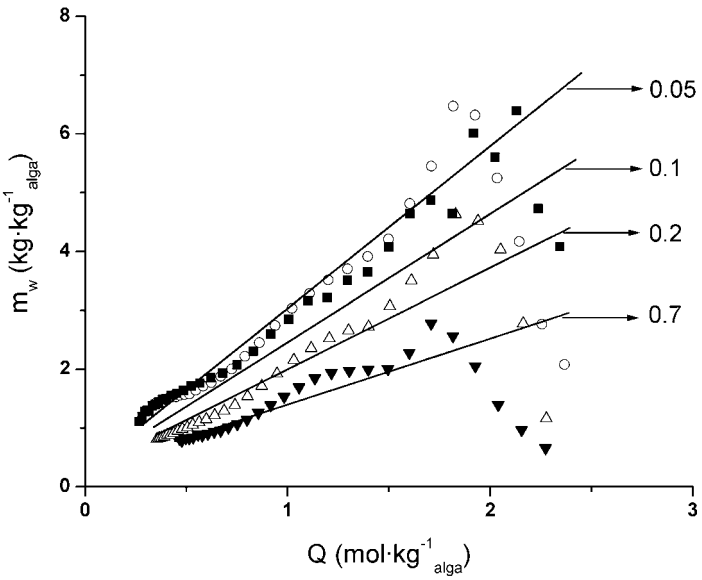

Figure 7.1.3. Water content of the proton-binding active layer of *S. muticum* in NaCl at different ionic strengths: 0.05 M (squares), 0.1 M (circles), 0.2 M (up triangles) and 0.7 M (down triangles). Values calculated on the basis of the Donnan model, using the charge-pH curve at 2 M as an approximation of the true master curve (see text for details). The lines correspond to estimates calculated from eq. (7.1.14) with the optimized parameters listed in **Table 7.1.1** (the numbers indicate the ionic strength in mol·L^{-1}).

The optimized coefficients for the different empirical expressions of $\bar{m}_w$ that were tested are summarized in **Table 7.1.1** together with the parameters of the Langmuir-Freundlich fit of the master curve data obtained in each case. For the sake of brevity, only the case of *S. muticum* is shown.

Table 7.1.1. Fitting parameters for the Donnan electrostatic and Langmuir-Freundlich heterogeneity description of the charge-pH data for *S. muticum*

$\bar{m}_w$ (kg·kg$^{-1}_{alga}$)	Q_{max} (mol·kg$^{-1}_{alga}$)[a]	Log K_H[a]	Γ[a]	SD[b]
		S. muticum in KNO_3		
3.6	2.36	3.24	0.62	0.047
1.0·pH	2.37	3.25	0.58	0.037
4.0·Q	2.41	3.31	0.53	0.034
$0.3\cdot pH^2$	2.39	3.27	0.55	0.032
$1.3+2.2\cdot Q^2$	2.39	3.30	0.53	0.030
$0.23\cdot I^{-0.61}$	2.36	2.90	0.66	0.037
$0.3+1.1\cdot I^{-0.35}\cdot Q$	2.40	3.23	0.55	0.030
		S. muticum in NaCl		
3.6	2.39	3.23	0.66	0.052
1.0·pH	2.39	3.22	0.61	0.042
3.7·Q	2.42	3.29	0.55	0.040
$0.3\cdot pH^2$	2.40	3.23	0.57	0.038
$1.5+1.8\cdot Q^2$	2.40	3.26	0.56	0.036
$0.51\cdot I^{-0.41}$	2.36	2.86	0.76	0.041
$0.3+1.0\cdot I^{-0.34}\cdot Q$	2.41	3.17	0.57	0.034

[a] Parameters obtained from the fitting of ($\bar{a}_H$, Q') data to a Langmuir-Freundlich isotherm.

[b] Standard deviation of the residuals in Q' (mol kg$^{-1}_{alga}$).

The first general conclusion is that the proton binding properties of each species are almost identical regardless the electrolyte used as background salt. In particular, the optimized parameters of the different empirical expressions for $\bar{m}_w$ show values almost identical in NaCl and KNO_3. This seems to indicate

that the shrinking/swelling behavior of the gel phase would not depend on the nature of the salt, for 1:1 electrolytes. The only exception seems to be the ionic strength-dependent expression of the Donnan volume, which yields rather different optimized parameters. This is probably related to the fact that the estimation of the activity coefficients becomes critical, due to the small values of $\overline{m}_w$ and, consequently, the high ionic strengths estimated by the model. For instance, the value of $\overline{m}_w$ for *S. muticum* in 2.0 M KNO_3, calculated from the I-dependent expression is 0.37 $kg \cdot kg^{-1}_{alga}$ (i.e. only a 27% of water in the gel phase). For algal biomass with an specific charge of 2 $mol \cdot kg^{-1}_{alga}$, the estimated ionic strength would be as high as 5.8 $mol \cdot kg^{-1}$. In such a concentrated environment it is reasonable to admit that the approximations included in the model might not be adequate.

In addition, the optimized $\overline{m}_w$ expressions obtained for each alga are also very similar among them, suggesting a common swelling behavior of the three species. Therefore, all the datasets were fitted simultaneously to obtain average values of the Donnan volume expressions. The results are listed in **Table 7.1.2**. For the case of no swelling (first row), the use of the ratio Donnan volume / total amount of binding sites (Q_{max}) is suggested as a way of accounting for the differences in the total content in functional groups (related to the percentage of alginate). It is known that the amount of alginate depends not only on the seaweed species, but also on the season, light supply, dynamics of water, etc. (Lobban and Harrison, 1994). A similar relationship was proposed by Schiewer and Wong (2000) for algal biomass. Analogously, Smith *et al.* (2004) expressed the Donnan volume in terms of the humic content of an acid-treated peat as a way of comparing different peat samples.

Table 7.1.2. Average empirical expressions of $\overline{m}_w$ for the three algae investigated in both electrolytes. [a] Standard deviation of the residuals in Q' ($mol\ kg^{-1}_{alga}$).

$\overline{m}_w$ ($kg \cdot kg^{-1}_{alga}$)	SD[a]
$1.4 \cdot Q_{max}$	0.063
$1.0 \cdot pH$	0.053
$3.5 \cdot Q$	0.049
$1.6+1.5 \cdot Q^2$	0.043
$0.6+0.8 \cdot I^{-0.37} \cdot Q$	0.042

A selection of the master curves calculated with different models to account for the particle swelling is shown in **Figure 7.1.4**. Except in the case of constant volume (no swelling), the calculated ($\bar{a}_H$, Q') curves merge fairly well to a single master curve for the ionic strengths studied. From the point of view of the convergence to the master curve, the use of a constant value of $\bar{m}_w$ is not fully satisfactory, as it leads to a higher dispersion of data and, consequently, to a worse fit (master curve not shown). The empirical dissociation-dependent or ionic strength-dependent expressions of $\bar{m}_w$ lead to well-merged curves and similar values of the standard deviation. The expressions of $\bar{m}_w$ as a function of pH or Q, and eq. (7.1.14) lead to a master curve that is almost superimposed to the titration curve at 2.0 $mol \cdot L^{-1}$, whereas the master curve obtained with the I-dependent expression of $\bar{m}_w$ shows a larger slope (see **Figure 7.1.4**). Consequently, in the latter case the heterogeneity becomes smaller (i.e., the calculated Γ value is closer to one) and the log K_H values are lower. The fact that different expressions of $\bar{m}_w$ may lead to an equally good convergence of the titration curves to different master curves demonstrates an ambiguity in the Donnan volume estimation and the necessity for an independent determination of $\bar{m}_w$. When no direct measurements of $\bar{m}_w$ are available the choice of a given model for the physical behavior of the gel phase may have an influence on the analysis of the intrinsic proton binding properties.

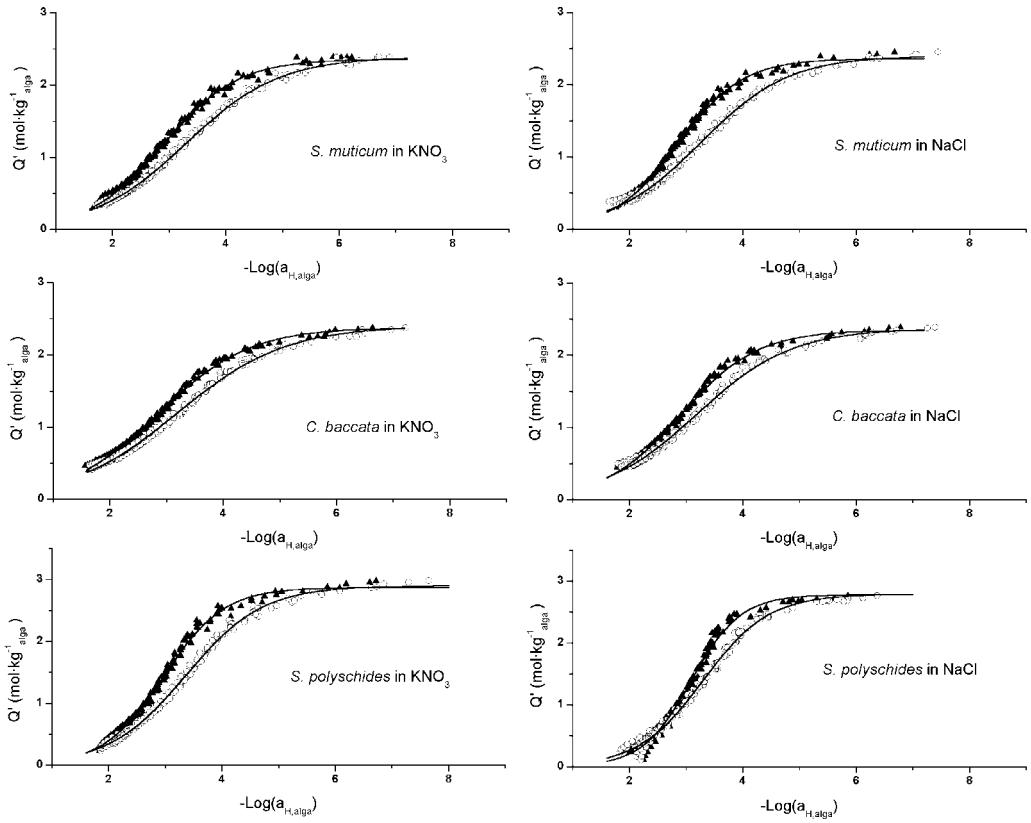

Figure 7.1.4. Calculated master curves for the three algae in NaCl and KNO_3. Filled triangles: $m_w = a \cdot I^{-b}$; open circles: $m_w = a + b \cdot I^c \cdot Q$; lines: Langmuir-Freundlich best fits.

7.1.4.4. Intrinsic proton binding

The proton affinity distribution functions F_{CA} obtained from the master curves of the three algae in KNO_3 are shown in **Figure 7.1.5**. It can be noted that the three affinity distributions are very similar, all showing a rather broad peak with a maximum in the log K_H range 3-3.5. In the case of *S. polyschides* the narrower peak suggests a lower degree of heterogeneity.

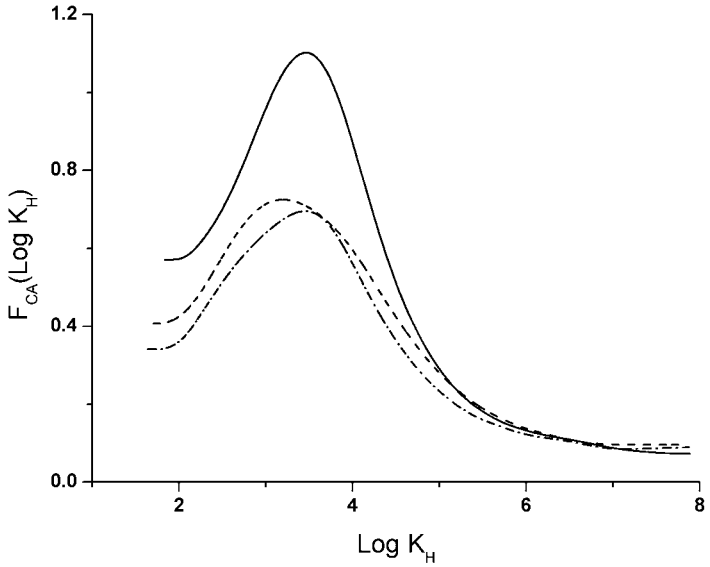

Figure 7.1.5. Non-normalized affinity distribution function, calculated with the CA method (Nederlof *et al.*, 1990) using a cubic smoothing spline of the master curve data obtained in KNO_3 under the assumption of $\bar{m}_w = a + b \cdot I^c \cdot Q$. Solid line: *S. Polyschides*; dashed line: *S. muticum*; dotted/dashed line: *C. baccata*.

The proton binding parameters of the Langmuir-Freundlich equation are listed in **Table 7.1.3**. The optimized Q_{max} values represent at least the 96 per cent of the values calculated from the first derivative of the electrode potential vs. titrant volume curves. The Γ heterogeneity factors lie between 0.5 and 0.75. The calculated log K_H values are very similar for the three species, ranging from 3.11 (*C. baccata*) to 3.24 (*S. polyschides*). In all the cases the I-dependent expression for $\bar{m}_w$ leads to a log K_H value ca. 0.3 logarithmic units lower.

Table 7.1.3. Parameters obtained from the fitting of ($\bar{a}_H$, Q') data (in both electrolytes) to a Langmuir-Freundlich isotherm, assuming $\bar{m}_w = a + b \cdot I^c \cdot Q$. [a] Standard deviation of the residuals in Q' (mol kg^{-1}_{alga}).

Species	log K_H	Γ	Q_{max} (mol·kg^{-1}_{alga})	SD[a]
S. muticum	3.18	0.58	2.40	0.035
C. baccata	3.11	0.50	2.38	0.041
S. polyschides	3.24	0.74	2.84	0.070

It is interesting to compare these results with the set of average values obtained by Milne *et al.* (2001) using the NICA-Donnan model for a number of humic and fulvic acid samples. It must be recalled that the NICA equation for proton binding is equivalent to a bimodal Langmuir-Freundlich isotherm (Benedetti *et al.*, 1996a). The median values of the first peak of the affinity distribution, often associated to the carboxylic moieties, are 2.3-2.9 and the corresponding heterogeneity factors have a value of 0.4-0.5. This would indicate that, in general, brown algal surfaces show a lower apparent heterogeneity and a slightly larger median affinity constant than humic substances.

Regardless of the swelling model employed, it can be noted that the proton binding behavior of *S. muticum* and *C. baccata* is very similar, in concordance with their morphological similitudes. *S. polyschides*, however, shows a smaller degree of heterogeneity, in agreement with what is observed in the intrinsic affinity distributions.

Figure 7.1.6 shows the experimental charge vs. pH data and the model estimates calculated under two assumptions: constant $\bar{m}_w$, and $\bar{m}_w$ as a function of Q and I (eq. 7.1.14). These two cases represent the worse and the best fits of the experimental data, respectively. It can be noted that even in the case of no swelling, the model can predict reasonably well the spacing between the charge curves at an intermediate dissociation degree, although the shape of the whole curve is not adequately reproduced. On the contrary, the more complex function (eq. 7.1.14) leads to a satisfactory fit throughout the pH range of study.

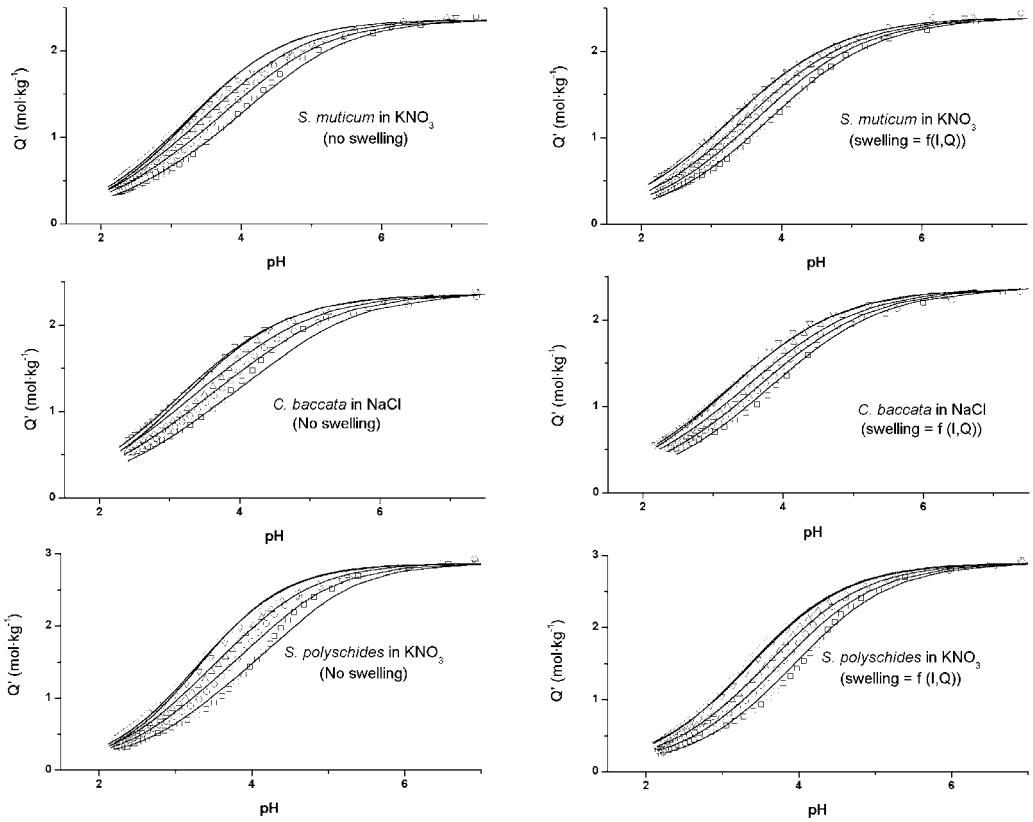

Figure 7.1.6. Charge vs. pH curves of *S. muticum* in KNO_3, *C. baccata* in NaCl and *S. polyschides* in KNO_3. Open symbols represent the experimental points at different ionic strengths: 0.05 M (squares), 0.1 M (circles), 0.2 M (up triangles), 0.7 M (down triangles) and 2 M (diamonds). Only every second point is shown for clarity. Lines represent model calculations under the assumption of constant m_w (panels on the left) and $m_w = a + b \cdot I^c \cdot Q$ (panels on the right). The lines that correspond to the 0.7 and 2 M ionic strengths are almost superimposed.

7.1.5. References

(2001) MatLab®. The MathWorks, Inc., Northampton, MA

Aderhold, D., Williams, C.J. and Edyvean, R.G.J. 1996. The removal of heavy-metal ions by seaweeds and their derivatives. *Bioresource Technol.*, **58**, 1-6.

Avena, M.J., Koopal, L.K. and van Riemsdijk, W.H. 1999. Proton binding to humic acids: electrostatic and intrinsic interactions. *J. Colloid Interf. Sci.*, **217**, 37-48.

Barriada, J.L., Brandariz, I. and Sastre de Vicente, M.E. 2000. Acid-base equilibria of monocarboxylic acids in various saline media: analysis of data using Pitzer equations. *J. Chem. Eng. Data*, **45**, 1173-1178.

Benedetti, M.F., van Riemsdijk, W.H. and Koopal, L.K. 1996a. Humic substances considered as a Heterogeneous Donnan Gel Phase. *Environ. Sci. Technol.*, **30**, 1805-1813.

Benedetti, M.F., van Riemsdijk, W.H., Koopal, L.K., Kinniburgh, D.G., Gooddy, D.C. and Milne, C.J. 1996b. Metal ion binding by natural organic matter: From the model to the field. *Geochim. Cosmochim. Acta*, **60**, 2503-2513.

Biesuz, R., Zagorodni, A.A. and Muhammed, M. 2001. Estimation of Deprotonation Coefficients for Chelating Ion Exchange Resins. Comparison of Different Thermodynamic Models. *J. Phys. Chem. B*, **105**, 4721-4726.

Borkovec, M., Jönsson, B. and Koper, G.J.M. 2001. Ionization processes and proton binding in polyprotic systems: small molecules, proteins, interfaces, and polyelectrolytes. In: Matijevic, E. (ed.), *Surface and colloid science*, vol 16, pp. 99-399. Kluwer Academic / Plenum Press, New York.

Brandariz, I., Fiol, S. and Sastre de Vicente, M.E. 1995. Study of the influence of ionic strength on the ionic product of water in saline media at 25ºC using the Pitzer equations. *Ber. Bunsenges Phys. Chem*, **99**, 749-752.

Brandariz, I., Vilariño, T., Alonso, P., Herrero, R., Fiol, S. and Sastre de Vicente, M.E. 1998. Effect of ionic strength on the formal potential of the glass electrode in various saline media. *Talanta*, **46**, 1469-1477.

Buffle, J. 1988. *Complexation reactions in aquatic systems: An analytical approach*. Ellis Horwood, Chichester.

Crist, R.H., Martin, J.R., Guptill, P.W., Eslinger, J.M. and Crist, D.R. 1990. Interaction of metals and protons with algae. 2. Ion exchange in adsorption and metal displacement by protons. *Environ. Sci. Technol.*, **24**, 337-342.

Crist, R.H., Oberholser, K., Schwartz, D., Marzoff, J., Ryder, D. and Crist, D.R. 1988. Interactions of metals and protons with algae. *Environ. Sci. Technol.*, **22**, 755-760.

Daniele, P.G., De Robertis, A., De Stefano, C., Sammartano, S. and Rigano, C. 1985. On the possibility of determining the thermodynamic parameters for the formation of weak complexes using a simple model for the dependence on ionic strength of activity coefficients: Na^+, K^+, and Ca^{2+} complexes of low molecular weight ligands in aqueous solution. *J. Chem. Soc. Dalton*, 2353-2361.

Daniele, P.G., De Stefano, C., Foti, C. and Sammartano, S. 1997. The effect of ionic strength and ionic medium on the thermodinamic parameters of protonation and complex formation. *Curr. Top. Solution Chem.*, **2**, 253-274.

Davis, T.A., Volesky, B. and Vieira, R.H.S.F. 2000. Sargassum seaweed as biosorbent for heavy metals. *Wat. Res.*, **34**, 4270-4278.

de Wit, J.C.M., van Riemsdijk, W.H. and Koopal, L.K. 1993a. Proton binding to humic substances. 1. Electrostatic effects. *Environ. Sci. Technol.*, **27**, 2005-2014.

de Wit, J.C.M., van Riemsdijk, W.H. and Koopal, L.K. 1993b. Proton binding to Humic substances. 2. Chemical heterogeneity and adsorption models. *Environ. Sci. Technol.*, **27**, 2015-2022.

de Wit, J.C.M., van Riemsdijk, W.H., Nederlof, M.M., Kinniburgh, D.G. and Koopal, L.K. 1990. Analysis of ion binding on humic substances and the determination of intrinsic affinity distributions. *Anal. Chim. Acta*, **232**, 189-207.

Figueira, M.M., Volesky, B., Ciminelli, V.S.T. and Roddick, F.A. 2000. Biosorption of metals in brown seaweed biomass. *Wat. Res.*, **34**, 196-204.

Fiol, S., Arce, F., Armesto, X.L., Penedo, F. and Sastre de Vicente, M.E. 1992. Analysis of Systematic Errors in Calibrating Glass Electrodes with H^+ as a Concentration Probe. *Fresenius J. Anal. Chem.*, **343**, 469-472.

Fiol, S., Vilariño, T., Herrero, R., Sastre de Vicente, M.E. and Arce, F. 1998. Protonation constants of valine, serine, and beta-alanine in artificial seawater at 25º C. *J. Chem. Eng. Data*, **43**, 393-395.

Forster, C.F. and Wase, D.A.J. 1997. *Biosorbents for metal ions*. Taylor & Francis, London.

Foti, C., Sammartano, S. and Signorino, G. 1998. The dependence on ionic strength of protonation constants of carboxylic acids in aqueous tetraethylammonium iodide solution, at different temperatures. *Fluid Phase Equilibr.*, **149**, 91-101.

Garcés, J.L., Mas, F., Cecília, J., Companys, E., Galceran, J., Salvador, J. and Puy, J. 2002. Complexation isotherms in metal speciation studies at trace concentration levels. Voltammetric techniques in environmental samples. *Phys. Chem. Chem. Phys.*, **4**, 3764-3773.

Grenthe, I. and Puigdomenech, I. (1997) Modeling in aquatic chemistry. OECD Nuclear Energy Agency, Paris

Haug, A. 1961. Dissociation of alginic acid. *Acta Chem. Scand.*, **15**, 950-952.

Haug, A., Larsen, B. and Smidsrod, O. 1966. A study of the constitution of alginic acid by partial acid hydrolysis. *Acta Chem. Scand.*, **20**, 183-190.

Haug, A., Larsen, B. and Smidsrod, O. 1974. Uronic acid sequence in alginate from different sources. *Carbohyd. Res.*, **32**, 217-225.

Holan, Z.R. and Volesky, B. 1994. Biosorption of lead and nickel by biomass of marine algae. *Biotechnol. Bioeng.*, **43**, 1001-1009.

Jensen, A. 1995. Production of alginate. In: Wiessner, W., Schnepf, E. and Starr, R.C. (eds.), *Algae, environment and human affairs*, pp. 79-92. Biopress, Bristol.

Kinniburgh, D.G., Milne, C.J., Benedetti, M.F., Pinheiro, J.P., Filius, J., Koopal, L.K. and van Riemsdijk, W.H. 1996. Metal ion binding by humic acid: application of the NICA-Donnan Model. *Environ. Sci. Technol.*, **30**, 1687-1698.

Klimmek, S., Stan, H.J., Wilke, A., Bunke, G. and Buchholz, R. 2001. Comparative analysis of the biosorption of cadmium, lead, nickel and zinc by algae. *Environ. Sci. Technol.*, **35**, 4283-4288.

Leusch, A., Holan, Z.R. and Volesky, B. 1995. Biosorption of heavy metals (Cd, Cu, Ni, Pb, Zn) by chemically-reinforced biomass of marine algae. *J.Chem.Technol. Biot.*, **62**, 279-288.

Lobban, C.S. and Harrison, P.J. 1994. *Seaweed ecology and physiology*. Cambridge University Press, Cambridge.

Lobo, V.M.M. and Quaresma, J.L. 1989. *Handbook of electrolyte solutions*. Elsevier, Amsterdam.

Lüning, K. 1990. *Seaweeds: their environment, biogeography, and ecophysiology*. John Wiley & Sons, New York.

Marinsky, J.A. 1987. A two-phase model for the interpretation of proton and metal ion interaction with charged polyelectrolyte gels and their linear analogs. In: Stumm, W. (ed.), *Aquatic Surface Chemistry. Chemical Processes at the Particle-Water Interface.*, pp. 49-81. J. Wiley & Sons, New York.

Marinsky, J.A., Wolf, A. and Bunzl, K. 1980. The binding of trace amounts of lead(II), copper(II), cadmium(II), zinc(II) and calcium(II) to soil organic matter. *Talanta*, **27**, 461-468.

Matheickal, J.T. and Yu, Q. 1999. Biosorption of lead(II) and copper(II) from aqueous solution by pre-treated biomass of Australian marine algae. *Bioresource Technol.*, **69**, 223-229.

May, P.M., Williams, D.R., Linder, P.W. and Torrington, R.G. 1982. The use of glass electrodes for the determination of formation constants I. *Talanta*, **29**, 249-256.

Milne, C.J., Kinniburgh, D.G. and Tipping, E. 2001. Generic NICA-Donnan model parameters for proton binding by humic substances. *Environ. Sci. Technol.*, **35**, 2049.

Morel, F.M.M. and Hering, J.G. 1993. *Principles and Applications of Aquatic Chemistry*. J. Wiley & Sons, New York.

Nederlof, M.M., de Wit, J.C.M., van Riemsdijk, W.H. and Koopal, L.K. 1993. Determination of proton affinity distributions for humic substances. *Environ. Sci. Technol.*, **27**, 846-856.

Nederlof, M.M., van Riemsdijk, W.H. and Koopal, L.K. 1990. Determination of adsorption affinity distributions: A general framework for methods related to local isotherm approximations. *J. Colloid Interf. Sci.*, **135**, 410-426.

Nederlof, M.M., van Riemsdijk, W.H. and Koopal, L.K. 1994. Heterogeneity analysis for binding data using an adapted smoothing spline technique. *Environ. Sci. Technol.*, **28**, 1037-1047.

Pitzer, K.S. 1991. Ion interaction approach: Theory and data correlation. In: Pitzer, K.S. (ed.), *Activity coefficients in electrolyte solutions*, pp. 75-153. CRC Press, Boca Raton, Florida.

Plette, A.C.C., van Riemsdijk, W.H., Benedetti, M.F. and van der Wal, A. 1995. pH dependent charging behavior of isolated cell walls of a Gram-positive soil bacterium. *J. Colloid Interf. Sci.*, **173**, 354-363.

Rey-Castro, C., Castro-Varela, R., Herrero, R. and Sastre de Vicente, M.E. 2003. Acid-base equilibria of phthalic acid in saline media: ion association from Pitzer equations. *Talanta*, **60**, 93-101.

Sastre de Vicente, M.E. 1997. Ionic strength effects on acid-base equilibria. A review. *Curr. Top. Solution Chem.*, **2**, 157-181.

Schiewer, S. and Volesky, B. 1997a. Ionic strength and electrostatic effects in biosorption of divalent metal ions and protons. *Environ. Sci. Technol.*, **31**, 2478-2485.

Schiewer, S. and Volesky, B. 1997b. Ionic strength and electrostatic effects in biosorption of protons. *Environ. Sci. Technol.*, **31**, 1863-1871.

Schiewer, S. and Wong, M.H. 2000. Ionic strength effects in biosorption of metals by marine algae. *Chemosphere*, **41**, 271-282.

Smith, E.J., Rey-Castro, C., Longworth, H., Lofts, S., Lawlor, A.J. and Tipping, E. 2004. Cation binding by acid-washed peat. *Eur. J. Soil Sci.* (in press).

Taboada-Pan, C., Brandariz, I., Barriada, J.L., Vilariño, T. and Sastre de Vicente, M.E. 2001. The salting coefficient and size of alkylamines in saline media at different temperatures: estimation from Pitzer equations and the mean spherical approximation. *Fluid Phase Equilibr.*, **180**, 313-325.

Tipping, E. 1998. Humic ion-binding model VI: An improved description of the interactions of protons and metal ions with humic substances. *Aquat. Geochem.*, **4**, 3-48.

Tipping, E. 2002. *Cation binding by humic substances*. Cambridge University Press, Cambridge.

Volesky, B. 1990. *Biosorption of heavy metals*. CRC Press, Boca Raton, Florida.

7.2. Surface charge and permeable gel descriptions of the ionic strength influence on proton binding to seaweed biomass

The development of physicochemical models for the description of cation binding to algal biomass is an essential issue for the practical application of seaweeds as biosorbents in wastewater treatment. These models should be able to account for the polyelectrolytic properties of these materials, and to reasonably describe and predict the ionic strength effect.

Data regarding the proton binding equilibria of *Sargassum muticum*, *Cystoseira baccata* and *Saccorhiza polyschides* in NaCl and KNO_3 were reported on a preceding paper. These data are re-analysed in this work, in order to compare two different electrostatic models (surface charge and Donnan models), representing two opposite idealised interface structures (planar surface and permeable gel). Simple analytical equations relating the apparent pK with both the dissociation degree and the ionic strength are derived for each case. The experimental data are reproduced with similar accuracy by the surface charge and the simplest Donnan model (rigid volume), although the latter seems to yield slightly better results. The comparison of the geometric parameters involved in each model (Donnan volume and specific area) with independent experimental measurements is not straightforward. Therefore, both models seem to be almost equivalent, within their respective assumptions. Nevertheless, Donnan has the advantage that provides a simple way to account for activity coefficient effects and non-specific binding.

7.2.1. Introduction

Brown seaweeds are very promising materials to be used as biosorbents in waste water treatment due to their abundance, low cost, high sorbent capacity and low environmental impact (Volesky, 1990). These features make the dead biomass obtained from seaweeds an excellent material for the removal of heavy metals and other pollutants from industrial effluents.

In recent years, a considerable effort has been focused on the development of physicochemical models capable to account for the effect of the different environmental conditions (ionic strength, pH, etc.) on the cation binding to these substances. In most of these works, pH and ionic strength have

been reported to strongly influence the heavy metal binding properties of algal biomass, although few studies provide a comprehensive model (Crist *et al.*, 1990; Schiewer and Volesky, 1997a; Schiewer and Volesky, 1997b).

Biosorption of proton and metal ions by algae is considered to take place in the cell wall (Crist *et al.*, 1988). In brown algae, the cell wall is constituted of a microfibrillar skeleton, mainly comprised of cellulose, and an amorphous embedding matrix, composed of polysaccharides with acid functional groups. The main components of this matrix in brown algae are alginates and fucoidans. Alginic acid is the common name of a family of linear polymers of 1,4-linked β-D-mannuronic and α-L-guluronic acids arranged in a non-regular, blockwise order along the chain. It usually constitutes around 20-40% of the dry weight (Percival and McDowell, 1967; Jensen, 1995). The term "fucoidans" covers a group of partially sulphated heteropolysaccharides that often contain uronic acids (Lobban and Harrison, 1994). In brown algae, the carboxylic groups from the cell wall polysaccharides are usually the most abundant acidic functional group and, therefore, the main functionality involved in acid-base reactions (Schiewer and Wong, 2000). The interested reader is referred to a very recent work reviewing the biochemistry of metal biosorption by seaweeds (Davis *et al.*, 2003).

In a previous study (Rey-Castro *et al.*, 2003) a combination of a Donnan model for the polyelectrolytic effect, and a Langmuir-Freundlich isotherm to describe the specific proton binding, was successfully applied to the description of the proton binding to seaweeds. The Donnan description of the electrostatic contribution to the proton binding assumes the algal particles to behave as a permeable three-dimensional gel that constitutes a separate phase in electrochemical equilibrium with the bulk solution. This picture is inspired by the structure of the cell walls, basically constituted of a hydrophilic gel-like matrix. The main drawback of this model lies on the difficulties that exist for the experimental determination of the effective gel volume (Schiewer and Volesky, 1997b). This fact makes it necessary to assume an empirical value. It was shown that a constant Donnan volume allows the satisfactory prediction of the shift in the charge vs. pH curves with ionic strength at a single value of the dissociation degree. The consideration of a variable volume (due to the shrinking/swelling properties of the biosorbent) provided a better description of the whole range of data, and therefore different empirical expressions to account for the particle swelling were studied.

Cation binding to a natural material may also be described as a sorption to a non-permeable two-dimensional surface. The so-called surface charge models have extensively been applied to the study of acid-base and complexation properties of a number of heterogeneous systems, such as oxides/hydroxides (Schindler and Stumm, 1987; Morel and Hering, 1993) or natural organic colloids (Bartschat *et al.*, 1992; Milne *et al.*, 1995). The comparison between surface charge and Donnan models applied to the study of humic substances is discussed, for instance, in (Avena *et al.*, 1999). To the authors' knowledge, a similar analysis regarding biosorption by algae has not been made yet. Therefore, the aim of the present work will be to compare both alternative approaches from the point of view of the interpretation of experimental proton dissociation data.

7.2.2. Models

The proton dissociation reaction of a polyelectrolyte:

$$AH = A^- + H^+ \tag{7.2.1}$$

can be described by an apparent dissociation constant, $K_{(\alpha)}$, as follows:

$$pK_{(\alpha)} = pH - \log\frac{\alpha}{1-\alpha} \tag{7.2.2}$$

where α is the dissociation degree, and pH is defined in the proton concentration scale (therefore, $K_{(\alpha)}$ is a stoichiometric constant).

As a result of the ionisation of the acid groups of the polyelectrolyte, a surface potential is generated. The observable change in Gibbs free energy related to the dissociation process can thus be split into two contributions (Schindler and Stumm, 1987; Morel and Hering, 1993), according to:

$$\Delta G_{dissociation} = \Delta G_{intrinsic} + \Delta G_{electrostatic} \tag{7.2.3}$$

where $\Delta G_{electrostatic}$ is the energy necessary to bring the proton from the surface site (at a potential ϕ_0) to the bulk solution:

$$\Delta G_{electrostatic} = -F\phi_0 \tag{7.2.4}$$

where F is the Faraday constant.

Thus, the corresponding equilibrium constants will be related by:

$$pK_{(\alpha)} = pK_{int(\alpha)} - \frac{F}{RT\ln 10}\phi_0 = pK_{int(\alpha)} - \frac{1}{\ln 10}\psi_0 \qquad (7.2.5)$$

where $\psi_0 = F\phi_0/(RT)$ is a nondimensional potential. The intrinsic constant (K_{int}) is assumed to be a function of the dissociation degree, as a result of the chemical heterogeneity of the system.

The proton concentration in the vicinity of the macromolecule site ($p\overline{H}$) can be related to its concentration in the bulk solution through a Boltzmann factor:

$$p\overline{H} = pH + \frac{1}{\ln 10}\psi_0 \qquad (7.2.6)$$

In general, ψ_0 is not accessible to direct experimental measurement (Westall, 1987). Consequently, it must be estimated using a model for the solid-liquid interface. Here, two opposite idealised cases will be compared. First, the algal particles will be regarded as a fully permeable homogeneous gel in Donnan equilibrium with the aqueous phase. Second, algae will be considered to behave as planar surfaces non-permeable to protons and background salt ions. For simplicity, only the case of a 1:1 background electrolyte will be shown.

7.2.2.1. Donnan permeable gel

The proton binding zone of the algal biomass is regarded as a three-dimensional structure constituted of an ionizable polyelectrolyte, i.e., a permeable polyelectrolytic gel. For this kind of systems, Marinsky proposed a model based on the Gibbs-Donnan formalism (Marinsky, 1987). From the initial assumptions of the model, it can be demonstrated that the activity ratio between the aqueous phase and the gel (indicated by a superscript bar) for the different monovalent cations follows the relation

$$\frac{\overline{a}_H}{a_H} = \frac{\overline{a}_M}{a_M} = \lambda \qquad (7.2.7)$$

where a_i is the activity of the *i* species, and M represents the counterion (here, Na^+ or K^+).

Assuming electroneutrality within the gel phase, and a state of equilibrium between phases for the diffusible background electrolyte MX, the following expression for the Donnan term can be easily derived (Rey-Castro *et al.*, 2003):

$$\lambda = \frac{\bar{\gamma}_M}{\gamma_M}\left(\frac{Q}{2V_D I} + \sqrt{\left(\frac{Q}{2V_D I}\right)^2 + \frac{\gamma_{\pm MX}^2}{\bar{\gamma}_M \bar{\gamma}_X}}\right) \tag{7.2.8}$$

where Q ($mol \cdot kg^{-1}_{alga}$) is the specific amount of charged groups, V_D ($L \cdot kg^{-1}_{alga}$) is the volume of the gel phase and I ($mol \cdot L^{-1}$) is the ionic strength of the bulk solution. Eq. (7.2.6) in terms of the Donnan term now rewrites as

$$p\bar{H} = pH - \log\left(\lambda \frac{\gamma_H}{\bar{\gamma}_H}\right) = pH - \log\lambda' \tag{7.2.9}$$

where the Donnan term formally represents the Boltzmann factor that relates the activities of the ions in the bulk solution and the gel phase.

If the following activity coefficient quotients are assumed equal to unity (Miyajima, 1995):

$$\frac{\gamma_H}{\bar{\gamma}_H}\frac{\bar{\gamma}_M}{\gamma_M} \approx 1 \quad \text{and} \quad \frac{\gamma_{\pm MX}^2}{\bar{\gamma}_M \bar{\gamma}_X} \approx 1 \tag{7.2.10}$$

then, a simplified expression can be obtained for the Donnan term

$$\lambda' = \left(\frac{Q}{2V_D I} + \sqrt{\left(\frac{Q}{2V_D I}\right)^2 + 1}\right) \tag{7.2.11}$$

and for the dependence of pK on the ionic strength and dissociation degree:

$$pK_{(\alpha)} = pK_{int(\alpha)} + \log\left(\frac{\bar{Q}}{2I} + \sqrt{\left(\frac{\bar{Q}}{2I}\right)^2 + 1}\right) \tag{7.2.12}$$

where $\overline{Q} = Q/V_D$ is the concentration of charged groups in the gel phase.

In the simplest case, the gel phase may be assumed rigid, and thus V_D will be constant. Nevertheless, this parameter is usually considered to depend on at least one of the titration variables: ionic strength (such as in the NICA-Donnan models for humic substances), pH or dissociation degree (Schiewer and Volesky, 1997b).

An alternative derivation of the Donnan model can also be made starting from the Poisson-Boltzmann equation. For a smeared-out charge homogeneously distributed within a finite volume, and assuming overall electroneutrality, Poisson-Boltzmann leads to (Wonders *et al.*, 1997):

$$\psi_0 = \psi_{Don} = \operatorname{arcsinh}\left(\frac{-\overline{Q}}{2I}\right) \tag{7.2.13}$$

if the gel dimensions are much larger than κ^{-1} (the Debye length). Ohshima and Kondo (1991) have reported a more general solution that does not assume overall electroneutrality in the gel.

7.2.2.2. Non-permeable planar surface

The algal particles can also be pictured as impenetrable solids with all their acid groups homogeneously distributed over the surface, which is assumed to be an infinite flat plane. Within the mean-field and smeared out charge approximations, the mean surface potential can be approximated by a diffuse-layer model such as Gouy-Chapman model. The non-linear Poisson-Boltzmann equation for this system can be exactly solved to obtain the following relation between ψ_0 and the surface charge density σ (Lyklema, 1995):

$$\sigma = \left(8 \cdot 10^3 \varepsilon\varepsilon_0 RTI\right)^{\frac{1}{2}} \sinh\left(\frac{\psi_0}{2}\right) \tag{7.2.14}$$

where σ = -QF/A (A being the specific surface area, in $m^2 \cdot kg^{-1}_{alga}$), ε is the permittivity constant, and ε_0 the dielectric constant of water. All the magnitudes are in SI units except I (in mol/L). Solving for ψ_0 yields:

$$\psi_0 = \psi_{GC} = 2\operatorname{arcsinh}\left(\frac{\overline{\sigma}}{I^{1/2}}\right) \tag{7.2.15}$$

Where $\bar{\sigma} = \sigma / \sqrt{8 \cdot 10^3 \varepsilon \varepsilon_0 RT}$

Substituting in eq. (7.2.5), yields (note that $\bar{\sigma} < 0$):

$$pK_{(\alpha)} = pK_{int(\alpha)} - 2\log\left(\frac{\bar{\sigma}}{I^{1/2}} + \sqrt{\left(\frac{\bar{\sigma}}{I^{1/2}}\right)^2 + 1}\right) \qquad (7.2.16)$$

7.2.2.3. Intrinsic heterogeneity

A usual criterion to check the validity of an electrostatic model is to plot the titration curves as a function of $p\bar{H}$. The curves obtained at different salt concentrations should then merge into one single master curve (de Wit *et al.*, 1990). It is expected that no influence of the bulk ionic strength will be observed if the model is correct. This master curve would reflect the intrinsic heterogeneity of the system. As a result of this heterogeneity, the intrinsic constant will be a function of the dissociation degree.

In this work, the intrinsic proton binding is described by a Langmuir-Freundlich (LF) isotherm:

$$\theta = \frac{Q_{max} - Q}{Q_{max}} = \frac{\left(K_H[\bar{H}]\right)^{\Gamma}}{1 + \left(K_H[\bar{H}]\right)^{\Gamma}} \qquad (7.2.17)$$

where $\theta = 1-\alpha$ is the coverage fraction of protonated sites, Q_{max} is the total specific amount of acid groups, $\log K_H$ is the mean value of the intrinsic affinity distribution, and Γ is a measure of the degree of heterogeneity ($0 < \Gamma \leq 1$, $\Gamma = 1$ represents homogeneity). From this equation, it easily follows that $pK_{int(\alpha=0.5)} = \log K_H$ (note that K_H formally represents a *binding* constant rather than a *dissociation* constant).

Although the choice of the isotherm may seem arbitrary, Garcés *et al.* (2002) showed that the important features of an adsorption isotherm are the average value and standard deviation of the affinity distribution rather than the exact form of the isotherm, for systems at intermediate coverages. Further work regarding the use of different isotherms for the analysis of biosorption data will be carried out in the future in order to support this assumption.

7.2.3. Methodology

Proton binding data obtained from potentiometric titrations of pre-treated seaweed biomass suspensions were available from an earlier study (Rey-Castro *et al.*, 2003). In that work, samples of three algal species (*Sargassum muticum*, *Cystoseira baccata* and *Saccorhiza polyschides*, collected from the coasts of A Coruña, NW Spain) were studied in two different background electrolytes (NaCl and KNO_3) at concentrations ranging from 0.05 to 2 mol/L. The original data sets consist of (Q, pH) pairs, of which Q was calculated from charge balance considerations, and pH (proton concentration scale) was determined potentiometrically with a glass electrode.

The best values of the Donnan volume and specific surface area were obtained following the procedure described in **Figure 7.2.1** and implemented in MatLab 6.1.

Values of pK at $\alpha = 0.5$, used for the nonlinear least squares fit of eqs. (7.2.12) and (7.2.16), were interpolated from the experimental curves using a cubic spline calculated with Origin 5.0.

7.2.4. Results and discussion

7.2.4.1. Analysis of the master curves

Table 7.2.1 lists the model parameters K_H, Γ and V_D or A obtained for each data set, together with the standard deviation of the residuals (SDR). It can be observed that the SDR values, although very similar, are systematically higher using the Gouy-Chapman electrostatic model. An example of the master curves obtained with both models is shown in **Figure 7.2.2.**. It can be observed that a satisfactory convergence is only obtained at intermediate coverages. The curves obtained with both models are very similar, although a slightly higher dispersion can be noticed in the Gouy-Chapman results, even in the central zone. The shape of the master curves can be improved if the influence of the particle swelling on the geometric parameter is taken into account, as shown by Rey-Castro *et al.* (2003), for the case of Donnan model.

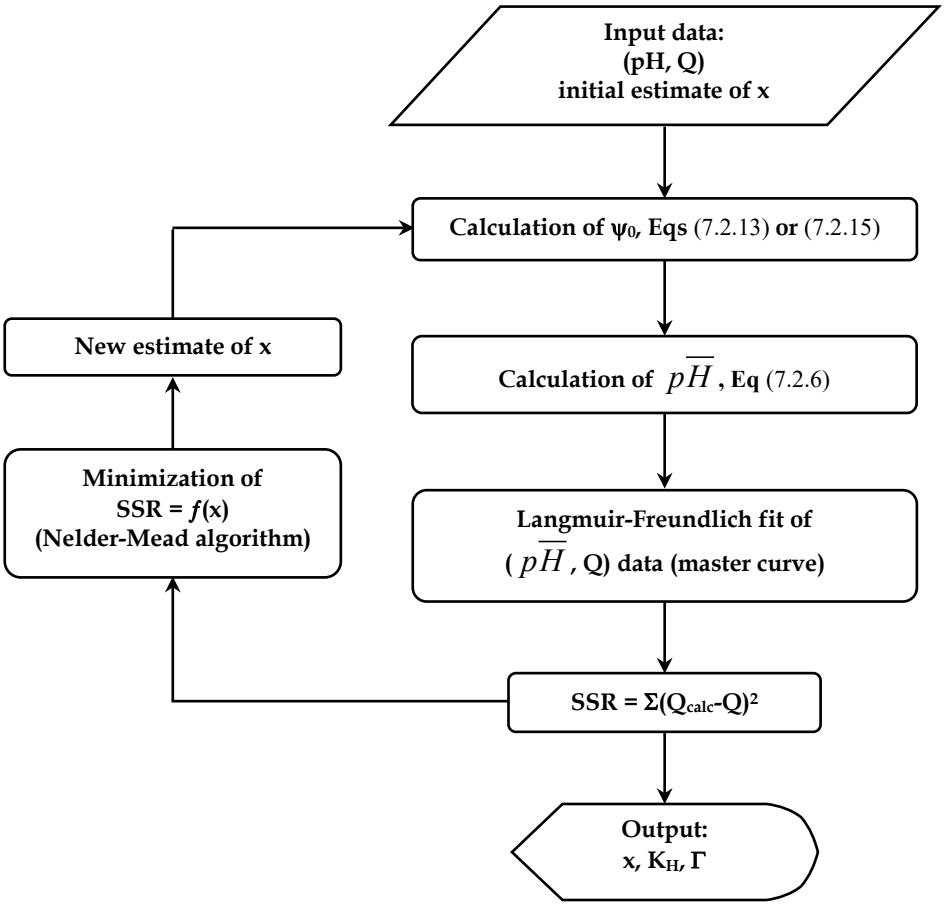

Figure 7.2.1. Iterative procedure for the calculation of the characteristic geometric parameter, x, which corresponds to V_D (permeable gel model) or A (surface charge model). SSR: sum of square residuals.

Table 7.2.1. Best-fit parameters for the Donnan and Gouy-Chapman electrostatic models in combination with a Langmuir-Freundlich isotherm. Original charge-pH data taken from (Rey-Castro *et al.*, 2003).

Species	Donnan				Gouy-Chapman			
	V_D ($L \cdot kg^{-1}_{alga}$)	$logK_H$	Γ	SDR[a]	A ($10^3\ m^2 \cdot kg^{-1}_{alga}$)	$logK_H$	Γ	SDR[a]
				KNO_3				
S. muticum	5.7	3.21	0.63	0.052	4800	3.09	0.69	0.065
C. baccata	5.1	3.12	0.54	0.044	4300	2.97	0.60	0.055
S. polyschides	6.9	3.30	0.77	0.083	6300	3.21	0.84	0.106
				NaCl				
S. muticum	5.2	3.20	0.66	0.048	4400	3.07	0.73	0.064
C. baccata	5.4	3.15	0.58	0.048	4600	3.02	0.64	0.058
S. polyschides	5.8	3.28	0.88	0.096	5400	3.17	0.98	0.122

[a] Standard deviation of the residuals in Q (mol kg^{-1}_{alga}).

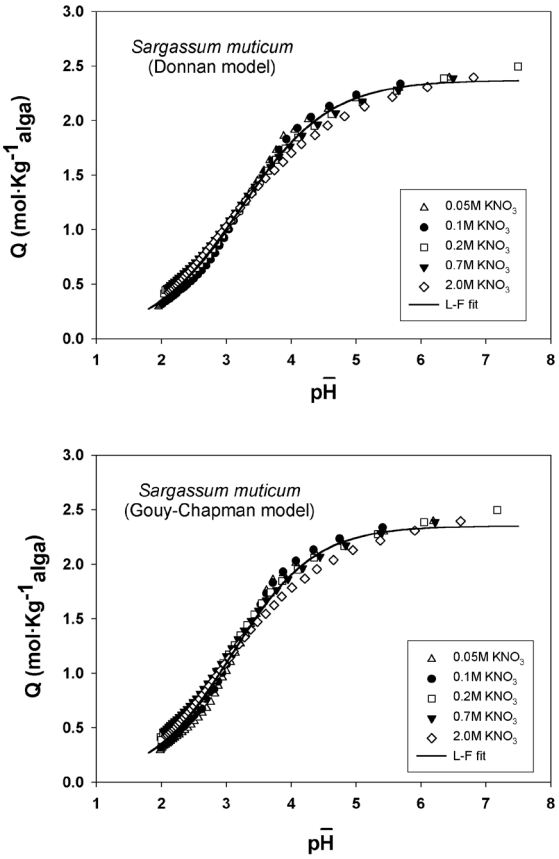

Figure 7.2.2. Q vs $\overline{pH}$ master curve calculated with both models for *S. muticum* in KNO_3. For clarity reasons, only every second point is shown. The lines represent the Langmuir-Freundlich fits.

Figure 7.2.3 shows a plot of pK_{int} vs. $\overline{pH}$ calculated with Donnan and Gouy-Chapman models. In both cases the intrinsic constants are almost independent of the ionic strength, as expected for a good correction of the electrostatic effect. The dependency of pK_{int} on pH (and, consequently, on α) is consistent with a heterogeneous character.

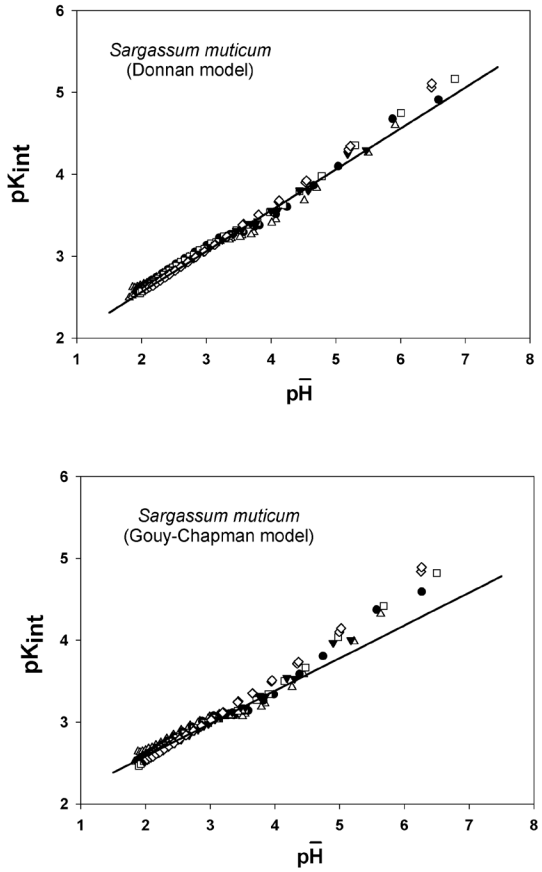

Figure 7.2.3. pK_{int} vs $p\overline{H}$ master curve calculated with both models for *S. muticum* in KNO_3. Symbols are the same as in **Figure 7.2.2.** The lines correspond to pK_{int} calculated from the Langmuir-Freundlich isotherm using the fitted parameters listed in **Table 7.2.1**.

The V_D values listed in **Table 7.2.1** are of the same order as the total specific volumes of algal biomass particles reported in bibliography (Schiewer and Volesky, 1997a; Schiewer and Volesky, 1997b; Schiewer and Wong, 2000). However, in these works it has been pointed out that V_D corresponds, in theory, only to the "effective" volume of the alginate layer where the proton binding reaction is supposed to take place and, therefore, it is expected to be smaller than the total particle volume.

The values of A obtained are much higher than the specific surface area determined in our laboratory from methylene blue adsorption on seaweed samples (see **Table 7.2.2**). Moreover, they are 1 or 2 orders of magnitude higher than the specific surface areas of most organic/inorganic sorbents, which are usually determined by the dye or gas adsorption methods. Nevertheless, the values reported in this work are in agreement with results obtained for different green and red algae from potentiometric titration data analysed using a double layer model (Wang *et al.*, 1997). The reason for the discrepancy between A and the specific areas determined from dye adsorption may be a different sorption mechanism for protons and dye molecules.

Table 7.2.2. Specific surface areas reported in bibliography for a sample of materials using different techniques. The value for *S. muticum* was experimentally determined for this work from methylene blue adsorption isotherms, using a molecular cross section of 108 $Å^2$ (van den Hul and Lyklema, 1968).

Material	Specific surface area (10^3 $m^2 \cdot Kg^{-1}$)	Method	Reference
Seaweed	537 (*S. muticum*)	dye adsorption	-
Different algal species	1030-28900	acid-base titration + double layer model	a
Charcoal	455-613	gas adsorption	b
Water hyacinth	223-243	dye adsorption	c
Hematite	ca. 30	different methods	d

References: Wang *et al.*, 1997[a]; Cao *et al.*, 2002[b]; Schneider *et al.*, 1995[c]; van den Hul and Lyklema, 1968[d].

The value of $A \cdot \kappa^{-1}$ (κ being the Debye parameter) may give an idea of the average double layer volume. The results (e.g. 6.5 $L \cdot Kg^{-1}_{alga}$, for *S. muticum* in 0.05M KNO_3) are in the order of V_D and the total specific volumes determined experimentally (Schiewer and Volesky, 1997b). The average surface area per group is around 3 nm^2 per site (*S. muticum*). As a matter of comparison, the length of the disaccharide unit in polymannuronic and polyguluronic acid fibres, determined by X-ray diffraction (Atkins *et al.*, 1973b; Atkins *et al.*, 1973a) is 1.04-0.87 nm.

It is probably incorrect to attach too much physical significance to A or V_D, due to the severe simplifications involved in the models shown here and the high complexity of the system. Nevertheless, the empirical values of these

parameters do not seem to be incompatible with the physical properties of the sorbent.

7.2.4.2. Analysis of the dependency of the apparent pK on I and α

These models are aimed to the simultaneous description of the effects of macromolecular charge and bulk ionic strength on the apparent proton dissociation of the algal biomass. The comparison between the model estimates and the experimental pK data is shown in **Figure 7.2.4**. In agreement with the results of the master curve calculations, the model estimates deviate significantly from experimental data at the lower and higher α values. It can be observed that both models reproduce in a similar way the data and may, therefore, be considered almost equivalent. Nevertheless, the surface charge model seems to predict a narrower distribution of the titration curves at low dissociation degrees (and the opposite at high α values). The accuracy of these plots may be increased by fitting the model parameters to the pK data rather than to the charge-pH curves. In addition, the Donnan model can be improved significantly by introducing a dependency for V_D, as shown elsewhere (Rey-Castro *et al.*, 2003).

Eqs. (7.2.12) and (7.2.16) allow the accurate description of the shift in the titration curves with ionic strength at a constant value of α. **Figure 7.2.5** shows a plot of the apparent pK at $\alpha = 0.5$ for *C. baccata* in KNO_3, and the least squares fits to eqs. (7.2.12) and (7.2.16) (note that in this case, the parameter values pK_{int} and V_D/A have been optimised for the particular case of $\alpha = 0.5$). Again, both models describe almost equally well the experimental data. Note that at constant α the intrinsic pK is supposed to be a constant, and thus no assumptions about the specific binding isotherm are required.

Eqs. (7.2.12) and (7.2.16) may also constitute useful functions to estimate the behaviour at ionic strengths below the experimental range. For simple ligands, the well-known Debye law imposes a linear relationship between pK and $I^{½}$ at low ionic strengths, whereas for the polyelectrolytic systems it is expected that pK will increase almost linearly with log I as the ionic strength decreases, which represents a significant difference. Another important feature of these models is that they do not involve the use of a thermodynamic equilibrium constant defined at zero ionic strength as a reference, as opposed to most of the models for simple ligands. Instead, in the

Donnan and surface charge models, the intrinsic pK would correspond to the apparent pK in the limit of high ionic strengths, where the difference in the electric potential between the surface and the bulk solution tends to zero.

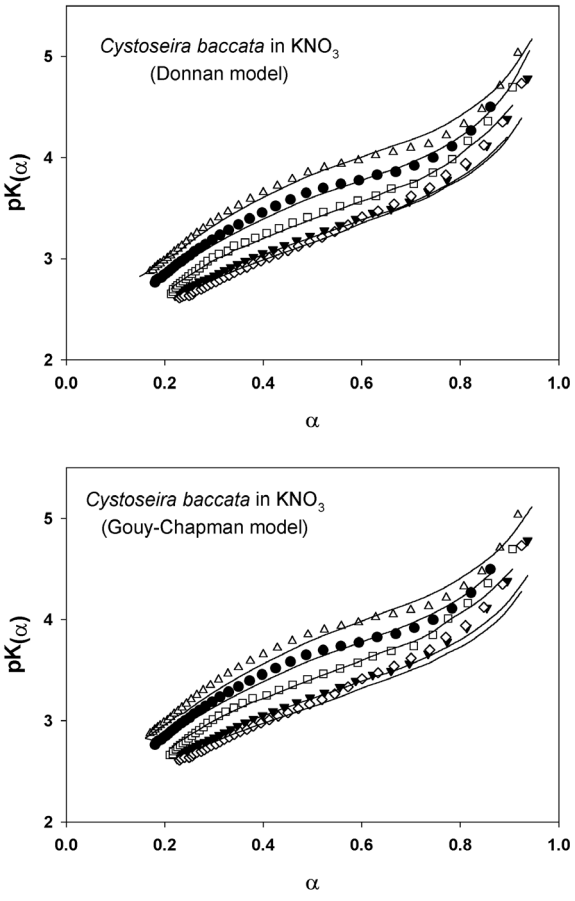

Figure 7.2.4. Plot of the apparent pK vs. the dissociation degree for *C. baccata* in KNO_3 at different ionic strengths. Symbols are the same as in **Figure 7.2.2**. The lines correspond to model calculations using the parameters obtained from the master curve optimisation (see **Table 7.2.1**).

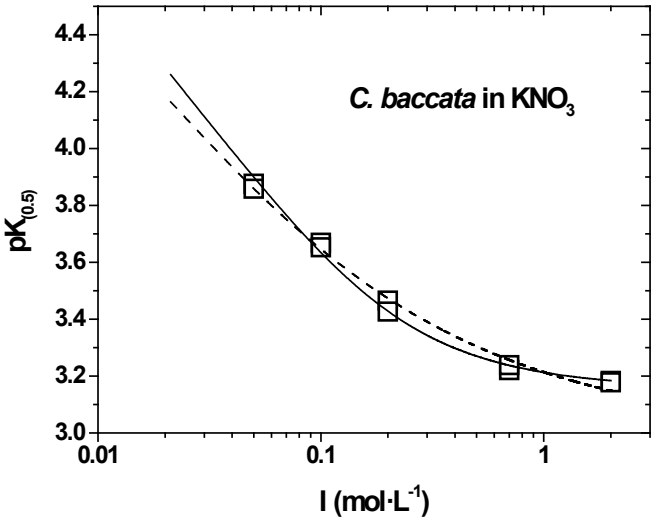

Figure 7.2.5. Plot of $pK_{(\alpha = 0.5)}$ for *C. baccata* in KNO_3, with the least squares fits to eqs. (7.2.12) (Donnan model, solid line) and (7.2.16) (Gouy-Chapman model, dashed line).

7.2.4.3. Consideration of activity coefficients

It has been assumed in both models that all non ideal behaviour of the species can be attributed to the effect of the electrostatic surface potential ψ_0. In the Donnan model, this involves the assumption of eq. (7.2.10), whereas in the case of the G-C model, it is implicitly assumed in the Boltzmann distribution (which has been formulated in terms of concentrations rather than activities) that activity coefficients of protons and co/counterions in the macromolecular vicinity and the bulk solution are equal.

From the point of view of the Donnan model, the activity coefficient influence becomes more important as ionic strength decreases, because the difference in the counterion concentrations in the gel phase and bulk solution increases. In practice, however, these effects are incorporated in the fitted parameter of the electrostatic model (V_D). When activity effects (other than the polyelectrolytic effect) are taken into account, it can be observed that the V_D values become lower and seem to depend less on the type of 1:1 electrolyte (Rey-Castro *et al.*, 2003).

7.2.4.4. Consideration of electrostatically bound protons

The models shown here consider all the bound protons as covalently bound. Nevertheless, a certain excess of proton ions in the double layer (with regard to the bulk solution) is expected. The amount of these "electrostatically bound" protons ($n_{H,e.b.}$, in $mol \cdot Kg^{-1}_{alga}$) can be accounted for in a simple way in Donnan model:

$$n_{H,e.b.} = V_D \cdot \left(\left[\overline{H} \right] - [H] \right) \tag{7.2.18}$$

In the case of the surface charge model, integration of the electrostatic potential over the thickness of the double layer is required. Nevertheless, this amount is only significant at very low ionic strengths and pH values.

7.2.5. Conclusions

A comparative study of two electrostatic models (Donnan and surface charge) was shown, for the particular case of proton binding equilibria of seaweed biomass. Both models lead to similar analytical expressions for the dependency of the apparent pK on the ionic strength and degree of dissociation. In each case, the use of the master curve procedure allows the estimation of two isotherm parameters describing the intrinsic heterogeneity, and a geometric parameter (V_D or A), which has been assumed to be independent of the titration conditions.

The quality of the master curve and the accuracy in the pK estimation are almost equivalent in both cases. It can be concluded that a discrimination between both models cannot be made from the experimental proton binding results when no reliable V_D or A values, determined in an independent way, are available.

These models need to be modified in order to improve the description of the experimental data. A significant improvement can be achieved in the Donnan model, by introducing a dependency for V_D and activity coefficient estimates, as shown in other works.

Future research will focus on the comparison of these models for the interpretation of metal binding data. A further analysis of the intrinsic proton

binding affinity of these materials and a study of additional seaweed species will also be carried out.

7.2.6. References

Atkins, E.D.T., Nieduszynski, I.A., Mackie, W., Parker, K.D. and Smolko, E.E. 1973a. Structural components of alginic acid. I. Crystalline structure of poly-β-D-mannuronic acid. Results of x-ray diffraction and polarized infrared studies. *Biopolymers*, **12**, 1865-1878.

Atkins, E.D.T., Nieduszynski, I.A., Mackie, W., Parker, K.D. and Smolko, E.E. 1973b. Structural components of alginic acid. II. Crystalline structure of poly-α-L-guluronic acid. Results of x-ray diffraction and polarized infrared studies. *Biopolymers*, **12**, 1879-1887.

Avena, M.J., Koopal, L.K. and van Riemsdijk, W.H. 1999. Proton binding to humic acids: electrostatic and intrinsic interactions. *J. Colloid Interf. Sci.*, **217**, 37-48.

Bartschat, B.M., Cabaniss, S.E. and Morel, F.M.M. 1992. Oligoelectrolyte model for cation binding by humic substances. *Environ. Sci. Technol.*, **26**, 284-294.

Cao, N., Darmstadt, H., Soutric, F. and Roy, C. 2002. Thermogravimetric study on the steam activation of charcoals obtained by vacuum and atmosferic pyrolysis of softwood bark residues. *Carbon*, **40**, 471-479.

Crist, R.H., Martin, J.R., Guptill, P.W., Eslinger, J.M. and Crist, D.R. 1990. Interaction of metals and protons with algae. 2. Ion exchange in adsorption and metal displacement by protons. *Environ. Sci. Technol.*, **24**, 337-342.

Crist, R.H., Oberholser, K., Schwartz, D., Marzoff, J., Ryder, D. and Crist, D.R. 1988. Interactions of metals and protons with algae. *Environ. Sci. Technol.*, **22**, 755-760.

Davis, T.A., Volesky, B. and Mucci, A. 2003. A review of the biochemistry of heavy metal biosorption by brown algae. *Wat. Res.*, **37**, 4311-4330.

de Wit, J.C.M., van Riemsdijk, W.H., Nederlof, M.M., Kinniburgh, D.G. and Koopal, L.K. 1990. Analysis of ion binding on humic substances and the

determination of intrinsic affinity distributions. *Anal. Chim. Acta*, **232**, 189-207.

Garcés, J.L., Mas, F., Cecília, J., Companys, E., Galceran, J., Salvador, J. and Puy, J. 2002. Complexation isotherms in metal speciation studies at trace concentration levels. Voltammetric techniques in environmental samples. *Phys. Chem. Chem. Phys.*, **4**, 3764-3773.

Jensen, A. 1995. Production of alginate. In: Wiessner, W., Schnepf, E. and Starr, R.C. (eds.), *Algae, environment and human affairs*, pp. 79-92. Biopress, Bristol.

Lobban, C.S. and Harrison, P.J. 1994. *Seaweed ecology and physiology*. Cambridge University Press, Cambridge.

Lyklema, J. 1995. *Fundamentals of interface and colloid science*. vol II. Academic Press, London.

Marinsky, J.A. 1987. A two-phase model for the interpretation of proton and metal ion interaction with charged polyelectrolyte gels and their linear analogs. In: Stumm, W. (ed.), *Aquatic Surface Chemistry. Chemical Processes at the Particle-Water Interface.*, pp. 49-81. J. Wiley & Sons, New York.

Milne, C.J., Kinniburgh, D.G., de Wit, J.C.M., van Riemsdijk, W.H. and Koopal, L.K. 1995. Analysis of proton binding by a peat humic acid using a simple electrostatic model. *Geochim. Cosmochim. Acta*, **59**, 1101-1112.

Miyajima, T. 1995. Evaluation of the electrostatic effect on metal ion - binding equilibria in negatively charged polyion systems. In: Marinsky, J.A. and Marcus, Y. (eds.), *Ion exchange and solvent extraction*, vol 12, pp. 275-351. Marcel Dekker, New York.

Morel, F.M.M. and Hering, J.G. 1993. *Principles and Applications of Aquatic Chemistry*. J. Wiley & Sons, New York.

Ohshima, H. and Kondo, T. 1991. On the electrophoretic mobility of biological cells. *Biophys. Chem.*, **39**, 191-198.

Percival, E. and McDowell, R.H. 1967. *Chemistry and Enzymology of marine algal polysaccharides*. Academic Press, London.

Rey-Castro, C., Lodeiro, P., Herrero, R. and Sastre de Vicente, M.E. 2003. Acid-base properties of brown seaweed biomass considered as a Donnan gel. A model reflecting electrostatic effects and chemical heterogeneity. *Environ. Sci. Technol.*, **37**, 5159-5167.

Schiewer, S. and Volesky, B. 1997a. Ionic strength and electrostatic effects in biosorption of divalent metal ions and protons. *Environ. Sci. Technol.*, **31**, 2478-2485.

Schiewer, S. and Volesky, B. 1997b. Ionic strength and electrostatic effects in biosorption of protons. *Environ. Sci. Technol.*, **31**, 1863-1871.

Schiewer, S. and Wong, M.H. 2000. Ionic strength effects in biosorption of metals by marine algae. *Chemosphere*, **41**, 271-282.

Schindler, P.W. and Stumm, W. 1987. The surface chemistry of oxides, hydroxides, and oxide minerals. In: Stumm, W. (ed.), *Aquatic Surface Chemistry. Chemical Processes at the Particle-Water Interface*, pp. 83-110. J. Wiley & Sons, New York.

Schneider, I.A.H., Rubio, J., Misra, M. and Smith, R.W. 1995. Eichhornia crassipes as biosorbent for heavy metal ions. *Minerals Engineering*, **8**, 979-988.

van den Hul, H.J. and Lyklema, J. 1968. Determination of specific surface areas of dispersed materials. Comparison of the negative adsorption method with some other methods. *J. Am. Chem. Soc.*, **90**, 3010-3015.

Volesky, B. 1990. *Biosorption of heavy metals*. CRC Press, Boca Raton, Florida.

Wang, X., Ma, Y. and Su, Y. 1997. Determining surface areas of marine alga cells by acid-base titration method. *Chemosphere*, **35**, 1131-1141.

Westall, J.C. 1987. Adsorption mechanisms in aquatic surface chemistry. In: Stumm, W. (ed.), *Aquatic Surface Chemistry. Chemical Processes at the Particle-Water Interface.*, pp. 3-32. J. Wiley & Sons, New York.

Wonders, J.H.A.M., Van Leeuwen, H.P. and Lyklema, J. 1997. Metal- and proton-binding properties of a core-shell latex: interpretation in terms of colloid surface models. *Colloid Surf. A*, **120**, 221-233.

APPENDIX A

Study of acrylic-maleic copolymers.
Supplementary data.

Table A.1. Experimental protonation constants of poly(acrylic co-maleic) acid (PAM3) in Et_4NI at different ionic strengths obtained by three and two parameter models at T = 25 °C

I/ mol L^{-1}	$logK_1$	$logK_0$	$logK_m$	σ_{fit}[a]	log K^H_n	n	σ_{fit}[a]
0.1	7.167	3.872	4.386	0.026	5.032	2.73	0.065
	7.217	3.910	4.393	0.025	5.057	2.75	0.064
	7.214	3.916	4.412	0.026	5.066	2.75	0.063
0.25	7.041	3.872	4.318	0.027	4.960	2.70	0.059
	7.200	3.916	4.256	0.028	4.989	2.77	0.066
	7.210	3.876	4.299	0.029	5.01	2.75	0.071
0.5	6.922	3.848	4.339	0.027	4.934	2.63	0.059
	7.009	3.909	4.291	0.028	4.951	2.67	0.062
	6.828	3.809	4.379	0.028	4.915	2.59	0.054

[a] std. dev. on the fit of equations (4.1.4), (4.1.5)

Table A.2. Experimental protonation constants of poly(acrylic co-maleic) acid (PAM3) in NaCl at different ionic strengths obtained by three and two parameter models at T = 25 °C

I/ mol L^{-1}	$logK_1$	$logK_0$	$logK_m$	σ_{fit}[a]	log K^H_n	n	σ_{fit}[a]
0.05	6.562	3.846	4.876	0.015	5.062	2.43	0.015
	6.614	3.828	4.883	0.016	5.075	2.47	0.019
	6.647	3.851	4.887	0.016	5.093	2.47	0.020
	6.316	3.760	4.892	0.013	4.975	2.34	0.016
	6.485	3.813	4.895	0.015	5.039	2.40	0.018
0.25	6.081	3.693	4.396	0.018	4.672	2.27	0.024
	6.001	3.646	4.430	0.017	4.653	2.24	0.022
	6.130	3.720	4.396	0.019	4.696	2.28	0.028
	6.089	3.740	4.398	0.019	4.690	2.25	0.025
1.0	5.791	3.611	4.140	0.022	4.458	2.15	0.032
	5.738	3.586	4.132	0.021	4.433	2.15	0.028
	5.744	3.598	4.152	0.020	4.448	2.14	0.028

[a] std. dev. on the fit of equations (4.1.4), (4.1.5)

Table A.3. Experimental protonation constants of poly(acrylic co-maleic) acid (PAM70) in Et_4NI at different ionic strengths obtained by Högfeldt model at T = 25 °C

I/ mol L^{-1}	$logK_1$	$logK_0$	$logK_m$	σ_{fit}[a]
0.1	7.670	3.864	4.863	0.018
	7.550	3.803	4.896	0.016
	7.607	3.821	4.898	0.017
0.25	7.478	3.818	4.720	0.018
	7.409	3.810	4.716	0.018
	7.467	3.814	4.721	0.019
0.5	7.330	3.816	4.686	0.019
	7.395	3.867	4.646	0.018
	7.326	3.830	4.702	0.020

[a] std. dev. on the fit of equation (4.1.5)

Table A.4. Experimental protonation constants of poly(acrylic co-maleic) acid (PAM70) in NaCl at different ionic strengths obtained by Högfeldt model at T = 25 °C

I/mol L^{-1}	$logK_1$	$logK_0$	$logK_m$	σ_{fit}[a]
0.05	6.559	3.958	5.226	0.010
	6.620	3.948	5.218	0.010
	6.594	3.920	5.239	0.011
0.1	6.465	3.874	4.919	0.013
	6.537	3.860	4.924	0.015
	6.418	3.891	4.953	0.012
0.5	6.311	3.839	4.310	0.022
	6.296	3.814	4.286	0.022
	6.370	3.856	4.274	0.022
1.0	6.058	3.703	4.151	0.023
	6.114	3.735	4.154	0.022
	6.094	3.697	4.123	0.023

[a] std. dev. on the fit of equation (4.1.5)

Table A.5. Apparent protonation constants in NaCl-$CaCl_2$ and NaCl/$MgCl_2$ mixtures for PAM3 at T = 25 °C

I/mol L^{-1}	C_{PAM3}	C_{Ca}	$logK_1$	$logK_0$	$logK_m$	σ_{fit}[b]
0.10	10.664[a]	6.793[a]	4.945	3.635	4.779	0.009
	13.584	3.127	5.403	3.692	4.833	0.012
	10.814	3.202	5.310	3.725	4.831	0.010
	11.510	5.203	5.149	3.698	4.814	0.011
	5.314	5.003	5.006	3.648	4.865	0.011
	5.323	7.504	4.827	3.640	4.813	0.008
	10.640	1.626	5.708	3.732	4.840	0.015
I/mol L^{-1}	C_{PAM3}	C_{Mg}	$logK_1$	$logK_0$	$logK_m$	σ_{fit}[b]
0.10	5.456[a]	3.013[a]	5.657	3.705	4.899	0.013
	5.323	10.044	5.263	3.701	4.761	0.012
	15.686	2.410	5.970	3.753	4.781	0.016
	16.383	3.817	5.834	3.769	4.751	0.013
	5.280	7.533	5.351	3.705	4.796	0.012
	11.036	5.022	5.577	3.712	4.819	0.013
	10.969	10.004	5.331	3.721	4.712	0.011

[a] mmol L^{-1}

[b] std. dev. on the fit of equation (4.1.5)

Table A.6. Apparent protonation constants in NaCl-$CaCl_2$ and NaCl/$MgCl_2$ mixtures for PAM70 at T = 25 °C

I/mol L^{-1}	C_{PAM70}	C_{Ca}	$logK_1$	$logK_0$	$logK_m$	σ_{fit}[b]
0.10	15.136[a]	2.501[a]	6.033	3.937	4.757	0.019
	15.210	5.003	5.384	3.855	4.861	0.010
	10.130	5.003	5.141	3.832	4.951	0.006
	9.653	10.006	4.531	3.728	4.916	0.003
	6.433	10.006	4.435	3.662	4.923	0.003
	8.318	2.001	5.787	3.931	4.939	0.015
0.50	29.170	6.740	5.601	3.676	4.540	0.010
	29.180	4.760	5.767	3.699	4.496	0.012
	15.780	7.930	5.296	3.590	4.665	0.005
	15.780	9.910	5.214	3.632	4.702	0.004
I/mol L^{-1}	C_{PAM70}	C_{Mg}	$logK_1$	$logK_0$	$logK_m$	σ_{fit}[b]
0.10	10.034[a]	2.009[a]	6.242	3.965	4.891	0.020
	6.747	3.013	5.882	3.940	4.974	0.014
	10.019	4.018	5.857	3.934	4.904	0.014
	5.708	4.319	5.684	3.953	4.954	0.011
	6.747	10.044	5.291	3.902	4.800	0.008
	5.046	15.066	5.063	3.837	4.754	0.007
	4.970	20.088	4.909	3.761	4.704	0.006

[a] mmol L^{-1}

[b] std. dev. on the fit of equation (4.1.5)

Table A.7. Comparison of the protonation constants of different polycarboxylic acids at I = 0.50 mol L^{-1} in different ionic media and T = 25 °C

		NaCl			Et_4NI		
ligand	MW	$logK^H_1$	$logK^H_0$	$\log \overline{K}^H$	$logK^H_1$	$logK^H_0$	$\log \overline{K}^H$
PAM[a]	3 kDa	6.01	3.69	4.64	6.92	3.86	5.04
	70 kDa	6.32	3.84	4.82	7.35	3.83	5.29
PMA[b]	4 kDa	5.67	4.72	5.30	6.47	4.76	5.71
	5.4 kDa	5.67	4.81	5.34	6.45	4.87	5.77
PAA[c]	2.2 kDa	5.54	4.30	4.78	6.80	4.50	5.38
	22 kDa	5.82	4.32	4.98	7.05	4.52	5.57

[a] poly(acrylic co-maleic) acids [this work]

[b] polymethacrylic acids (De Stefano *et al.* 2002)

[c] polyacrylic acids (De Stefano *et al.* 2003a)

APPENDIX B

Numerical solution of the NLPB equation in mixed 1-1 / 1-2 electrolyte solutions

This appendix was written with the valuable assistance of members of the Grup de Fisicoquímica de Sistemes Macromolèculars d'Interès Ambiental (U. of Lleida and U. of Barcelona). Doctors E. Companys, J.L. Garcés, J. Cecilia, J. Galceran, J. Puy and F. Mas are especially acknowledged.

The most popular methods for numerically solving differential equations such as the non-linear Poisson-Boltzmann (NLPB) equation are those based on finite differences (FD) schemes. In particular, the fourth-order Runge-Kutta algorithm (Press *et al.*, 1986) was employed in many works on this subject (Anderson and Record, 1990; Fogolari *et al.*, 1992; Schmitz, 1993; Ni *et al.*, 1999). However, the FD methods, while conceptually simple and straightforward, often may be inaccurate and unstable.

An alternative approach to the solution of these differential equations relies on the use of the Finite Element Method, FEM (Hughes, 1987), which consists in transforming the original differential problem into an integral one, and then approximating the solution by a set of basis functions defined on a suitable grid. The coefficients of this set are calculated in such a way that the residuals are minimized. The FEM is a specially powerful tool for the solution of differential equations that involve irregular geometries in two or three dimensions. For instance, it has recently been applied to the description of the electrostatic interactions (through NLPB) in large macromolecules of complex shape (Baker *et al.*, 2001).

Here, the Galerkin Finite Element Method (GFEM) using a set of linear Lagrangian basis functions on the grid has been implemented in order to solve the NLPB, following the procedure described in Companys (2003).

The FEM is specially suitable for solving the NLPB equation for conditions of low ionic strength and high surface charges, because in these cases the electrostatic potential changes sharply when approaching to the surface of the polyelectrolyte. Since there is no restriction on the position of the nodes of the grid, the spacing between the points has been chosen to be inversely proportional to the expected gradient of the electrostatic potential (the sought function).

NLPB equations in cylindrical and spherical geometry

The non-linear Poisson Boltzmann (NLPB) equation for the electrostatic potential created by a infinitely diluted polyelectrolyte in a mixed solution of 1-1 and 1-2 background salts is:

$$\nabla^2\psi = -\frac{\rho}{\varepsilon} = \kappa^2 \frac{k_B T}{e}\left\{\alpha_1 \sinh\left(\frac{e\psi}{k_B T}\right) + \alpha_2\left[\exp\left(\frac{e\psi}{k_B T}\right) - \exp\left(\frac{-2e\psi}{k_B T}\right)\right]\right\} \quad \text{(B.1)}$$

where κ is the reciprocal of Debye's length

$$\kappa = \left(\frac{e^2 N_A 2I}{\varepsilon k_B T}\right)^{1/2} \quad \text{(B.2)}$$

associated to the background salt ions dissolved in the solution, which screen the charges of the ionisable groups of the polyelectrolyte. I is the ionic strength, *e* is the elementary charge. N_A is Avogadro number, ε is the bulk dielectric constant, k_B is Boltzmann constant and T is the temperature.

Coefficients α_i in Eq. (B.1) are defined in terms of the ratio $\rho = C_2/C_1$ (where C_2 and C_1 are the overall concentrations of the 1-2 and 1-1 salts):

$$\alpha_1 = \frac{1}{1+3\rho} \text{ and } \alpha_2 = \frac{\rho}{1+3\rho} \quad \text{(B.3)}$$

where $1<\alpha_1<0$ and $0<\alpha_2<1/3$, the limiting values corresponding to the pure 1:1 or 1:2 salt solutions.

The solution of the NLPB equation depends on the geometry of the polyelectrolyte (considered a rigid and impermeable surface), which is taken as a sphere or an infinite (very large) cylinder. The solution also depends on the charge of the polyelectrolyte through the boundary condition at the surface. The other boundary conditions prescribes that the electrostatic potential vanishes at infinite (far away from any molecule of polyeletrolyte in dilute situations). The value boundary problem is, then:

$$\psi(\infty) = 0 \; ; \; \left(\frac{d\psi}{dr}\right)_{r=a} = -\frac{\sigma}{\varepsilon} \quad \text{(B.4)}$$

where *a* represents the surface coordinate, i.e., either the radius of the cylinder or the radius of the sphere, respectively, and σ is the surface charge density.

By means of an electrostatic potential defined as a dimensionless magnitude,

$$\tilde{\psi} \equiv \frac{e\psi}{k_B T} \tag{B.5}$$

the NLPB equation becomes an ordinary differential equation (ODE) of second order, which in a compact form (for both geometries) can be written as

$$\frac{d^2\tilde{\psi}}{dr^2} + \frac{g}{r}\frac{d\tilde{\psi}}{dr} = \kappa^2 \left\{ \alpha_1 \sinh\tilde{\psi} + \alpha_2 \left[\exp\left(\tilde{\psi}\right) - \exp\left(-2\tilde{\psi}\right) \right] \right\} \tag{B.6}$$

where g = 1 for cylindrical geometry and g =2 for spherical geometry.

Taking dimensionless radial coordinates in logarithmic space

$$\begin{aligned} y &\equiv \kappa\, r; \quad x = \ln y \\ y_0 &\equiv \kappa\, a; \quad x_0 = \ln y_0 \end{aligned} \tag{B.7}$$

the NLPB equation (B.6) becomes

$$\frac{d^2\tilde{\psi}}{dx^2} + (g-1)\frac{d\tilde{\psi}}{dx} = e^{2x} \left\{ \alpha_1 \sinh\tilde{\psi} + \alpha_2 \left[\exp\left(\tilde{\psi}\right) - \exp\left(-2\tilde{\psi}\right) \right] \right\} \tag{B.8}$$

and the value boundary problem (B.4) becomes

$$\tilde{\psi}(\infty) = 0 \tag{B.9}$$

$$\left(\frac{d\tilde{\psi}}{dx}\right)_{x=x_0} = -2\beta \tag{B.10}$$

for cylindrical geometry and

$$\left(\frac{d\tilde{\psi}}{dx}\right)_{x=x_0} = -\beta \tag{B.11}$$

for spherical geometry. β is related to the dimensionless surface charge density. In cylindrical geometry, β is defined as

$$\beta = \xi^{cyl}\alpha_d \tag{B.12}$$

in terms of the structural charge density, $\xi^{cyl} = l_B/b$, which relates the distance of separation of the charged ionised functional groups (b) with l_B, the Bjerrum length (the typical distance at which the electrostatic energy of elementary charges equals the thermal energy):

$$l_B = \frac{e^2}{4\pi\varepsilon k_B T} \tag{B.13}$$

For the spherical geometry:

$$\beta = \xi^{sph} n_p \alpha_d \tag{B.14}$$

where $\xi^{sph} = l_B/a$, n_p is the maximun number of ionisable groups over the surface (in practice, of the whole polyelectrolyte), and α_d is the dissociation degree.

Use of the GFEM method

For the sake of simplicity we detail here the particular case of cylindrical geometry (g = 1).

Using the GFEM method, the integral formulation of eq. (B.8) reads

$$\int_{x_0}^{L} \omega_k(x)\left(e^{2x} f(\psi) - \frac{d^2\psi}{dx^2}\right)dx - \omega_k(x_0)\left\{\left(\frac{d\psi}{dx}\right)_{x=x_0} + 2\beta\right\} = 0 \tag{B.15}$$

where L is an arbitrary distance, sufficiently large so that the boundary condition at $x \to \infty$ is fulfilled at this position, $\{\omega_k(x)\}$ is a set of arbitrary functions of the space functions, and

$$f(\psi) = \alpha_1 \sinh\psi + \alpha_2\left[\exp(\psi) - \exp(-2\psi)\right] \tag{B.16}$$

Then, integration by parts of the above integral equation yields the weak formulation of the NLPB ODE equation:

$$\int_{x_0}^{L} \omega_k(x) e^{2x} f(\psi)dx + \int_{x_0}^{L}\left(\frac{d\omega_k(x)}{dx}\right)\left(\frac{d\psi}{dx}\right)dx - \omega_k(x_0)2\beta = 0 \tag{B.17}$$

Now, the unknown function, $\psi(x)$, is expanded as a function of linear spatial interpolants with two sets of unknown coefficients m_j and u_j:

$$\psi(x) = \sum_{j=0}^{N-1} m_j \omega_j(x) \tag{B.18}$$

$$f\left[\psi(x)\right] = \alpha_1 \sinh\psi(x) + \alpha_2\left\{\exp\left[\psi(x)\right] - \exp\left[-2\psi(x)\right]\right\} = \\ = \sum_{j=0}^{N-1} u_j \omega_j(x) \tag{B.19}$$

The interpolants are linear piecewise functions (see **Figure B.1**) defined as

$$\omega_j(x) = \begin{cases} \dfrac{x - x_{j-1}}{x_j - x_{j-1}} & ; \quad x_{j-1} \le x \le x_j \\ \dfrac{x - x_{j+1}}{x_j - x_{j+1}} & ; \quad x_j \le x \le x_{j+1} \\ 0 & ; \quad \begin{cases} x \le x_{j-1} \\ x \ge x_{j+1} \end{cases} \end{cases} \tag{B.20}$$

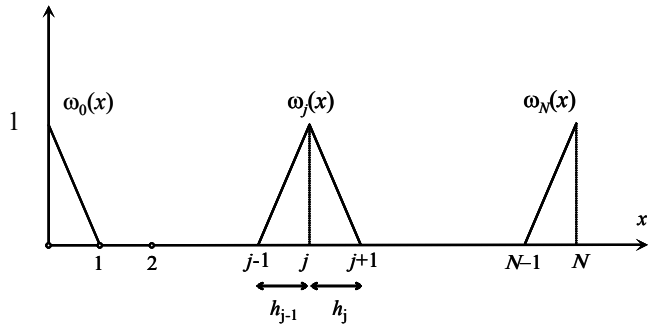

Figure B.1. Mesh and base functions used to interpolate the solution function.

In order to relate the two unknown set of coefficients, we notice that at a point grid j, all the interpolants (except ω_j which becomes 1) vanish, so the value of the function $\psi(x)$ takes the value m_j at $x = x_j$. In a similar way, the

function $f\left[\psi(x)\right]$ takes the value u_j at $x = x_j$; therefore we conclude that $u_j = \alpha_1 \sinh m_j + \alpha_2 \left\{\exp(m_j) - \exp(-2m_j)\right\}$.

Then, the terms of the above integral equation can be computed analytically and it reduces to a system of N non-linear equations, which can be written in a matrix form as

$$\mathbf{A}u + \mathbf{C}m + w = \mathbf{0} \tag{B.21}$$

where

$$u = \begin{pmatrix} u_0 \\ u_1 \\ \\ \vdots \\ u_{N-1} \end{pmatrix} = \begin{pmatrix} \sinh m_0 \\ \sinh m_1 \\ \\ \vdots \\ \sinh m_{N-1} \end{pmatrix} \; ; \; m = \begin{pmatrix} m_0 \\ m_1 \\ \\ \vdots \\ m_{N-1} \end{pmatrix} \; ; \; w = \begin{pmatrix} -2\beta \\ 0 \\ \\ \vdots \\ 0 \end{pmatrix} \tag{B.22}$$

and the matrices are

$$\mathbf{A} = \tag{B.23}$$

$$= \begin{pmatrix}
\frac{e^{2x_1}}{2}\beta(h_0) & e^{2x_0}\gamma(h_0) & 0 & 0 & \dots & 0 & 0 \\
e^{2x_0}\gamma(h_0) & \frac{e^{2x_0}}{2}\alpha(h_0)+\frac{e^{2x_2}}{2}\beta(h_1) & e^{2x_1}\gamma(h_1) & 0 & \dots & 0 & 0 \\
0 & e^{2x_1}\gamma(h_1) & \frac{e^{2x_1}}{2}\alpha(h_1)+\frac{e^{2x_3}}{2}\beta(h_2) & e^{2x_2}\gamma(h_2) & \dots & 0 & 0 \\
0 & 0 & e^{2x_2}\gamma(h_2) & \frac{e^{2x_2}}{2}\alpha(h_2)+\frac{e^{2x_4}}{2}\beta(h_3) & \dots & 0 & 0 \\
\vdots & \vdots & \vdots & \vdots & \ddots & \vdots & \vdots \\
0 & 0 & 0 & \dots & e^{2x_{N-3}}\gamma(h_{N-3}) & \frac{e^{2x_{N-3}}}{2}\alpha(h_{N-3})+\frac{e^{2x_{N-1}}}{2}\beta(h_{N-2}) & e^{2x_{N-2}}\gamma(h_{N-2}) \\
0 & 0 & 0 & \dots & 0 & e^{2x_{N-2}}\gamma(h_{N-2}) & \frac{e^{2x_{N-2}}}{2}\alpha(h_{N-2})+\frac{e^{2x_N}}{2}\beta(h_{N-1})
\end{pmatrix}$$

where

$$\alpha(h) \equiv \frac{1}{2h^2}\left(e^{2h}-1\right)+e^{2h}\left(1-\frac{1}{h}\right)$$

$$\beta(h) \equiv \frac{1}{2h^2}\left(1-e^{-2h}\right)-e^{-2h}\left(1+\frac{1}{h}\right) \qquad \text{(B.24)}$$

$$\gamma(h) \equiv \frac{1}{4h}\left\{e^{2h}\left(1-\frac{1}{h}\right)+\left(1+\frac{1}{h}\right)\right\}$$

and

$$\mathbf{C} = \begin{pmatrix} \frac{1}{h_0} & -\frac{1}{h_0} & 0 & \cdots & 0 & 0 \\ -\frac{1}{h_0} & \frac{1}{h_0}+\frac{1}{h_1} & -\frac{1}{h_1} & \cdots & 0 & 0 \\ 0 & -\frac{1}{h_1} & \frac{1}{h_1}+\frac{1}{h_2} & \cdots & 0 & 0 \\ \vdots & \vdots & \vdots & \ddots & \vdots & \vdots \\ 0 & 0 & 0 & \cdots & \frac{1}{h_{N-3}}+\frac{1}{h_{N-2}} & -\frac{1}{h_{N-2}} \\ 0 & 0 & 0 & \cdots & -\frac{1}{h_{N-2}} & \frac{1}{h_{N-2}}+\frac{1}{h_{N-1}} \end{pmatrix} \qquad \text{(B.25)}$$

with $h_j \equiv x_{j+1} - x_j$, representing the distance between the points in the grid, which in general can vary adapting to the requirements of the particular problem at different positions. Here, due to the fact that we have chosen the radial distance in logarithmic space, there is no need to use an uneven grid, so $h_j = h$ has been used. We have used 200 points in the grid with L sufficiently large.

This system of non-linear equations is solved numerically using a Newton-Raphson method (Press *et al.*, 1986). The solution of the linearized Poisson-Boltzmann equation (under the Debye-Hückel approximation) was chosen as initial estimate in the iterative procedure.

References

Anderson, C.F. and Record, M.T.J. (1990). Ion distributions around DNA and other cylindrical polyions: Theoretical descriptions and physical implications. *Annu. Rev. Biophys. Biophys. Chem*, **19**, 423-465.

Baker, N.A., Sept, D., Holst, M.J. and McCammon, J.A. (2001). The adaptative multilevel finite element solution of the Poisson-Boltzmann equation on massively parallel computers. *IBM J. Res. & Dev.*, **45**, 427-438.

Companys, E. (2003). Speciation of heavy metals in macromolecular systems by electroanalytical techniques. PhD Thesis. Universitat de Lleida.

Fogolari, F., Manzini, G. and Quadrifoglio, F. (1992). Polyelectrolytes in mixed salts: Scatchard plots obtained by means of Poisson-Boltzmann calculations. *Biophys. Chem.*, **43**, 213-219.

Hughes, T.J.R. (1987). *The finite Element Method*. Prentice Hall, Englewood Cliffs, N.J.

Ni, H., Anderson, C.F. and Record, M.T.J. (1999). Quantifying the thermodynamic consequences of cation (M^{2+}, M^{+}) accumulation and anion (X^{-}) exclusion in mixed salt solutions of polyanionic DNA using Monte Carlo and Poisson-Boltzmann calculations of ion-polyion preferential interaction coefficients. *J. Phys. Chem. B*, **103**, 3489-3504.

Press, W.H., Flannery, B.P., Teukolsky, S.A. and Vetterling, W.T. (1986). *Numerical recipes*. Cambridge University Press, Cambridge.

Schmitz, K.S. (1993). *Macroions in solution and colloidal suspension*. VCH, New York.